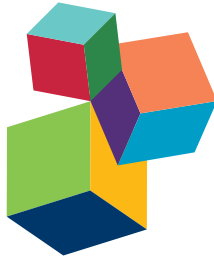


ADVANCEMENTS IN ALGAL BIOFUELS RESEARCH – RECENT EVALUATION OF ALGAL BIOMASS PRODUCTION AND CONVERSION METHODS FOR FUELS AND HIGH VALUE CO-PRODUCTS

EDITED BY: Umakanta Jena and S. Kent Hoekman

PUBLISHED IN: Frontiers in Energy Research &
Frontiers in Bioengineering and Biotechnology



frontiers

Frontiers Copyright Statement

© Copyright 2007-2017 Frontiers Media SA. All rights reserved.

All content included on this site, such as text, graphics, logos, button icons, images, video/audio clips, downloads, data compilations and software, is the property of or is licensed to Frontiers Media SA ("Frontiers") or its licensees and/or subcontractors. The copyright in the text of individual articles is the property of their respective authors, subject to a license granted to Frontiers.

The compilation of articles constituting this e-book, wherever published, as well as the compilation of all other content on this site, is the exclusive property of Frontiers. For the conditions for downloading and copying of e-books from Frontiers' website, please see the Terms for Website Use. If purchasing Frontiers e-books from other websites or sources, the conditions of the website concerned apply.

Images and graphics not forming part of user-contributed materials may not be downloaded or copied without permission.

Individual articles may be downloaded and reproduced in accordance with the principles of the CC-BY licence subject to any copyright or other notices. They may not be re-sold as an e-book.

As author or other contributor you grant a CC-BY licence to others to reproduce your articles, including any graphics and third-party materials supplied by you, in accordance with the Conditions for Website Use and subject to any copyright notices which you include in connection with your articles and materials.

All copyright, and all rights therein, are protected by national and international copyright laws.

The above represents a summary only. For the full conditions see the Conditions for Authors and the Conditions for Website Use.

ISSN 1664-8714

ISBN 978-2-88945-198-2

DOI 10.3389/978-2-88945-198-2

About Frontiers

Frontiers is more than just an open-access publisher of scholarly articles: it is a pioneering approach to the world of academia, radically improving the way scholarly research is managed. The grand vision of Frontiers is a world where all people have an equal opportunity to seek, share and generate knowledge. Frontiers provides immediate and permanent online open access to all its publications, but this alone is not enough to realize our grand goals.

Frontiers Journal Series

The Frontiers Journal Series is a multi-tier and interdisciplinary set of open-access, online journals, promising a paradigm shift from the current review, selection and dissemination processes in academic publishing. All Frontiers journals are driven by researchers for researchers; therefore, they constitute a service to the scholarly community. At the same time, the Frontiers Journal Series operates on a revolutionary invention, the tiered publishing system, initially addressing specific communities of scholars, and gradually climbing up to broader public understanding, thus serving the interests of the lay society, too.

Dedication to quality

Each Frontiers article is a landmark of the highest quality, thanks to genuinely collaborative interactions between authors and review editors, who include some of the world's best academicians. Research must be certified by peers before entering a stream of knowledge that may eventually reach the public - and shape society; therefore, Frontiers only applies the most rigorous and unbiased reviews.

Frontiers revolutionizes research publishing by freely delivering the most outstanding research, evaluated with no bias from both the academic and social point of view.

By applying the most advanced information technologies, Frontiers is catapulting scholarly publishing into a new generation.

What are Frontiers Research Topics?

Frontiers Research Topics are very popular trademarks of the Frontiers Journals Series: they are collections of at least ten articles, all centered on a particular subject. With their unique mix of varied contributions from Original Research to Review Articles, Frontiers Research Topics unify the most influential researchers, the latest key findings and historical advances in a hot research area! Find out more on how to host your own Frontiers Research Topic or contribute to one as an author by contacting the Frontiers Editorial Office: researchtopics@frontiersin.org

ADVANCEMENTS IN ALGAL BIOFUELS RESEARCH – RECENT EVALUATION OF ALGAL BIOMASS PRODUCTION AND CONVERSION METHODS FOR FUELS AND HIGH VALUE CO-PRODUCTS

Topic Editors:

Umakanta Jena, New Mexico State University, USA

S. Kent Hoekman, Desert Research Institute, USA

Algae biomass has enormous potential to produce fuels and value-added products. Algae-derived biofuels and bioproducts offer great promise in contributing to U.S. energy security and in mitigating the environmental concerns associated with conventional fuels. Algae's ability to grow in low quality water/wastewater and to accumulate lipids has encouraged scientists to investigate algae as a medium for wastewater treatment and a potential source of fuel and bioproducts. There are growing demands for biomass-based transportation fuels, including biodiesel, bio-oil, biomethane, biohydrogen, and other high-value products (nutraceuticals, proteins, omega-3 etc.). Algae can help address these needs.

The topic of algae energy includes the production and characterization of algae cultures, conversion into fuel feedstocks and high value products, and optimization of product isolation and use. In view of the increasing efforts in algae biomass production and conversion into energy and high-value products, the current research topic covers important aspects of algal strain selection, culture systems, inorganic carbon utilization, lipid metabolism and quality, biomass harvesting, extraction of lipids and proteins, and thermochemical conversion of algal feedstocks into biocrude.

Citation: Jena, U., Hoekman, S. K., eds. (2017). *Advancements in Algal Biofuels Research – Recent Evaluation of Algal Biomass Production and Conversion Methods for Fuels and High Value Co-Products*. Lausanne: Frontiers Media. doi: 10.3389/978-2-88945-198-2

Table of Contents

- 04** ***Editorial: Recent Advancements in Algae-to-Biofuels Research: Novel Growth Technologies, Conversion Methods, and Assessments of Economic and Environmental Impacts***
Umakanta Jena and S. Kent Hoekman
- Section I: Algal Biology and Biomass Production**
- 06** ***Strategies for Optimizing Algal Biology for Enhanced Biomass Production***
Amanda N. Barry, Shawn R. Starkenburg and Richard T. Sayre
- 11** ***The Marine Microalga, *Heterosigma Akashiwo*, Converts Industrial Waste Gases into Valuable Biomass***
Jennifer J. Stewart, Colleen M. Bianco, Katherine R. Miller and Kathryn J. Coyne
- 19** ***Evaluation of Diverse Microalgal Species as Potential Biofuel Feedstocks Grown Using Municipal Wastewater***
Sage R. Hiibel, Mark S. Lemos, Brian P. Kelly and John C. Cushman
- 27** ***Quantitative Assessment of Microalgae Biomass and Lipid Stability Post-Cultivation***
Katerine Napan, Tyler Christianson, Kristen Voie and Jason C. Quinn
- 33** ***Design, Construction, and Validation of an Internally Lit Air-Lift Photobioreactor for Growing Algae***
Esteban Hincapie and Ben J. Stuart
- 40** ***Biomass and Neutral Lipid Production in Geothermal Microalgal Consortia***
Kathryn F. Bywaters and Christian H. Fritsen
- Section II: Biomass Conversion into Fuel and High-Value Products**
- 51** ***Pyrolysis of Algal Biomass Obtained from High-Rate Algae Ponds Applied to Wastewater Treatment***
Fernanda Vargas e Silva and Luiz Olinto Monteggia
- 57** ***Demineralization of *Sargassum* spp. Macroalgae Biomass: Selective Hydrothermal Liquefaction Process for Bio-Oil Production***
Liz M. Díaz-Vázquez, Arnulfo Rojas-Pérez, Mariela Fuentes-Caraballo, Isis V. Robles, Umakanta Jena and K. C. Das
- 68** ***Optimization of Protein Extraction from *Spirulina Platensis* to Generate a Potential Co-Product and a Biofuel Feedstock with Reduced Nitrogen Content***
Naga Sirisha Parimi, Manjinder Singh, James R. Kastner, Keshav C. Das, Lennart S. Forsberg and Parastoo Azadi
- 77** ***Solvent Extraction and Characterization of Neutral Lipids in *Oocystis* sp.***
Renil Anthony and Ben Stuart



Editorial: Recent Advancements in Algae-to-Biofuels Research: Novel Growth Technologies, Conversion Methods, and Assessments of Economic and Environmental Impacts

Umakanta Jena^{1*} and S. Kent Hoekman²

¹Chemical and Materials Engineering, New Mexico State University, Las Cruces, NM, USA, ²Desert Research Institute, Reno, NV, USA

Keywords: algal biology, wastewater treatment, CO₂ utilization, thermochemical conversion, biofuels

Editorial on the Research Topic

Recent Advancements in Algae-to-Biofuels Research: Novel Growth Technologies, Conversion Methods, and Assessments of Economic and Environmental Impacts

OPEN ACCESS

Edited and Reviewed by:

Uwe Schröder,
Braunschweig University of
Technology, Germany

*Correspondence:

Umakanta Jena
ujena@nmsu.edu

Specialty section:

This article was submitted to
Bioenergy and Biofuels,
a section of the journal
Frontiers in Energy Research

Received: 04 February 2017

Accepted: 16 February 2017

Published: 06 March 2017

Citation:

Jena U and Hoekman SK (2017)
Editorial: Recent Advancements in
Algae-to-Biofuels Research: Novel
Growth Technologies, Conversion
Methods, and Assessments of
Economic and Environmental
Impacts.
Front. Energy Res. 5:2.
doi: 10.3389/fenrg.2017.00002

Biomass-derived fuels and chemicals provide an alternative to conventional petroleum-based feedstocks owing to their greater energy security, reduced environmental impacts, foreign exchange savings, and socioeconomic benefits (Demirbas, 2009). In the past two decades, there has been increasing research and technological development of biofuels and bioenergy by academia, industry, and other organizations (Brenan and Owende, 2010). Algae are one of the most studied potential sources of biofuels and bioenergy (Menetrez, 2012). Algal fuels are attractive to energy researchers, engineers, post-graduate and advanced undergraduate students, and others interested in pursuing research of bioenergy and bio-based products. Research into identification of productive algal species and conversion of algae into alternative fuels and other bioproducts is taking place in both public and private arenas. Although research has been conducted on algal strain selection, maintenance of pure species, growth and cultivation of algal biomass, there is still significant room for improvement in these areas (Hannon et al., 2010). Also, macroalgae (commonly known as “seaweed”) have not been fully exploited as a biofuel resource. Minimizing land, water, and nutrient use is critical to sustainable algal production. Recycling of process water, nutrients, and energy is crucial to large-scale algal production (Darzins et al., 2010; Hannon et al., 2010). The downstream processing of algal components into fuel and high-value coproducts poses a different set of challenges. Through processing technologies such as anaerobic digestion, pyrolysis, gasification, catalytic cracking, and enzymatic or chemical transesterification, whole algal biomass or algal extracts can be converted into different fuels, including biogas, kerosene, ethanol, jet fuel, and bio-hydrogen (Chisti, 2007; Christenson and Sims, 2011; Jena and Das, 2011; Milledge et al., 2014). Other areas of interest include development of higher efficiency harvesting and dewatering technologies, improved high-value product extraction and downstream processing, and development of novel conversion methods suitable for wet algae.

In view of increasing efforts on algal biomass production and its conversion into energy and high-value products, this research topic covers important aspects of algal strain selection, culture systems, inorganic carbon utilization, lipid metabolism and quality, biomass harvesting, extraction of lipids and proteins, and thermochemical conversion of algal feedstocks into biocrude.

Most of the articles in this current Research Topic fit within the category of Recent Advancements in Algae-to-Biofuels Research, including novel growth technologies and conversion methods. For example, strategies for optimizing algal biology for enhanced biomass production have been reviewed and detailed by Barry et al. These include modification of photosynthetic light-harvesting antenna size to increase energy capture and conversion efficiency, as well as development of advanced molecular breeding techniques (Barry et al.). Novel design and construction of an internally lit air-lift photobioreactor for growing algae have been described and validated in a separate chapter (Hincapie and Stuart). Other topics include utilization of municipal wastewater for algal growth (Hiibel et al.) and use of carbon dioxide through conversion of industrial waste gases to produce algae biomass (Napan et al.; Stewart et al.). Several experimental efforts directed at producing algae-derived fuels and high-value products are also reported here. These include production of neutral lipids using geothermal microalgae consortia (Bywaters and Fritsen), hydrothermal liquefaction (HTL) of macroalgae (Díaz-Vázquez et al.), pyrolysis of algae into bio-oil (Vargas e Silva and Monteggia), solvent extraction and characterization of neutral lipids (Anthony and Stuart), and novel protein extraction and subsequent HTL into biocrude (Parimi et al.).

REFERENCES

- Brennan, L., and Owende, P. (2010). Biofuels from microalgae – a review of technologies for production, processing, and extractions of biofuels and co-products. *Renew. Sustain. Energy Rev.* 14, 557. doi:10.1016/j.rser.2009.10.009
- Chisti, Y. (2007). Biodiesel from microalgae. *Biotechnol. Adv.* 25, 294. doi:10.1016/j.biotechadv.2007.02.001
- Christenson, L., and Sims, R. (2011). Production and harvesting of microalgae for wastewater treatment, biofuels, and bioproducts. *Biotechnol. Adv.* 29, 686. doi:10.1016/j.biotechadv.2011.05.015
- Darzens, A., Pienkos, P., and Edye, L. (2010). *Current Status and Potential for Algal Biofuels Production, International Energy Agency, Bioenergy Task 39, Report T39-T2*. Available at: http://www.globalbioenergy.org/uploads/media/1008_IEA_Bioenergy_Task_39_-_Current_status_and_potential_for_algal_biofuels_production.pdf
- Demirbas, A. (2009). Political, economic and environmental impacts of biofuels: a review. *Appl. Energy* 86, S108–S117. doi:10.1016/j.apenergy.2009.04.036
- Hannon, M., Gimpel, J., Tran, M., Rasala, B., and Mayfield, S. (2010). Biofuels from algae: challenges and potential. *Biofuels* 1, 763–784. doi:10.4155/bfs.10.44
- Jena, U., and Das, K. C. (2011). Comparative evaluation of thermochemical liquefaction and pyrolysis for bio-oil production from microalgae. *Energy Fuels* 25, 5472. doi:10.1021/ef201373m
- Menetrez, M. (2012). An overview of algae biofuel production and potential environmental impact. *Environ. Sci. Technol.* 46, 7073–7085. doi:10.1021/es300917r
- Milledge, J. J., Smith, B., Dyer, P. W., and Harvey, P. (2014). Macroalgae-derived biofuel: a review of methods of energy extraction from seaweed biomass. *Energies* 7, 7194–7222. doi:10.3390/en7117194

Conflict of Interest Statement: The authors declare that the research was conducted in the absence of any commercial or financial relationships that could be construed as a potential conflict of interest.

Copyright © 2017 Jena and Hoekman. This is an open-access article distributed under the terms of the Creative Commons Attribution License (CC BY). The use, distribution or reproduction in other forums is permitted, provided the original author(s) or licensor are credited and that the original publication in this journal is cited, in accordance with accepted academic practice. No use, distribution or reproduction is permitted which does not comply with these terms.

Along with a summary of relevant basic standard methods practiced in microalgae culture, harvesting, and processing, the current research topic presents an up-to-date overview of advancements in the still exciting field of algal biofuel research. Each chapter opens with fundamental explanations and goes on to provide experimental details and discuss the results. All chapters are supported by numerous clear, informative diagrams and tables.

We sincerely thank the authors of all the chapters for their cooperation and their willingness to revise the manuscripts in a timely manner. We also acknowledge the assistance of reviewers, who in spite of their busy professional activities, helped to evaluate the manuscripts and provide critical inputs to refine and improve the chapters. Finally, we warmly thank the team of Frontier Energy for their cooperation and communication in this effort.

AUTHOR CONTRIBUTIONS

UJ contributed to preparation and submission of the manuscript and was responsible for editing eight chapters in this research topic. SH contributed to editing two chapters in the current research topic.



Strategies for optimizing algal biology for enhanced biomass production

Amanda N. Barry, Shawn R. Starkenburg and Richard T. Sayre*

Los Alamos National Laboratory, New Mexico Consortium, Los Alamos, NM, USA

Edited by:

Umakanta Jena, Desert Research Institute, USA

Reviewed by:

Alberto Scorma, Ghent University, Belgium

Suyin Gan, The University of Nottingham Malaysia Campus, Malaysia

Chris Fritsen, Desert Research Institute, USA

*Correspondence:

Richard T. Sayre, Los Alamos National Laboratory, New Mexico Consortium, 100 Entrada Dr, Los Alamos, NM 87544, USA

e-mail: rsayre@newmexicoconsortium.org

One of the most environmentally sustainable ways to produce high-energy density (oils) feed stocks for the production of liquid transportation fuels is from biomass. Photosynthetic carbon capture combined with biomass combustion (point source) and subsequent carbon capture and sequestration has also been proposed in the intergovernmental panel on climate change report as one of the most effective and economical strategies to remediate atmospheric greenhouse gases. To maximize photosynthetic carbon capture efficiency and energy-return-on-investment, we must develop biomass production systems that achieve the greatest yields with the lowest inputs. Numerous studies have demonstrated that microalgae have among the greatest potentials for biomass production. This is in part due to the fact that all alga cells are photoautotrophic, they have active carbon concentrating mechanisms to increase photosynthetic productivity, and all the biomass is harvestable unlike plants. All photosynthetic organisms, however, convert only a fraction of the solar energy they capture into chemical energy (reduced carbon or biomass). To increase aerial carbon capture rates and biomass productivity, it will be necessary to identify the most robust algal strains and increase their biomass production efficiency often by genetic manipulation. We review recent large-scale efforts to identify the best biomass producing strains and metabolic engineering strategies to improve aerial productivity. These strategies include optimization of photosynthetic light-harvesting antenna size to increase energy capture and conversion efficiency and the potential development of advanced molecular breeding techniques. To date, these strategies have resulted in up to twofold increases in biomass productivity.

Keywords: algae, biomass, biofuel, photosynthesis, lipid, carbohydrate, *Chlorella sorokiniana*, *Chlamydomonas reinhardtii*

INTRODUCTION

Over the past 5 years, tremendous progress has been made in the technical and economic development of algal biofuel production systems (Chisti, 2008; Mata et al., 2010; Campbell et al., 2011; National Research Council, 2012; NAABB Final Report, 2014). In 2010, the “state of the art” technologies used to produce biodiesel from algae included paddle-wheel driven pond cultivation, centrifugation-based harvesting, biomass drying, and transesterification and resulted in fuel costs of over \$100/gge (National Research Council, 2012). Recent advances in algal biofuel production technologies have rapidly moved the industry from an economic uncertainty to an economic feasibility (Chisti, 2008; Williams and Laurens, 2010; Campbell et al., 2011; Richardson et al., 2014; NAABB Final Report, 2014). For example, the recent close-out report for the National Alliance of Advanced Biofuels and Bioproducts (NAABB) describes an integrated pathway from algal biomass production to fuel conversion that approaches an estimated cost of \$8.00/gge while achieving nearly 90% recovery of all carbon in biomass as fuel (NAABB Final Report, 2014). An important part of the cost reduction of producing algal biofuels was the use of hydrothermal liquefaction (HTL) (elevated temperature, 250–350°C, and pressure, 10–20 MPa, treatment) of wet biomass to produce biocrude coupled with catalytic hydrogen

gasification of the water soluble fraction remaining from HTL to produce methane (Jena et al., 2011a,b; NAABB Final Report, 2014). Algal biocrude was successfully converted into diesel, gasoline, and/or aviation fuel with the appropriate catalysts and treatments (NAABB Final Report, 2014). Significantly, NAABB supported life cycle analyses (LCA) also identified the major constraints limiting the production of fuels from algae at economic parity with petroleum. The major constraints limiting economic parity of algal biofuels with petroleum include (1) the limited production of algal biomass per unit land area, and (2) the energy and economic costs associated with scalable algae harvesting (National Research Council, 2012; NAABB Final Report, 2014). For algal biofuels to achieve economic parity with petroleum, algal biomass yields will need to be increased approximately threefold from 12 to >30 gdw/m²/day on a sustained basis. In addition, the energy-return-on-investment (EROI) for harvesting algae from ponds ideally would need to be >20, i.e., no more than 5% of the energy content of the algae is used for harvest (NAABB Final Report, 2014).

Focusing only on commodity scale production of fuels from algae is, however, not the only approach for achieving economic parity with petroleum. One approach for reducing the costs of producing fuels from algae is the co-production of high-value products along with the biofuel feedstock (National Research

Council, 2012; NAABB Final Report, 2014). In addition, a new potential economic driver for the reduction in algal biofuel costs is emerging; i.e., the potential for carbon capture and sequestration. The recent Intergovernmental Panel for Climate Change (IPCC) report has identified biological energy production coupled with carbon capture and sequestration (BECCS) as the most technological and economically viable solutions for removing carbon from the atmosphere to mitigate the impact of greenhouse gases on Climate Change (2014). Briefly, carbon removed from the atmosphere through photosynthesis is converted into biofuel. Energy generated from biofuel combustion at a point source generates income while also reducing demand for fossil fuels. The concentrated CO₂ released from biofuel combustion at the point source is subsequently captured and sequestered before entering the atmosphere. Coupling bioenergy production with carbon sequestration (BECCS), including subterranean CO₂ injection or biochar carbon sequestration, results in a net removal of carbon from the atmosphere (Climate Change, 2014). If enacted, tax credits and/or carbon credit policies could provide cost reductions for producing bioenergy from algae coupled with carbon capture and sequestration. In the following review, we consider various strategies for increasing overall algal bioenergy production yields while reducing costs and enhancing carbon capture. These strategies include selection of the most robust and greatest yielding algal biomass strains coupled with genetic improvements to increase photosynthetic efficiency.

RECENT PROGRESS IN ENHANCING MICROALGAL BIOFUEL FEED STOCK PRODUCTION

Recently, it has been recognized that the EROI for downstream algal biomass conversion to fuel technologies is less constrained by the biochemical composition (oil versus carbohydrate and protein) of the biomass than previously thought (Sayre, 2010; Subramanian et al., 2013). To date, much of the focus on improving algal biofuel production yields has focused on increasing lipid content or the energy density of the biomass, often at the expense of total biomass yield (Huerlimann et al., 2010; Sharma et al., 2012; Subramanian et al., 2013). Since total energy yield is the product of both the biomass energy density and the total biomass yield, the most efficient means to increase overall biomass to fuel EROI is to determine the ideal balance between biomass energy density (lipid, carbohydrate, and protein composition) and biomass yield that gives the greatest total energy yield. In addition, we must also consider the optimal algal biochemical composition that yields the greatest EROI during biomass conversion to fuel. Recently, analyses of the thermodynamics of solar energy conversion by algae into combustible energy storage products (oil and carbohydrate) indicate that carbohydrate production is thermodynamically more efficient than oil production (Subramanian et al., 2013). The overall EROI from photosynthetically captured red photons to heat of combustion is 59% for triacylglycerol (TAG, C₅₅H₉₈O₆) and 64% for starch (C₆H₁₂O₆) on a per carbon basis (Table S1 in Supplementary Material). Furthermore, carbohydrate production may be kinetically less constrained than lipid production and starch may serve as a reduced carbon source for lipid production (Subramanian et al., 2013). Relevant to this hypothesis, recent analyses of the EROI for algal biomass conversion into biocrude by HTL indicates

that the biomass to fuel conversion EROI is similar for algal biomass feed stocks having a broad range of carbohydrate to oil ratios (Campbell et al., 2011). The EROI for biocrude production using *Nannochloropsis* (32% oil, 57% protein, 8% carbohydrate) was 66%, while for *Porphyridium* (8% oil, 43% protein, 40% carbohydrate), which has a fourfold lower oil content and a fivefold higher carbohydrate content, the EROI for biocrude production was 52% (Table S2 in Supplementary Material). Thus, HTL treatment of algal biomass generates a biocrude product having similar EROIs from feed stocks having a broad range of lipid content. To optimize total bioenergy yield from sun to fuel, we need to select, breed, or design algae that are not only the most efficient at energy capture, conversion, and storage, but which have the optimal carbohydrate:lipid ratios that will give both the greatest total energy yield in production and the greatest EROI for biomass to fuel conversion.

EMERGING BIOENERGY PRODUCTION STRAINS

Whereas *Chlamydomonas* has many features that make it an ideal model organism for evaluating various metabolic engineering and breeding strategies to improve crop yield and robustness, it has limited potential as a production strain due primarily to limitations in the maximal cell number or biomass density achieved at saturating or stationary phase cultures (NAABB Final Report, 2014). The NAABB consortium conducted an extensive bioprospecting effort to identify wild algal isolates that had the highest biomass yield and energy densities (Branyikova et al., 2011; Li et al., 2013; NAABB Final Report, 2014). One of the most productive species identified by two independent groups within the NAABB consortium was *Chlorella sorokiniana*. *C. sorokiniana* has an optimal growth temperature of 37°C, and is able to grow heterotrophically on a variety of sugars that enhance oil accumulation. Under N-starvation, *C. sorokiniana* was shown to accumulate neutral lipids, accumulate oil droplets, and exhibited an increased oxidative stress response with damage to photosystem II (PSII) (Zhang et al., 2013). Growth in an optimized mixo- and heterotrophic bioreactor supplemented with glucose enabled *C. sorokiniana* UTEX 1230 to accumulate 30–40% of its cell mass as lipids (Rosenberg et al., 2014). Furthermore, while growing in the absence of nitrogen (following pre-growth with ammonia at dry weight production rates equivalent to growth in the presence of ammonia), the energy content of the algae increased by nearly 50% on a dry weight basis (Sangeeta Negi, personal communication). This increase in energy content was associated with elevated TAG levels. The ability to grow at unimpeded rates while increasing energy density in the absence of nitrogen for extended periods of time is not commonly observed in many algal species, which typically have reduced growth rates as they become nitrogen starved of the course of several weeks. Pre-loading production strains with sufficient nutrients to produce high biomass and lipid yields in the absence of macro-nutrients, or using so-called nutrient-pulse technology, is potentially one way of controlling weedy or competing algal contaminants in production systems.

Currently, we are improving and annotating the genomes of three independent *C. sorokiniana* isolates (Table 1; NAABB Final Report, 2014). Two of these genomes, strain “1412” and UTEX 1230, were drafted by the NAABB Consortium (NAABB Final Report, 2014) and most recently, a genome assembly and

Table 1 | Genome statistics for strains of *C. sorokiniana* (NAABB Final Report, 2014).

Strain	1412	UTEX 1230	1228
Quality	Improved draft	Improved draft	Improved draft
Platform(s)	Illumina	Illumina + Pacbio	Pacbio + Opgen
Assembly size	59.3 MB	60 MB	61 MB
Contigs	5949	746	66
Contig N50	19.5 kb	812 kb	2.35 MB
Max contig size	122 kb	2.6 MB	4.56 MB
Chromosomes	N.D.	N.D.	12
% Unique ^a	93.9%	95.8%	N.A.

^aIndicates the percentage of unique nucleotide sequence (<90% identity) between strains of *C. sorokiniana*. The unique sequence indicated for *C. sorokiniana* strain UTEX 1230 was calculated from a comparison to *C. sorokiniana* strain 1228. The percentage of unique sequence indicated for *C. sorokiniana* strain 1412 was calculated from a comparison to both strain 1230 and 1228.

N.D., not determined; N.A., not applicable.

annotation project was initiated for a new strain; *C. sorokiniana* 1228. Preliminary analysis of the improved drafts from these three strains indicates that all *C. sorokiniana* species have approximate genome sizes of 60 MB and that the dominant generation is diploid. Despite the similarity in genome size, only 4–6% of each genome is highly conserved (4–6 MB of each genome share >90% nucleotide identity), which suggests that each strain has unique genotypic/phenotypic properties that can be combined to further improve the performance in a production environment (Table 1).

With respect to strain improvement, we have developed nuclear transformation vectors for *C. sorokiniana* based on the use of *C. sorokiniana* gene promoters identical to those identified to be optimal for gene expression in *Chlamydomonas* (Kumar et al., 2013). PCR positive transformants of codon-optimized foreign genes have also been identified based on paromomycin selection. In the future, breeding algae for improved performance will likely be a part of the repertoire for crop improvement. Using advanced molecular assisted breeding techniques, gene tagging and activation strategies, and mutagenesis approaches to breed for strains with enhanced yield and range of environmental performance may substantially increase crop yields. The major challenge for many diploid algae has been the identification of conditions that induce meiosis, gametogenesis, and mating. Recently, it has been observed that diploid *Chlorella* species have genes essential for meiosis as well as flagellar genes, required for mating (Blanc et al., 2010). As indicated above, we have observed substantial genetic variation in independent isolates of *C. sorokiniana* suggesting that there is considerable opportunity for crop improvement through molecular assisted breeding and genome editing technologies.

INCREASING SOLAR ENERGY CAPTURE AND CONVERSION EFFICIENCY FOR ENHANCED FUEL PRODUCTION

The earliest event in photosynthesis is the capture of photons by the light-harvesting antenna protein-pigment complexes of the chloroplast thylakoid membranes (Zhu et al., 2010; Subramanian et al., 2013). In chlorophytic (green) algae, the majority (>70%) of

chlorophyll (Chl) is associated with the light-harvesting antenna complexes (Perrine et al., 2012). The antenna complexes capture and transfer energy to the reaction center complexes (PS I and II) where charge separation occurs. Significantly, energy migration within the light-harvesting antenna complex is very efficient occurring by quantum coherence processes (Subramanian et al., 2013). Highly efficient light capture by large antenna, even though wasteful, confers a selective advantage in mixed species populations by limiting light availability for competing species as well as facilitating light capture at low light flux densities deep in the canopy or water column (Blankenship et al., 2011). However, the very large apparent optical cross sections of light-harvesting complexes trap substantially more photons than accommodated by the photosynthetic electron transfer apparatus (Perrine et al., 2012). Indeed, at full sunlight intensities the rate of photon capture is 10-fold faster than the rate-limiting step (1–10 ms) in electron transfer associated with plastoquinone oxidation by the cytochrome b6/f complex (Perrine et al., 2012). As a result, 80% of the trapped energy is dissipated as heat or Chl fluorescence at full sunlight intensities [2000 μmol photosynthetically active (400–700 nm) photons/m²/s (Mussgnug et al., 2005; Perrine et al., 2012)].

Photosynthetic carbon dioxide fixation is challenged by various constraints as well including: photorespiratory energy and C losses from RuBisCO oxygenase activity, limiting abundance of critical metabolic enzymes, and metabolic feedback from inefficiencies in C flux from source to sinks (Giordano et al., 2005; Spalding, 2009; Zhu et al., 2010; Branyikova et al., 2011; Johnson and Alric, 2013). Overall, the maximum thermodynamic efficiency for photosynthesis using red photons to produce carbohydrate is 25–30% (Subramanian et al., 2013). If the entire solar spectrum is factored into the energy efficiency calculations then the maximum solar-to-biomass conversion efficiency only approaches 11% (Giordano et al., 2005; Zhu et al., 2010; Subramanian et al., 2013; Torzillo et al., 2014). In reality, the thermodynamic efficiency for harvestable biomass production is typically <3%, due in part to kinetic constraints in photosynthesis, respiratory losses, and negative feedback regulation by the sink (Zhu et al., 2010; Johnson and Alric, 2013; Subramanian et al., 2013).

Substantial improvements in photosynthesis and biomass yield have been achieved in algae. The greatest yield improvements, to date, have been achieved by optimizing the size of the light-harvesting antenna complex to reduce inefficiencies in energy conversion (Mussgnug et al., 2005; Perrine et al., 2012). Engineering “intermediate” antenna sizes in *Chlamydomonas reinhardtii* improved photosynthetic rates and biomass yields on the order of 10–30% in laboratory cultures (Polle et al., 2001; Mussgnug et al., 2005; Melis, 2009; Perrine et al., 2012). To achieve an intermediate antenna size, the synthesis of Chl b, which is bound only to the peripheral light-harvesting antenna complex proteins, was reduced by inhibiting the synthesis of Chl a oxygenase, the enzyme that converts Chl a into Chl b, using RNAi technology (Perrine et al., 2012). Most recently, this approach to reduce antenna size, and thus increase biomass productivity, was performed in *C. sorokiniana*, where UV mutagenesis was utilized to isolate truncated antenna mutants (Cazzaniga et al., 2014). PSII antenna reduction (48% of LHClI protein content compared to

wild-type) resulted in a 32% increased mean biomass productivity over wild-type strains when grown in photobioreactors.

CONCLUDING REMARKS

Overall, there continues to be a need to identify and or engineer the best and most robust algal strains to produce the greatest amount of biomass. Additional traits that are desirable for sustainable algal biomass production include; heat tolerance (to reduce the need for evaporative cooling and to seal ponds to reduce water demand), inducible self-flocculation (to reduce harvesting costs), herbivore resistance, and traits that reduce competition by unwanted algal contaminants. Furthermore, it is understood that different algal species will be optimal in different environments and produce greater biomass at different seasons of the year. Rotating production strains (crops) during the year to optimize yields is one strategy successfully used in agriculture to optimize yield. For algal crop improvement to approach the historical yield increases achieved in crop plants, a combination of using the best producing species, development of diverse breeding populations, and application of genome editing and transgenic approaches will need to be developed. There is great potential for yield improvement in this largely untapped resource of genetic and phenotypic diversity.

SUPPLEMENTARY MATERIAL

The Supplementary Material for this article can be found online at <http://www.frontiersin.org/Journal/10.3389/fenrg.2015.00001/abstract>

REFERENCES

- Blanc, G., Duncan, G., Agarkova, I., Borodovsky, M., Gurnon, J., Kuo, A., et al. (2010). The *Chlorella variabilis* NC64A genome reveals adaptation to photosymbiosis, coevolution with viruses, and cryptic sex. *Plant Cell* 22, 2943–2955. doi:10.1105/tpc.110.076406
- Blankenship, R. E., Tiede, D. M., Barber, J., Brudvig, G. W., Fleming, G., Ghirardi, M., et al. (2011). What is the solar energy conversion efficiency of natural photosynthesis compared to photovoltaic cells? *Science* 332, 805–809. doi:10.1126/science.1200165
- Branyikova, I., Marsalkova, B., Doucha, J., Branyik, T., Bisova, K., Zachleder, V., et al. (2011). Microalgae – novel highly efficient starch producers. *Biotechnol. Bioeng.* 108, 766–776. doi:10.1002/bit.23016
- Campbell, P. K., Beer, T., and Batten, D. (2011). Life cycle assessment of biodiesel production from microalgae in ponds. *Bioresour. Technol.* 102, 50–56. doi:10.1016/j.biortech.2010.06.048
- Cazzaniga, S., Dall'Osto, L., Szaub, J., Scibilia, L., Ballottari, M., Purton, S., et al. (2014). Domestication of the green alga *Chlorella sorokiniana*: reduction of antenna size improves light-use efficiency in a photobioreactor. *Biotechnol. Biofuels* 7, 157–170. doi:10.1186/s13068-014-0157-z
- Chisti, Y. (2008). Biodiesel from microalgae beats bioethanol. *Trends Biotechnol.* 26, 126–131. doi:10.1016/j.tibtech.2007.12.002
- Climate Change. (2014). *Mitigation of Climate Change*. Intergovernmental Panel on Climate Change. Available at: <http://www.ipcc.ch/>
- Giordano, M., Beardall, J., and Raven, J. A. (2005). CO₂ concentrating mechanisms in algae: mechanisms, environmental modulation, and evolution. *Annu. Rev. Plant Biol.* 56, 99–131. doi:10.1146/annurev-arplant.56.032604.144052
- Huerlimann, R., de Nys, R., and Heimann, K. (2010). Growth, lipid content, productivity, and fatty acid composition of tropical microalgae for scale-up production. *Biotechnol. Bioeng.* 107, 245–257. doi:10.1002/bit.22809
- Jena, U., Vaidyanathan, N., Chinnasamy, S., and Das, K. C. (2011a). Evaluation of microalgae cultivation using recovered aqueous co-product from thermoliquefaction of algal biomass. *Bioresour. Technol.* 102, 3380–3387. doi:10.1016/j.biortech.2010.09.111
- Jena, U., Das, K. C., and Kastner, J. R. (2011b). Effect of operating conditions of thermoliquefaction on biocrude production from *Spirulina platensis*. *Bioresour. Technol.* 102, 6221–6229. doi:10.1016/j.biortech.2011.02.057
- Johnson, X., and Alric, J. (2013). Central carbon metabolism and electron transport in *Chlamydomonas reinhardtii*: metabolic constraints for carbon partitioning between oil and starch. *Eukaryotic Cell* 12, 776–793. doi:10.1128/EC.00318-12
- Kumar, A., Falcao, V. R., and Sayre, R. T. (2013). Evaluating nuclear transgene expression systems in *Chlamydomonas reinhardtii*. *Algal Res.* 2, 321–332. doi:10.1016/j.algal.2013.09.002
- Li, T., Zheng, Y., Yu, L., and Chen, S. (2013). High productivity cultivation of a heat-resistant microalgae, *Chlorella sorokiniana* for biofuel production. *Bioresour. Technol.* 131, 60–67. doi:10.1016/j.biortech.2012.11.121
- Mata, T. M., Martins, A. A., and Caetano, N. S. (2010). Microalgae for biodiesel production and other applications: a review. *Renew. Sustain Energy Rev.* 14, 217–232. doi:10.1016/j.rser.2009.07.020
- Melis, A. (2009). Solar energy conversion efficiencies in photosynthesis: minimizing the chlorophyll antennae to maximize efficiency. *Plant Sci.* 177, 272–280. doi:10.1016/j.plantsci.2009.06.005
- Mussgnug, J. H., Wobbe, L., Elles, I., Claus, C., Hamilton, M., Fink, A., et al. (2005). NAB1 is an RNA binding protein involved in the light-regulated differential expression of the light-harvesting antenna of *Chlamydomonas reinhardtii*. *Plant Cell* 17, 3409–3421. doi:10.1105/tpc.105.035774
- NAABB Final Report. (2014). *National Alliance for Advanced Biofuels and Bioproducts Synopsis (NAABB) Final Report*. Available at: <http://energy.gov/eere/bioenergy/downloads/national-alliance-advanced-biofuels-and-bioproducts-synopsis-naabb-final>
- National Research Council. (2012). *Sustainable Development of Algal Biofuels*. Washington, DC: The National Academies Press.
- Perrine, Z., Negi, S., and Sayre, R. T. (2012). Optimization of photosynthetic light energy utilization by microalgae. *Algal Res.* 1, 134–142. doi:10.1016/j.algal.2012.07.002
- Polle, J., Kanakagiri, S., Benemann, J. R., and Melis, A. (2001). “Maximizing photosynthetic efficiencies and hydrogen production by microalgal cultures,” in *Biohydrogen II: An Approach to Environmentally Acceptable Technology*, eds J. Miyake, T. Matsunaga, and A. San Pietro (Oxford: Pergamon Press), 111–130.
- Richardson, J. W., Johnson, M. D., Zhang, X., Zemke, P., Chen, W., and Hu, Q. (2014). A financial assessment of two alternative cultivation systems and their contributions to algae biofuel economic viability. *Algal Res.* 4, 96–104. doi:10.1016/j.algal.2013.12.003
- Rosenberg, J. N., Kobayashi, N., Barnes, A., Noel, E. A., Betenbaugh, M. J., and Oyler, G. A. (2014). Comparative analyses of three chlorella species in response to light and sugar reveal distinctive lipid accumulation patterns in the microalga *C. sorokiniana*. *PLoS ONE* 9:e92460. doi:10.1371/journal.pone.0092460
- Sayre, R. T. (2010). Microalgal biofuels; carbon capture and sequestration. *Bioscience* 60, 722–727. doi:10.1525/bio.2010.60.9.9
- Sharma, K. K., Schuhmann, H., and Schenk, P. M. (2012). High lipid induction in microalgae for biodiesel production. *Energies* 5, 1532–1553. doi:10.3390/en5051532
- Spalding, M. H. (2009). *CO₂-Concentrating Mechanism and Carbon Assimilation*. Oxford: Academic Press.
- Subramanian, S., Barry, A. N., Pieris, S., and Sayre, R. T. (2013). Comparative energetics and kinetics of autotrophic lipid and starch metabolism in chlorophytic microalgae: implications for biomass and biofuel production. *Biotechnol. Biofuels* 6, 150–162. doi:10.1186/1754-6834-6-150
- Torzilla, G., Scoma, A., Faraloni, C., and Giannelli, L. (2014). Advances in the biotechnology of hydrogen production with the microalga *Chlamydomonas reinhardtii*. *Crit. Rev. Biotechnol.* doi:10.3109/07388551.2014.900734
- Williams, P. J. B., and Laurens, L. M. L. (2010). Microalgae as biodiesel & biomass feedstocks: review & analysis of the biochemistry, energetics & economics. *Energy Environ. Sci.* 3, 554–590. doi:10.1039/b924978h
- Zhang, Y. M., Chen, H., He, C. L., and Wang, Q. (2013). Nitrogen starvation induced oxidative stress in an oil-producing green alga *Chlorella sorokiniana* C3. *PLoS ONE* 8:e69225. doi:10.1371/journal.pone.0069225
- Zhu, X. G., Long, S. P., and Ort, D. R. (2010). Improving photosynthetic efficiency for greater yield. *Annu. Rev. Plant Biol.* 61, 235–261. doi:10.1146/annurev-arplant-042809-112206

Conflict of Interest Statement: The authors declare that the research was conducted in the absence of any commercial or financial relationships that could be construed as a potential conflict of interest.

Received: 29 September 2014; accepted: 13 January 2015; published online: 02 February 2015.

Citation: Barry AN, Starkenburg SR and Sayre RT (2015) Strategies for optimizing algal biology for enhanced biomass production. *Front. Energy Res.* 3:1. doi: 10.3389/fenrg.2015.00001

This article was submitted to *Bioenergy and Biofuels*, a section of the journal *Frontiers in Energy Research*.

Copyright © 2015 Barry, Starkenburg and Sayre. This is an open-access article distributed under the terms of the Creative Commons Attribution License (CC BY). The use, distribution or reproduction in other forums is permitted, provided the original author(s) or licensor are credited and that the original publication in this journal is cited, in accordance with accepted academic practice. No use, distribution or reproduction is permitted which does not comply with these terms.

The marine microalga, *Heterosigma akashiwo*, converts industrial waste gases into valuable biomass

Jennifer J. Stewart^{1*}, Colleen M. Bianco², Katherine R. Miller³ and Kathryn J. Coyne¹

¹ College of Earth, Ocean, and Environment, University of Delaware, Lewes, DE, USA, ² Department of Microbiology, University of Illinois at Urbana-Champaign, Urbana, IL, USA ³ Department of Chemistry, Salisbury University, Salisbury, MD, USA

OPEN ACCESS

Edited by:

Umakanta Jena,
Desert Research Institute, USA

Reviewed by:

Alberto Scoma,
Ghent University, Belgium
Probir Das,
Qatar University, Qatar
Liz M. Diaz,
University of Puerto Rico, USA

*Correspondence:

Jennifer J. Stewart,
College of Earth, Ocean, and
Environment, University of Delaware,
700 Pilottown Road, Lewes, DE
19958, USA
jen@udel.edu

Specialty section:

This article was submitted to
Bioenergy and Biofuels, a section of
the journal *Frontiers in Energy
Research*

Received: 03 December 2014

Accepted: 26 February 2015

Published: 16 March 2015

Citation:

Stewart JJ, Bianco CM, Miller KR and
Coyne KJ (2015) The marine
microalga, *Heterosigma akashiwo*,
converts industrial waste gases into
valuable biomass.
Front. Energy Res. 3:12.
doi: 10.3389/fenrg.2015.00012

Heterosigma akashiwo is an excellent candidate for growth on industrial emissions since this alga has the ability to metabolize gaseous nitric oxide (NO) into cellular nitrogen via a novel chimeric protein (NR2-2/2HbN) and also tolerates wide fluctuations in temperature, salinity, and nutrient conditions. Here, we evaluated biomass productivity and composition, photosynthetic efficiency, and expression of NR2-2/2HbN for *Heterosigma* growing on simulated flue gas containing 12% CO₂ and 150 ppm NO. Biomass productivity of *Heterosigma* more than doubled in flue gas conditions compared to controls, reflecting a 13-fold increase in carbohydrate and a 2-fold increase in protein productivity. Lipid productivity was not affected by flue gas and the valuable omega-3 fatty acids, eicosapentaenoic acid and docosahexaenoic acid, constituted up to 16% of total fatty acid methyl esters. Photochemical measurements indicated that photosynthesis in *Heterosigma* is not inhibited by high CO₂ and NO concentrations, and increases in individual fatty acids in response to flue gas were driven by photosynthetic requirements. Growth rates and maximum cell densities of *Heterosigma* grown on simulated flue gas without supplemental nitrogen, along with a significant increase in NR2-2/2HbN transcript abundance in response to flue gas, demonstrated that nitrogen derived from NO gas is biologically available to support enhanced CO₂ fixation. Together, these results illustrate the robustness of this alga for commercial-scale biomass production and bioremediation of industrial emissions.

Keywords: bioremediation, biofuel, algae, carbon dioxide, nitric oxide, raphidophyte, biomass

Introduction

The globally distributed algal species *Heterosigma akashiwo* (Y. Hada) Y. Hada ex Y. Hara & M. Chihara (Hara and Chihara, 1987) is a unicellular chromophyte alga within the class Raphidophyceae and is well known for forming dense blooms in coastal and estuarine systems worldwide (Zhang et al., 2006; Martínez et al., 2010). *Heterosigma* has been identified as a promising candidate for the production of high quality biodiesel and is capable of achieving a higher total lipid content than several other microalgal species traditionally used in biodiesel production (Fuentes-Grünwald et al., 2013; 2012; 2009). This robust organism tolerates wide fluctuations in temperature, salinity, and nutrient conditions (Martínez et al., 2010), suggesting that this alga would be a viable option for commercial-scale biomass production. *Heterosigma* is also an excellent candidate for growth on industrial emissions (i.e., “flue gases”), since this alga has the ability to metabolize gaseous NO into cellular nitrogen via a novel chimeric protein, NR2-2/2HbN (Stewart and Coyne, 2011).

Developing innovative CO₂ utilization strategies is essential for overcoming the barriers to economic and sustainable algal biomass production, since CO₂ supplementation is a requirement for commercial biomass production due to carbon limitation at atmospheric CO₂ levels (Benemann, 2013). Utilizing flue gas CO₂ would have the dual advantage of simultaneously decreasing biomass production costs while also mitigating the effects of harmful greenhouse gas emissions. CO₂ accounts for 82% of anthropogenically derived greenhouse gas emissions in the United States (EPA, 2012), and it is widely accepted that remediation of CO₂ emissions is essential for mitigating global climate change. In addition, flue gas also contains cytotoxic nitrogen oxides (NO_x, > 90% as nitric oxide), and the reaction products of NO_x emissions, ozone (O₃) and nitrous oxide (N₂O), are also potent greenhouse gases (EPA, 2014). Harnessing both CO₂ and NO_x emissions from flue gas as nutrient sources for *Heterosigma* growth could theoretically reduce operating costs for biomass production by 50% (Douskova et al., 2009; Nagarajan et al., 2013).

Utilization of industrial CO₂ for algal growth has been investigated for a variety of algal species, including *Spirulina* sp. (Chen et al., 2012), *Chlorella* sp. (Doucha et al., 2005; Douskova et al., 2009; Borkenstein et al., 2011; Chiu et al., 2011), and *Dunaliella* sp. (Harter et al., 2013). The green alga, *Scenedesmus* sp., is able to grow in high CO₂ and NO_x environments and is currently being evaluated for growth on industrial emissions (Jin et al., 2008; Santiago et al., 2010; Basu et al., 2013; Jiang et al., 2013; Lara-Gil et al., 2014; Wilson et al., 2014). Continued identification and characterization of algal species that thrive in these harsh conditions is a critical step toward economically viable production of algal biofuels and bioproducts. To address this critical research gap, we evaluated biomass productivity, cellular composition, photosynthetic efficiency, and expression of *NR2-2/2HbN* for *H. akashiwo* growing on simulated flue gas containing 12% CO₂ and 150 ppm NO. Results of this work will support the development of commercial platforms for cultivating algal biomass on flue gas for the biofuels and bioproducts industries.

Materials and Methods

Strains and Experimental Culture Conditions

H. akashiwo CCMP 2393 (NCMA; Boothbay Harbor, ME, USA) was maintained in seawater diluted to a salinity of 20 ppt and amended with *f/2* nutrients (-Si) (Guillard, 1975), buffered with 20 mM HEPES (pH = 7.35), and grown at room temperature and an irradiance of ~80 μmol quanta m⁻² s⁻¹ on a 12:12 h light:dark cycle. Light provided by cool white fluorescent bulbs was measured using an LI-250A light meter (LI-COR Biosciences, Lincoln, NE, USA) placed against the external wall of the culture vessel at a point closest to the light source. Cultures were grown in 1 L narrow-mouth polycarbonate bottles (diameter = 99 mm; Thermo Fisher Scientific, Waltham, MA, USA) sealed with screw caps retrofitted with inlet and outlet ports attached to PTFE tubing (3/16" ID, 1/4" OD, 1/32" wall). Cultures were bubbled continuously (2 mL min⁻¹) with compressed air (control) or a simulated flue gas mixture consisting of 12% CO₂ and 150 ppm NO balanced in N₂ through rigid PTFE tubing that extended to the bottom of

the vessel. The headspace was vented through a short piece of PTFE tubing stuffed with cotton fitted to the outlet port.

Cultures were maintained in batch growth under experimental conditions for five cycles (35 days) by replacing culture with fresh media every 7 days to achieve an initial density of 180,000 cells/mL at the start of each batch cycle. During the sixth cycle, replicate cultures (500 mL; *n* = 4) were sampled during mid-log growth for analysis of total carbohydrate, protein and lipid content, lipid profiles, gene expression, seawater chemistry, particulate carbon and nitrogen, and photochemistry as described below.

In a separate experiment, cells acclimated to growth on either air or simulated flue gas for five cycles were used to seed replicate cultures (500 mL; *n* = 4) and cultivated in modified *f/2* media containing either 0 or 220 μM sodium nitrate (NaNO₃). Growth was monitored daily for 12 days using an improved Neubauer hemocytometer (Thermo Fisher Scientific) to calculate cell density. Specific growth rate (μ) was calculated using the following equation:

$$\mu = [\ln(N_2 \div N_1)] \div (t_2 - t_1) \quad (1)$$

where *N*₂ and *N*₁ are cell densities (cells/mL) at *t*₂ and *t*₁, respectively.

Cell Counts, Cell Size, and Cell Weight

Cell counts and cell sizes were determined using a Multisizer 3 Coulter Counter (Beckman Coulter, Indianapolis, IN, USA). Dry weight (DW) was determined from a calibration curve of DW (mg/L) versus cell counts (cells/mL) of serially diluted *H. akashiwo* harvested during exponential growth. Specifically, triplicate samples of each dilution were filtered onto pre-combusted and pre-weighed GF/F glass fiber filters (Whatman/GE Lifesciences, Pittsburgh, PA, USA) and washed with 0.5 M ammonium bicarbonate to remove salts. Samples were dried at 90°C to constant weight to obtain DW. Cell concentrations (cells/mL) obtained during the experiment were then converted to DW (mg/L) equivalents. Volumetric productivity (mg L⁻¹ day⁻¹) for biomass and biochemical constituents was calculated using the following equation:

$$\text{Productivity} = (N_2 - N_1) \div (t_2 - t_1) \quad (2)$$

where *N*₂ and *N*₁ are biomass or biochemical constituent concentrations (mg L⁻¹) at *t*₂ and *t*₁, respectively.

Carbon Chemistry

Culture samples were collected in glass vials fitted with conical caps, preserved with 5% HgCl₂, and stored at 4°C until analysis. Dissolved inorganic carbon (DIC) was determined by the method of Sharp et al. (2009) using a custom built acid sparging instrument described in Friederich et al. (2002) fitted with a high precision flow control infrared analyzer (LI-COR Biosciences). Partial pressure of CO₂ was calculated from DIC and pH using the CO₂calc application version 1.0.3. Calculations were performed using the GEOSECS (Li et al., 1969) option for acidity constants, the borate acidity constant of Dickson (1990), and the seawater pH scale.

Expression of NR2-2/2HbN

Cultures were filtered on 3- μm polycarbonate membrane filters and immediately submerged in Buffer RLT (Qiagen, Germantown, MD, USA) for gene expression analysis. Total RNA was extracted using the RNEasy Plant Mini Kit (Qiagen) and resuspended in RNase-free water. The purity of total RNA was analyzed spectroscopically (Nanodrop, Thermo Fisher Scientific) and RNA was treated with DNase I (Invitrogen/Life Technologies, Grand Island, NY, USA) as previously described (Coyne and Cary, 2005). Approximately 1 μg of DNase-treated total RNA was reverse transcribed with oligodT primer using the Superscript III First Strand Synthesis System (Invitrogen). Duplicate reactions for each DNase-treated RNA sample without reverse transcriptase were also evaluated by PCR. Transcript abundances for nitrate reductase (NR2-2/2HbN) and glyceraldehyde 3-phosphate dehydrogenase (HaGAP, as a reference gene) were determined by quantitative real time-PCR using the Stratagene MX3005P Sequence Detection System (Agilent Technologies, Santa Clara, CA, USA) as previously described (Stewart and Coyne, 2011).

Total Lipid, Protein, and Carbohydrate Quantification

Culture was centrifuged for 5 min at 4000 RPM using a swinging bucket rotor centrifuge (Thermo Fisher Scientific). Total lipid content was determined using the colorimetric sulfo-phosphovanillin assay for microalgae as described by Cheng et al. (2011) and optimized during this study for *H. akashiwo*. Lipids were extracted from centrifuged algal cells using the method developed by Folch et al. (1957). Briefly, the frozen algal pellet was homogenized with a 2:1 chloroform-methanol mixture then washed with 0.2 volumes of 0.05 M NaCl in deionized water, making a final critical ratio of 2:1:0.8 chloroform-methanol-sodium chloride solution. For the assay, 100 μL of the lower phase containing the pure lipid extract or corn oil standards containing 5–160 μg lipids in chloroform were added directly to a 96-well PCR plate. Methanol was added to each well to obtain a 2:1 chloroform-methanol ratio. The solvent was evaporated by placing the plate in a warm water bath, and then 100 μL of concentrated sulfuric acid was added to each well. The plate was then incubated at 90°C for 20 min and cooled on ice for 2 min. Equal volumes of samples and standards were transferred to a 96-well polypropylene microplate (Costar, Corning Life Sciences, Tewksbury, MA, USA) and background absorbance was measured at 540 nm. Vanillin-phosphoric acid reagent (0.2 mg/mL vanillin in 17% phosphoric acid) was immediately added to obtain a final vanillin concentration of 0.06 mg/mL. After 5 min of color development, the absorbance was measured at 540 nm on an Omega Star Microplate Reader (BMG LABTECH, Ortenburg, Germany) and total lipid content was determined by linear regression using corn oil standards.

Proteins were extracted from the centrifuged algal cells by sonication in 200 mM potassium phosphate buffer. Total protein was measured using the BCA Protein Assay Kit (Pierce, Rockford, IL, USA) according to manufacturer instructions and protein content was determined by linear regression analysis.

Carbohydrate content was determined using the phenol-sulfuric acid colorimetric method described by Dubois et al. (1956). Centrifuged algal cells were re-suspended in deionized

water, and phenol and sulfuric acid were added to give a final concentration of 0.66% and 13.0 M, respectively. Samples were incubated in a room temperature water bath for 30 min, and then transferred to a 96-well plate and the absorbance was measured at 482 nm on an Omega Star Microplate Reader (BMG LABTECH). Carbohydrate content was determined by linear regression using a standard curve of known glucose concentrations (range 0–3 mM).

Particulate Carbon and Nitrogen Analysis

Particulate organic carbon and particulate organic nitrogen were quantified using a particulate autoanalyzer (Costech Elemental Analyzer, Costech Analytical Technologies, Valencia, CA, USA) as described by Hutchins et al. (2002). Briefly, 5 mL of culture were filtered onto pre-combusted GF/F Whatman glass-fiber filters, stored at -80°C and dried in an 80°C oven prior to analysis. Phenylalanine and ethylenediaminetetraacetic acid were used as standards.

Photosynthetic Physiology

Cultures were filtered onto GF/A glass fiber filters and chlorophyll *a* (chl *a*) was extracted in 5 mL of 90% acetone for 24 h at -20°C. Chl *a* fluorescence was measured on a Turner 10-AU fluorometer. A 1 mL subsample of culture was held under low light conditions for 20 min and dark adapted for 2 min (Hennige et al., 2013), prior to measuring fluorescence with a Fast Repetition Rate Fluorometer (FRRF; Chelsea Technologies Group, West Molesey, UK). The following photosynthetic parameters were quantified (Cosgrove and Borowitzka, 2011): maximum photochemical efficiency of PSII (F_v/F_m), the functional absorption cross section of PSII (σ), energy transfer between PSII units (p), the time constant for reoxidation of Q_A acceptor in the PSII reaction center (τ), minimum fluorescence (F_o), and maximum (F_m) fluorescence.

FAME Analysis

Fatty acid methyl esters (FAMES) were prepared by acid catalyzed direct transesterification (Ichihara and Fukubayashi, 2010). Briefly, the lyophilized cells were re-suspended in 0.2 mL toluene. Then 1.5 mL methanol and 0.3 mL 8% (w/v) HCl in methanol solution were added to the mixture. This solution was incubated at 45°C overnight. FAMES were subsequently extracted in 1 mL hexane. Tridecanoic acid (C13:0; final concentration of 30.1 μM) was added as an internal standard. Extracted FAMES were stored at -20°C until analysis. FAMES were analyzed by gas chromatography on a Hewlett Packard HP 5890 Series equipped with a flame ionization detector and a Zebron ZB-Wax column (60 m \times 0.32 mm \times 0.25 μm , Phenomenex, Torrance, CA, USA). Supelco 37 component FAME mix (Sigma Aldrich, St. Louis, MO, USA) was used as a standard for fatty acid identification and quantification. FAMES were resolved using splitless injection and heating the column as follows: initial oven temperature 190°C, increased by a 15°C/min to 250°C, and held at 250°C for 25 min.

Estimation of Biodiesel Parameters

The following equations were used to estimate saponification number (SN, Eq. 3), iodine number (IN, Eq. 4), and cetane

number (CN, Eq. 5) (Lei et al., 2012):

$$SN = \sum (560 \times P_i) \div MW_i \quad (3)$$

$$IN = \sum (254 \times D \times P_i) \div MW_i \quad (4)$$

$$CN = 46.3 + 5458 \div SN - 0.225 \times IN \quad (5)$$

where P_i is the weight percent of each FAME, MW_i is the molecular weight of each FAME, and D is the number of double bonds in each FAME.

Statistical Analysis

Statistical analysis was performed using JMP Pro v11.2 software (SAS, Cary, NC, USA). Prior to comparison of means, data were assessed for normality and equality of variance. Raw data that did not meet assumptions of equal variance (by Levene's test) and/or normality (by the Kolmogorov-Smirnov test) were transformed prior to statistical analysis. Differences were determined to be statistically significant when $P < 0.05$.

For mean comparisons of total carbohydrate, protein and lipid content, lipid profiles, gene expression, seawater chemistry, particulate carbon and nitrogen, and photochemistry between air and simulated flue gas cultures, SDs were calculated from the average of replicates ($n = 4$) and means were compared using the Student's t -test. In cases where transformed data did not meet assumptions of equal variance and normality, the non-parametric Wilcoxon Rank-Sum test was used to compare means.

For mean comparisons of growth rate and maximum cell density between combinations of air, flue gas, $0 \mu\text{M}$ NaNO_3 , and $220 \mu\text{M}$ NaNO_3 , interaction effects were tested using a full factorial two-way ANOVA. There were no significant interaction effects for this dataset, so means were compared using a one-way ANOVA with Tukey HSD *post hoc* analysis.

Results

Carbon Chemistry

pH was significantly lower for flue gas (6.916 ± 0.037) versus air (7.336 ± 0.155) cultures ($P < 0.01$), which increased the proportion of dissolved CO_2 in the total DIC pool from 4.0% to 9.6% (Table 1). Flue gas treatment resulted in a large increase in both DIC and pCO_2 levels in cultures. Maximum pCO_2 levels in cultures treated with a model flue gas (12% CO_2) were 82-fold higher than cultures treated with atmospheric levels of CO_2 .

Expression of NR2-2/2HbN

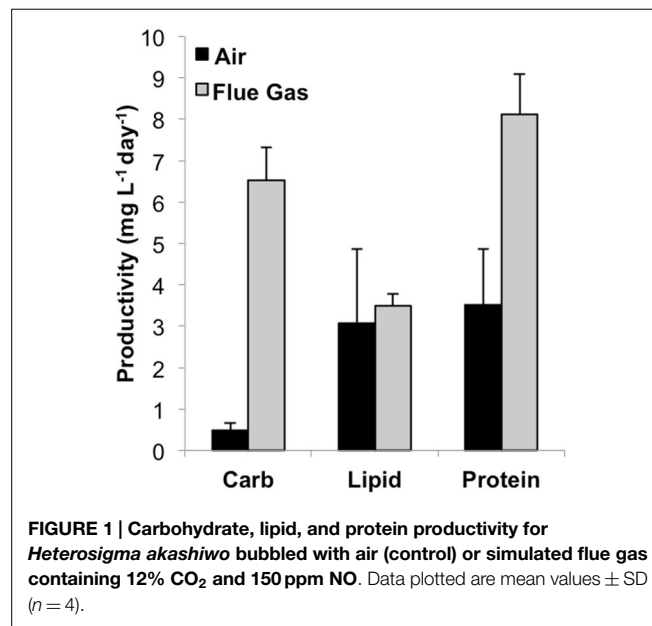
Relative expression of the *NR2-2/2HbN* transcript significantly differed between air grown cultures (1.4 ± 0.8) and flue gas cultures (6.2 ± 1.8), resulting in a 4.4-fold increase in transcript abundance in response to treatment conditions ($P < 0.02$).

Productivity

Total biomass productivity was significantly higher for flue gas cultures [$18.2 (\pm 2.6) \text{mg L}^{-1} \text{day}^{-1}$] versus air cultures [$7.0 (\pm 1.9) \text{mg L}^{-1} \text{day}^{-1}$, $P < 0.001$]. In addition to an increase in growth rate, a significant increase in average cell diameter from

TABLE 1 | Carbon chemistry of *Heterosigma akashiwo* cultures bubbled with air (control) or a simulated flue gas containing 12% CO_2 and 150 ppm NO.

	Air	Flue Gas
DIC (μM)	223 (± 53)	7767 (± 259)
pCO_2 (μatm)	282 (± 112)	23,247 (± 1317)
HCO_3^- ($\mu\text{mol/kg SW}$)	210 (± 49)	6980 (± 276)
CO_3^{2-} ($\mu\text{mol/kg SW}$)	3 (± 1)	38 (± 5)
CO_2 ($\mu\text{mol/kg SW}$)	9 (± 4)	748 (± 42)



$10.5 \mu\text{m}$ in air to $12.0 \mu\text{m}$ in flue gas cultures was also observed ($P < 0.03$). The effect of flue gas on the productivity of biochemical constituents varied (Figure 1). While there was a 13-fold increase in carbohydrate ($P < 0.001$) and a 2-fold increase in protein ($P < 0.001$), both total lipid productivity and cellular lipid composition (pg/cell basis, data not shown) were unaffected. Chlorophyll a content also increased in flue gas cultures compared to controls (1.09 ± 0.05 and 0.92 ± 0.09 pg/cell, respectively, $P < 0.001$). The simultaneous increase in both carbohydrates and proteins was reflected in the maintenance of C:N ratios between air (7.2 ± 0.7) and flue gas (7.8 ± 0.9) cultures.

Photosynthetic Physiology

Dark-adapted photosynthetic measurements are summarized in Table 2. Maximum photochemical efficiency of PSII (F_v/F_m) and the rate of PSII re-oxidation (t) were both significantly lower in flue gas cultures ($P < 0.001$), while the functional absorption cross section (S_{PSII}) did not change in response to flue gas. Both minimum (F_o) and maximum (F_m) raw fluorescence significantly increased in flue gas cultures ($P < 0.001$), which coincided with a significant increase in chl a content as previously noted.

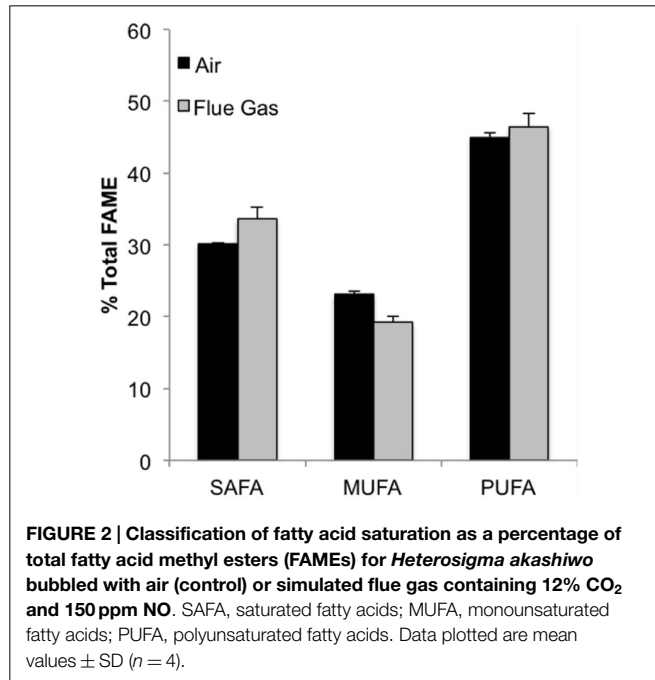
FAME Analysis

The following fatty acids were the predominant constituents in all growth conditions: C18:4, C16:0, C20:5n3, and C16:1. In

TABLE 2 | Maximum photochemical efficiency of PSII (F_v/F_m), functional absorption cross section (S_{PSII}), rate of PSII re-oxidation (t), minimum (F_o) and maximum (F_m) fluorescence measured in the dark for *Heterosigma akashiwo* grown on air (control) or simulated flue gas (treatment).

	Air	Flue Gas
F_v/F_m	0.498 (± 0.009)	0.458 (± 0.002)
S_{PSII} ($\text{\AA}^2 \text{ quantum}^{-1}$)	1.10 (± 0.03)	1.10 (± 0.02)
t (μs)	708 (± 8)	621 (± 20)
F_o (RFU)	6144 (± 1)	11,758 (± 1)
F_m (RFU)	12,250 (± 1)	21,764 (± 1)

Error represents SD ($n = 4$).



response to flue gas, the proportion of saturated fatty acids (SAFA) significantly increased ($P < 0.01$), the proportion of mono-unsaturated fatty acids (MUFA) significantly declined ($P < 0.001$), while the proportion of polyunsaturated fatty acids (PUFA) remained constant (Figure 2). The proportional composition of individual FAMES in the total FAME pool showed that the significant increase in total SAFA was driven by a 1.8-fold increase in C14:0 ($P < 0.001$; Figure 3A). Conversely, the significant decrease in total MUFA was attributable to a decline in C17:1 and C22:1n9 ($P < 0.02$ in both cases). Total PUFA remained constant due to balanced increases and decreases in several individual PUFAs. Notably, the presence of C18:2n6 was only detected at a low concentration in one air (control) replicate, but represented 2.2 (± 0.3)% of total FAMES in response to flue gas. In addition, the proportion of C18:4 also increased in response to flue gas ($P < 0.05$) while both C20:5n3 and C22:2 declined ($P < 0.005$ and $P < 0.04$, respectively).

When FAMES are plotted on a cellular basis, additional patterns emerged (Figure 3B). The predominant fatty acids (C18:4, C16:0, C20:5n3, and C16:1) are all significantly increased on a per cell basis in response to flue gas. There was a 1.83-fold increase in

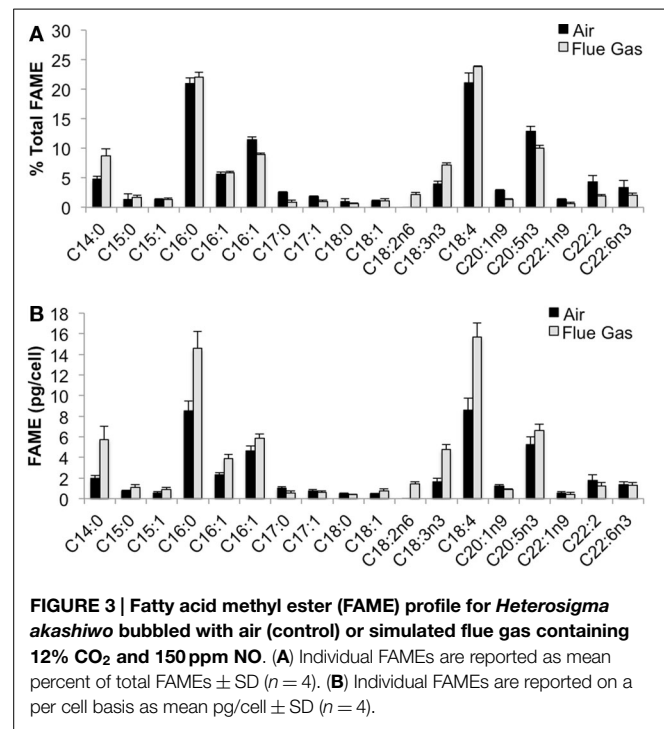


TABLE 3 | Calculated values for estimated biodiesel quality based on FAME profiles for *Heterosigma akashiwo* grown on air (control) or simulated flue gas (treatment).

	Pre-extraction		Post-extraction (70%)		Post-extraction (100%)	
	Air	Flue gas	Air	Flue gas	Air	Flue gas
SN	197 (± 1)	200 (± 1)	178 (± 2)	185 (± 2)	170 (± 2)	179 (± 2)
IN	177 (± 4)	175 (± 5)	133 (± 4)	141 (± 2)	114 (± 5)	126 (± 1)
CN	34 (± 1)	34 (± 1)	47 (± 1)	44 (± 0.2)	53 (± 2)	48 (± 0.1)

SN, saponification number; IN, iodine number; CN, cetane number were calculated for biomass under three scenarios: without EPA/DHA extraction, with 70% extraction recovery of EPA/DHA, and with total recovery of EPA/DHA. Error represents SD ($n = 4$).

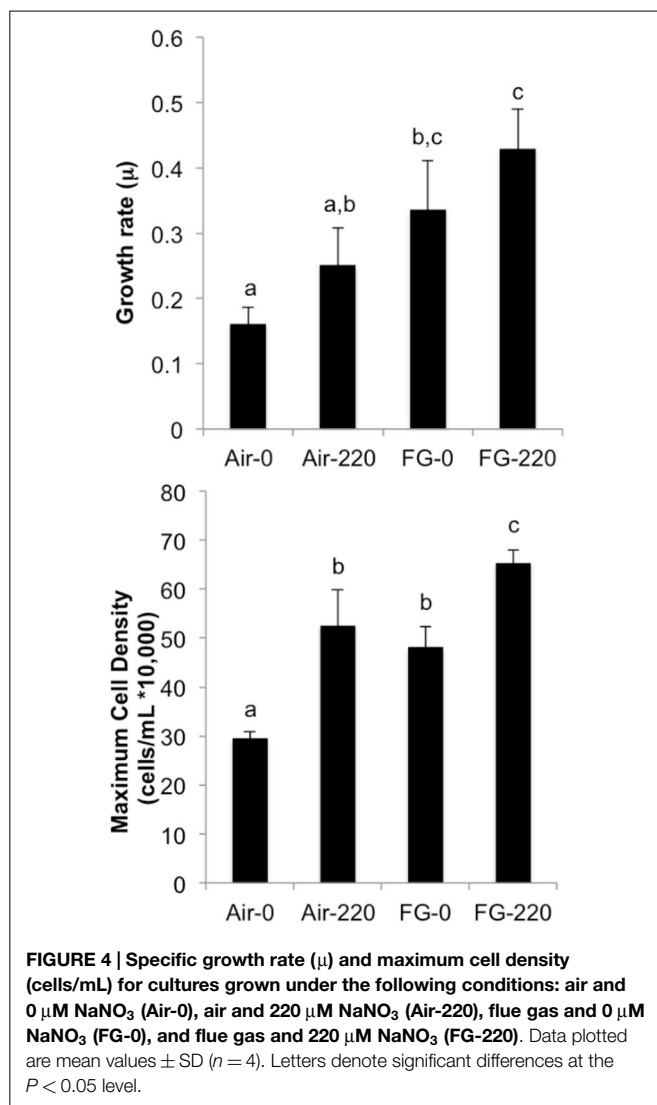
C18:4 ($P < 0.001$), a 1.70-fold increase in C16:0 ($P < 0.002$), a 1.25-fold increase in C20:5n3 ($P < 0.05$), and a total 1.97-fold increase in total isomers of C16:1 ($P < 0.01$).

Estimation of Biodiesel Parameters

Calculated values for estimated biodiesel quality are summarized in Table 3. Both air and flue gas cultures have an estimated cetane number (CN) of 34. Eicosapentaenoic acid (EPA) and docosahexaenoic acid (DHA) are long chain, polyunsaturated fatty acids, and their presence resulted in high estimated saponification number (SN) and iodine number (IN) values, which contributed to a decrease in estimated CN. Therefore, CN was also calculated after extraction of EPA/DHA.

Effect of Nitrate Levels on Growth in Air Versus Simulated Flue Gas

Figure 4 summarizes specific growth rate (μ) and maximum cell density (cells/mL) achieved in cultures grown under the following



conditions: air and 0 μM NaNO_3 (Air-0), air and 220 μM NaNO_3 (Air-220), flue gas and 0 μM NaNO_3 (FG-0), and flue gas and 220 μM NaNO_3 (FG-220). There was not a significant interaction effect of gas type and nitrate concentration on growth rate or maximum cell density. FG-0 grew at the same rate as both Air-220 and FG-220 cultures. All cultures grew faster than Air-0, which was observed to be the only treatment to form resting cysts during stationary phase. FG-220 achieved the highest maximum cell density, while maximum cell densities for FG-0 and Air-220 were not significantly different.

Discussion

Growth on a simulated flue gas with relevant NO_x levels more than doubled the biomass productivity of *H. akashiwo*. Flue gas treatment drastically increased the amount of bioavailable carbon in the media (Table 1), and the accumulation of large amounts of storage carbohydrates suggests that *Heterosigma* is effective at fixing this excess CO_2 . Maintenance of the C:N ratio along with

an increase in protein content suggests that CO_2 assimilation in flue gas cultures was not limited by nitrogen availability. Photochemical measurements also indicated that photosynthesis in *Heterosigma* is not inhibited by high CO_2 and NO concentrations (Table 2). For example, the rate of PSII re-oxidation (t) was 87 μs faster, suggesting that photosynthetic electron transport was enhanced during growth on flue gas and that cells maintained overall photosynthetic efficiency despite an observed decline in dark-acclimated F_v/F_m . Growth rates and maximum cell densities of *Heterosigma* grown on simulated flue gas without supplemental nitrogen (FG-0) demonstrated that nitrogen derived from NO gas is biologically available to support enhanced CO_2 fixation (Figure 4). In addition, the increase in *NR2-2/HbN* transcript abundance observed here supports the hypothesis that this chimeric enzyme is involved in maintaining cell growth in the presence of NO (Stewart and Coyne, 2011). Collectively, these results support the hypothesis that *Heterosigma* is an ideal candidate for the commercial production of algal biomass using industrial emissions containing high levels of CO_2 and NO .

Heterosigma biomass was subsequently analyzed for its potential to become a biofuel feedstock. In the conventional algae to biofuel pathway, algal lipids are extracted and upgraded to biodiesel (Davis et al., 2012). The residual biomass, which accounts for 50–75% of the total biomass, is then processed into non-fuel products, such as animal feeds and high value chemicals, or is subjected to anaerobic digestion (Davis et al., 2012). In the present study, growth on simulated flue gas did not reduce total lipid yields, so changes in lipid profiles were investigated to assess the potential for converting this lipid fraction to quality biodiesel. The American Society for Testing and Materials standards specify that the CN must be a minimum of 47 for B100 biodiesel and a minimum of 40 for blended B6 to B20 biodiesels (ASTM International, 2014). CNs based on total lipid composition for both air and flue gas cultures were well below this standard unless at least 70% of EPA/DHA was theoretically extracted prior to the transesterification of lipids (Table 3). The omega-3 fatty acids, eicosapentaenoic acid (EPA, C20:5n3) and docosahexaenoic acid (DHA, C22:6n3), are potential value-added products from this species with an estimated bulk wholesale value of \$12,540/kg for >70% pure oil (J Edwards International, Inc., personal communication). In this study, EPA and DHA constituted approximately 12–16% of total FAMES. Since the removal of these polyunsaturated fatty acids from the lipid mixture before conversion to biodiesel also enhances the quality of the resulting fuel, purification of these lipids prior to further processing could be economically feasible (Molina Grima et al., 2003; Chauton et al., 2014).

Interestingly, the predominant fatty acids profiled here (C18:4, C16:0, C20:5n3, and C16:1) are the main fatty acyl substituents of the thylakoid sulfolipid, sulfoquinovosyl diacylglycerol (SQDG), which is produced at high levels in *Heterosigma* (Keusgen et al., 1997). Enhanced synthesis of these fatty acids in the presence of high CO_2 and NO (Figure 3) likely functioned to support an increase in thylakoid number or surface area as suggested by a significant 17% increase in chlorophyll content (Benning, 1998; Minoda et al., 2002). This subsequently explains the increase in C14:0, which is linked to the fatty acid synthase enzyme prior to the two carbon elongation cycle that produces C16:0,

where C16:0 is then released from fatty acid synthase as the precursor to long chain saturated and unsaturated fatty acid synthesis. Here, it appears that changes in individual fatty acid content on a cellular basis were driven by photosynthetic requirements.

In this study, lipid production did not benefit from growth on flue gas, whereas carbohydrate and protein output was significantly enhanced. A recent advancement in algal biomass processing provides an alternative to focusing solely on lipids as the primary feedstock for biofuel production. Whole algae hydrothermal liquefaction can produce fuels using the entire biomass in lieu of separating its biochemical components and has been characterized as a technically and economically feasible processing scheme (Biddy et al., 2013). Under this scheme, the primary goal is to maximize overall biomass productivity, with increases in growth rates and/or increases in the storage of any cellular product contributing to the target outcome. With hydrothermal liquefaction, the large increase in carbohydrates and protein in response to flue gas observed in the present study (Figure 1) is advantageous for increasing total biofuel yields. In contrast to green algae, *Heterosigma* stores photosynthetic energy not only in the form of lipids, but also as water-soluble carbohydrates stored within vacuoles (Chiovitti et al., 2006),

and the dramatic increase in carbohydrates seen here indicates that *Heterosigma* is metabolically suited to fix large amounts of anthropogenic CO₂ into valuable biomass. Together, these results illustrate the robustness of this alga and support continued efforts to assess the viability of this species for commercial-scale biomass production and bioremediation of industrial emissions.

Acknowledgments

This work was supported by the United States Department of Agriculture (USDA-NIFA-2011-67012-31175 to JS), the National Oceanic and Atmospheric Administration through Delaware Sea Grant (Award #NA10OAR4170084-12 to JS and KC and Award #NA14OAR4170087 to JS and KC), and the National Science Foundation (Award #1314003 to JS). We would like to acknowledge Catherine Fitzgerald at Salisbury University for her assistance in developing the GC protocol for the resolution of long chain FAMES. We would also like to thank Mark Warner (University of Delaware) and Joséé Nina Bouchard (Algenol, Fort Myers, FL, USA) for technical support.

References

- ASTM International. (2014). *Standard Specification for Biodiesel Fuel Blend Stock (B100) for Middle Distillate Fuels: Designation D6751-14*. West Conshohocken, PA: ASTM International.
- Basu, S., Roy, A. S., Mohanty, K., and Ghoshal, A. K. (2013). Enhanced CO₂ sequestration by a novel microalga: *Scenedesmus obliquus* SA1 isolated from bio-diversity hotspot region of Assam, India. *Bioresour. Technol.* 143, 369–377. doi:10.1016/j.biortech.2013.06.010
- Benemann, J. (2013). Microalgae for biofuels and animal feeds. *Energies* 6, 5869–5886. doi:10.3390/en6115869
- Benning, C. (1998). Biosynthesis and function of the sulfolipid sulfoquinovosyl diacylglycerol. *Annu. Rev. Plant Physiol. Plant Mol. Biol.* 49, 53–75. doi:10.1146/annurev.arplant.49.1.53
- Biddy, D., Jones, R., Zhu, S., Bilal, K.; Pacific Northwest National Laboratory, and National Renewable Energy Laboratory. (2013). *Whole Algae Hydrothermal Liquefaction Technology Pathway: Technical Report NREL/TP-5100-58051*. Washington, DC: U.S. Department of Energy.
- Borkenstein, C. G., Knokelechner, J., Frühwirth, H., and Schagerl, M. (2011). Cultivation of *Chlorella emersonii* with flue gas derived from a cement plant. *J. Appl. Phycol.* 23, 131–135. doi:10.1007/s10811-010-9551-5
- Chauton, M. S., Reitan, K. I., Norsker, N. H., Tveterås, R., and Kleivdal, H. T. (2014). A techno-economic analysis of industrial production of marine microalgae as a source of EPA and DHA-rich raw material for aquafeed: research challenges and possibilities. *Aquaculture* 436, 95–103. doi:10.1016/j.aquaculture.2014.10.038
- Chen, H. W., Yang, T. S., Chen, M. J., Chang, Y. C., Lin, C. Y., Wang, E. I., et al. (2012). Application of power plant flue gas in a photobioreactor to grow *Spirulina* algae, and a bioactivity analysis of the algal water-soluble polysaccharides. *Bioresour. Technol.* 120, 256–263. doi:10.1016/j.biortech.2012.04.106
- Cheng, Y., Zheng, Y., and VanderGheynst, J. S. (2011). Rapid quantitative analysis of lipids using a colorimetric method in a microplate format. *Lipids* 46, 95–103. doi:10.1007/s11745-010-3494-0
- Chiovitti, A., Ngoh, J. E., and Wetherbee, R. (2006). 1, 3-β-d-glucans from *Harmomonas dimorpha* (Raphidophyceae). *Botanica Marina* 49, 360–362. doi:10.1515/BOT.2006.045
- Chiu, S. Y., Kao, C. Y., Huang, T. T., Lin, C. J., Ong, S. C., Chen, C. D., et al. (2011). Microalgal biomass production and on-site bioremediation of carbon dioxide, nitrogen oxide and sulfur dioxide from flue gas using *Chlorella* sp. cultures. *Bioresour. Technol.* 102, 9135–9142. doi:10.1016/j.biortech.2011.06.091
- Cosgrove, J., and Borowitzka, M. A. (2011). “Chlorophyll fluorescence terminology: an introduction,” in *Chlorophyll a Fluorescence in Aquatic Sciences: Methods and Applications*, eds D. J. Suggett, O. Prasil, and M. A. Borowitzka (New York, NY: Springer), 1–18.
- Coyne, K. J., and Cary, S. C. (2005). Molecular approaches to the investigation of viable dinoflagellate cysts in natural sediments from estuarine environments. *J. Euk. Microbiol.* 52, 90–94. doi:10.1111/j.1550-7408.2005.05202001.x
- Davis, R., Fishman, D., Frank, E. D., Wigmosta, M. S., et al. (2012). *Renewable Diesel from Algal Lipids: An Integrated Baseline for Cost, Emissions, and Resource Potential from a Harmonized Model*. NREL/TP-5100-55431. Washington, DC: U.S. Department of Energy.
- Dickson, A. G. (1990). Standard potential of the reaction – AGCL(S)+1/2H₂(G)=AG(S)+HCL(AQ) and the standard acidity constant of the ion HSO₄– in synthetic sea-water from 273.15-k to 318.15-k. *J. Chem. Thermodyn.* 22, 113–127. doi:10.1016/0021-9614(90)90074-Z
- Doucha, J., Straka, F., and Lívanský, K. (2005). Utilization of flue gas for cultivation of microalgae *Chlorella* sp. in an outdoor open thin-layer photobioreactor. *J. Appl. Phycol.* 17, 403–412. doi:10.1007/s10811-005-8701-7
- Douskova, I., Doucha, J., Livansky, K., Machat, J., Novak, P., Umysova, D., et al. (2009). Simultaneous flue gas bioremediation and reduction of microalgal biomass production costs. *Appl. Microbiol. Biotechnol.* 82, 179–185. doi:10.1007/s00253-008-1811-9
- Dubois, M., Gilles, K., Hamilton, J., Rebers, P., and Smith, F. (1956). Colorimetric method for determination of sugars and related substances. *Anal. Chem.* 28, 350–356. doi:10.1021/ac60111a017
- EPA. (2012). *Overview of Greenhouse Gases: Carbon Dioxide Emissions*. Available at: <http://www.epa.gov/climatechange/ghgemissions/gases/co2.html>
- EPA. (2014). *Ground Level Ozone: Basic Information*. Available at: <http://www.epa.gov/climatechange/ghgemissions/gases/co2.html>
- Folch, J., Lees, M., Stanley, G. H. S., Han, J. I., and Park, J. K. (1957). A simple method for the isolation and purification of total lipids from animal tissues. *J. Biol. Chem.* 226, 497–509.
- Friederich, G. E., Walz, P. M., Burczynski, M. G., and Chavez, F. P. (2002). Inorganic carbon in the central California upwelling system during the 1997 – 1999 el niño – la niña event. *Prog. Oceanogr.* 54, 185–203. doi:10.1016/S0079-6611(02)00049-6
- Fuentes-Grünwald, C., Garcés, E., Alacid, E., Rossi, S., and Camp, J. (2013). Biomass and lipid production of dinoflagellates and raphidophytes in indoor and outdoor photobioreactors. *Mar. Biotechnol.* 15, 37–47. doi:10.1007/s10126-012-9450-7

- Fuentes-Grünewald, C., Garcés, E., Alacid, E., Sampedro, N., Rossi, S., and Camp, J. (2012). Improvement of lipid production in the marine strains *Alexandrium minutum* and *Heterosigma akashiwo* by utilizing abiotic parameters. *J. Ind. Microbiol. Biotechnol.* 39, 207–216. doi:10.1007/s10295-011-1016-6
- Fuentes-Grünewald, C., Garcés, E., Rossi, S., and Camp, J. (2009). Use of the dinoflagellate *Karlodinium veneficum* as a sustainable source of biodiesel production. *J. Ind. Microbiol. Biotechnol.* 36, 1215–1224. doi:10.1007/s10295-009-0602-3
- Guillard, R. R. L. (1975). "Culture of phytoplankton for feeding marine invertebrates," in *Culture of Marine Invertebrate Animals*, eds W. L. Smith and M. H. Chanley (New York, NY: Plenum Press), 26–60.
- Hara, Y., and Chihara, C. (1987). Morphology, ultrastructure and taxonomy of the raphidophycean alga, *Heterosigma akashiwo*. *Bot. Mag.* 100, 151–163. doi:10.1007/BF02488320
- Harter, T., Bossier, P., Verreth, J. A. J., Bode, S., van der Ha, D., Deebber, A. E., et al. (2013). Carbon and nitrogen mass balance during flue gas treatment with *Dunaliella salina* cultures. *J. Appl. Phycol.* 25, 359–368. doi:10.1007/s10811-012-9870-9
- Hennige, S. J., Coyne, K. J., Macintyre, H., Liefer, J., and Warner, M. E. (2013). The photobiology of *Heterosigma akashiwo*: photoacclimation, diurnal periodicity, and its ability to rapidly exploit exposure to high light. *J. Phycol.* 49, 349–360. doi:10.1111/jpy.12043
- Hutchins, D. A., Hare, C. E., Weaver, R. S., Zhang, Y., Firme, G. F., DiTullio, G. R., et al. (2002). Phytoplankton iron limitation in the Humboldt current and Peru upwelling. *Limnol. Oceanogr.* 47, 997–1011. doi:10.4319/lo.2002.47.4.0997
- Ichihara, K., and Fukubayashi, Y. (2010). Preparation of fatty acid methyl esters for gas-liquid chromatography. *J. Lipid Res.* 51, 635–640. doi:10.1194/jlr.D001065
- Jiang, Y., Zhang, W., Wang, J., Chen, Y., Shen, S., and Liu, T. (2013). Utilization of simulated flue gas for cultivation of *Scenedesmus dimorphus*. *Bioresour. Technol.* 128, 359–364. doi:10.1016/j.biortech.2012.10.119
- Jin, H. F., Santiago, D. E. O., Park, J., and Lee, K. (2008). Enhancement of nitric oxide solubility using Fe(II)EDTA and its removal by green algae *Scenedesmus* sp. *Biotechnol. Bioprocess Eng.* 13, 48–52. doi:10.1007/s12257-007-0164-z
- Keusgen, M., Curtis, J. M., Thibault, P., Walter, J. A., Windust, A., and Ayer, S. W. (1997). Sulfoquinovosyl diacylglycerols from the alga *Heterosigma carterae*. *Lipids* 32, 1101–1112. doi:10.1007/s11745-997-0142-9
- Lara-Gil, J. A., Álvarez, M. M., and Pacheco, A. (2014). Toxicity of flue gas components from cement plants in microalgae CO₂ mitigation systems. *J. Appl. Phycol.* 26, 357–368. doi:10.1007/s10811-013-0136-y
- Lei, A., Chen, H., Shen, G., Hu, Z., Chen, L., and Wang, J. (2012). Expression of fatty acid synthesis genes and fatty acid accumulation in *Haematococcus pluvialis* under different stressors. *Biotechnol. Biofuels* 5, 1–11. doi:10.1186/1754-6834-5-18
- Li, Y. H., Takahashi, T., and Broecker, W. S. (1969). Degree of saturation of CaCO₃ in oceans. *J. Geophys. Res.* 74, 5507. doi:10.1371/journal.pone.0016069
- Martínez, R., Orive, E., Laza-Martínez, A., and Seoane, S. (2010). Growth response of six strains of *Heterosigma akashiwo* to varying temperature, salinity and irradiance conditions. *J. Plankton Res.* 32, 529–538. doi:10.1093/plankt/fbp135
- Minoda, A., Sato, N., Nozaki, H., Okada, K., Takahashi, H., Sonoike, K., et al. (2002). Role of sulfoquinovosyl diacylglycerol for the maintenance of photosystem II in *Chlamydomonas reinhardtii*. *Eur. J. Biochem.* 269, 2353–2358. doi:10.1046/j.1432-1033.2002.02896.x
- Molina Grima, E., Belarbi, E. H., Acién Fernández, F. G., Robles Medina, A., and Chisti, Y. (2003). Recovery of microalgal biomass and metabolites: process options and economics. *Biotechnol. Adv.* 20, 491–515. doi:10.1016/S0734-9750(02)00050-2
- Nagarajan, S., Chou, S. K., Cao, S., Wu, C., and Zhou, Z. (2013). An updated comprehensive techno-economic analysis of algae biodiesel. *Bioresour. Technol.* 145, 150–156. doi:10.1016/j.biortech.2012.11.108
- Santiago, D. E. O., Jin, H. F., and Lee, K. (2010). The influence of ferrous-complexed EDTA as a solubilization agent and its auto-regeneration on the removal of nitric oxide gas through the culture of green alga *Scenedesmus* sp. *Process Biochem.* 45, 1949–1953. doi:10.1016/j.procbio.2010.04.003
- Sharp, J. H., Yoshiyama, K., Parker, A. E., Schwartz, M. C., Curless, S. E., Beauregard, A. Y., et al. (2009). A biogeochemical view of estuarine eutrophication: seasonal and spatial trends and correlations in the Delaware estuary. *Estuaries Coast.* 32, 1023–1043. doi:10.1007/s12237-009-9210-8
- Stewart, J. J., and Coyne, K. J. (2011). Analysis of raphidophyte assimilatory nitrate reductase reveals unique domain architecture incorporating a 2/2 hemoglobin. *Plant Mol. Biol.* 77, 565–575. doi:10.1007/s11103-011-9831-8
- Wilson, M. H., Groppo, J., Placido, A., Graham, S., Morton, S. A. III, Santillan-Jimenez, E., et al. (2014). CO₂ recycling using microalgae for the production of fuels. *Appl. Petrochem. Res.* 4, 41–53. doi:10.1007/s00253-012-4362-z
- Zhang, Y., Fu, F.-X., Whereat, E., Coyne, K. J., and Hutchins, D. A. (2006). Bottom-up controls on a mixed-species HAB assemblage: a comparison of sympatric *Chattonella subsalsa* and *Heterosigma akashiwo* (Raphidophyceae) isolates from the Delaware Inland Bays, USA. *Harmful Algae* 5, 310–320. doi:10.1016/j.hal.2005.09.001

Conflict of Interest Statement: Jennifer J. Stewart and Kathryn J. Coyne. (2013). Novel Nitrate Reductase Fusion Proteins and Uses Thereof. U.S. Patent No. 8,409,827. Washington, DC: U. S. Patent and Trademark Office. The other co-authors declare that the research was conducted in the absence of any commercial or financial relationships that could be construed as a potential conflict of interest.

Copyright © 2015 Stewart, Bianco, Miller and Coyne. This is an open-access article distributed under the terms of the Creative Commons Attribution License (CC BY). The use, distribution or reproduction in other forums is permitted, provided the original author(s) or licensor are credited and that the original publication in this journal is cited, in accordance with accepted academic practice. No use, distribution or reproduction is permitted which does not comply with these terms.

Evaluation of diverse microalgal species as potential biofuel feedstocks grown using municipal wastewater

Sage R. Hiibel^{1,2}, Mark S. Lemos¹, Brian P. Kelly¹ and John C. Cushman^{1*}

¹ Department of Biochemistry and Molecular Biology, University of Nevada Reno, Reno, NV, USA, ² Department of Civil and Environmental Engineering, University of Nevada Reno, Reno, NV, USA

OPEN ACCESS

Edited by:

Umakanta Jena,
Desert Research Institute, USA

Reviewed by:

Arumugam Muthu,
Council of Scientific and Industrial
Research, India
Probir Das,
Qatar University, Qatar
Sivasubramanian Velusamy,
Phycospectrum Environmental
Research Centre, India

*Correspondence:

John C. Cushman,
Department of Biochemistry and
Molecular Biology, University of
Nevada Reno, MS 330, 1664 N.
Virginia Street, Reno, NV
89557-0330, USA
jcushman@unr.edu

Specialty section:

This article was submitted to
Bioenergy and Biofuels, a section of
the journal *Frontiers in Energy
Research*

Received: 16 February 2015

Accepted: 17 April 2015

Published: 11 May 2015

Citation:

Hiibel SR, Lemos MS, Kelly BP and
Cushman JC (2015) Evaluation of
diverse microalgal species as
potential biofuel feedstocks grown
using municipal wastewater.
Front. Energy Res. 3:20.
doi: 10.3389/fenrg.2015.00020

Microalgae offer great potential as a third-generation biofuel feedstock, especially when grown on wastewater, as they have the dual application for wastewater treatment and as a biomass feedstock for biofuel production. The potential for growth on wastewater centrate was evaluated for forty microalgae strains from fresh (11), brackish (11), or saltwater (18) genera. Generally, freshwater strains were able to grow at high concentrations of centrate, with two strains, *Neochloris pseudostigmata* and *Neochloris conjuncta*, demonstrating growth at up to 40% v/v centrate. Fourteen of 18 salt water *Dunaliella* strains also demonstrated growth in centrate concentrations at or above 40% v/v. Lipid profiles of freshwater strains with high-centrate tolerance were determined using gas chromatography–mass spectrometry and compared against those obtained on cells grown on defined maintenance media. The major lipid compounds were found to be palmitic (16:0), oleic (18:1), and linoleic (18:2) acids for all freshwater strains grown on either centrate or their respective maintenance medium. These results demonstrate the highly concentrated wastewater can be used to grow microalgae, which limits the need to dilute wastewater prior to algal production. In addition, the algae produced generate lipids suitable for biodiesel or green diesel production.

Keywords: microalgae, fresh water, brackish water, salt water, biofuel, municipal wastewater, centrate

Introduction

The world's demand for petroleum fuels continues to grow even as supplies dwindle. In recent years, there has been a strong push to develop alternative energy sources to help supplement or potentially replace fossil fuels. Wind turbines and photovoltaic technologies offer renewable sources of electric power; however, liquid fuels for the transportation sector make up more than 70% of the energy consumed in US (Forsberg, 2009). Biofuels have great potential to help fill this need, and there has been significant research in this area. First- and second-generation liquid biofuels, such as corn ethanol and soy biodiesel, have received considerable interest and resources in the last 20 years, and are considered technically mature. Third-generation biofuels, such as lignocellulosics and microalgae, although not as technologically advanced, hold great promise as sustainable biofuels because they avoid the food *versus* fuel debate that has plagued corn and soy-based biofuels. As part of the Renewable Fuel Standard II, the US government has tapped the third-generation biofuels for 21×10^9 barrels/year of fuel by 2022, with 4×10^9 barrels/year of that coming from non-cellulosic

and non-corn-based biodiesel fuels, such as those derived from microalgae (Schnepf and Yacobucci, 2010).

As with many third-generation fuels, microalgae have great potential as a biofuel feedstock source. They are among the most rapidly growing photosynthetic organisms on the planet (Chisti, 2007), and they can be cultured year-round in even cold climates if growth is coupled to a low-cost heat source (i.e., waste or low-grade geothermal). Large-scale production of algae biomass has been demonstrated, but several technical hurdles remain that must be addressed before microalgae can become a viable biofuel feedstock. Currently, biomass harvesting and oil extraction are key processing steps that are energy intensive and cost prohibitive. From the algal growth perspective, a sustainable water source and nutrient supply are paramount to economic microalgae production. Regardless of the strain used (salt or fresh water), a non-saline water supply will be required to make up for evaporative loss in an open-pond cultivation system. Lastly, off-setting part or all of the nutrient supply required to grow microalgae with non-petroleum-derived fertilizer such as municipal wastewater can help improve the carbon budget of microalgal-based biofuel production systems (Chisti, 2007; Wang et al., 2010; Bhatt et al., 2014; Dong et al., 2014; Mu et al., 2014).

Wastewater offers the possibility of serving as both a freshwater and a nutrient source, with most municipalities having a continuous supply. Ideally, the wastewater could be used in its raw state or with minimal treatment so as to reduce the costs of the wastewater treatment plant (WWTP) (Pittman et al., 2011; Bhatt et al., 2014; Mu et al., 2014). Centrate, the liquid fraction after anaerobic digestion, offers a feed stream high in nitrogen and phosphorous, which are two of the main nutrients required for microalgae and also two compounds that cause high removal costs for most municipal WWTPs (Wang et al., 2010; Li et al., 2011a; Bhatt et al., 2014; Dong et al., 2014; Mu et al., 2014). In addition to decreasing the nutrient load to the plant, diverting centrate to algae production also decreases the treatment volume, thereby decreasing treatment costs of other chemical constituents (Li et al., 2011a; Mu et al., 2014). Metal content of wastewaters or centrate are unlikely to inhibit microalgal growth (Wang et al., 2010; Dong et al., 2014).

In this work, centrate was used as a water and nutrient source for the growth of green algae as a biofuel feedstock. A total of 40 microalgae strains comprised of isolates from freshwater, brackish water, and saltwater strains were evaluated for tolerance to and growth in centrate. The growth characteristics, biomass and lipid yields, and lipid profiles were determined for the two most tolerant freshwater strains, *Neochloris conjuncta* and *Neochloris pseudostigmata*, to evaluate the potential of utilizing municipal wastewater centrate to grow microalgae as a biofuel feedstock.

Materials and Methods

Strains and Media

Eleven freshwater *Neochloris* strains, 11 brackish water *Nannochloropsis* strains, and 18 saltwater *Dunaliella* strains were evaluated for their ability to grow on municipal wastewater centrate (Table 1). The cultures were obtained from the Culture Collection of Algae at The University of Texas at Austin (UTEX),

the Culture Collection of Algae and Protozoa (CCAP), the Canadian Phycological Culture Centre [PCCC; formerly known as the University of Toronto Culture Collection of Algae and Cyanobacteria (UTCC)], or the Culture Collection of Algae at the University of Göttingen, Germany (SAG). All cultures were grown at room temperature under an 18/6 h light/dark cycle on their respective maintenance media. The freshwater *Neochloris* strains were maintained on Bold's modified Bristol medium (Bold, 1949): 2.94 mM NaNO₃, 0.17 mM CaCl₂ (2H₂O), 0.3 mM MgSO₄ (7H₂O), 0.43 mM K₂HPO₄, 1.29 mM KH₂PO₄, and 0.43 mM NaCl at pH = 7.7. Saltwater *Dunaliella* strains were maintained on a modified 2ASW (artificial seawater) medium (Gomord et al., 2010); 33.6 g/L of sea salts were used in place of the NaCl. The brackish water *Nannochloropsis* strains were maintained on slightly modified f/2 Medium of Guillard and Ryther (1962) in which the vitamin solution from the 2ASW medium (Gomord et al., 2010), which contained additional vitamin components, was used in place of that described for the original f/2 medium.

Centrate Characteristics

Centrate was collected from the Truckee Meadows Water Authority Reclamation Facility, the local municipal WWTP facility located in Sparks, Nevada. Centrate was filtered through Miracloth (typical pore size 22–25 μm, EMD Millipore), then autoclaved and stored at 4°C until use (<3 days). Average nitrogen, phosphorus, and potassium content of centrate from this facility have been previously reported as 1003.0 ± 174.6 mg/L NH₄-N, 244.5 ± 34.5 mg/L *ortho*-P, and 202 ± 54 mg/L K⁺, respectively (Herrera, 2009). The raw centrate had an average pH = 7.8 and contained 1.284 mg/L TDS and 726.2 mg/L bicarbonate, and the major ions by concentration were sodium (77.0 ± 36.5 mg/L) and chloride (189.2 ± 132.4 mg/L). A detailed characterization of the centrate can be found in Herrera (2009).

Preliminary Screening

All strains were screened initially for their tolerance to grow on centrate using a 96-well titer plate format. Plates were loaded with 200 μL of medium and 25 μL of inoculum culture per well and then incubated at 22°C and a 18/6 h light/dark cycle under 100 μmol/m² s on an orbital shaking table rotating at 100 rpm. For the *Neochloris* and *Nannochloropsis* strains, the medium consisted of centrate diluted with nanopure water to 0, 2, 4, 6, 8, 10, 12, 14, 15, 20, 25, 30, 40, 50, 60, 70, 80, 90, and 100% v/v. The *Dunaliella* strains were screened with the same centrate concentrations, but dilutions were made with a 33.6 g/L sea-salt solution, as no growth was observed without the addition of sea salts (data not shown). The appropriate maintenance media and sterile water were used as positive and negative growth medium controls, respectively. Each culture was inoculated in duplicate on two plates (four total replicates) to allow for statistical testing power. The 96-well titer plates were monitored visually to monitor growth (Figure S1 in Supplementary Material).

Microalgae Growth

The two freshwater strains with the highest centrate tolerance, *N. pseudostigmata* (UTEX 1249) and *N. conjuncta* (CCAP 254/1),

TABLE 1 | The 40 strains evaluated, their original culture collection source, and the maximum centrate concentration at which growth was observed for each strain in preliminary plate screening tests.

	Species	Source	Max % v/v	Origin and source ^a
Freshwater <i>Neochloris</i>	<i>N. aquatica</i>	UTEX 138	14	Bloomington, IN (USA); aquarium
	<i>N. minuta</i>	UTEX 776	14	Santa Marta (Cuba); sugar cane field soil
	<i>N. pyrenoidosa</i>	UTEX 777	12	Jovallanos (Cuba); sugar cane field soil
	<i>N. oleoabundans</i>	UTEX 1185	12	Rub al Kali (Saudi Arabia); sand dune
	<i>N. pseudostigmata</i>	UTEX 1249	40	Enchanted Rock, TX (USA); soil
	<i>N. cohaerens</i>	UTEX 1707	0	Bastrop State Park, TX (USA); soil
	<i>N. vigensis</i>	UTEX 1981	20	Travis County, TX (USA); pond
	<i>N. fusispora</i> ^b	UTEX b778	10	Ranchuelo (Cuba); sugar cane field soil (Arce and Bold, 1958)
	<i>N. terrestris</i> ^c	UTEX b947	14	Daniel Town (Jamaica); corn field soil
	<i>N. wimmeri</i> ^d	CCAP 213/4	0	Czechoslovakia; freshwater
	<i>N. conjuncta</i>	CCAP 254/1	40	Travis County, TX (USA); freshwater
Brackish <i>Nannochloropsis</i>	<i>N. sp.</i>	CCAP 211/78	14	Unknown; marine
	<i>N. sp.</i>	CCAP 849/8	14	Qingdao (China); marine
	<i>N. sp.</i>	CCAP 849/9	14	Japan; marine
	<i>N. gaditana</i>	CCAP 849/5	14	Cadiz Bay (Spain); marine
	<i>N. oceanica</i>	CCAP 849/10	14	Western Norway; marine fish hatchery (Bligh and Dyer, 1959)
	<i>N. oculata</i>	CCAP 849/1	0	Skate Point, Isle of Cumbrae (Scotland); marine
	<i>N. oculata</i>	CCAP 849/7	0	Lake of Tunis (Tunisia); marine
	<i>N. salina</i>	CCAP 849/2	4	Skate Point, Isle of Cumbrae (Scotland); marine
	<i>N. salina</i>	CCAP 849/3	12	Skate Point, Isle of Cumbrae (Scotland); marine
	<i>N. salina</i>	CCAP 849/4	12	Skate Point, Isle of Cumbrae (Scotland); marine
	<i>N. salina</i> ^e	CCAP 849/6	12	Great South Bay, Long Island, NY (USA); marine
Saltwater <i>Dunaliella</i>	<i>D. bardawil</i>	UTEX LB 2538	50	Bardawil Lagoon, North Sinai (Israel); salt pond
	<i>D. bioculata</i>	UTEX LB 199	50	(Russia); salt lake
	<i>D. salina</i>	UTEX LB 200	50	(Russia); dirty salt lake
	<i>D. tertiolecta</i>	UTEX LB 999	50	Oslo Fjord (Norway); brackish
	<i>D. salina</i>	UTEX LB 1644	30	Baja, CA (USA); marine
	<i>D. primolecta</i>	UTEX LB 1000	40	Plymouth, Devon (England); marine
	<i>D. peircei</i>	UTEX LB 2192	50	Lake Marina, CA (USA); brackish
	<i>D. salina</i>	UTCC 197	0	Unknown
	<i>D. tertiolecta</i>	UTCC 420	50	Unknown; marine
	<i>D. sp.</i>	UTCC 457	40	Sarnia, Ontario (Canada); surface brine storage pond
	<i>D. salina</i>	CCAP 19/18	50	Hutt Lagoon (Western Australia); hypersaline brine
	<i>D. tertiolecta</i>	CCAP 19/6B	50	Oslo Fjord (Norway); brackish
	<i>D. tertiolecta</i>	CCAP 19/24	50	Unknown; possibly marine
	<i>D. tertiolecta</i>	CCAP 19/27	50	Halifax (Canada); unknown
	<i>D. maritima</i>	SAG 42.89	50	Former USSR; marine
	<i>D. sp.</i>	SAG 19-5	14	Wad al Neifur (Egypt); marine
<i>D. terricola</i>	SAG 43.89	40	Former USSR; marine	
	<i>D. granulata</i>	SAG 41.89	14	Former USSR; marine

Max % v/v refers to the maximum volume percent centrate at which growth was observed; the saltwater species were supplemented with 33.6 g/L sea salt. UTEX – Culture Collection of Algae at The University of Texas at Austin; CCAP – the Culture Collection of Algae and Protozoa (CCAP); UTCC – University of Toronto Culture Collection of Algae and Cyanobacteria [now referred to as the Canadian Phycological Culture Centre (CPC)]; SAG – the Culture Collection of Algae at the University of Göttingen, Germany.

^aUnless noted, origin and source information obtained from the originating culture collection.

^bCurrently regarded as a taxonomic synonym of *Ettlia fusispora*.

^cCurrently regarded as a taxonomic synonym of *Ettlia terrestris*.

^dCurrently listed with CCAP as *Ettlia carolinosa*.

^eCurrently listed with CCAP as *Nannochloropsis gaditana*.

were grown in 2-L Erlenmeyer flasks to determine growth characteristics. Optical density (measured as absorbance at 600 nm) was used to monitor the cell density of the cultures and to determine the growth phase of the culture. Maximum growth rates were determined by plotting the A_{600} values versus time (Figures S2 and S3 in Supplementary Material) and taking the slope of growth rate plot during the exponential growth phase. Each medium was prepared by mixing the filtered and autoclaved centrate with nanopure water to 10, 25, or 40% v/v centrate, then the pH adjusted to 7.7 with 0.1N HCl or NaOH as required. Bold's modified Bristol medium (Bold, 1949) at pH = 7.7 was also prepared and used as

a baseline. Each batch of medium was divided into 1.5 L aliquots, transferred to the flasks, and then autoclaved. After sterilization, flasks were inoculated with 30 mL of mid-log phase culture and then stoppered with a bubbler apparatus (sterile two-holed stopper with two glass tubes with a small amount of cotton batting). Cultures were grown in a growth chamber (Conviron PGR15) with a 18/6 h light/dark cycle at 26/20°C and 140 $\mu\text{mol}/\text{m}^2$ s light supplied by a mixture of fluorescent and incandescent lamps. Using an aquarium pump, atmospheric air was pumped through a 2-L flask with sterile water, which served to both filter and humidify the air, and then was split into eight flasks using a manifold.

The air bubbles served as both a CO₂ source and agitation for the flasks.

Centrate Acclimation Testing

In a separate experiment, cells were grown to mid-log phase in Bold's modified Bristol medium (Sandnes et al., 2006) or in 10, 25, or 40% v/v centrate. To evaluate the effects of pre-acclimation, 30 mL of each of the liquid cultures were transferred to 2-L Erlenmeyer flasks with their respective fresh media. The cultures were grown and monitored as described above.

Harvesting, Drying, and Lipid Extraction

The algae were harvested via centrifugation (6000 × g for 5 min) in early stationary phase (3–5 days after log phase) and the algae paste was then stored at –80°C. The samples were lyophilized to remove all moisture and dry weights were determined. The dried samples were then re-suspended in water (1 mL/g dry algae) overnight at 4°C. A modified Bligh and Dyer (1959) extraction method was used to extract the lipids (and other chloroform-soluble components). Modifications include centrifugation-assisted phase separation (2800 × g for 10 min) and a second extraction on the non-lipid phase to ensure complete extraction. Chloroform was evaporated under a stream of nitrogen and dry weights of the lipids were determined.

FAME Preparation and GC/MS

Fatty acid profiles were determined via GC/MS analysis of fatty acid methyl esters (FAMES). Briefly, the dried lipid extracts were esterified to FAMES using the rapid BF₃-methanol esterification procedure (Metcalf et al., 1966). After esterification, samples were dried completely under nitrogen then re-suspended in 1 mL carbon disulfide. FAME profiles were obtained by the Nevada Proteomics Center using GC/MS (Thermo Polaris Q) on an Agilent HP – INNOWAX column (P/N 19091N-136; 60 m × 0.250 mm, 0.25 μm film thickness) using helium as the carrier gas at 1.0 mL/min constant flow and a split ratio of 1:10 (split flow 10 mL/min) with 1 μL injection volumes. The GC was operated with an inlet temperature of 225°C and a column temperature starting at 180°C and ramping at 5°C/min to 240°C with a 30 min hold. The transfer line temperature between the GC and the MS was maintained at 250°C. The MS was operated in Full Scan mode with a mass range of 40–450 m/z at 70 eV and an ion source temperature of 200°C. Chromatograms and spectra were analyzed using XCalibur (Thermo Fisher Scientific, v1.3).

Results and Discussion

Preliminary Centrate Screening

Preliminary screening of the various microalgae strains revealed a wide range of tolerance to centrate (Table 1). Autoclaved centrate was used to avoid the possible complicating influence of undefined microbial flora on algal growth. Sterile centrate has been used in several other investigations (Wang et al., 2010; Li et al., 2011a; Zhu et al., 2013; Dong et al., 2014). Of the 11 freshwater *Neochloris* strains, two (*N. cohaerens* and *N. wimmeri*) were unable to grow in the presence of any centrate, while two strains (*N. conjuncta* and *N. pseudostigmata*) were tolerant of

concentrations up to 40% v/v. Growth was observed at maximum centrate concentrations between 10 and 20% v/v for the remaining seven strains. The brackish water *Nannochloropsis* strains had a lower centrate tolerance, with growth observed at a maximum of 14% v/v centrate for five strains and two strains unable to grow in the presence of any centrate. This low centrate tolerance might possibly be due to a lack of salts in the growth medium (centrate diluted with nanopure water) rather than as a function of the centrate concentration itself. As expected, saltwater *Dunaliella* strains were unable to grow when the centrate lacked salt and was diluted using nanopure water alone (data not shown). However, when sea salts were added to match the salt concentration of the 2ASW (33.6 g/L) to the diluting water, all but one of the saltwater strains (*D. salina* UTC 197) were able to grow at 14% v/v or greater centrate (Table 1). Of the 18 species or strains tested, 11 grew at 50% v/v centrate, and an additional 3 grew at 40% v/v centrate levels. Interestingly, of four different *D. salina* strains (e.g., UTEX LB 200, UTEX LB 1644, UTCC 197, and CCAP 19/18) evaluated, two UTEX strains (LB 200 and LB 1644) and CCAP 19/18 all demonstrated high-centrate tolerance, while UTCC 197 was the only *Dunaliella* strain unable to grow in centrate. Recent work suggests that UTEX 200 should not be designated as *D. salina* based on physiological and molecular markers (Ben-Amotz et al., 2009).

These tolerances to centrate were lower than those reported previously for several other algal species and strains (Wang et al., 2010; Li et al., 2011a; Zhu et al., 2013). However, such differences might be due to differences in centrate characteristics arising from the unique inputs and processing steps of a particular WWTP. Wang and Lan (2011) reported growth with a wild-type *Chlorella* sp. on a 100% centrate medium, which contained 72 mg/L total N, and would correspond to ~7% v/v centrate used in this work on a total N basis. Further evaluation with this same centrate source found a total of fourteen strains from genera *Chlorella*, *Haematococcus*, *Scenedesmus*, *Chlamydomonas*, and *Chlorococcum* that were able to grow on the pure centrate (Li et al., 2011b). From the present work, the two freshwater strains (*N. conjuncta* and *N. pseudostigmata*) were considered for further evaluation because of their high-centrate tolerance and no need for additional salt supplementation.

Microalgal Growth

The *N. conjuncta* and *N. pseudostigmata* were grown in 2-L flasks with modified Bristol medium and various concentrations of centrate. No significant differences ($p > 0.05$) were observed in the maximum growth rates for either species (Table 2). For both species, no significant difference in the acclimation period was observed between modified Bristol medium and 10% v/v centrate. However, significant time lag periods in growth were observed for both species when the centrate concentration was increased to 25% v/v ($p < 0.01$), and additional lags were observed when the concentration was increased to 40% ($p < 0.01$ for *N. conjuncta*; $p < 0.05$ for *N. pseudostigmata*). At the highest centrate concentrations, a delay of more than 40 days was observed for both species. This increase in the lag time with increasing centrate concentration suggested the presence of a compound(s) that inhibit microalgal growth in the centrate, although the cells were able to

TABLE 2 | Maximum growth rate (μ_{\max}) and observed lag time of *N. conjuncta* and *N. pseudostigmata* grown in 10, 25, and 40% v/v centrate and in Bold's modified Bristol medium (Bold, 1949).

	<i>N. conjuncta</i>		<i>N. pseudostigmata</i>	
	μ_{\max} (1/days)	Lag (days)	μ_{\max} (1/days)	Lag (days)
NON-ACCLIMATED CELLS				
Bristol medium	0.004 ± 0.001	2.3 ± 1.5	0.0072 ± 0.0004	0.8 ± 1.5
10% Centrate	0.006 ± 0.002	2.3 ± 1.5	0.007 ± 0.001	1.5 ± 1.7
25% Centrate	0.009 ± 0.003	16.0 ± 7.7	0.008 ± 0.002	17.8 ± 3.8
40% Centrate	0.007 ± 0.002	46.3 ± 3.4	0.009 ± 0.002	41.5 ± 20
PRE-ACCLIMATED CELLS				
Bristol medium	0.009 ± 0.002	0.0 ± 0.0	0.0099 ± 0.0006	0.0 ± 0.0
10% Centrate	0.011 ± 0.001	2.0 ± 0.0	0.012 ± 0.004	1.5 ± 1.2
25% Centrate	0.006 ± 0.002	7.0 ± 0.0	0.007 ± 0.001	10.0 ± 6.5
40% Centrate	0.015 ± 0.005	33.8 ± 9.8	0.016 ± 0.003	44.3 ± 4.0

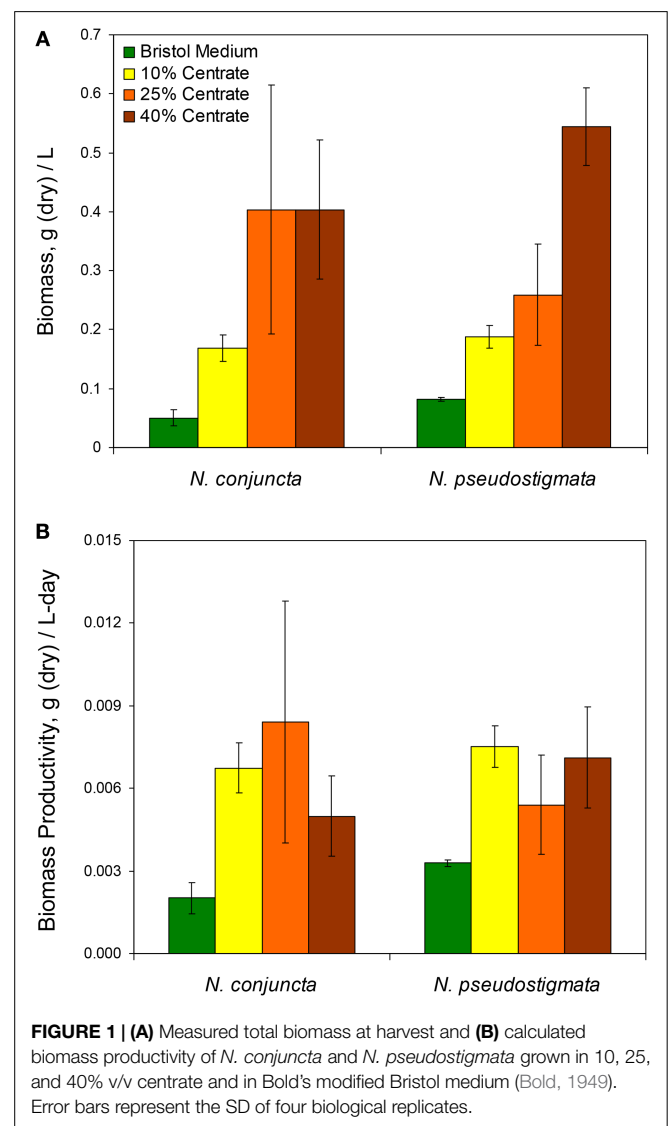
Error ranges represent the SD of four biological replicates.

grow given enough time. The identity of the putative inhibitor(s) is unknown, but likely candidates might include ammonia or urea (Moazeni, 2013). Additional studies are needed to verify the presence of ammonia or urea in centrate and to test this possibility in future studies. However, neither metals nor ammonia ions were reported to be likely candidates for toxicity responses to centrate (Dong et al., 2014).

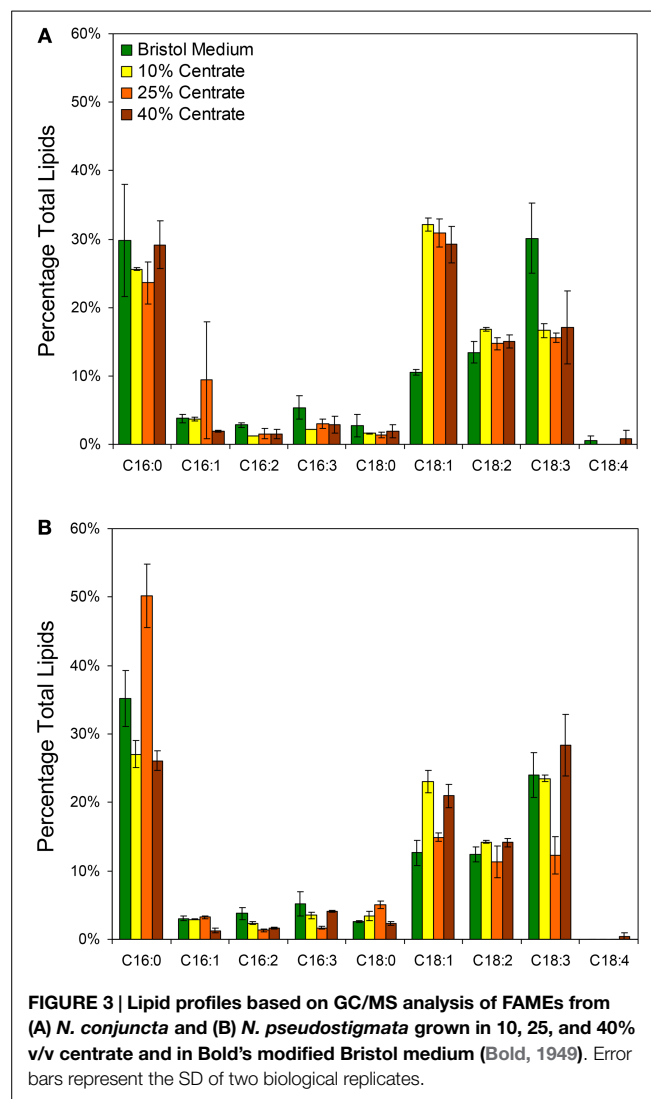
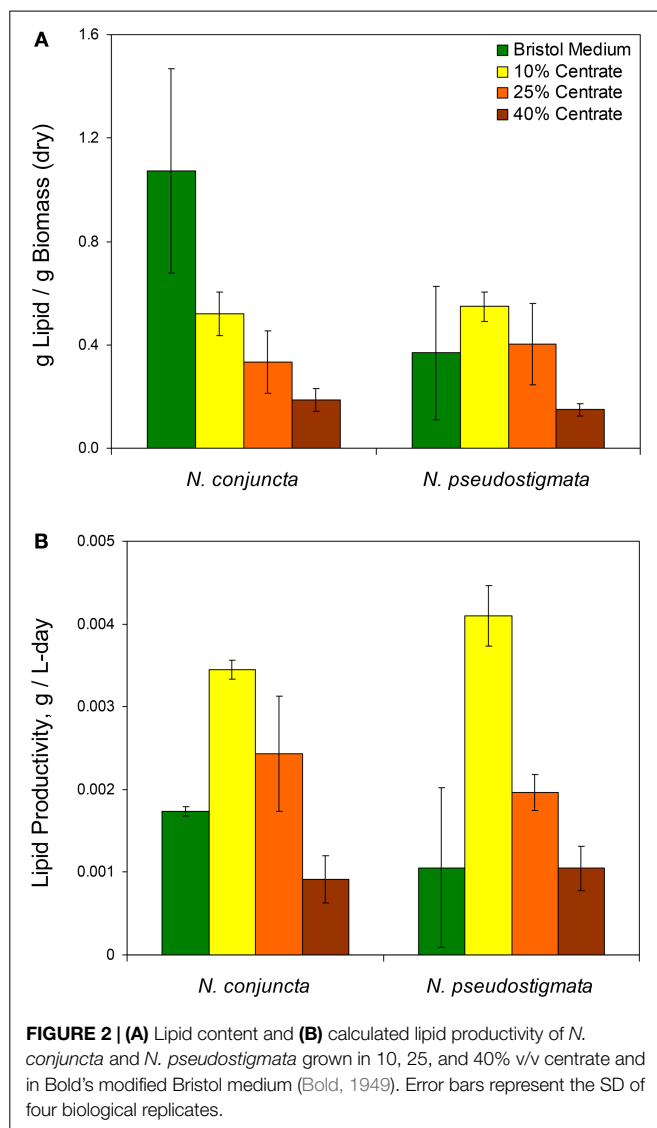
The long lag period in growth at elevated centrate concentrations would be problematic for large-scale cultivation, especially in open-pond systems, due to the prolonged opportunities for contamination of the cultures by other species (Chisti, 2007; Bhatt et al., 2014). To evaluate whether the cells could be acclimating to the inhibiting compound(s), and thereby decrease the observed lag time, cells exposed to centrate were used as inoculum for serial growth trials. For these tests, *N. conjuncta* and *N. pseudostigmata* grown in either Bold's modified Bristol medium (Bold, 1949) or in 10, 25, and 40% v/v centrate were inoculated into fresh batches of their respective medium and monitored (Table 2; Figures S2 and S3 in Supplementary Material). In general, the maximum growth rates of the pre-acclimated cells increased relative to the non-acclimated cells. As expected, no difference in the lag time was observed with the cells grown in Bristol medium and the 10% v/v centrate for either species. However, the average lag times for the pre-acclimated *N. conjuncta* decreased by 9 and 12.5 days when grown on 25 and 40% v/v centrate, respectively. The trend was not as strong with the pre-acclimated *N. pseudostigmata* cells, although the average lag time of those grown on 25% v/v centrate decreased 7.8 days (Table 2; Figures S2 and S3 in Supplementary Material). These results suggest that the inhibitory compound found in centrate is one that the freshwater *Neochloris* species may be able to acclimate to, and a further reduction in the lag time might be achieved with additional acclimation cycles.

Biomass Production and Productivity

The *N. conjuncta* and *N. pseudostigmata* cultures were harvested via centrifugation ~5 days after reaching stationary phase, as determined by A_{600} measurements. After harvesting, the cell pellets were frozen and then water removed via lyophilization. For both species, the dry biomass obtained (normalized to the culture volume harvested) increased with increasing centrate concentrations (Figure 1A). Biomass concentrations ranged over nearly



an order of magnitude, from 0.045 to 0.404 g dry biomass/L for *N. conjuncta* and from 0.107 to 0.544 g dry biomass/L for *N. pseudostigmata*. The *N. conjuncta* cultures grown on centrate



all had significantly ($p = 0.0026$) more biomass than the Bristol culture, whereas only the *N. pseudostigmata* cultures grown on the two higher centrate concentrations had significantly ($p < 0.05$ for 25% v/v; $p < 0.01$ for 40% v/v) more biomass. Because centrate has a very high nutrient content (e.g., ~1000 mg/L N and ~200 mg/L P), the greater biomass amounts were expected.

Despite the greater biomass amounts with increasing centrate concentrations, the amount of dry biomass obtained per day did not appear to be affected by the centrate concentration (**Figure 1B**). There was no significant difference ($p > 0.05$) for either species across the various centrate concentrations, with productivity values ranging from 0.0050 to 0.0084 g dry biomass/L-day. However, biomass productivity of *N. conjuncta* was significantly ($p = 0.012$) lower at 0.0018 g dry biomass/L-day when grown on Bristol medium. These values were lower than those obtained by Wang and Lan (2011) who reported a biomass productivity of 0.233 g dry biomass/L-day with *N. oleoabundans* grown on secondary municipal wastewater effluents enriched with nitrogen. Sun et al. (2014) also reported higher biomass

productivities of 0.113 g dry biomass/L-day for *N. oleoabundans* grown in basal SE medium. Although biomass was not measured for the cultures inoculated with pre-acclimated cells, the reduction in lag times with the higher centrate concentrations would be expected to result in higher biomass productivities due to the shorter cultivation times. However, biomass productivities can vary as a result of other influences, such as mixing of the cultures, CO₂ supplementation, light intensity, and carbon source.

Lipid Production and Productivity

Unlike the biomass, the mass of lipids produced (per mass of dry biomass) was found to decrease with increasing centrate concentrations for both *Neochloris* species (**Figure 2A**). The *N. conjuncta* grown in Bristol medium was found to have a lipid content (1.07 ± 0.4 g lipid/g dry biomass) significantly ($p = 0.0004$) higher than any other species/medium combination, which ranged from 0.5 to 50 g lipid/g dry biomass. These values agree with the 0.27 (Sun et al., 2014), 0.50 (Griffiths et al., 2012), and 0.52 (Gouveia et al., 2009) g lipid/g dry biomass reported for *N. oleoabundans*.

The lipid productivity also decreased with increasing centrate concentrations for both species (**Figure 2B**). Interestingly, the highest lipid productivity (0.0041 g lipid/L-day, *N. pseudostigmata*) was observed with 10% v/v centrate rather than on the Bristol medium with both species. The lowest productivities (0.001 g lipid/g dry biomass) were observed with 40% v/v centrate. This range is similar to the 0.003 g lipid/L-day (Sun et al., 2014) and 0.0029 g lipid/L-day (Griffiths et al., 2012) reported for *N. oleoabundans* under nitrogen-limited conditions. As mentioned previously, the lipid productivities would be expected to increase with the higher centrate concentrations when pre-acclimated cells are used. Therefore, centrate-grown cultures all would likely have greater lipid productivities than those grown in Bristol medium.

In addition to the total lipid measurements, fatty acid profiles were obtained for the two species grown with Bristol medium and various centrate concentrations with the most prevalent fatty acids presented in **Figure 3**. The dominant fatty acids for both *Neochloris* species were palmitic (C16:0), oleic (C18:1), linoleic (C18:2), and linolenic (C18:3). Although the lipid profiles varied by species, the profiles in **Figure 3** agree generally with what others have observed for various *Neochloris* species (Griffiths et al., 2012; Sun et al., 2014) and other green algae (Islam et al., 2013). The most notable differences between the lipid profiles of *N. conjuncta* was the significant increase in C18:1 ($p < 0.01$) and decrease in C18:3 ($p < 0.05$) when changing from Bristol medium to centrate (**Figure 3A**). There were no significant differences in any of the other fatty acids with any growth media for the *N. conjuncta*. Interestingly, very similar changes (e.g., C18:1 increase, C18:3 decrease) were observed when going from nitrogen-replete to nitrogen-limited conditions using *N. oleoabundans* (Griffiths et al., 2012). Lipid accumulation in microalgae is known to occur as a result of stress events, including nutrient starvation, temperature or pH shock, or light limitation (Wang et al., 2010; Li et al., 2011a; Sharma et al., 2012). With these experiments, the cultures were grown until early stationary phase (based on A_{600}) before harvesting, which corresponds to ~5 days of growth when at least one nutrient was limiting. The differences in lipid productivity observed between the cells grown in Bristol medium and the centrate solutions are possibly due to a different nutrient becoming limited. Xin et al. (2010) demonstrated that *Scenedesmus* subjected to nitrogen starvation had a 30% increase in lipids, whereas the same cells subjected to phosphorus starvation had a 53% increase, suggesting that nutrient stress affects the degree of lipid accumulation (Xin et al., 2010).

The *N. pseudostigmata* profiles had more variability (**Figure 3B**), but a significant decrease in C18:1 ($p < 0.05$) was observed in the Bristol medium compared to the 10 and 40% v/v centrate cultures. The increase in C18:3 in Bristol was not observed, as was the case with *N. conjuncta*. Instead, a decrease in C18:3 with corresponding increases in C16:0 and C16:3 were observed for the *N. pseudostigmata* culture grown in 25% v/v centrate. Sun et al. (2014) also observed increases in C16:0 accumulation with increasing nutrient stress duration for *N. oleoabundans*; however, they also found an increase in C18:1, which is in contradiction of what was observed here for *N. conjuncta*.

Conclusion

Wastewater centrate offers a promising alternative water source for the cultivation of microalgae for biofuels production. Forty microalgae species were screened for tolerance; two freshwater species were found to grow in up to 40% v/v centrate and multiple saltwater species could grow in up to 50% v/v centrate when supplemented with sea salt. Despite these promising results, many of the strains evaluated were very sensitive to centrate and failed to grow at even low concentrations, and even those strains with high tolerance to centrate had increased lag times with increasing centrate concentration. This lag time could be partially reduced by pre-acclimating the cells to the centrate. Using the two freshwater *Neochloris* strains as models, improvements in both biomass productivity and lipid productivity were observed when the cells were grown on centrate, relative to defined maintenance medium. The lipid profiles of the microalgae grown with centrate and with the maintenance medium were similar, although a significant increase in C18:1 and significant decrease in C18:3 were observed in *N. conjuncta*. Screening of additional microalgae strains should be continued, especially of environmental strains with pre-exposure to the centrate, to identify those strains that can be grown with higher centrate concentrations and also those strains with high lipid content to be used for biofuel feedstock production. The identification of microalgal species or strains adapted to the nutrient profile of a particular waste stream would likely be less expensive than the potential costs associated with supplementing the nutrient profile of a particular waste stream in order to attain optimal growth. Lastly, high performing strains should be evaluated in larger volumes and in raceway ponds or photobioreactors to further evaluate their applicability for full-scale use.

Author Contributions

SRH conducted the research, designed experiments, and wrote the bulk of the manuscript. MSL assisted with experimental design and experimentation and assisted with the preparation of the manuscript. BPK assisted with centrate testing studies, contributed to interpretation of results, and assisted with the preparation of the manuscript. JCC initiated research on wastewater algae, conceived of the study, helped design experiments, and revised the manuscript.

Acknowledgments

Financial support was provided by Department of Energy's Nevada Renewable Energy Consortium (Grant DE-EE0000272). The Nevada Proteomics Center receives financial support from Nevada INBRE, which is funded by NIH Grant number P20 RR-016464 from the INBRE Program of the National Center for Research Resources. The authors would also like to thank Rebecca Albion for all of her assistance in the lab and Rebekah Woolsey for performing the GC-MS analyses.

Supplementary Material

The Supplementary Material for this article can be found online at <http://journal.frontiersin.org/article/10.3389/fenrg.2015.00020>

References

- Arce, G., and Bold, H. (1958). Some Chlorophyceae from Cuban soils. *Am. J. Bot.* 45, 492–503. doi:10.2307/2439186
- Ben-Amotz, A., Polle, J., and Rao, D. (2009). *The Alga Dunaliella: Biodiversity, Physiology, Genomics, and Biotechnology*. Enfield, NH: Science Publishers, Inc.
- Bhatt, N., Panwar, A., Bisht, T., and Tamta, S. (2014). Coupling of algal biofuel production with wastewater. *ScientificWorldJournal* Article ID 210504, 10. doi:10.1155/2014/210504
- Bligh, E., and Dyer, W. (1959). A rapid method of total lipid extraction and purification. *Can. J. Physiol. Pharmacol.* 37, 911–917. doi:10.1139/y59-099
- Bold, H. (1949). The morphology of *Chlamydomonas chlamydogama* sp. nov. *Bull. Torrey Botanical Club* 76, 101–108. doi:10.2307/2482218
- Chisti, Y. (2007). Biodiesel from microalgae. *Biotechnol. Adv.* 25, 294–306. doi:10.1016/j.biotechadv.2007.02.001
- Dong, B., Ho, N., Ogden, K., and Arnold, R. (2014). Cultivation of *Nannochloropsis salina* in municipal wastewater or digester centrate. *Ecotoxicol. Environ. Saf.* 103, 45–53. doi:10.1016/j.ecoenv.2014.02.001
- Forsberg, C. (2009). Sustainability by combining nuclear, fossil, and renewable energy sources. *Prog. Nucl. Energy* 51, 192–200. doi:10.1016/j.pnucene.2008.04.002
- Gomord, V., Fitchette, A., Menu-Bouaouiche, L., Saint-Jore-Dupas, C., Plasson, C., Michaud, D., et al. (2010). Plant-specific glycosylation patterns in the context of therapeutic protein production. *Plant Biotechnol. J.* 8, 564–587. doi:10.1111/J.1467-7652.2009.00497.X
- Gouveia, L., Marques, A., Da Silva, T., and Reis, A. (2009). *Neochloris oleoabundans* UTEX #1185: a suitable renewable lipid source for biofuel production. *J. Ind. Microbiol. Biotechnol.* 36, 821–826. doi:10.1007/s10295-009-0559-2
- Griffiths, M., Van Hille, R., and Harrison, T. (2012). Lipid productivity, settling potential and fatty acid profile of 11 microalgal species grown under nitrogen replete and limited conditions. *J. Appl. Phycol.* 24, 989–1001. doi:10.1007/s10811-011-9723-y
- Guillard, R., and Ryther, J. (1962). Studies of marine planktonic diatoms. *Cyclotella nana* Hustedt and *Detonula confervaceae* (Cleve) Gran. *Can. J. Microbiol.* 8, 229–239. doi:10.1139/m62-029
- Herrera, N. (2009). *Analysis of Centrate Composition and Evaluation of its Applicability as a Nutrient Supplement to Irrigation Water*. M.S. Reno: University of Nevada.
- Islam, M., Magnusson, M., Brown, R., Ayoko, G., Nabi, M., and Heimann, K. (2013). Microalgal species selection for biodiesel production based on fuel properties derived from fatty acid profiles. *Energies* 6, 5676–5702. doi:10.3390/en6115676
- Xin, L., Hong-ying, H., Ke, G., and Ying-xue, S. (2010). Effects of different nitrogen and phosphorus concentrations on the growth, nutrient uptake, and lipid accumulation of a freshwater microalga *Scenedesmus* sp. *Bioresour. Technol.* 101, 5494–5500. doi:10.1016/j.biortech.2010.02.016
- Li, Y., Chen, Y.-F., Chen, P., Min, M., Zhou, W., Martinez, B., et al. (2011a). Characterization of a microalga *Chlorella* sp. well adapted to highly concentrated municipal wastewater for nutrient removal and biodiesel production. *Bioresour. Technol.* 102, 5138–5144. doi:10.1016/j.biortech.2011.01.091
- Li, Y., Zhou, W., Hu, B., Min, M., Chen, P., and Ruan, R. (2011b). Integration of algae cultivation as biodiesel production feedstock with municipal wastewater treatment: strains screening and significance evaluation of environmental factors. *Bioresour. Technol.* 102, 10861–10867. doi:10.1016/j.biortech.2011.09.064
- Metcalfe, L., Schmitz, A., and Pelka, J. (1966). Rapid preparation of fatty acid esters from lipids for gas chromatographic analysis. *Anal. Chem.* 38, 514–515. doi:10.1021/ac60235a044
- Moazeni, F. (2013). *Investigating the Feasibility of Growing Algae for Fuel in Southern Nevada*. Ph.D. Dissertation Las Vegas: University of Nevada.
- Mu, D., Min, M., Krohn, B., Mullins, K., Ruan, R., and Hill, J. (2014). Life cycle environmental impacts of wastewater-based algal biofuels. *Environ. Sci. Technol.* 48, 11696–11704. doi:10.1021/es5027689
- Pittman, J., Dean, A., and Osundeko, O. (2011). The potential of sustainable algal biofuel production using wastewater resources. *Bioresour. Technol.* 102, 17–25. doi:10.1016/j.biortech.2010.06.035
- Sandnes, J., Ringstad, T., Wenner, D., Heyerdahl, P., Kallqvist, I., and Gislerod, H. (2006). Real-time monitoring and automatic density control of large-scale microalgal cultures using near infrared (NIR) optical density sensors. *J. Biotechnol.* 122, 209–215. doi:10.1016/j.jbiotec.2005.08.034
- Schnepf, R., and Yacobucci, B. (2010). *Renewable Fuel Standard (RFS): Overview and Issues*. Washington, DC: Congressional Research Service.
- Sharma, K., Schuhmann, H., and Schenk, P. (2012). High lipid induction in microalgae for biodiesel production. *Energies* 5, 1532–1553. doi:10.3390/en5051532
- Sun, X., Cao, Y., Xu, H., Liu, Y., Sun, J., Qiao, D., et al. (2014). Effect of nitrogen-starvation, light intensity and iron on triacylglyceride/carbohydrate production and fatty acid profile of *Neochloris oleoabundans* HK-129 by a two-stage process. *Bioresour. Technol.* 155, 204–212. doi:10.1016/j.biortech.2013.12.109
- Wang, B., and Lan, C. (2011). Biomass production and nitrogen and phosphorus removal by the green alga *Neochloris oleoabundans* in simulated wastewater and secondary municipal wastewater effluent. *Bioresour. Technol.* 102, 5639–5644. doi:10.1016/j.biortech.2011.02.054
- Wang, L., Min, M., Li, Y., Chen, P., Chen, Y., Liu, Y., et al. (2010). Cultivation of green algae *Chlorella* sp. in different wastewaters from municipal wastewater treatment plant. *Appl. Biochem. Biotechnol.* 162, 1174–1186. doi:10.1007/s12010-009-8866-7
- Zhu, L., Wang, Z., Shu, Q., Takala, J., Hiltunen, E., Feng, P., et al. (2013). Nutrient removal and biodiesel production by integration of freshwater algae cultivation with piggery wastewater treatment. *Water Res.* 47, 4294–4302. doi:10.1016/j.watres.2013.05.004

Conflict of Interest Statement: The authors declare that the research was conducted in the absence of any commercial or financial relationships that could be construed as a potential conflict of interest.

Copyright © 2015 Hiibel, Lemos, Kelly and Cushman. This is an open-access article distributed under the terms of the Creative Commons Attribution License (CC BY). The use, distribution or reproduction in other forums is permitted, provided the original author(s) or licensor are credited and that the original publication in this journal is cited, in accordance with accepted academic practice. No use, distribution or reproduction is permitted which does not comply with these terms.



Quantitative assessment of microalgae biomass and lipid stability post-cultivation

Katerine Napan, Tyler Christianson, Kristen Voie and Jason C. Quinn*

Department of Mechanical and Aerospace Engineering, Utah State University, Logan, UT, USA

Edited by:

Umakanta Jena, Desert Research Institute, USA

Reviewed by:

S. Kent Hoekman, Desert Research Institute, USA

Ben J. Stuart, Ohio University, USA

*Correspondence:

Jason C. Quinn, Department of Mechanical and Aerospace Engineering, Utah State University, 4130 Old Main Hill, Logan, UT 84322-4130, USA
e-mail: jason.quinn@usu.edu

Processing of microalgal biomass to biofuels and other products requires the removal of the culture from a well-controlled growth system to a containment or preprocessing step at non-ideal growth conditions, such as darkness, minimal gas exchange, and fluctuating temperatures. The conditions and the length of time between harvest and processing will impact microalgal metabolism, resulting in biomass and lipid degradation. This study experimentally investigates the impact of time and temperature on *Nannochloropsis salina* harvested from outdoor plate photobioreactors. The impact of three temperatures, 4, 40, or 70°C, on biomass and lipid content (as fatty acid methyl esters) of the harvested microalgae was evaluated over a 156 h time period. Results show that for *N. salina*, time and temperature are key factors that negatively impact biomass and lipid yields. The temperature of 70°C resulted in the highest degradation with the overall biofuel potential reduced by 30% over 156 h. Short time periods, 24 h, and low temperatures are shown to have little effect on the harvested biomass.

Keywords: microalgae, biomass, lipid, FAME, losses, harvest, *Nannochloropsis salina*, microalgal storage

INTRODUCTION

Microalgae cultivation has been intensely studied in the past decades due to inherent advantages such as high biomass and lipid productivities, capacity to be grown in non-arable land, utilization of low quality and saline water, and integration with point source waste streams (Khan et al., 2009; Mata et al., 2010). Technological hurdles in the growth, dewater, and conversion steps of the feedstock to biofuel process has limited the scale at which production has been demonstrated (Quinn et al., 2012). Cultivation systems, which include photobioreactors (PBR) and open raceway ponds, have been used at pilot plant scale to produce biomass, which is typically harvested, preserved, and processed off site. Large-scale systems will integrate on site processing based on environmental and economic benefits (Batan et al., 2010; Lundquist et al., 2010; Davis et al., 2011, 2014; Beal et al., 2012; Quinn et al., 2014; Rogers et al., 2014; Thilakaratne et al., 2014; Woertz et al., 2014). Current uncertainties in the structure of a large-scale algal based biorefineries make it possible that microalgae biomass will be temporarily stored in holding tanks based on dewatering processing capacity. Further, the possibility exists for long-term storage due to equipment malfunction or limitations in downstream processing. The tolerance of algal biomass to time and temperature must be understood such that yield is not impacted from biomass and lipid degradation prior to recovery.

During microalgae production, cells are exposed to conditions that ensure biomass multiplication and lipid accumulation. Environmental conditions such as nutrient load, carbon dioxide, light, and temperature are well constrained by the cultivation system and optimized for microalgae growth and stability. However, during harvesting and preprocessing, these conditions are abruptly terminated and new conditions, previously avoided in

a controlled growth system develop. Depending on the harvesting method and processing capacity, the conditions and time of exposure vary. Generally, during the collection and transport of microalgae from the cultivation system to a centralized separation facility, the cells are not exposed to sunlight and the culture temperature is a function of meteorological conditions. During this time period, microalgae are still carrying out physiological activities under non-ideal conditions. As a result, the cells and their contents will undergo physiological changes that could negatively affect the biomass and bio-products yields.

Several factors are known to contribute to biomass and lipid losses. These losses are known to be accelerated by rising temperatures. Low temperatures can reduce the reaction rate of enzyme-catalyzed metabolic reactions in microalgal cells (Mishra and Gamage, 2007). The length of harvest is also known to influence biomass, as organisms need energy to continue cell functions (Montaini et al., 1995). Microalgae-related literature addressing these factors is limited with few studies presenting data related to biomass and lipid degradation. Previous work has focused on carbon isotope fractionation, microalgae respiration rate, and microalgae decomposition in natural environments. The application of results to microalgae biorefinery systems is limited. Additionally, several techno-economic and life cycle assessments of the microalgae biofuel process do not consider the impact of storage time or preprocessing temperatures on yield as all assume a seamlessly integrated co-located growth and processing facility (Batan et al., 2010; Beal et al., 2012; Sills et al., 2012; Jones et al., 2014; Quinn et al., 2014; Rogers et al., 2014; Thilakaratne et al., 2014; Woertz et al., 2014). Current assessments of the microalgae to biofuels process make simplifying assumption due to the lack of large-scale processing data (Davis et al.,

2014). Currently, there is a need to develop data that can be leveraged to validate engineering system process models for improved fidelity in large-scale feasibility assessments of microalgae biofuel systems.

This study experimentally evaluates the impact of time and temperature on microalgae biomass and lipid composition as applied for use as a biodiesel feedstock. The experimental system was designed to be representative of a large-scale microalgae processing system through the harvesting phase. In large-scale systems, it is expected, based on variable production and fixed processing capacity, there will be storage of culture for a non-trivial time period. This study presents results in terms of changes in *Nannochloropsis salina* biomass and lipid quantity (produced in outdoor flat-plate PBR) stored under three different temperatures, 4°C (refrigeration), 40°C (outdoor storage in summer), and 70°C (pasteurization or upper storage bound), over the course of 156 h. Discussion includes the impact of the results on the microalgae industry and on scalability assessments.

MATERIALS AND METHODS

Nannochloropsis salina was cultivated in outdoor PBR with the collected biomass analyzed as a function of time and temperature. Harvested biomass was collected in 50 mL aliquots and exposed to three different temperatures. Periodic collection of samples were centrifuged and analyzed for biomass and lipid content. Experiments were performed in triplicate with the baseline biomass and lipid content being time 0.

ORGANISM PRODUCTION

Nannochloropsis salina was grown in flat-plate PBR (110 cm × 241 cm × 5 cm) with a maximum capacity of 130 L of culture. The PBRs were located in a greenhouse with supplemental high pressure sodium lighting (Utah State University Research Greenhouse). Temperature was maintained at 23°C in the PBR through a chilled water heat exchanger. Mixing of the system was maintained through sparge air supplied through a stainless steel manifold in the bottom of the PBR. The pH was maintained at 7.3 through automatic injection of carbon dioxide into the sparge air based on pH feedback. Prior to inoculation, PBRs were washed and bleached overnight, followed by rinsing with tap water.

Nutrient medium was prepared using tap water, sodium chloride (NaCl, 17.5 g L⁻¹), calcium chloride dihydrate (CaCl₂ × 2H₂O, 1.5 × 10⁻¹ g L⁻¹), potassium chloride (KCl, 4.8 × 10⁻¹ g L⁻¹), sodium metasilicate non-ahydrate (Na₂SiO₃ × 9H₂O, 5.7 × 10⁻² g L⁻¹), magnesium sulfate heptahydrate (MgSO₄ × 7H₂O, 1.48 g L⁻¹), potassium nitrate (KNO₃, 1.02 g L⁻¹), potassium phosphate monobasic (KH₂PO₄, 6.8 × 10⁻² g L⁻¹), ammonium ferric citrate (5.2 × 10⁻³ g L⁻¹), boric acid (H₃BO₃, 9.0 × 10⁻⁴ g L⁻¹), disodium molybdenate dihydrate (Na₂MoO₄ × 2H₂O, 1.2 × 10⁻⁵ g L⁻¹), manganese chloride tetrahydrate (MnCl₂ × 4H₂O, 3.0 × 10⁻⁴ g L⁻¹), zinc sulfate heptahydrate (ZnSO₄ × 7H₂O, 6.0 × 10⁻⁵ g L⁻¹), cupric sulfate pentahydrate (CuSO₄ × 5H₂O, 2.0 × 10⁻⁵ g L⁻¹), 0.1 mM biotin (40.9 μL), 6.5 mM thiamine (26.08 μL), and 0.135 mg mL⁻¹ vitamin B₁₂ (14.81 μL). Microalgae were harvested from the PBRs when the culture concentration reached at least 2 g L⁻¹.

DEGRADATION EXPERIMENTAL SET-UP

This study is a time series experiment with time as an independent variable and temperature as controlled variable. The dependent variable or measured responses were either biomass or lipid content. The measured response at different times is compared against the initial conditions before the temperature treatment (in this case, the biomass and lipid content at time 0). The duration of the experiment was at the least 156 h with sampling events within 12 and 24 h from each other (one sample event was lost during the lipid analysis).

For the determination of biomass degradation, microalgae cultivated in flat-plate PBR located at the USU Research Greenhouse facility were harvested and were immediately transferred into seventy two 50 mL polypropylene centrifuge tubes. The vials were separated into three groups of 24 vials. From each group of 24 vials, 3 vials, to be used as samples at time 0, were immediately centrifuged (RC-6 Plus, Thermo Fisher, USA), the supernatant was discarded and the pellet was preserved in a -80°C freezer. The biomass content in these vials was used as the initial untreated response. The remaining 21 vials left in each batch were placed in one of three water baths maintained at 4°C (represent refrigeration), 40°C (represent outdoor storage in summer), or 70°C (represent pasteurization or upper storage bound). The water baths were maintained in complete darkness with minimal light exposure during sampling. During sampling, three vials were collected from each water bath. The vials were immediately centrifuged, and the pellets were preserved at -80°C. Frozen biomass pellets were put in a lyophilizer (FreeZone 6, Labconco, USA) overnight at -50°C under 0.1 mBar vacuum for complete dewatering. Freeze dried samples were used to determine biomass loss. Biomass was measured through analyzing the mass remaining in harvested samples after centrifugation. At the end of the experiment, the freeze dried microalgae were powdered using a mortar and pestle and was preserved at -80°C until fatty acid methyl ester (FAME) analysis.

LIPID ANALYSIS

Total lipids were quantified through FAME content with results expressed as percent FAME content based on microalgal biomass dry weight (% of total DW). This approach to measure lipids accurately reflects the biofuel potential (Wycken and Laurens, 2013). FAMES were produced through an acid-catalyzed *in situ* transesterification technique. Approximately, 100 mg was transferred into test tubes (borosilicate tubes with screw cap, Fisher Scientific, USA). A 2 mL solution of a 2% sulfuric acid in methanol (v/v) was added to the vials that were then sealed. Vials were digested at 80°C for 90 min in a digital reactor block (DBR200, HACH, USA) shaking the tube contents vigorously every 15 min. Digested contents were transferred to a borosilicate test tube. Digestion vials were then rinsed three times with 1 mL chloroform and the rinsing solution transferred to the test tubes.

The methanol, sulfuric acid, chloroform, and biomass mixture were then washed with an equal volume of deionized water delivered using a washing/dispensing bottle (with nozzle) that allowed for a well stirred solution. Vials were then centrifuged for phase separation. The upper methanol and water phase was discarded and the water washing step was repeated two times more. The bottom phase containing the chloroform and FAME was transferred

to a 10 mL volumetric flask using a 5 mL glass gas-tight syringe. The syringe and the test tube were rinsed two times more using chloroform with the rinse transferred into the 10 mL volumetric flask. The final volume in the volumetric flask was adjusted to 10 mL using chloroform, and the contents were mixed thoroughly. From this solution, 1 mL was transferred to an amber borosilicate screw top vial for analysis by gas chromatograph (Model 7890A GC System, Agilent Technologies, USA) equipped with a flame ionization detector (FID) and autosampler. The column used was a capillary column with polyethylene glycol stationary phase Stabilwax-DA (RESTEK), length 30 m, internal diameter 0.32 mm, and film thickness 0.25 μm . The inlet temperature used was of 250°C, oven temperature used was of 100°C for 1 min, 25°C/min up to 200°C, and held for 1 min, 5°C/min up to 250°C and held for 7 min. The FID was held at 280°C. Standards using methyl myristate, methyl palmitoleate, and methyl oleate were prepared in a chloroform matrix and run in parallel with the prepared samples.

RESULTS

Time and temperature were shown to be critical factors for *N. salina* biomass yields. **Figure 1** shows the decrease of biomass with time at the three temperatures tested. For experiments at 4°C biomass losses were minimal, with biomass content becoming statistically different to the initial biomass after 132 h (ANOVA, $p < 0.05$). In contrast, for experiments at 40 and 70°C the biomass contents were statistically different to the initial biomass (ANOVA, $p < 0.05$) starting at the first sampling of the experiment, 12 h. The slope of the decrease in biomass content was more pronounced at the beginning of the experiment (during the first 60 h) and became mild after this period.

The time evolution of percent FAME content (% of total DW) at 4, 40, and 70°C is shown in **Figure 2**. **Figure 2A** shows an initial increase in percent FAME (% of total DW). Similar behavior was observed by Montaini et al. (1995). A second experiment was performed to further investigate initial lipid increase. Results from this study are presented in **Figure 3** and show a slight increase in percent FAME initially for the 40°C experiment with minimal

degradation in the latter part of the experiment. The 70°C experiment was not statistically different from the initial percent FAME content (% of total DW) while the 4°C experiment was slightly

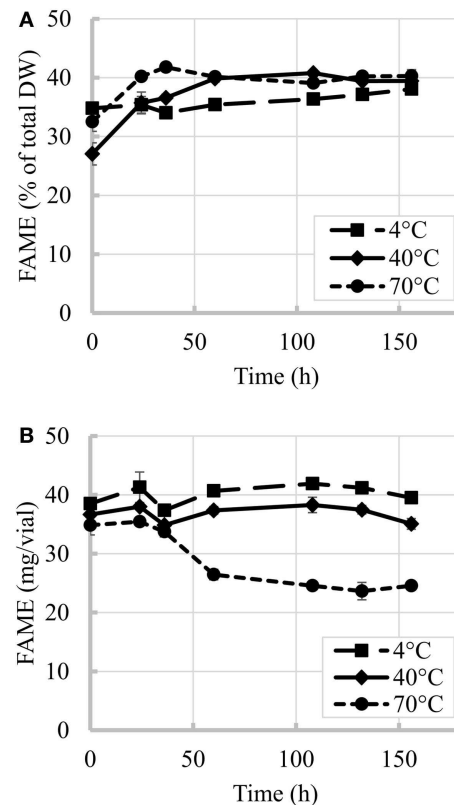


FIGURE 2 | Time evolution of FAME content at three different temperatures. (A) Percent FAME per unit of biomass (% total DW), **(B)** Total FAME per vial. Initial biomass was 2 g/L. Error bars represent SD from three independent experiments. SD not visible is overlapped with the symbols.

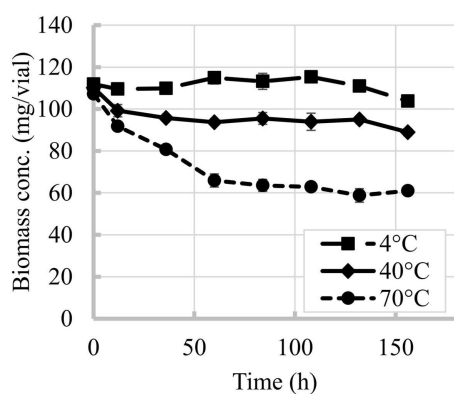


FIGURE 1 | Time evolution of *N. salina* biomass content at different temperatures. Error bars represent SD from three independent experiments. SD not visible is overlapped with the symbols.

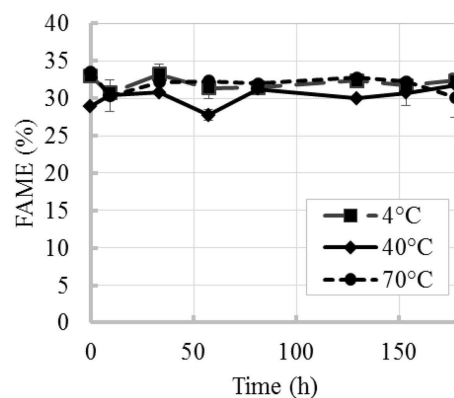


FIGURE 3 | Time evolution of percent FAME content (% total DW) at three different temperatures (repeated experiment). Error bars represent SD from three independent experiments. SD not visible is overlapped with the symbols.

different only between 9 and 81 h (ANOVA, $p < 0.05$). In terms of the overall lipid content in the vials (mg FAME/vial), **Figure 2B** shows that the total lipid content in each vial as a function of time. Results show a 4.4% reduction in the 40°C experiment and 29.5% reduction in the 70°C experiment strictly based on FAME not incorporating biomass loss.

The losses per vial during the overall experiment were greater for biomass than for lipids. Biomass losses reached 43% when vials were exposed to 70°C while at the lowest temperature tested (4°C) the impact was minimal. Losses of up to 30% in the overall lipid content per vial were observed in this study for 70°C experiment after 156 h, while temperature of 40°C and below seemed to cause minimal impacts.

DISCUSSION

OVERALL BIOMASS AND LIPID CONTENT

The harvesting process exposes microalgae to prolonged darkness, limited gas exchange conditions, and changes in temperature, which will impact the overall composition of the cell. Under normal growth conditions microalgae perform primarily photosynthesis and minimal respiration. During photosynthesis, exogenous carbon dioxide is consumed as a carbon source, water is the electron donor, NADP is the electron acceptor, and molecular oxygen is produced as a byproduct and biomass is produced (Richmond, 2004). However, when microalgae are transferred into a containment with minimal illumination photosynthesis stops and instead respiration occurs (Montaini et al., 1995). During respiration, microalgae consume intracellular carbon reserves as carbon sources, consume molecular oxygen, and carbon dioxide and water are by-products. The respiratory metabolism of stored carbon resources and the parallel oxygen consumption ensure enough energy for temporary survival of cells. Studies have shown that *Tetraselmis suecica* maintained in unsealed vials at 4°C in darkness still had viable cells after 5 months of incubation, while hermetically sealed vessels presented limited survival (Montaini et al., 1995).

Respiration occurring during harvesting is expected to produce changes in the biochemical composition of the biomass. It has been shown in previous studies that during respiration under oxic or anoxic conditions microalgae preferentially consume energy reserves in the form of carbohydrate, followed by proteins and ultimately lipids, which were otherwise supplied by photosynthesis (Rodger Harvey et al., 1995; Aji, 2011). The consumption of internal food reserves results in mass loss (Mishra and Gamage, 2007). Such is the case of the reduction of particulate matter in *Chlorella pyrenoidosa* incubations under anoxic axenic conditions observed by Foree and McCarty (1970). Also, green microalgae *Coelastrum sphaericum* and *Scenedesmus falcatus* incubated under dark conditions at various temperatures (16, 22, and 28°C) reported an overall biomass loss between 2 and 10% during the first 12 h of darkness (Grobelaar and Soeder, 1985). In addition, it has been shown that respiration in *Dunaliella salina* exposed to 10–30°C produced total carbon losses in the order of 50–60% in 20 days (Degens et al., 1968).

During respiration, the energy obtained for cell maintenance is primarily derived from consumption of reserves other than lipids (Montaini et al., 1995; Rodger Harvey et al., 1995; Aji,

2011). Literature shows that total fatty acid content remained unchanged in microalgae *T. suecica* regardless of the time of incubation although cells were presenting loss of viability (conditions: 60 g L⁻¹, preserved at 4°C in hermetically sealed vials up to 90 days) (Montaini et al., 1995). This same experiment with *T. suecica* also showed an increase in percent of total fatty acids (% of total DW) in comparison to the value obtained for the fresh biomass at the beginning of the incubation period. Interestingly, 15 days of incubation produced a 30.4% increase, while 22 days produced 28.4% increase (Montaini et al., 1995). These results agree with the increases of percent FAME (% of total DW) observed in this study. This percent FAME (% of total DW) increase could be the result of (i) mass loss due to consumption of reserves (Montaini et al., 1995), and (ii) liberation of fatty acids from complex proteins and carbohydrates being consumed during respiration processes (Laurens et al., 2012).

The variability in the increases of percent FAME (% of total DW) between the first and second experiment can also originate from variability inherent to microalgal biomass. In the repeated experiment (results in **Figures 2A** and **3**), the biomass used in these two experiments came from different production batches resulting in the differences in initial harvested percent FAME, which impacted the trend. Several factors during microalgae cultivation affect cell composition and lipid profiles (Mayers et al., 2014; Scholz et al., 2014), e.g., different lipids convert to FAME with different efficiencies (e.g., mono-glycerides yields 83.2% FAME, triglycerides yields 100% FAME and phospholipids yields 64.4% FAME) (Laurens et al., 2012). Regardless of the increments in percent FAME (% of total DW) observed in this study, the total lipid content per vial decreased with increase in temperature and was only maintained constant at low temperatures and short incubation times, thus confirming that temperature and time resulting from delays during harvesting can affect final biofuel potential.

In addition to internal reserve consumption, the perishability of biomass can also occur due to toxic effects caused by respiration/fermentation by-products accumulated in the vials (Mishra and Gamage, 2007). Literature shows in a closed container the rate of cell mortality is increased under accumulation of carbon dioxide and excretion of organic acids from fermentation (Degens et al., 1968; Montaini et al., 1995). After the respiration process consumes the available oxygen in an hermetically sealed containment (preventing gas exchange), an oxygen-limited environment will be formed (Mishra and Gamage, 2007). Under limited oxygen conditions, the rate of respiration is dramatically reduced (Grobelaar and Soeder, 1985) and ultimately can lead to anaerobic environments. Anaerobic conditions are harsh as they lead to fermentation and decay (Mishra and Gamage, 2007). Loss of viability and increased broken cells has been observed in microalgae stored under dark anoxic conditions (Montaini et al., 1995; Heasman and Fisheries, 2001; Aji, 2011). In these systems, lower temperatures increased viability of the stored cells.

Reduction of temperature is a method for hindering mass loss and degradation, mainly because respiration and metabolic processes in live cells, as well as several post-mortem processes (e.g., catabolism, autolysis) are enzymatically driven,

with enzyme reaction rates reduced with low temperatures (Kroemer et al., 1995; Mishra and Gamage, 2007). As found in this study, losses were generally reduced at lower temperatures. Despite low temperatures, the mechanisms producing these losses do not completely stop, hence after some time degradation will still occur.

IMPLICATIONS

Biomass and lipid losses due to unexpected delays during harvesting (e.g., equipment malfunction, uncooperative weather, and other unforeseen circumstances) or preprocessing could impact logistic and production costs. Lowering culture temperature minimizes losses but implies investments in transportation with cooled containments, thus rising equipment and operational costs. Cost of inventory will need to be considered in order to maintain reliability as a supplier, with large inventories resulting in costly stock and low inventories increasing the risk (Garstang et al., 2002). The losses observed in this study can also impact plant design parameters, such as the distance from the cultivation site to the location of the separation units as well as the number of processing units needed. In addition to economic implications, the mass losses can also affect the final net environmental impact (Chaoui and Eckhoff, 2014). The final decision about implementation of any preservation strategy will be a result of the techno-economic analysis, which needs to include the potential risks that losses during harvesting represent. Further, the experimental work presented is limited to one strain. It is expected that similar trends would be seen in other strains of microalgae.

ACKNOWLEDGMENTS

The authors would like to acknowledge the Utah State University and the Department of Energy Grant DE-EE0003114 for funding of this study, Dr. Bruce Bugbee and Dr. Curtis Adams for their support with the microalgae cultivation and Hao-Chieh Hsieh and Danna Quinn for their support.

REFERENCES

- Aji, L. P. (2011). The use of algae concentrates, dried algae and algal substitutes to feed bivalves. *Makara J. Sci.* 15. doi:10.7454/mss.v15i1.868
- Batan, L., Quinn, J., Willson, B., and Bradley, T. (2010). Net energy and greenhouse gas emission evaluation of biodiesel derived from microalgae. *Environ. Sci. Technol.* 44, 7975–7980. doi:10.1021/es102052y
- Beal, C., Hebner, R., Webber, M., Ruoff, R., and Seibert, A. F. (2012). The energy return on investment for algal biocrude: results for a research production facility. *Bioenerg. Res.* 5, 341–362. doi:10.1007/s12155-011-9128-4
- Chaoui, H., and Eckhoff, S. (2014). “Biomass feedstock storage for quantity and quality preservation,” in *Engineering and Science of Biomass Feedstock Production and Provision*, eds Y. Shastri, A. Hansen, L. Rodríguez, and K. C. Ting (New York, NY: Springer), 165–193.
- Davis, R., Aden, A., and Pienkos, P. T. (2011). Techno-economic analysis of autotrophic microalgae for fuel production. *Appl. Energy* 88, 3524–3531. doi:10.1016/j.apenergy.2011.04.018
- Davis, R. E., Fishman, D. B., Frank, E. D., Johnson, M. C., Jones, S. B., Kinchin, C. M., et al. (2014). Integrated evaluation of cost, emissions, and resource potential for algal biofuels at the national scale. *Environ. Sci. Technol.* 48, 6035–6042. doi:10.1021/es4055719
- Degens, E. T., Guillard, R. R. L., Sackett, W. M., and Hellebust, J. A. (1968). Metabolic fractionation of carbon isotopes in marine plankton – I. Temperature and respiration experiments. *Deep Sea Res. Oceanogr. Abstr.* 15, 1–9. doi:10.1016/0011-7471(68)90024-7
- Foree, E. G., and McCarty, P. L. (1970). Anaerobic decomposition of algae. *Environ. Sci. Technol.* 4, 842–849. doi:10.1021/es60045a005
- Garstang, J., Weekes, A., Poulter, R., and Bartlett, D. (2002). *Identification and Characterization of Factors Affecting Losses in the Large-Scale, Non-Ventilated Bulk Storage of Wood Chips and Development of Best Storage Practices*. Gloucestershire: Report to the UK Department of Trade and Industry.
- Grobbelaar, J. U., and Soeder, C. J. (1985). Respiration losses in planktonic green algae cultivated in raceway ponds. *J. Plankton Res.* 7, 497–506. doi:10.1093/plankt/7.4.497
- Heasman, M. P., and Fisheries, N. (2001). *Production of Micro-algal Concentrates for Aquaculture: Development and Evaluation of Harvesting, Preservation, Storage and Feeding Technology*. Nelson Bay: NSW Fisheries.
- Jones, S., Davis, R., Zhu, Y., Kinchin, C., Anderson, D., Hallen, R., et al. (2014). *Process Design and Economics for the Conversion of Algal Biomass to Hydrocarbons: Whole Algae Hydrothermal Liquefaction and Upgrading*. Richland, WA: U.S. Department of Energy Bioenergy Technologies Office.
- Khan, S. A., Rashmi, Hussain, M. Z., Prasad, S., and Banerjee, U. C. (2009). Prospects of biodiesel production from microalgae in India. *Renew. Sustain. Energ. Rev.* 13, 2361–2372. doi:10.1016/j.rser.2009.04.005
- Kroemer, G., Petit, P., Zamzami, N., Vayssière, J. L., and Mignotte, B. (1995). The biochemistry of programmed cell death. *FASEB J.* 9, 1277–1287.
- Laurens, L. L., Quinn, M., Van Wychen, S., Templeton, D., and Wolfrum, E. (2012). Accurate and reliable quantification of total microalgal fuel potential as fatty acid methyl esters by in situ transesterification. *Anal. Bioanal. Chem.* 403, 167–178. doi:10.1007/s00216-012-5814-0
- Lundquist, T. J., Woertz, I. C., Quinn, N. W. T., and Benemann, J. R. (2010). *A Realistic Technology and Engineering Assessment of Algae Biofuel Production*. Berkeley, CA: Energy Biosciences Institute.
- Mata, T. M., Martins, A. A., and Caetano, N. S. (2010). Microalgae for biodiesel production and other applications: a review. *Renew. Sustain. Energ. Rev.* 14, 217–232. doi:10.1016/j.rser.2009.07.020
- Mayers, J. J., Flynn, K. J., and Shields, R. J. (2014). Influence of the N:P supply ratio on biomass productivity and time-resolved changes in elemental and bulk biochemical composition of *Nannochloropsis* sp. *Bioresour. Technol.* 169, 588–595. doi:10.1016/j.biortech.2014.07.048
- Mishra, V. K., and Gamage, T. V. (2007). “Postharvest physiology of fruit and vegetables,” in *Handbook of Food Preservation*, Second Edn, ed. M. S. Rahman (London: CRC press).
- Montaini, E., Chini Zittelli, G., Tredici, M. R., Molina Grima, E., Fernández Sevilla, J. M., and Sánchez Pérez, J. A. (1995). Long-term preservation of *Tetraselmis suecica*: influence of storage on viability and fatty acid profile. *Aquaculture* 134, 81–90. doi:10.1016/0044-8486(95)00034-Y
- Quinn, J. C., Smith, T. G., Downes, C. M., and Quinn, C. (2014). Microalgae to biofuels lifecycle assessment-multiple pathway evaluation. *Algal Res.* 4, 116–122. doi:10.1186/1754-6834-6-88
- Quinn, J. C., Yates, T., Douglas, N., Weyer, K., Butler, J., Bradley, T. H., et al. (2012). *Nannochloropsis* production metrics in a scalable outdoor photobioreactor for commercial applications. *Bioresour. Technol.* 117, 164–171. doi:10.1016/j.biortech.2012.04.073
- Richmond, A. (2004). *Handbook of Microalgal Culture Biotechnology and Applied Phycology*. Oxford: Ames, IA: Blackwell Science. Available at: <http://site.ebrary.com/id/10249036>
- Rodger Harvey, H., Tuttle, J. H., and Tyler Bell, J. (1995). Kinetics of phytoplankton decay during simulated sedimentation: changes in biochemical composition and microbial activity under oxic and anoxic conditions. *Geochim. Cosmochim. Acta* 59, 3367–3377. doi:10.1016/0016-7037(95)00217-N
- Rogers, J. N., Rosenberg, J. N., Guzman, B. J., Oh, V. H., Mimbela, L. E., Ghassemi, A., et al. (2014). A critical analysis of paddlewheel-driven raceway ponds for algal biofuel production at commercial scales. *Algal Res.* 4, 76–88. doi:10.1016/j.algal.2013.11.007
- Scholz, M. J., Weiss, T. L., Jing, J., Roth, R., Goodenough, U., Posewitz, M. C., et al. (2014). “Ultrastructure and composition of the *Nannochloropsis gaditana* cell wall,” in *4th International Conference on Algal Biomass, Biofuels and Bioproducts*.
- Sills, D. L., Paramita, V., Franke, M. J., Johnson, M. C., Akabas, T. M., Greene, C. H., et al. (2012). Quantitative uncertainty analysis of life cycle assessment for algal biofuel production. *Environ. Sci. Technol.* 47, 687–694. doi:10.1021/es3029236

- Thilakaratne, R., Wright, M. M., and Brown, R. C. (2014). A techno-economic analysis of microalgae remnant catalytic pyrolysis and upgrading to fuels. *Fuel* 128, 104–112. doi:10.1016/j.fuel.2014.02.077
- Woertz, I. C., Benemann, J. R., Du, N., Unnasch, S., Mendola, D., Mitchell, B. G., et al. (2014). Life cycle GHG emissions from microalgal biodiesel – a CA-GREET model. *Environ. Sci. Technol.* 48, 6060–6068. doi:10.1021/es403768q
- Wyche, S. V., and Laurens, L. M. L. (2013). *Determination of Total Lipids as Fatty Acid Methyl Esters (FAME) by In situ Transesterification*. Golden, CO: National Renewable Energy Laboratory.

Conflict of Interest Statement: The authors declare that the research was conducted in the absence of any commercial or financial relationships that could be construed as a potential conflict of interest.

Received: 01 September 2014; accepted: 21 March 2015; published online: 15 April 2015.

Citation: Napan K, Christianson T, Voie K and Quinn JC (2015) Quantitative assessment of microalgae biomass and lipid stability post-cultivation. *Front. Energy Res.* 3:15. doi: 10.3389/fenrg.2015.00015

This article was submitted to *Bioenergy and Biofuels*, a section of the journal *Frontiers in Energy Research*.

Copyright © 2015 Napan, Christianson, Voie and Quinn. This is an open-access article distributed under the terms of the Creative Commons Attribution License (CC BY). The use, distribution or reproduction in other forums is permitted, provided the original author(s) or licensor are credited and that the original publication in this journal is cited, in accordance with accepted academic practice. No use, distribution or reproduction is permitted which does not comply with these terms.



Design, construction, and validation of an internally lit air-lift photobioreactor for growing algae

Esteban Hincapie¹ and Ben J. Stuart^{2*}

¹ Department of Mechanical Engineering, Russ College of Engineering and Technology, Ohio University, Athens, OH, USA

² Department of Civil Engineering, Russ College of Engineering and Technology, Ohio University, Athens, OH, USA

Edited by:

Umakanta Jena, Desert Research Institute, USA

Reviewed by:

Alberto Scoma, Ghent University, Belgium

Ashish Bhatnagar, Maharshi Dayanand Saraswati University, India
K. C. Das, University of Georgia, USA

*Correspondence:

Ben J. Stuart, 122 Stocker Center, Athens, OH 45701, USA
e-mail: stuart@ohio.edu

A novel 28 L photobioreactor for growing algae was developed using fiber optics for internal illumination. The proposed design uses the air-lift principle to enhance the culture circulation and induce light/dark cycles to the microorganisms. Optical fibers were used to distribute photons inside the culture media providing an opportunity to control both light cycle and intensity. The fibers were coupled to an artificial light source; however, the development of this approach aims for the future use of natural light collected through parabolic solar collectors. This idea could also allow the use of opaque materials for photobioreactor construction significantly reducing costs and increasing durability. Internal light levels were determined in dry conditions and were maintained above $80 \mu\text{mol}/(\text{s}\cdot\text{m}^2)$. The hydrodynamic equations of the air-lift phenomena were explored and used to define the geometric characteristics of the unit. The reactor was inoculated with the algae strain *Chlorella* sp. and sparged with air. The reactor was operated under batch mode and daily monitored for biomass concentration. The specific growth rate constant of the novel device was determined to be 0.011 h^{-1} . The proposed design can be effectively and economically used in carbon dioxide mitigation technologies and in the production of algal biomass for biofuel and other bioproducts.

Keywords: algae photobioreactor, air-lift, internally lit, hydrodynamic design, specific growth rate

INTRODUCTION

Microalgae have several advantages over other biological sources as a feedstock for biofuels and bioproducts. Algae have a higher ratio of oil production to required cultivated area compared with common bioenergy sources such as corn, soybean, rapeseed, jatropha, and others (Chisti, 2008). Microalgae can also be used for starch production and its subsequent ethanol production through yeast fermentation, achieving efficiencies similar to the best available crops (Harun et al., 2010). Another characteristic of algae is that it can double its biomass at an exponential rate requiring less surface area for the production of biofuels and bioproducts (Framptona et al., 2013). Microalgae could also be used for carbon dioxide capture and recycling since 1.7 kg of CO_2 is required for every kilogram of biomass generated (Ghorbani et al., 2014).

There are several advantages of photobioreactors over conventional open algal cultivation systems. Closed systems allow more precise control over critical algal growth parameters including pH, nutrient delivery, light intensity, light cycle duration, ultraviolet exposure, and mixing (Kunjapur and Eldridge, 2010). Also, photobioreactors provide an isolated environment with a much lower probability of contamination by other algal strains or microorganisms. Typically, these reactors require less land for the same biomass production (Borowitzka, 1999). Finally, photobioreactors could extend the growth potential from a current few microorganism strains used in open systems to more than thousands of strains of phototrophic algae (Tredici, 1999).

However, the design and scale up of photobioreactors still require further development. The most important areas have been

identified as (1) efficient lighting processes, (2) efficient supply of carbon dioxide and oxygen removal, and (3) energy consumption for adequate mixing (Clemens, 2009). Light delivery remains a challenging problem for photobioreactor scale up. Surface lit photobioreactors require a large surface area to volume ratio to transmit enough light to support the photosynthetic process (Janssen et al., 2003). Extensive transparent surfaces are difficult and expensive to build, and the cells closer to the surface of the photobioreactor may be photo inhibited while cells in the center of the vessel may be photo limited affecting algal productivity (Gris et al., 2014). The literature present other internal lighting approaches such as plastic light guides (Zijffers et al., 2008) or internal fluorescent bulbs surrounded by glass containers (Ogbonna et al., 1996).

Fiber optics have also been proposed in the past to deliver light to microalgal cultures inside the reactor as an alternative to using glass tubes with outside radiation. Xue et al. (2013) proposed an air-lift photobioreactor using fiber optics but they encountered leakage problems in their design. Another bubble column bioreactor design incorporated optical fibers to control illumination where the fiber optics were introduced from the top of the column to avoid leakage issues (Bayless, 2007). This current work pursued the integration of an air-lift reactor design that incorporated fiber optic illumination. Here, we present the design process of the novel photobioreactor to address uniform light distribution, fiber optic support, and leakage prevention and results that indicate that this approach can be used for microalgal production.

MATERIALS AND METHODS

PHOTOBIOREACTOR DESIGN AND CONSTRUCTION

The development of the novel air-lift photobioreactor followed the stages typical of a design process. The first part considered general aspects of the systems such as light and dark areas, size, and structural support. Subsequent considerations focused on fiber optic support and the hydrodynamic modeling of the system.

The conceptual design for the reactor is depicted in **Figure 1**. The height was 1171 mm with a volume of 28 L. The air-lift reactor was composed of two zones; one illuminated and the other dark. This division combined with the induced circulation imposed light/dark cycles upon the microorganisms. Microalgae are continuously exposed to such cycles in nature as consequence of the mixing in the bodies of water (Peers et al., 2009), and the proposed photobioreactor provided an environment which simulated the natural conditions for microalgae. Although the specific design proposed by the researchers induces light cycles, the idea of using fiber optics inside the bioreactor could provide continuous exposure to light by extending the fiber array to both chambers of the bioreactor.

The containment vessel comprised materials that offer ease of construction and may be made leak proof at a reasonable cost compared to glass. A commercial material that was easy to obtain and work with was chosen for the construction, and material homogeneity was crucial to constructability and to maintain compatibility of the sub-components. It was also necessary to take into consideration important constraints of the material application such as permanent immersion under water, tolerance with microalgae, and stabilization properties.

Steel pipes were eliminated from consideration because of difficulty in fabrication (i.e., drilling and cutting) and the potential for corrosion in aqueous environments, and stainless steel was expensive. Acrylic was considered as it has been used in past photobioreactor applications (Hsieh and Wu, 2009); however, the acrylic bonding process is more complicated than other plastics and requires more expensive products. As the bonding process is well known and used in everyday plumbing applications, PVC was chosen as the best commercial material for the laboratory unit. Both header and draft tube pipes were made of white PVC to maximize the reflection of the light inside the illuminated area. The reflection of the light waves by white plastic is beneficial for light availability in algal cultures (Slegers et al., 2013). This also provided a separation between the dark and light cycles. It should be noted that other materials will need to be evaluated in the future since it has been suggested that PVC could promote biofilm formation (Guzman et al., 2007).

The riser was illuminated with fiber optics that were directed through the header pipe placed in the center of the reactor as shown in **Figures 1** and **2**. The header served as the conduit to carry the fiber optic cables inside the reactor volume, as well as the gas supply line and provided ease of construction to avoid leakage problems. The optical fibers carried inside the header minimized interference with the algal growth and provided sufficient space for the 44 optical fibers (**Figure 2**). Once the fibers were directed from the light source into the header, a subsystem of plastic bolts was developed to uniformly distribute photons within the algal culture. The header and bolts also provided the structural support required

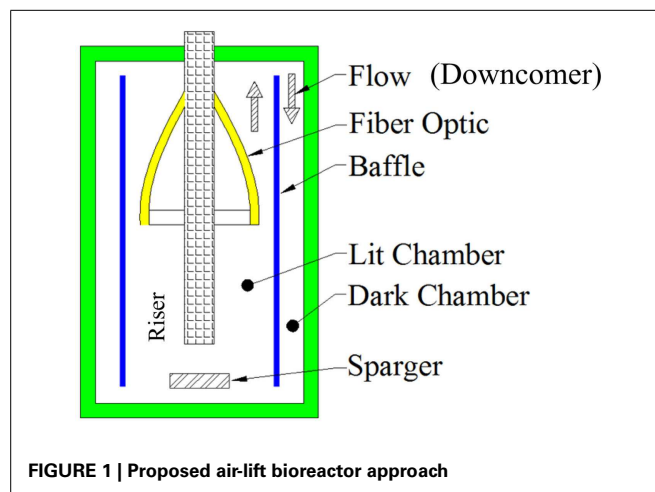


FIGURE 1 | Proposed air-lift bioreactor approach

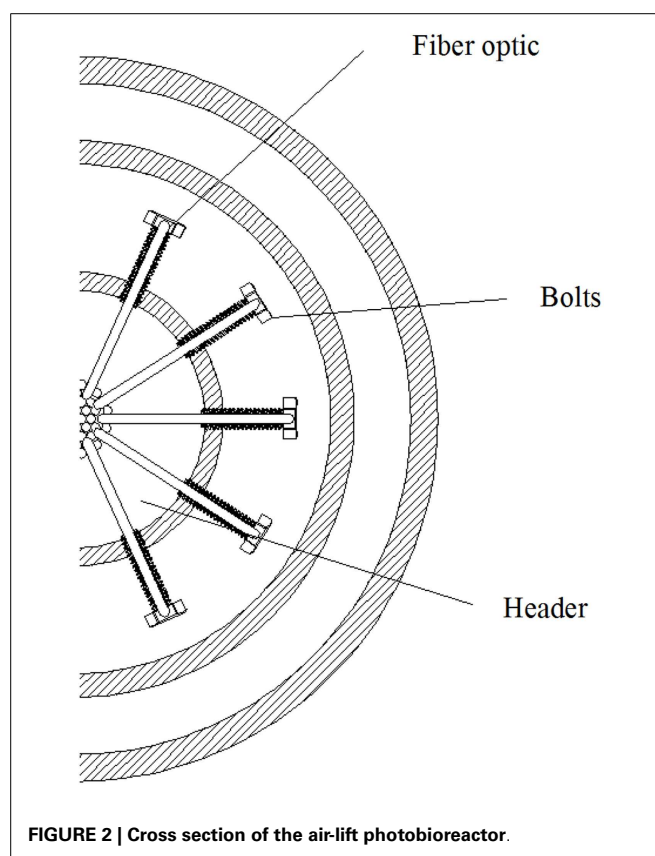


FIGURE 2 | Cross section of the air-lift photobioreactor.

to hold the fiber optics in a specific location in the flow path of the growth media that carried the algal culture. A draft tube served as the required baffle to allow circulation of the growth media inside the air-lift device. The liquid flowed upwards in the area contained between the header and draft tube, while the media moved downward between the draft tube and the containment vessel (**Figure 1**, as indicated by arrows).

Adequate structural support for all system components was also addressed. The downcomer and riser were supported in a way to guarantee stability and prevent leaking of the algal culture.

Since the air-lift reactor has an internal baffle, the design process also considered a support for the embedded system (not shown). The sparger was designed with four injection points as shown in **Figure 6** to allow for adequate distribution of the gas inside the riser chamber while minimizing the possibility of biofouling. The position of the sparger was defined inside the baffle such that it optimizes the circulation flow as explained elsewhere (Chisti, 1989).

The size of the containment vessel was determined by a combination of two criteria; (1) the availability of the materials in the commercial market, and (2) air-lift systems should follow a general geometric rule. In order to guarantee smooth flow between the components, the ratio of downcomer area (A_d) to riser area (A_r) should be approximately unity (Chisti, 1989):

$$\frac{A_r}{A_d} \cong 1 \quad (1)$$

The proposed design accommodated this geometric restriction through the selection of appropriate pipe diameters. Additionally, this ratio affects retention time in each section of the reactor and could easily be manipulated as a method of controlling light/dark cycle.

LIGHT SYSTEM

The proposed design used plastic optical fiber (POF) cables (PGR-FB3000®, Moritex, USA) instead of glass primarily because POFs are stronger, supporting more stress and pressure than glass ones. Further, POFs have more flexibility and a smaller bending radius than glass systems, which is a primary reason they are broadly used in architectural and automobile applications. Finally, POFs are traditionally less expensive than optical fibers made of glass (Bailey, 2003).

This research used an artificial source to provide the light for growing the microalgae. The light source was a microscope illuminator powered with a EKE light bulb of 21 V and 150 W (GE lighting, Cleveland, OH, USA). Previous publications have suggested an optimum light intensity for microalgae between 80 and 120 $\mu\text{mol}/(\text{s}\cdot\text{m}^2)$ (Csavina, 2008; Li et al., 2012). In order to achieve the required light intensity inside the photobioreactor, it was necessary to determine the number of optical fibers at each level in the system to achieve the minimum target of 80 $\mu\text{mol}/(\text{s}\cdot\text{m}^2)$. This approach was based on the theoretical treatment of light as a particle (photon). First, the intensity provided by the light source was measured using a Li-cor LI 190 quantum sensor facing directly toward the light bulb. It was then possible to determine the number of micromoles of photons per fiber based on the area of each cable. Finally, the number of fibers required was computed taking into consideration the area of the riser previously defined and was determined to be eleven POFs per level (**Table 1**).

To confirm that the target light intensity [80 $\mu\text{mol}/(\text{s}\cdot\text{m}^2)$] was achieved with the eleven fibers per level, a column mock-up was developed as shown in **Figure 3**. The rig was constructed using the same pipe dimensions as defined previously with two mounted optical fibers (**Figure 3A**). The results of the light readings are shown in **Table 2**. **Figure 4** provides a front view of the

Table 1 | Light intensity calculations for the photobioreactor.

Variable	Magnitude	Units
Measured photon density of the light source	11,000 \pm 500	$\mu\text{mol}/(\text{s}\cdot\text{m}^2)$
Area of the fiber	7	mm^2
Photons per fiber	0.08	$\mu\text{mol}/(\text{s}\cdot\text{fiber})$
Number of fibers per level	11	fibers
Total incident light per level	0.91	$\mu\text{mol}/\text{s}$
Average irradiance per level	73	$\mu\text{mol}/(\text{s}\cdot\text{m}^2)$

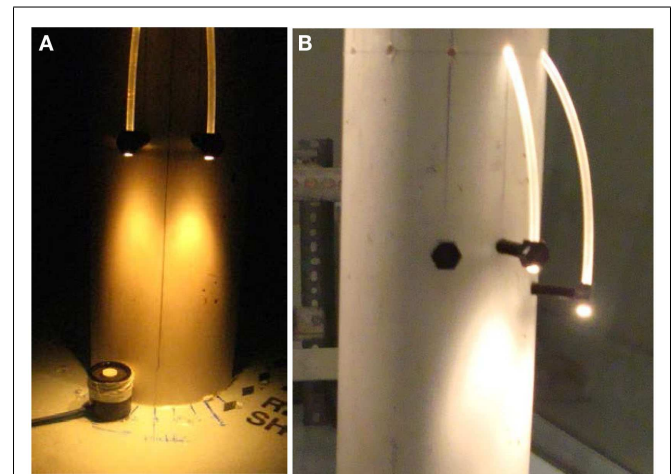


FIGURE 3 | (A) Measurement of light levels inside the photobioreactor; **(B)** Different level spacing's under consideration.

Table 2 | Light intensity levels inside the reactor.

Level distance (mm)	Light intensity $\mu\text{mol}/(\text{s}\cdot\text{m}^2)$ for each position							
	1	2	3	4	5	6	7	Peak
35	55	437	544	215	599	603	98	603
95	124	170	206	213	211	185	144	213
120	63	84	99	103	105	98	69	105

measurement taken between two POFs. Positions 1 and 7 measured the lowest light intensity since the light sensor was placed outside both POFs, respectively as indicated in **Figure 4**. Positions 2 and 3 were beneath the first POF light stream, positions 5 and 6 were beneath the second POF, while position 4 was in the middle of both POFs. The average and peak light intensities at all distances exceeded the required target; however, since actual light levels during growth conditions will be lower as the concentration of microalgae increases, it was concluded that the proposed spacing of 120 mm will meet the minimum light requirement even with high density cultures.

Bolts provided the necessary support required while maintaining a structurally sound point for the fiber optic cables (**Figures 3** and **4**). To maintain material compatibility with the pipes, PVC

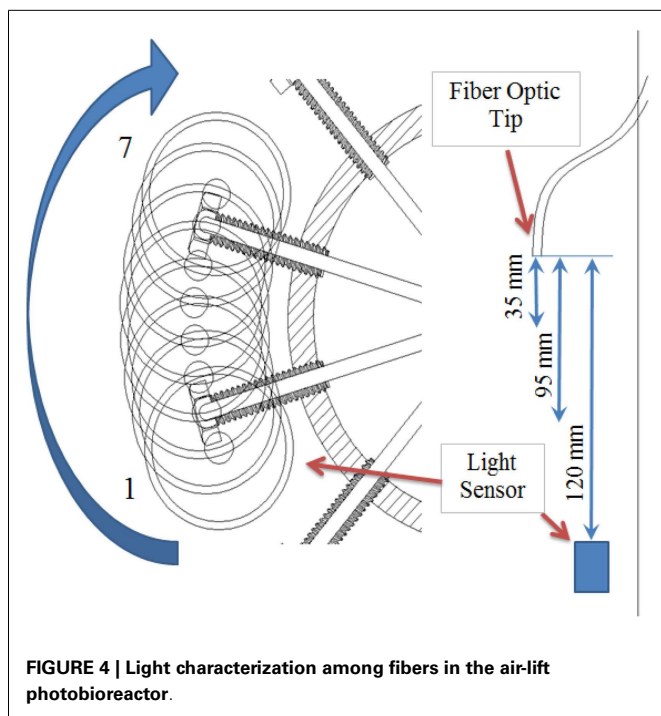


FIGURE 4 | Light characterization among fibers in the air-lift photobioreactor.

bolts were chosen as the element to provide the support. The proposed design consisted of eleven bolts per level, where each bolt had a hole in the head equal to the diameter of the POF. The bolts were attached to the header via a threaded hole, providing enough strength for a robust construction. This was important to assure that the bending force of the fiber optic did not loosen or release the bolts from their place. Additionally, the threaded joints permitted quick disassembly of the bolts to allow for future modifications to the number of fibers or levels.

FINAL DIMENSIONS AND CIRCULATION MODEL

The optimum mixing velocity in algal cultures is a tradeoff between efficient mass transfer and minimizing shear stresses. An extensive literature review was performed to determine liquid and gas velocities used in past algal bioreactors (Table 3). Previous studies have been successful growing algae in the superficial gas velocity (U_g) range of 0.07–2.5 cm s^{-1} , while an upper limit of 3.4 cm s^{-1} was reported as the onset of cell damage due to shear stress. Therefore, the average of the lowest and highest reported values was used as the superficial gas velocity for the demonstration tests.

The modeling equations proposed by Chisti were solved by iteration of Eq. 2:

$$U_{Lr} = \left[\frac{2gh_D(\epsilon_r - \epsilon_d)}{K_B \left(\frac{A_r}{A_d} \right)^2 \frac{1}{(1-\epsilon_d)^2}} \right]^{0.5} \quad (2)$$

where U_{Lr} is the superficial liquid velocity, g is gravity, h_d is the height of the column, ϵ_r and ϵ_d are the gas holdup in the riser and downcomer, and K_b is the frictional loss coefficient. The gas hold up is the volumetric ratio of gas in the liquid (volume of gas per

Table 3 | Calculated superficial gas velocities for previous air-lift and bubble column reactors reported in the literature.

Study	Reactor diameter (cm)	Type	U_g (cm s^{-1})	Gas Flow (L min^{-1})
Ranjbar et al. (2008)	4.6	Air Lift	0.07	0.1
Ranjbar et al. (2008)	4.6	Air Lift	0.13	0.1
Vasconcelos Barbosa (2003)	3.5	Bubble Column	0.50	0.3
Vasconcelos Barbosa (2003)	21	Bubble Column	0.60	12.5
García Camacho et al. (1999)	8	Bubble Column	1.00	3.0
This research	20.3	Air Lift	1.80	13.3
Vasconcelos Barbosa (2003)	21	Bubble Column	2.50	52.0
Vasconcelos Barbosa (2003)	3.5	Bubble Column	3.40	2.0
García Camacho et al. (1999)	8	Bubble Column	5.00	15.1

volume of liquid), and the superficial liquid velocity is the velocity of the liquid without the gas fraction. The true liquid velocity considers the gas fraction in the volume and therefore is higher than the superficial liquid velocity. Velocities for different gas flow rates are shown in Table 4 with the selected gas flow rate for our design shown in gray.

The expected superficial liquid velocity in the riser was 9.2 cm s^{-1} and the true liquid velocity was 9.6 cm s^{-1} . Based on the length of the riser (70 cm), the model predicted a mean cell residence time (MCRT) of 8 s in the riser section. This period is also the light side period of the circulation. The model also predicted a true liquid velocity in the downcomer of 14 cm s^{-1} , yielding a MCRT in the dark side of the system of 5 s. As the total system MCRT was expected to be 18 s, an algal cell would be in the riser for 8 s, in the downcomer for 5 s, and held up in the bottom and upper connection chambers of the system for an additional 5 s.

CIRCULATION TESTS

A non-reactive tracer test was performed to determine the velocities and mixing characteristics of the proposed photobioreactor. A peristaltic pump was used to sample at a constant volumetric flow rate from two points of the reactor (top and bottom) through separate sample lines. The reactor was filled with RO water and 10 mL of a 1 mM NaCl solution was injected through the top flange at the beginning of the test. Three aliquots were sampled every 5 s to measure the change in the Chloride ion concentration. The vials were analyzed via Ion Chromatograph (Dionex, 25A) equipped with an AS14A Column.

PRODUCTIVITY TESTS

Five tests were performed to determine the specific growth rate in the photobioreactor and develop the operation and maintenance procedures of the bioreactor. The alga that was used for all the tests was *Chlorella* sp. (UTEX, 2714) and two experiments used the

Table 4 | Calculated MCRTs for different gas flow rates.

Gas hold up (%)	Gas flow rate (L min ⁻¹)	Total MCRT (s)	MCRT riser (s)	Superficial gas velocity (cm s ⁻¹)	Superficial liquid velocity (cm s ⁻¹)	True liquid velocity (cm s ⁻¹)
3.0	9	20	11	0.9	7.8	8.1
3.7	11	19	10	1.2	8.5	8.9
4.2	13.3	18	10	1.8	9.2	9.6
4.8	16	17	9	2.2	9.7	10.2
5.3	18	16	9	2.5	10.2	10.8

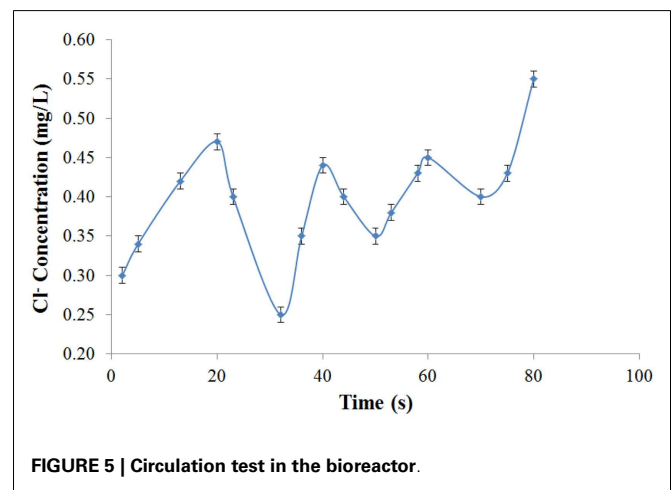
commercial nutrient product Botanicare® and three experiments used Bristol media (as recommended by UTEX). The motivation for investigating the commercial product Botanicare® was to replace the expense of a defined media (Bristol) with a more economical nutrient source. Botanicare® is composed of 3% soluble nitrogen, 2% P₂O₅, 4% K₂O, 1% Ca, and 0.5% Mg. However, as explained below, it was necessary to transition to Bristol media due to pH control issues when using Botanicare® (UTEX Bristol Media Recipe).

All productivity tests were performed under the same air flow rate of 13.3 LPM. As the bubble flow in the constrained space (riser) provided a continuous agitation over the optical fiber tips, it was assumed this action would keep them clean from algal attachment and fouling. The disassembling and inspection of the internal components of the reactor between each run verified the cleaning action of the bubbles when using Botanicare® as the media as shown in **Figure 6**. However, the tests performed with Bristol media demonstrated significant algal attachment to the internal walls of the bioreactor. Nevertheless, the tips of POF were never covered by microalgae ensuring the light delivery through the growth cycle.

GROWTH RATE MEASUREMENT

Samples were obtained through a draining valve which was flushed prior to sample collection to assure that the sampled liquid was representative of the current culture. A 40 mL aliquot of the algal culture was drained daily from the reactor and three 8 mL volumes were separated from the sample and their *in vivo* fluorescence determined and recorded. The standard deviation shown in **Figures 7** and **8** correspond to $n=3$ for each reading. The fluorometer used to determine the chlorophyll *a* readings was a TD 700 (Turner Designs, CA, USA). The fluorometer calibration was checked biweekly by the use of a Red Solid Standard. The remaining sample volume was used to determine the pH using a pHtestr 3+ (Oakton, Vernon Hills, IL, USA). The target pH was 6.8 ± 1.0 based on the UTEX media specifications. However, maintaining this target was particularly difficult when using Botanicare® since this product has a pH close to 2 in a concentrated solution without buffer. This created pH swings that affected the growth of the microalgae in the bioreactor for Test #1.

To develop the correlation between cell count and fluorescence, samples were diluted until a chlorophyll *a* concentration lower than $10 \mu\text{g L}^{-1}$ was achieved. The dilution was recorded and the number of cells in the diluted sample was determined using a microscope and a Nannoplankton chamber (ID#533, Phycotech, MI, USA). The variation in the number of cells was compared to

**FIGURE 5 | Circulation test in the bioreactor.**

the *in vivo* fluorescence of the algal strain and a linear correlation was obtained with an R^2 of 0.965.

The specific growth rate constant (μ) for different intervals was calculated for each test based on Eq. 3 where N_i and N_f are the cell populations at the initial and final time. This equation was used to calculate μ for specific time intervals as described below (Wood et al., 2005).

$$\mu = \frac{\ln(N_i/N_f)}{t_f - t_i} \quad (3)$$

RESULTS AND DISCUSSION

CIRCULATION TIME

A mixing characterization experiment was developed to validate the theoretical model. The change in chloride concentration with time is provided in **Figure 5**. The oscillation in the concentration is caused by the upward and downward circulation in the air-lift system as predicted by the equations and can be analyzed to determine experimental MCRT. These results show that the MCRT of the system is between 21 and 22 s; slightly longer than the predicted time of 18 s. The increased experimental MCRT is most likely attributable to slightly larger than predicted holdup volumes at the top and bottom of the reactor.

PRODUCTIVITY

The increase in cell density and the corresponding pH values over time for Tests 1 and 2 using Botanicare® as the growth media is presented in **Figure 7**. In Test 1, the biomass increased for 91 h,

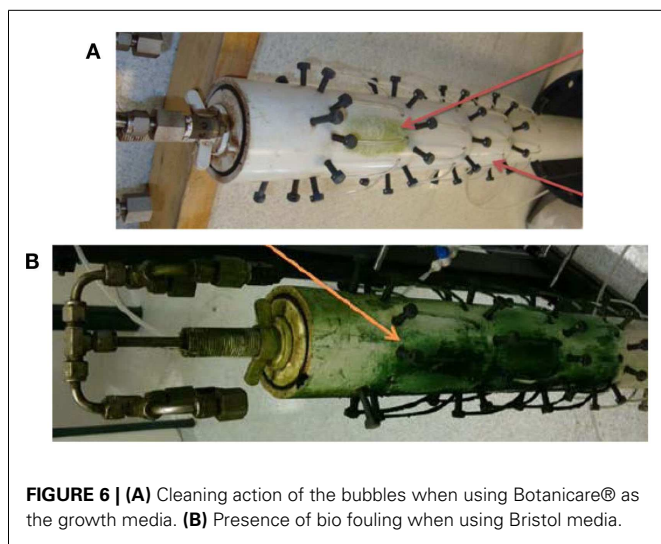


FIGURE 6 | (A) Cleaning action of the bubbles when using Botanicare® as the growth media. **(B)** Presence of bio fouling when using Bristol media.

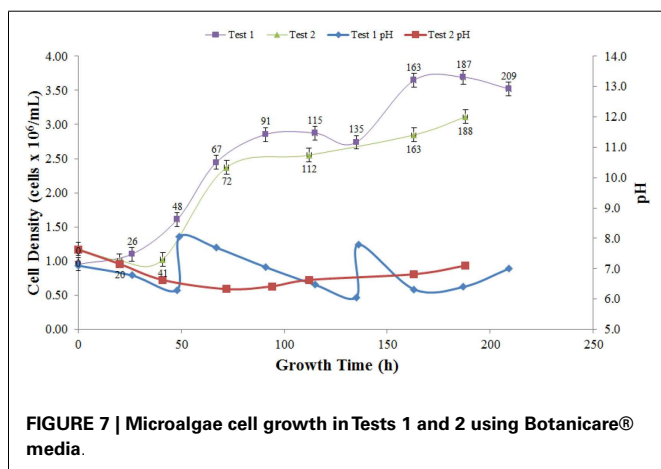


FIGURE 7 | Microalgae cell growth in Tests 1 and 2 using Botanicare® media.

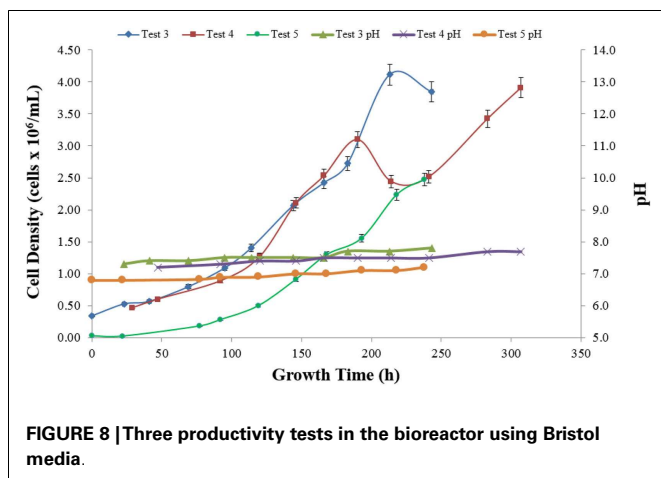


FIGURE 8 | Three productivity tests in the bioreactor using Bristol media.

then decreased slightly until hour 135. It is hypothesized that the drop in pH inhibited optimal growth conditions since the Botanicare media did not have any pH buffer. The increases in pH during Test 1 seen in Figure 7 correspond to an addition of NaOH needed

Table 5 | Selected productivity rates.

Test	Interval (h)	Growth rate (h ⁻¹)	Linear coefficient of determination
1	0–91	0.013	0.95
2	41–112	0.012	0.78
3	0–213	0.011	0.99
4	0–190	0.012	0.98
5	0–238	0.021	0.94

to raise the pH to a more suitable biological range. The exponential growth constant for Test 1 between 0 and 91 h was 0.013 h⁻¹ ($R^2 = 0.955$), with maximum growth between hours 48 and 67 ($\mu = 0.022$ h⁻¹). Test 2 exhibited a slight decrease in Chlorophyll *a* concentration during the first 41 h, indicating that a period of acclimatization was experienced by the algae. This was followed by a consistent increase over the remaining 160 h, resulting in an average growth rate between hours 41 and 112 of 0.012 h⁻¹ ($R^2 = 0.78$) and a maximum specific growth rate over interval 41–72 h of 0.027 h⁻¹.

Figure 8 presents the growth curves for Tests 3–5 and growth rate data for selected intervals representative of the average of the five tests are presented in Table 5. The *Chlorella* culture in Test 3 exhibited sustained growth from 0.4 to 4.0 × 10⁶ cells mL over 213 h, resulting in a calculated productivity of 0.011 h⁻¹ with an R^2 coefficient of 0.99. The biomass decrease at the end was assumed to be due to achievement of stationary phase of the culture. Test 4 demonstrated an increase in biomass over time, resulting in an average specific growth rate over the first 161 h of 0.012 h⁻¹ and a maximum rate between hours 120 and 146 of 0.020 h⁻¹. The decrease in fluorescence at hour 214 corresponds with an interruption in the light source (burned-out bulb), but recovery upon replacement was immediate and aggressive. Test 5 exhibited a specific growth rate of 0.022 h⁻¹ with an R^2 of 0.94. This rate is similar to the maximum growth rate seen in each of the previous tests and is the same as the value of 0.022 h⁻¹ reported in the literature for optimized systems (Miron Sanchez et al., 2000).

Table 5 summarizes the growth rate data for all five tests. Overall, the novel internally lit photobioreactor achieved growth rates previously reported in the literature for optimized systems indicating that fiber optics could be used as tool for light delivery to microalgal cultures. Further work is required to optimize system operation (e.g., pH control), explore larger volumes, and develop a comparison between internally lit and outdoor designs.

CONCLUSION

The novel internally lit air-lift algae bioreactor was able to operate successfully for 3 months without leakage of the media or major modifications. All internal components of the system and subsystems remained operative and a simple maintenance procedure was developed for cleaning and continued operation. The minimum average light intensity in the illuminated chamber was 89 μmol/(s·m²) with the proposed arrangement of 11 fiber optic cables per level; in excess of the defined lower target of 80 μmol/(s·m²) and validating the calculation that determined

the number of fibers required from the reactor section mock-up. Although some biofilm was detected on the walls of the reactor for three of the tests, the air bubbles demonstrated an effective cleaning effect over the fiber optics as evidenced by the fact that the fiber optic cables tips were never found to be clogged during the visual inspections after three months of operation.

Chlorella vulgaris was successfully grown at different specific constant growth rates in the air-lift system. A mean specific growth rate constant of 0.011 h^{-1} was achieved for periods over 140 h with maximum rates exceeding 0.020 h^{-1} for each of the five tests. Further, Test 5 demonstrated a sustained a growth rate of 0.020 h^{-1} over the 240 h duration of the experiment. These results collectively demonstrate that an internally lit photobioreactor can be used for microalgal cultures as an option to current glass photobioreactors. More work is required to scale up the system and perform a comparison with outdoor designs.

ACKNOWLEDGMENTS

This work was funded in part by a grant from the US Department of Energy (award number DE-FG36-08GO88083).

REFERENCES

- Bailey, D. (2003). *Practical Fiber Optics*. Perth: Elsevier, 81–93.
- Bayless, D. (2007). *Apparatus and Method for Growing Biological Organisms for Fuel and Other Purposes*. United States of America Patent 0264708.
- Borowitzka, A. (1999). Commercial production of microalgae: ponds, tanks, tubes and fermenters. *J. Biotechnol.* 70, 313–321. doi:10.1016/S0168-1656(99)00083-8
- Chisti, Y. (1989). *Air Lift Bioreactors*. New York, NY: Elsevier Applied Science, 12–29.
- Chisti, Y. (2008). Biodiesel from microalgae beats bioethanol. *Trends Biotechnol.* 26, 126–131. doi:10.1016/j.tibtech.2007.12.002
- Clemens, P. (2009). Design principles of photo-bioreactors for cultivation of microalgae. *Eng. Life Sci.* 9, 165–177. doi:10.1007/s00449-013-0898-2
- Csavina, J. (2008). *The Optimization of Growth Rate and Lipid Content from Select Algae Strains*. MS thesis, Ohio University, Athens.
- Frampton, M. F., Gurneya, R. H., Dunstana, G. A., Clementsona, L. A., Toiflc, M. C., Pollardc, C. B., et al. (2013). Evaluation of growth, nutrient utilization and production of bioproducts by a wastewater-isolated microalga. *Bioresour. Technol.* 130, 261–268. doi:10.1016/j.biortech.2012.12.001
- García Camacho, F., Contreras Gómez, A., Ación Fernández, F. G., Fernández Sevilla, J., and Grima, E. M. (1999). Use of concentric-tube airlift photobioreactors for microalgal outdoor mass cultures. *Enzyme Microb. Technol.* 24, 164–172. doi:10.1016/S0141-0229(98)00103-3
- Ghorbani, A., Rahimpour, H. R., Ghasemi, Y., Zoughi, S., and Rahimpour, M. R. (2014). A review of carbon capture and sequestration in Iran: microalgal biofixation potential in Iran. *Renew. Sust. Energy Rev.* 35, 73–100. doi:10.1016/j.rser.2014.03.013
- Gris, B., Morosinotto, T., Giacometti, G. M., Bertucco, A., and Sforza, E. (2014). Cultivation of *Scenedesmus obliquus* in photobioreactors: effects of light intensities and light–dark cycles on growth, productivity, and biochemical composition. *Appl. Biochem. Biotechnol.* 172, 2377–2389. doi:10.1007/s12010-013-0679-z
- Guzman, K., La Motta, E. J., McCorquodale, J. A., Rojas, S., and Ermogenous, M. (2007). Effect of biofilm formation on roughness coefficient and solids deposition in small-diameter PVC sewer pipes. *J. Environ. Eng.* 133, 364–371. doi:10.1061/(ASCE)0733-9372(2007)133:4(364)
- Harun, R., Danquaha, M. K., and Fordea, G. M. (2010). Microalgal biomass as a fermentation feedstock for bioethanol production. *J. Chem. Technol. Biotechnol.* 85, 199–203. doi:10.1002/jctb.2287
- Hsieh, C. H., and Wu, W. T. (2009). A novel photobioreactor with transparent rectangular chambers for cultivation of microalgae. *Biochem. Eng. J.* 46, 300–305. doi:10.1016/j.bej.2009.06.004
- Janssen, M., Tramper, J., Mur, L. R., and Wijffels, R. H. (2003). Enclosed outdoor photobioreactors: light regime, photosynthetic efficiency, scale-up, and future prospects. *Biotechnol. Bioeng.* 81, 193–210. doi:10.1002/bit.10468
- Kunjapur, A. M., and Eldridge, R. B. (2010). Photobioreactor design for commercial biofuel production from microalgae. *Ind. Eng. Chem. Res.* 49, 3516–3526. doi:10.1021/ie901459u
- Li, Y., Zhou, W., Hu, B., Min, M., Chen, P., and Ruan, R. (2012). Effect of light intensity on algal biomass accumulation and biodiesel production for mixotrophic strains *Chlorella kessleri* and *Chlorella protothecoide* cultivated in highly concentrated municipal wastewater. *Biotechnol. Bioeng.* 109, 2222–2229. doi:10.1002/bit.24491
- Miron Sanchez, A., Garcia Camacho, F., Contreras Gomez, A., and Molina Grima, E. (2000). Bubble column and airlift photobioreactors for algal culture. *AIChE J.* 46, 1872–1887. doi:10.1002/aic.690460915
- Ogbonna, J. C., Yada, H., Masui, H., and Tanaka, H. (1996). A novel internally illuminated stirred tank photobioreactor for large-scale cultivation of photosynthetic cells. *J. Ferment. Bioeng.* 82, 61–67. doi:10.1016/0922-338X(96)89456-6
- Peers, G., Truong, T., Ostendorf, E., Busch, A., Elrad, D., Grossman, A., et al. (2009). An ancient light-harvesting protein is critical for the regulation of algal photosynthesis. *Nature* 462, 518–521. doi:10.1038/nature08587
- Ranjbar, R., Inoue, R., Katsuda, T., Yamaji, H., and Katoh, S. (2008). High efficiency production of astaxanthin in an air lift photobioreactor. *J. Biosci. Bioeng.* 106-2, 204–207. doi:10.1263/jbb.106.204
- Slegers, P. M., van Beveren, P. J., Wijffels, R. H., van Straten, G., and van Boxtel, A. J. (2013). Scenario analysis of large scale algae production in tubular photobioreactors. *Appl. Energy* 105, 395–406. doi:10.1016/j.apenergy.2012.12.068
- Tredici, M. (1999). *The Encyclopedia of Bioprocess Technology*. New York, NY: John Wiley.
- UTEX. Available at: <http://www.sbs.utexas.edu/utex/algaeDetail.aspx?algaeID=5235>
- UTEX Bristol Media Recipe. Available at: <http://www.sbs.utexas.edu/utex/mediaDetail.aspx?mediaID=29>
- Vasconcelos Barbosa, M. (2003). *Microalgal Photobioreactors: Scale Up and Optimization*. Ph. D. thesis. Wageningen: Wageningen University.
- Wood, A. M., Everroad, R. C., and Wingard, L. M. (2005). *Measuring Growth Rates in Microalgal Cultures. Algal Culturing Techniques*. San Diego, CA: Elsevier Academic Press, 269–285.
- Xue, S., Zhang, Q., Wu, X., Yan, C., and Wei, C. (2013). A novel photobioreactor structure using optical fibers as inner light source to fulfill flashing light effects of microalgae. *Bioresour. Technol.* 138, 141–147. doi:10.1016/j.biortech.2013.03.156
- Zijffers, J. W. E., Janssen, M., Tramper, J., and Wijffels, R. H. (2008). Design process of an area-efficient photobioreactor. *Mar. Biotechnol.* 10, 404–415. doi:10.1007/s10126-007-9077-2

Conflict of Interest Statement: The authors declare that the research was conducted in the absence of any commercial or financial relationships that could be construed as a potential conflict of interest.

Received: 31 August 2014; accepted: 20 December 2014; published online: 23 January 2015.

Citation: Hincapie E and Stuart BJ (2015) Design, construction, and validation of an internally lit air-lift photobioreactor for growing algae. *Front. Energy Res.* 2:65. doi: 10.3389/fenrg.2014.00065

This article was submitted to *Bioenergy and Biofuels*, a section of the journal *Frontiers in Energy Research*.

Copyright © 2015 Hincapie and Stuart. This is an open-access article distributed under the terms of the Creative Commons Attribution License (CC BY). The use, distribution or reproduction in other forums is permitted, provided the original author(s) or licensor are credited and that the original publication in this journal is cited, in accordance with accepted academic practice. No use, distribution or reproduction is permitted which does not comply with these terms.



Biomass and neutral lipid production in geothermal microalgal consortia

Kathryn F. Bywaters^{1,2} and Christian H. Fritsen^{1*}

¹ Division of Earth and Ecosystem Sciences, Desert Research Institute, Reno, NV, USA

² Graduate Program of Environmental Science, University of Nevada Reno, Reno, NV, USA

Edited by:

Umakanta Jena, Desert Research Institute, USA

Reviewed by:

Reeta Rani Singhania, Blaise Pascal University, France

May M. Wu, Argonne National Laboratory, USA

*Correspondence:

Christian H. Fritsen, Division of Earth and Ecosystem Sciences, Desert Research Institute, 2215 Raggio Parkway, Reno, NV 89512, USA
e-mail: christian.fritsen@dri.edu

Recently, technologies have been developed that offer the possibility of using algal biomass as feedstocks to energy producing systems – in addition to oil-derived fuels (Bird et al., 2011, 2012). Growing native mixed microalgal consortia for biomass in association with geothermal resources has the potential to mitigate negative impacts of seasonally low temperatures on biomass production systems as well as mitigate some of the challenges associated with growing unialgal strains. We assessed community composition, growth rates, biomass, and neutral lipid production of microalgal consortia obtained from geothermal hot springs in the Great Basin/Nevada area that were cultured under different thermal and light conditions. Biomass production rates ranged from 39.0 to 344.1 mg C L⁻¹ day⁻¹. The neutral lipid production in these consortia with and without shifts to lower temperatures and additions of bicarbonate (both environmental parameters that have been shown to enhance neutral lipid production) ranged from 0 to 38.74 mg free fatty acids (FFA) and triacylglycerols (TAG) L⁻¹ day⁻¹; the upper value was approximately 6% of the biomass produced. The higher lipid values were most likely due to the presence of *Achnanthydium* sp. Palmitic and stearic acids were the dominant free fatty acids. The S/U ratio (the saturated to unsaturated FA ratio) decreased for cultures shifted from their original temperature to 15°C. Biomass production was within the upper limits of those reported for individual strains, and production of neutral lipids was increased with secondary treatment. All results demonstrate a potential of culturing and manipulating resultant microalgal consortia for biomass-based energy production and perhaps even for biofuels.

Keywords: algae, geothermal, biofuel, energy, biomass

INTRODUCTION

Environmental and biological fluctuations (e.g., temperature, light levels, nutrient availability, pH, grazers, etc.) make the maintenance of unialgal strains as a feedstock for fuels/biofuels challenging (Sheehan et al., 1998; Brennan and Owende, 2010). During the aquatic species program (ASP) that conducted a myriad of activities aimed at producing algae for oil (Sheehan et al., 1998), biomass recycling was an example of a method employed for species maintenance. Even when such measures were employed, shifts in the dominant taxa often occurred (Weissman and Benemann, 1979; Sheehan et al., 1998). Some have henceforth concluded that for successful cultivation for fuels, the best approach would be to allow a native species to invade production ponds (Sheehan et al., 1998). However, these native contaminants would have to be maintained/manipulated to be oleaginous for fuels production.

Recently, additional technologies have been developed that offer the possibility of using algal biomass as feedstocks to other energy producing systems beyond oil-derived fuels (Bird et al., 2011, 2012). Such developments make algal biomass – beyond that which is oleaginous – possible feedstocks that could help in meeting energy demands.

It is apparent that for such biomass-to-energy pathways to be developed and realized, high productivity, high yield, and low-cost-low-maintenance systems will be required. High

production and yields that are able to be maintained despite time-varying conditions in temperatures and irradiances (that can vary on time scales of minutes to seasons) will be highly desirable.

Growing algal biomass in association with geothermal resources has the potential to mitigate negative impacts of low temperatures on biomass production systems – and thus, has the potential for maintaining production in areas where low seasonal temperatures might otherwise preclude high production. Moreover, cultivating microalgae in high-temperature environments has the potential to increase intrinsic growth rates and productivity. Throughout much of the arid west/southwest geothermal resources are abundant (Faulds et al., 2004) and are being further developed as a source of energy (United States Congress Senate Committee On et al., 1984). Moreover, the arid west/southwest is a location where irradiances are favorable for algal growth throughout much of the year (Davis, 2012). If water downstream from these power plants – or even directly from hot springs or wells – were to be used to heat algal production systems (either directly or indirectly), the likelihood that such systems might become viable, for use in some fashion in the algal production industry, would be expanded.

To help in the overall evaluation of the potential for growing algal biomass in high productivity systems at moderately high temperatures, we cultivated mixed consortia from two hot

springs in Nevada, evaluated their growth at moderately high varying temperatures and then evaluated potential manipulations that could possibly increase their oleaginous production as well. Results are evaluated in context of evaluating the potential of long-term maintenance of highly productive consortia as feedstock for energy.

MATERIALS AND METHODS

SAMPLE COLLECTION

Samples were collected for culturing from two geothermal hot spring sites: (1) Hazen (also known as Patua), located in central Nevada near Hwy 50 between Fernley and Fallon (39°35' 57.0" N, -119°6' 40.0" W) on 5/19/2011 and (2) Monitor (also known as Potts), located in central Nevada approximately 45 miles south-east of Austin (39°04' 43.3" N, -116°38' 24.3" W) on 10/29/2011. A benthic algal and sediment sample was collected at (1) Hazen at a temperature of 38°C and pH of 7.28 and (2) Monitor at a temperature of 41°C and pH of 6.87.

Algae and nutrient samples were collected for culturing and water chemistry. Algae samples were inoculated into 3N media prepared with 0.2 μm capsule filtered geothermal water from each site (here after referred to as Geo3). Water samples, for chemical analysis, were filtered *in situ* using a 0.4-μm pore polycarbonate filter and then frozen immediately until analysis. Water samples were analyzed using (1) a Lachat QuikChem FIA+ 8000 series for soluble reactive phosphorus (ortho-P), ammonium (NH₄⁺), silicon oxide (SiOx), and total combined NO₂⁻ and NO₃⁻ [ortho-P, 10-115-01-1-M (Liao, 2002); NH₄⁺, 10-107-06-2-C (Prokopy, 2003); SiOx, 31-114-27-1-D (Wolters, 2002); NOx, 10-107-04-1-C (Pritzlaff, 2000)] and (2) a Dionex ICS-1500 ion chromatograph for the anions and cations [fluoride (F⁻), chloride (Cl⁻), bromide (Br⁻), sulfate (SO₄²⁻), lithium (Li⁺), sodium (Na⁺), potassium (K⁺), magnesium (Mg²⁺), and calcium (Ca²⁺)]. Determination of anions and cations was performed using an IonPac® analytical separatory column, guard columns (anions, AS14A and AG14A; cations, CS12A and CG12A), eluents (anions, sodium carbonate, and sodium bicarbonate; cations, methane sulfanic acid), and Dionex standards (anions, Seven Anion Standard II; cations, Six Anion Standard II).

INITIAL MIXED CULTURE MAINTENANCE AND EXPERIMENTAL INITIATION

Consortia (250 mL) were used to inoculate 750 mL of media in 2 L baffled culture flasks. The cultures were maintained at 30°C (Hazen) or 40°C (Monitor) initially under continuous irradiance of 200 μE m⁻² s⁻¹, then transferred to a light:dark cycle of 12:12 hours, before being transferred to natural lighting within temperature controlled enclosures (Ecopods) in a green house setting.

MIXED CULTURE SEMI-CONTINUOUS PHASE AND INCUBATION VARIANCE

The cultures were maintained in batch mode until they reached later stages of logarithmic growth, when they were then switched to semi-continuous cultures. The volumes for the dilutions were determined by the apparent growth rates using *in vivo* fluorescence (Fo) measures. Fo measures were performed using a Spectromax Gemini EM 96-well plate spectrofluorometer (excitation 440 nm,

emission 680 nm). During the semi-continuous phase, samples were collected and cultures were diluted with fresh media on a daily basis.

GROWTH RATES

Growth rates were determined, by Fo measures, over the time series when the culture was in the exponential growth phase using Eq. 1:

$$\mu = [\ln(Fo_{t2}) - \ln(Fo_{t1})] / \Delta t$$

where μ was the growth rate, ln(Fo_{t2}) was the natural log of the Fo reading at the end of the determined growth phase, ln(Fo_{t1}) was the natural log of the Fo reading at the beginning of the determined growth phase, and Δt was the time interval. The upper and lower limits were determined by a 95% confidence interval on the natural log of the exponential growth phase. P-values were generated and all values were below the critical value 0.05.

The microalgal consortia sub-cultures were taken and transferred to three separate incubation conditions. The incubation conditions for Hazen samples were natural light in a greenhouse (EcoPod – EP) at (1) 30 ± 3°C, (2) 35 ± 2°C, and (3) 40 ± 3°C. The incubation conditions for Monitor samples were EP at (1) 35 ± 2°C, (2) 40 ± 3°C, and (3) 45 ± 3°C. After the cultures had acclimated to their respective conditions they were maintained in a semi-continuous state (Figure 1).

MIXED CULTURE SECONDARY TREATMENT

When a near steady-state was obtained, mixed cultures were combined and then split into 12 separate × 500 mL culture flasks for a given incubation condition. From the 12 replicates, 4 treatments (3 replicates per treatment) were achieved and each treatment was either: maintained at temperature, maintained at temperature with the addition of sodium bicarbonate (final concentration 4 mM), incubated at 15°C, or incubated at 15°C with the addition of sodium bicarbonate (final concentration 4 mM) – with the exception of the 40°C Hazen cultures that only underwent the temperature shift and the temperature shift with the addition of bicarbonate.

All mixed cultures were incubated for a 5-day period. Samples were taken daily for microscopy (fixed with glutaraldehyde 0.5% final concentration), measures of Fo, and stained with Nile Red (NR) for quantification of neutral lipids (15 μL of NR solution was added to 1 mL algal suspension, vortexed and 300 μL loaded into wells of a 96-well plate; fluorescence intensity was measured using a Spectromax Gemini EM 96-well plate spectrofluorometer: excitation 530 nm and emission 575 nm). Samples for measures of water chemistry, triacylglycerides (TAG), free fatty acids (FFA), and ash free dry weight (AFDW) were taken at the beginning and end of the 5-day period. AFDW samples were vacuum filtered onto pre-combusted (500°C for 1 h) GF/F filters, dried, and stored with desiccant. AFDW was then determined gravimetrically using standard methods (Clesceri et al., 1998). TAG and FFA samples were analyzed using electrospray tandem mass spectrometry (ESI-MS/MS) and ultra-performance liquid chromatography-tandem mass spectrometric (UPLC/MS) methods (Samburova et al., 2013).

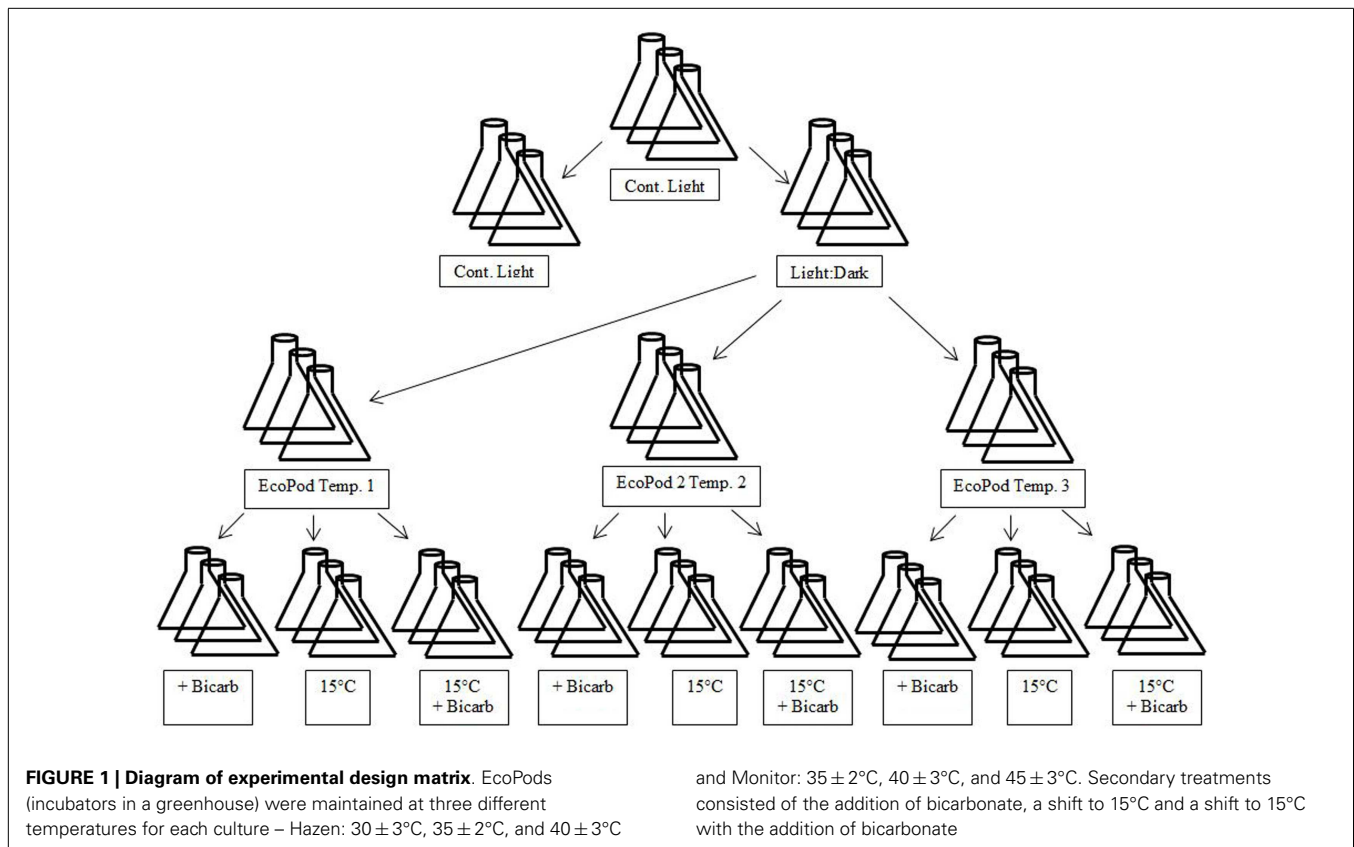


Table 1 | Chemical composition of geothermal hot springs water from Hazen and Monitor hot springs.

Site	Ortho-P (μM)	NH_4 (μM)	SiOx (μM)	$\text{NO}_2 + \text{NO}_3$ (μM)	Li^+ (μM)	Na^+ (μM)	K^+ (μM)	Mg^{2+} (μM)	Ca^{2+} (μM)	F^- (μM)	Cl^- (μM)	Br^- (μM)	SO_4^{2-} (μM)
Hazen	1.29	14.55	1560.14	0.61	260.93	28248.66	989.30	26.98	1789.47	247.23	25163.14	36.13	3751.43
Monitor	0.31	13.87	468.91	n.d.	33.08	2082.41	329.22	97.18	1357.61	79.34	314.06	n.d.	560.00

BIOMASS, TAG, AND FFA DETERMINATIONS

Biomass, TAG, and FFA production rates were determined using the AFDW data. Biomass productivity was determined by AFDW at the beginning and end of the growth phase over the time of the growth phase (estimates of carbon production were made using an average C:AFDW ratio of 0.5g:g). The concentration of TAG and FFA (determined by ESI-MS/MS and UPLC/MS methods) for each sample was divided by the AFDW, for that sample, to determine the total TAG and FFA content per unit biomass.

RESULTS

CHEMICAL COMPOSITION OF GEOTHERMAL WATERS

The chemical composition of the geothermal hot spring waters – Hazen and Monitor – was different; the majority of cation and anion concentrations in Hazen water were considerably higher (Table 1). Sodium was over 13 times higher in Hazen than Monitor water. Cations: lithium, potassium, and calcium were also higher in Hazen water, except magnesium, which was almost four

times higher in Monitor water. Silica, nitrate plus nitrite, and phosphorous were higher in Hazen, as well.

CULTURE EXPERIMENTS – EcoPods AND SECONDARY TREATMENT

Community composition

The dominant taxa of the Hazen geothermal consortia, at 30, 35, and 40°C, were similar and consisted of *Achnanthydium* sp., *Aphanocapsa* sp., *Synechocystis* sp., and *Leptolyngbya* sp (Tables 2–4). The algal assemblage at the beginning and end of the treatment period was consistent for replicates of a specific treatment. Shifts in the dominant algal genus in the consortia, were seen at 30°C with the addition of bicarbonate, at 35°C, and at 35°C with the addition of bicarbonate. Dominance in the assemblages shifted from *Achnanthydium* sp. to either *Synechocystis* sp. or *Leptolyngbya* sp.

Dominant taxa in the Monitor geothermal consortia, at 35, 40, and 45°C, were similar and consisted of *Oscillatorian* sp., *Synechocystis* sp., and *Leptolyngbya* sp. at the beginning of the secondary treatment phase. The algal assemblage at the beginning

Table 2 | Relative percentage of dominate taxa by biovolume for the EcoPod (natural light) cultures at 30°C before and after secondary treatment; N = 3 for all counts, ±1 SD.

	EP30 6/28	EP30 8/22	EP30/30 8/27	EP30/30 + B 8/27	EP30/15 8/27	EP30/15 + B 8/27
<i>Leptolyngbya</i>	0 ± 0	5 ± 1	3 ± 0	20 ± 3	9 ± 1	8 ± 1
<i>Aphanocapsa</i>	26 ± 6	22 ± 4	24 ± 7	10 ± 1	29 ± 2	27 ± 2
<i>Synechocystis</i>	34 ± 11	34 ± 16	43 ± 17	52 ± 4	53 ± 11	46 ± 18
<i>Achnantheidium</i>	34 ± 12	25 ± 13	22 ± 13	1 ± 1	4 ± 4	15 ± 13
<i>Chroococcus</i>	6 ± 5	15 ± 3	7 ± 5	18 ± 10	5 ± 5	5 ± 7
<i>Synechococcus</i>	0 ± 0	0 ± 0	0 ± 0	0 ± 0	0 ± 0	1 ± 1

Table 3 | Relative percentage of dominate taxa by biovolume for the EcoPod (natural light) cultures at 35°C before and after secondary treatment; N = 3 for all counts, ±1 SD.

	EP35 7/18	EP35 8/22	EP35/35 8/27	EP35/35 + B 8/27	EP35/15 8/27	EP35/15 + B 8/27
<i>Leptolyngbya</i>	0 ± 0	13 ± 3	44 ± 13	16 ± 5	29 ± 4	20 ± 9
<i>Aphanocapsa</i>	53 ± 24	56 ± 8	35 ± 9	29 ± 2	40 ± 11	53 ± 5
<i>Synechocystis</i>	24 ± 21	15 ± 3	13 ± 3	51 ± 10	0 ± 0	0 ± 0
<i>Achnantheidium</i>	18 ± 18	16 ± 3	8 ± 2	4 ± 1	31 ± 2	27 ± 7
<i>Chroococcus</i>	0 ± 0	0 ± 0	0 ± 0	0 ± 0	0 ± 0	0 ± 0
<i>Synechococcus</i>	4 ± 5	0 ± 0	0 ± 0	0 ± 0	0 ± 0	0 ± 0

Table 4 | Relative percentage of dominate taxa by biovolume for the EcoPod (natural light) cultures at 40°C before and after secondary treatment; N = 3 for all counts, ±1 SD.

	EP40 7/28	EP40 8/22	EP40/15 8/27	EP40/15 + B 8/27
<i>Leptolyngbya</i>	0 ± 0	19 ± 5	7 ± 1	9 ± 1
<i>Aphanocapsa</i>	21 ± 5	39 ± 15	31 ± 5	52 ± 12
<i>Synechocystis</i>	45 ± 14	11 ± 4	61 ± 25	38 ± 6
<i>Achnantheidium</i>	21 ± 20	2 ± 2	0 ± 0	0 ± 0
<i>Chroococcus</i>	12 ± 21	0 ± 0	0 ± 0	0 ± 0
<i>Synechococcus</i>	1 ± 1	29 ± 11	1 ± 2	2 ± 2

and end of the treatment period were consistent for replicates of a specific treatment. Shifts in the dominant genus in the consortia were seen at 45°C with and without the addition of bicarbonate to *Leptolyngbya* dominated assemblages.

Specific growth rates

Hazen. Cultures maintained at temperature with the addition of bicarbonate had higher growth rates (ranging from 0.63 to 0.79 doublings day⁻¹) than those just maintained at temperature (ranging from 0.46 to 0.60 doublings day⁻¹). The highest growth rate was observed in the cultures at 30°C with the addition of bicarbonate, averaging 0.79 doublings day⁻¹. The temperature shift to 15°C decreased the growth rates in all cultures, and in some cases to a growth rate of 0 (Figure 2; Table 5).

Monitor. Cultures maintained at temperature with the addition of bicarbonate had higher growth rates (ranging from 0.29 to

0.62 doublings day⁻¹) than those just maintained at temperature (ranging from 0.21 to 0.50 doublings day⁻¹). The highest growth rate was achieved by the cultures at 40°C with the addition of bicarbonate, averaging 0.62 doublings day⁻¹. The temperature shift to 15°C decreased the growth rates in all cultures, and in some case to a growth rate of 0 (Figure 3; Table 5).

Biomass productivity

Hazen. Biomass productivity followed the same trends as the measured growth rates. The cultures maintained at 30°C with the addition of bicarbonate produced the greatest biomass – 344.1 mg CL⁻¹ day⁻¹. The culture at 35°C had the lowest biomass production – 118.9 mg CL⁻¹ day⁻¹. The cultures maintained at temperature (excluding 45°C) – with the addition of bicarbonate – had an average percent increase in biomass production of 163% more than the cultures that did not have bicarbonate additions (Table 5).

Monitor. Biomass productivity also followed the same trends as the measured growth rates. The cultures maintained at 40°C with the addition of bicarbonate produced the greatest biomass – 382.3 mg CL⁻¹ day⁻¹. The culture at 45°C had the lowest biomass production – 39.0 mg CL⁻¹ day⁻¹. The cultures maintained at temperature – with the addition of bicarbonate – had an average percent increase in biomass production of 102% more than the cultures that did not have bicarbonate additions (Table 5).

Nile Red, FFA, and TAGs productivity and composition

The NR values showed an average increase in neutral lipid accumulation per unit biomass of only 6–8% with secondary treatments

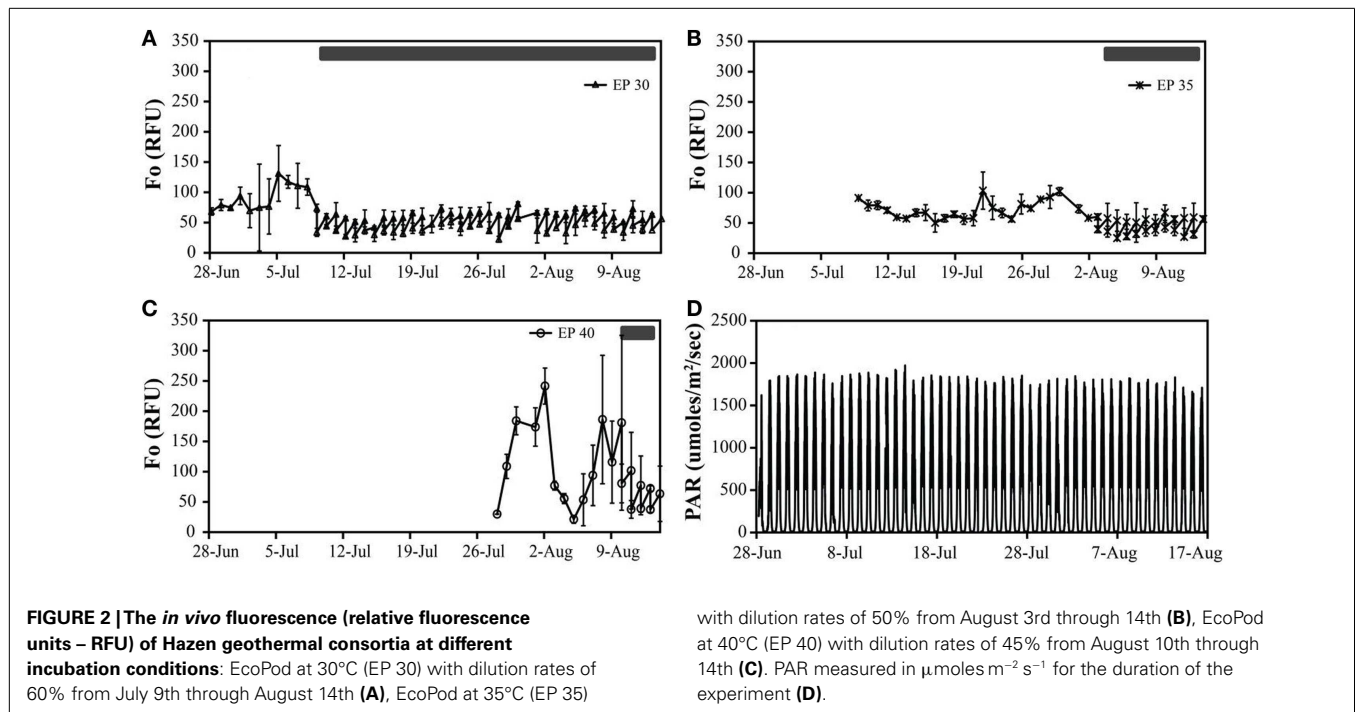


Table 5 | Growth rates, triacylglycerides (TAG), and free fatty acids (FFA), biomass production rates of Hazen and Monitor consortia incubated at different temperatures with and without the addition of bicarbonate.

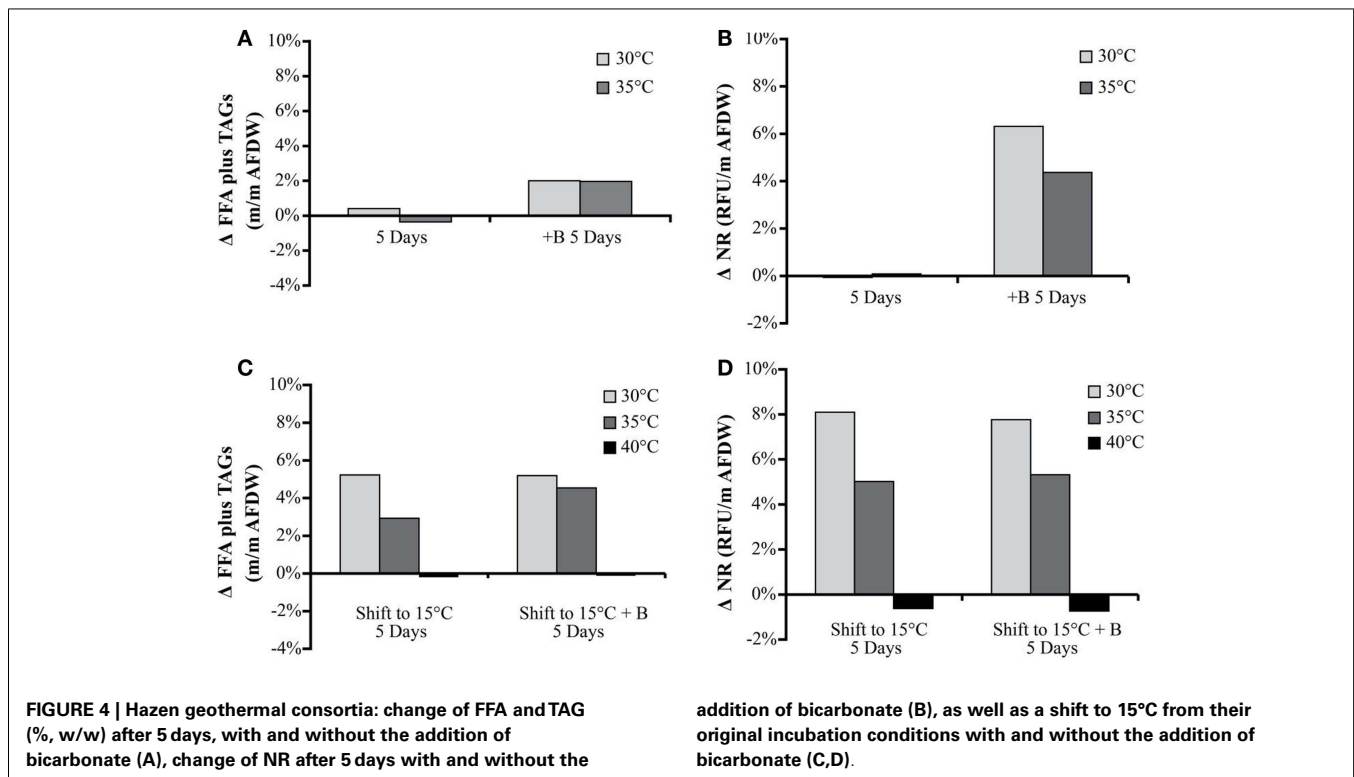
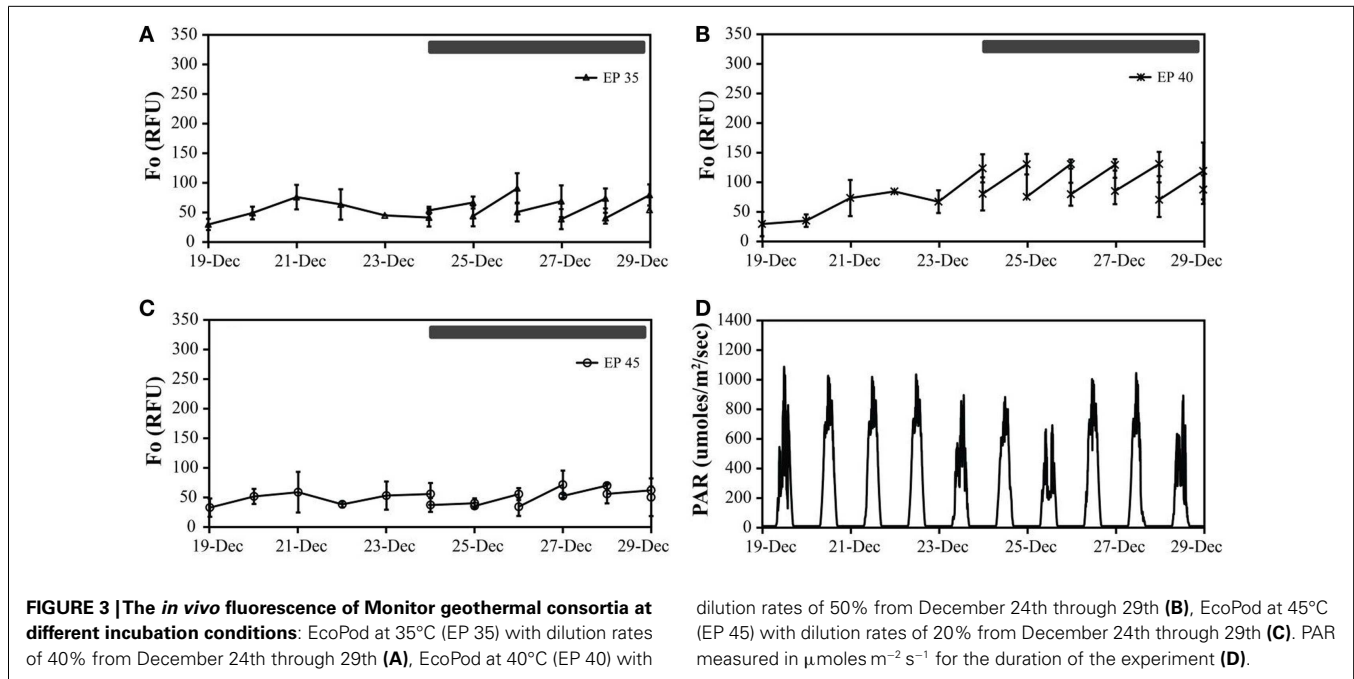
Initial temp/ secondary treatment	Hazen growth rate (doublings day^{-1}) $N = 3, \pm 1 \text{ SD}$	Monitor growth rate (doublings day^{-1}) $N = 3, \pm 1 \text{ SD}$	Hazen estimated biomass production rates ($\text{mg CL}^{-1} \text{ day}^{-1}$)	Monitor estimated biomass production rates ($\text{mg CL}^{-1} \text{ day}^{-1}$)	Hazen estimated TAG and FFA production rates ($\text{mg L}^{-1} \text{ day}^{-1}$)	Monitor estimated TAG and FFA production rates ($\text{mg L}^{-1} \text{ day}^{-1}$)
30/30	0.60 ± 0.24	n.a.	129.7	n.a.	2.82	n.a.
30/30 + B	0.79 ± 0.48	n.a.	344.1	n.a.	17.80	n.a.
30/15	0.35 ± 0.15	n.a.	0.00	n.a.	38.74	n.a.
30/15 + B	0.22 ± 0.09	n.a.	0.00	n.a.	38.52	n.a.
35/35	0.46 ± 0.09	0.40 ± 0.20	119.0	123.4	0.95	n.a.
35/35 + B	0.63 ± 0.10	0.53 ± 0.05	309.0	266.3	16.06	n.a.
35/15	0.07 ± 0.02	0.13 ± 0.11	0.00	0.00	21.61	n.a.
35/15 + B	0.07 ± 0.03	0.00 ± 0.19	0.00	0.00	31.03	n.a.
40/40	n.a.	0.50 ± 0.28	n.a.	140.0	n.a.	3.34
40/40 + B	n.a.	0.62 ± 0.21	n.a.	382.4	n.a.	24.65
40/15	0.02 ± 0.02	0.00 ± 0.15	0.00	0.00	0.20	16.82
40/15 + B	0.10 ± 0.06	0.00 ± 0.17	0.00	0.00	n.d.	10.67
45/45	n.a.	0.21 ± 0.19	n.a.	39.0	n.a.	n.a.
45/45 + B	n.a.	0.29 ± 0.17	n.a.	46.5	n.a.	n.a.
45/15	n.a.	0.00 ± 0.03	n.a.	0.00	n.a.	n.a.
45/15 + B	n.a.	0.00 ± 0.05	n.a.	0.00	n.a.	n.a.

n.a., not applicable; n.d., not detected.

(except 40°C, which actually showed a decrease) (Figure 4). The change in Nile Red values in the biomass was similar to the trends observed in TAG and FFA accumulation.

The FFA and TAG concentration per amount of biomass, for the Hazen cultures, marginally increased with the addition of bicarbonate – from approximately 1–3%. The

addition of bicarbonate, for cultures maintained at temperature, increased the estimated FFA and TAG productivity from (1) 2.82 to 17.8 $\text{mg L}^{-1} \text{ day}^{-1}$ for 30°C and (2) 0.95 to 16.06 $\text{mg L}^{-1} \text{ day}^{-1}$ for 35°C (Table 5). The amount of FFA and TAG per amount biomass increased with decreasing temperature by 3–5% – except in the 40°C cultures (Figure 4).



A decrease in temperature increased the estimated FFA and TAG productivity, to 21.61–38.74 $\text{mg L}^{-1} \text{day}^{-1}$. The Monitor cultures showed an increase in TAG and FFA per amount biomass with both the addition of bicarbonate and a temperature drop (from 3.34 $\text{mg L}^{-1} \text{day}^{-1}$ to a maximum value of 24.65 $\text{mg L}^{-1} \text{day}^{-1}$).

FFA and TAG profiles were analyzed for the following treatment conditions: (1) maintained at temperature, (2) maintained at temperature with the addition of bicarbonate, (3) shifted to 15°C, and (4) shifted to 15°C with the addition of bicarbonate. FFA composition stayed relatively constant with both the addition of bicarbonate and with the temperature shift (Table 6). The TAG

Table 6 | The composition of FFA in Hazen geothermal consortia (% w/w) at 0 and 5 days, with and without the addition of bicarbonate (A) as well as a shift to 15°C from their original incubation conditions, with and without the addition of bicarbonate (B).

Free fatty acid	0 Days		5 Days			5 Days + Bicarb			
	30°C	35°C	30°C	35°C		30°C	35°C		
(A)									
Linolenic acid C18:3	0.5	0.4	1.4	1.0		n.d.	1.1		
Linoleic acid C18:2	1.6	2.9	5.0	2.9		0.6	2.7		
Palmitic acid C16:0	29.7	26.5	14.6	20.3		29.6	18.6		
Palmitoleic acid C16:1	17.7	19.6	37.6	28.4		15.1	40.8		
Oleic acid C18:1	4.7	5.7	9.3	8.7		3.9	8.0		
Hexadecatrienoic acid C16:3	n.d.	n.d.	0.1	n.d.		n.d.	n.d.		
Hexadecadienoic acid C16:2	1.6	1.6	6.4	3.2		n.d.	0.6		
Stearic acid C18:0	42.7	36.3	11.6	21.9		50.3	17.0		
Arachidonic acid C20:4	1.6	6.5	13.2	13.2		0.6	11.1		
Eicosadienoic acid C20:2	n.d.	0.4	0.5	0.3		n.d.	n.d.		
Eicosenoic acid C20:1	n.d.	n.d.	0.2	n.d.		n.d.	n.d.		
(B)									
Free fatty acid	0 Days			5 Days			5 Days + Bicarb		
	30°C	35°C	40°C	30°C	35°C	40°C	30°C	35°C	40°C
Linolenic acid C18:3	0.5	0.4	n.d.	5.9	1.9	n.d.	5.7	5.2	n.d.
Linoleic acid C18:2	1.6	2.9	1.6	5.5	2.5	10.1	4.6	6.4	11.4
Palmitic acid C16:0	29.7	26.5	32.4	12.8	17.3	26.8	12.5	13.1	24.0
Palmitoleic acid C16:1	17.7	19.6	7.6	39.8	48.6	6.1	40.8	38.0	15.3
Oleic acid C18:1	4.7	5.7	5.9	7.3	3.4	14.5	7.3	7.1	13.1
Hexadecatrienoic acid C16:3	n.d.	n.d.	n.d.	0.4	0.1	n.d.	0.4	0.3	n.d.
Hexadecadienoic acid C16:2	1.6	1.6	n.d.	9.2	4.3	n.d.	9.4	9.0	n.d.
Stearic acid C18:0	42.7	36.3	52.4	5.9	16.8	42.5	7.9	10.1	36.2
Arachidonic acid C20:4	1.6	6.5	n.d.	12.8	4.8	n.d.	11.1	10.3	n.d.
Eicosadienoic acid C20:2	n.d.	0.4	n.d.	0.4	0.2	n.d.	0.2	0.4	n.d.
Eicosenoic acid C20:1	n.d.	n.d.	n.d.	0.1	0.1	n.d.	0.1	0.1	n.d.

n.d., limit of detection ($0.03 \mu\text{g mL}^{-1}$).

diversity increased after the fifth day of the incubation period in all cultures. A shift was seen in the TAG composition to a decrease in chain length and increase in unsaturation at the cooler temperatures (Table 7).

DISCUSSION

Owing to the potential for energy production, it is imperative to determine algal consortia production rate of biomass and lipids, from high-temperature environments under culturing conditions. Cultivation conditions, such as temperatures and secondary treatment, can maximize production rates of algal biomass or increase neutral lipid concentrations. Microalgal consortia collected from naturally high-temperature environments present the possibility of robust communities, potentially having the advantage of resistance to invasion in production systems, and for elevated growth rates – therefore, biomass. Growing algae at higher temperature requires more energy to maintain; however, coupling this system with a geothermal resource would reduce energy requirements

for heating and have the added bonus of consistent temperatures in all seasons. High biomass production rate were obtained from geothermal microalgal consortia.

Biomass production rate were similar for both Hazen and Monitor cultures over the range of temperature treatments (except Monitor at 45°C, which had <50% the production rate of the other cultures). Microalgae have evolved so that their optimum temperature is the same as their environmental temperature (Brock, 1967), which would explain why increasing the incubation temperature did not increase biomass production rates.

Biomass production rates ($39.0\text{--}344.1 \text{ mg C L}^{-1} \text{ day}^{-1}$) achieved by geothermal microalgal consortia (Hazen/Monitor) were comparable to those reported for individual strains. The reported biomass production rates of various strains (taxa and incubation temperature: *Nannochloropsis* sp. $28 \pm 1^\circ\text{C}$, *Isochrysis* sp. $22 \pm 2^\circ\text{C}$, *Tetraselmis* sp. $28 \pm 1^\circ\text{C}$, *Neochloris oleoabundans* 25.6°C , *Chlorella* sp. $23\text{--}29^\circ\text{C}$, *Dunaliella salina* $23\text{--}29^\circ\text{C}$, and *Chlorella vulgaris* $23\text{--}29^\circ\text{C}$) range from 42.3 to $7100 \text{ mg C L}^{-1} \text{ day}^{-1}$ (Huerlimann et al.,

Table 7 | The composition of TAG in Hazen geothermal consortia (% w/w) at 0 and 5 days, with and without the addition of bicarbonate (A) as well as a shift to 15°C from their original incubation conditions, with and without the addition of bicarbonate (B).

TAG	0 Days		5 Days			5 Days + Bicarb			
	30°C	35°C	30°C	35°C		30°C	35°C		
(A)									
C16:1/C16:1/C16:1	n.d.	n.d.	10.8	10.0		16.9	10.4		
C16:0/C16:1/C16:1	n.d.	25.0	35.0	34.6		34.1	34.5		
C16:0/C16:0/C16:1	n.d.	25.0	26.8	28.5		22.9	24.7		
C16:0/C16:0/C16:0	n.d.	n.d.	0.6	0.8		0.3	0.6		
C18:3/C16:1/C16:1	n.d.	n.d.	1.3	0.8		0.7	0.6		
C18:3/C16:1/C16:0	n.d.	n.d.	1.9	2.3		1.7	1.7		
C18:3/C16:0/C16:0	n.d.	n.d.	3.2	3.8		4.1	3.4		
C18:1/C16:1/C16:0	n.d.	n.d.	5.1	5.4		6.9	6.3		
C18:1/C16:0/C16:0	n.d.	n.d.	3.2	3.1		3.3	3.1		
C18:0/C16:0/C16:0	n.d.	n.d.	n.d.	n.d.		0.1	0.1		
C18:3/C18:1/C16:1	n.d.	n.d.	5.1	4.6		5.4	8.8		
C18:3/C18:1/C16:0	n.d.	n.d.	2.5	2.3		1.4	3.4		
C18:1/C18:1/C16:1	n.d.	n.d.	1.3	0.8		0.7	1.2		
C18:1/C18:1/C16:0	n.d.	n.d.	0.6	0.8		0.3	0.3		
C18:1/C18:0/C16:0	n.d.	n.d.	0.6	n.d.		0.2	0.2		
C18:0/C18:0/C16:0	n.d.	n.d.	n.d.	n.d.		n.d.	n.d.		
C18:0/C18:1/C18:3	n.d.	n.d.	n.d.	n.d.		0.2	0.2		
C18:1/C18:1/C18:1	n.d.	n.d.	0.6	0.8		0.1	0.2		
C18:0/C18:1/C18:1	n.d.	n.d.	n.d.	n.d.		0.1	0.1		
C18:0/C18:0/C18:1	100.0	50.0	1.3	1.5		0.3	0.1		
C20:4/C18:1/C16:2	n.d.	n.d.	n.d.	n.d.		0.3	0.2		
(B)									
TAG	0 Days			5 Days			5 Days + Bicarb		
	30°C	35°C	40°C	30°C	35°C	40°C	30°C	35°C	40°C
C16:1/C16:1/C16:1	n.d.	n.d.	n.d.	20.8	14.4	n.d.	18.5	18.8	n.d.
C16:0/C16:1/C16:1	n.d.	25.0	n.d.	27.9	39.0	n.d.	34.3	37.1	n.d.
C16:0/C16:0/C16:1	n.d.	25.0	n.d.	19.3	22.5	n.d.	19.6	19.8	n.d.
C16:0/C16:0/C16:0	n.d.	n.d.	n.d.	0.1	0.1	n.d.	0.1	0.1	n.d.
C18:3/C16:1/C16:1	n.d.	n.d.	n.d.	1.7	0.7	n.d.	1.0	0.9	n.d.
C18:3/C16:1/C16:0	n.d.	n.d.	n.d.	6.2	4.1	n.d.	3.8	4.0	n.d.
C18:3/C16:0/C16:0	n.d.	n.d.	n.d.	6.5	5.6	n.d.	6.7	7.2	n.d.
C18:1/C16:1/C16:0	n.d.	n.d.	n.d.	7.3	7.3	n.d.	8.8	8.7	n.d.
C18:1/C16:0/C16:0	n.d.	n.d.	n.d.	2.2	1.8	n.d.	1.8	1.4	20.0
C18:0/C16:0/C16:0	n.d.	n.d.	n.d.	n.d.	n.d.	n.d.	n.d.	n.d.	n.d.
C18:3/C18:1/C16:1	n.d.	n.d.	n.d.	4.6	2.3	n.d.	3.2	0.1	n.d.
C18:3/C18:1/C16:0	n.d.	n.d.	n.d.	1.3	0.7	n.d.	0.7	0.5	20.0
C18:1/C18:1/C16:1	n.d.	n.d.	n.d.	1.0	0.6	n.d.	0.6	0.6	20.0
C18:1/C18:1/C16:0	n.d.	n.d.	n.d.	0.4	0.3	n.d.	0.3	0.3	20.0
C18:1/C18:0/C16:0	n.d.	n.d.	n.d.	0.1	0.1	n.d.	0.1	0.1	n.d.
C18:0/C18:0/C16:0	n.d.	n.d.	n.d.	n.d.	n.d.	n.d.	n.d.	n.d.	n.d.
C18:0/C18:1/C18:3	n.d.	n.d.	n.d.	0.1	0.1	n.d.	0.1	0.1	n.d.
C18:1/C18:1/C18:1	n.d.	n.d.	n.d.	0.1	0.1	n.d.	0.1	n.d.	20.0
C18:0/C18:1/C18:1	n.d.	n.d.	n.d.	0.1	0.1	n.d.	n.d.	n.d.	n.d.
C18:0/C18:0/C18:1	100	50.0	n.d.	n.d.	n.d.	100	n.d.	0.1	n.d.
C20:4/C18:1/C16:2	n.d.	n.d.	n.d.	0.4	0.2	n.d.	0.3	0.2	n.d.

n.d., limit of detection ($0.03 \mu\text{g mL}^{-1}$).

2010; Araujo et al., 2011; Kim, 2011; Zhou et al., 2011; Murray et al., 2012). The incubation temperatures for the strains reported in the literature were mainly below those that were used in this experiment. The production rates, with the addition of bicarbonate, were enhanced. The addition of bicarbonate allows for enhanced inorganic carbon uptake to produce cellular material and thereby achieving maximum productivity. The poor solubility of CO₂ in water (1.25 g kg⁻¹ water at 30°C and 1 atm) can lead to growth inhibition due to carbon limitations (Smith and Bidwell, 1989; Giordano et al., 2005; Aishvarya et al., 2012). CO₂ solubility decreases with increasing temperature and at higher temperature ranges there can be severe loss of gaseous CO₂ in aquatic systems (Dodds et al., 1956; Carroll et al., 1991). Given what is known about CO₂ solubility it is logical to propose that geothermal systems might be carbon limited (due to being at elevated temperatures); the demonstrated increase in biomass production with the addition of bicarbonate further supports this hypothesis. The result of higher biomass production validates the idea that biomass yields can be increased with the utilization of native geothermal consortia.

Biomass production ranged from approximately 3.8–34.5 g C m⁻² day⁻¹ with the addition of bicarbonate. The long-term industry standard, set by U.S. Department of Energy's Aquatic Species Program, for biomass production from microalgae is 50 g dry weight m⁻² day⁻¹ to be cost effective and competitive with fossil fuels (Sheehan et al., 1998). Production rates were converted from a volume basis (L) to an area production bases (m²) assuming that volumetric bases can be maintained in a raceway pond at a height of 30 cm – optimal depth for an open-race way pond for comparison to the industrial standard (Sheehan et al., 1998). The majority of open-race way ponds range from 10 to 50 cm in depth. The shallow depths used in cultivation have several advantages: (1) effective utilization of mixing energy, (2) less concentration needed at harvesting, and (3) dense cultures maintain photosynthetic efficiency because at deeper depths light becomes attenuated due to self-shading (Terry and Raymond, 1985; Sheehan et al., 1998; Brennan and Owende, 2010; Stephenson et al., 2011). However, the production rates are based on the experimental culture conditions (2 L culture flasks with a media height of 10 cm) and it remains to be seen how the cultures would perform on a larger scale within a pond or bioreactor.

The neutral lipid production of the cultures showed variations based on treatment. The FFA and TAG production from geothermal microalgal consortia, with and without secondary treatment, ranged from 0 to 38.74 mg L⁻¹ day⁻¹. Zhou et al. (2011) investigated the lipid productivity of 17 strains, mainly *Chlorella* sp. (incubated at unknown temperature) and reported values ranging between 0.0369 and 94.8 mg L⁻¹ day⁻¹, with an average lipid productivity of 54.97 mg L⁻¹ day⁻¹. Mata et al. (2010) reported values of lipid productivity for 29 strains that ranged from 10.3 to 142.0 mg L⁻¹ day⁻¹. Lipid production from the microalgal consortia was affected by the addition of bicarbonate and for some cultures by a temperature drop, with the exception of the 40°C cultures. The addition of bicarbonate in the lower temperature experiment (that came from the 30°C cultures), did not increase

TAG and FFA accumulation. This lack of accumulation could have been due to increased CO₂ solubility at lower temperatures rendering the additional carbon source unnecessary. In the 40°C culture the lower temperature experiment (with and without the addition of bicarbonate) showed reduced TAG and FFA content; this could have been due to general loss in culture biomass. Adequate dissolved inorganic carbon must be present for new lipid synthesis from carbon fixation. Inorganic carbon (in the form of bicarbonate) was supplied because it is an effective lipid accumulation trigger that induces carbon storage metabolic activity (Gardner et al., 2012, 2013; White et al., 2013). Although the addition of bicarbonate increased lipid productivity, values were still in the lower range of those reported for algal strains. Unfavorable growth conditions can cause a cessation of cellular replication and thereby also increasing the accumulation of FFA and TAG (Renaud et al., 1991; Sheehan et al., 1998; Widjaja et al., 2009). The highest values of FFA and TAG production were seen in the Hazen cultures, with a shift to 15°C with and without the addition of bicarbonate, and were approximately 6% of the biomass produced. The neutral lipid production in these cultures was most likely due to the presence of *Achnantheidium* sp.; however, these values were still below the average of the reported values for oleaginous strains.

The composition of FFA and TAG were also affected by the temperature decrease. FFA and TAG compositions followed the general trend of increasing unsaturation with decreasing temperature (Hu et al., 2008). The S/U ratio (the saturated to unsaturated FA ratio) decreased for cultures shifted from their original temperature to 15°C: (1) from 2.62 to 0.22 at 30°C, (2) from 1.69 to 0.41 at 35°C, and (3) from 5.61 to 1.89 at 40°C. Cultures from both 30 and 35°C, when shifted to 15°C, increased in palmitoleic acid (C16:1) content. A desaturation of palmitic acid to palmitoleic acid has been seen in *Anabaena variabilis* (Sato and Murata, 1980). The trend toward a decrease in chain length and an increase in unsaturation is based on maintaining membrane fluidity at cooler temperatures (Cronan and Gelmann, 1975; McElhaney and Souza, 1976; Hochachka and Somero, 1984). Triacylglycerides diversity increased by the end of the incubation period in all cultures and the trend of decreased chain length and increased unsaturation was seen at cooler temperatures.

The degree of unsaturation and common chain length of the FFAs found in the geothermal microalgal consortia were suitable for biodiesel production (Leonardi et al., 2011). The content of linolenic acid in all cultures – before and after secondary treatment – was below 12% (% m/m), which is the maximum allowed by the European standard EN 14214. The most common chain length for polyunsaturated fatty acid (PUFA) was 16, with a maximum of 20.

The biomass production rates reported in this study show the potential of consortia as a source of alternative energy. Biomass production was within the upper limits of those reported for individual strains. Production of neutral lipids was increased with secondary treatment but still not comparable with oleaginous strains. Further work needs to be done on various high-temperature, microalgal consortia to establish the expected range for consortia production rates.

AUTHOR CONTRIBUTIONS

Kathryn F. Bywaters: conception of experimental design, performed experiments, post processed and analysed of data, and drafted the paper. Christian H. Fritsen: conception of experimental design, analysis of data, and drafted the paper.

ACKNOWLEDGMENTS

This research was supported by the Department of Energy DE-EE0000600. We would like to thank Dr. Samburova and Dr. Zielinska for the FFA and TAG analysis, William Coloumbe for aiding with Ecopod operations and Eric Wirthlin, Jeramie Memmott, Clinton Davis, Teresa Schwedhelm, and Emily Ulrich for lab assistance.

REFERENCES

- Aishvarya, V., Pradhan, N., Nayak, R. R., Sukla, L. B., and Mishra, B. K. (2012). Enhanced inorganic carbon uptake by *Chlorella* sp. IMMTCC-2 under autotrophic conditions for lipid production and CO₂ sequestration. *J. Appl. Phycol.* 24, 1455–1463. doi:10.1007/s10811-012-9801-9
- Araujo, G. S., Matos, L., Goncalves, L. R. B., Fernandes, F. A. N., and Farias, W. R. L. (2011). Bioprospecting for oil producing microalgal strains: evaluation of oil and biomass production for ten microalgal strains. *Bioresour. Technol.* 102, 5248–5250. doi:10.1016/j.biortech.2011.01.089
- Bird, M. I., Wurster, C. M., De Paula Silva, P. H., Bass, A. M., and De Nys, R. (2011). Algal biochar – production and properties. *Bioresour. Technol.* 102, 1886–1891. doi:10.1016/j.biortech.2010.07.106
- Bird, M. I., Wurster, C. M., De Paula Silva, P. H., Paul, N. A., and De Nys, R. (2012). Algal biochar: effects and applications. *Glob. Change Biol. Bioenergy* 4, 61–69. doi:10.1111/j.1757-1707.2011.01109.x
- Brennan, L., and Owende, P. (2010). Biofuels from microalgae – a review of technologies for production, processing, and extractions of biofuels and co-products. *Renew. Sustain. Energy. Rev.* 14, 557–577. doi:10.1016/j.rser.2009.10.009
- Brock, T. D. (1967). Micro-organisms adapted to high temperatures. *Nature* 214, 882. doi:10.1038/214882a0
- Carroll, J. J., Slupsky, J. D., and Mather, A. E. (1991). The solubility of carbon-dioxide in water at low-pressure. *J. Phys. Chem. Ref. Data* 20, 1201–1209. doi:10.1063/1.555900
- Clesceri, L. S., Greenberg, A. E., and Eaton, A. D. (eds) (1998). *Standard Methods for the Examination of Water and Wastewater*. Baltimore, MD: American Public Health Association, American Water Works Association, Water Environment Federation.
- Cronan, J. E., and Gelmann, E. P. (1975). Physical-properties of membrane lipids – biological relevance and regulation. *Bacteriol. Rev.* 39, 232–256.
- Davis, C. J. (2012). *Periphyton Ecology in Great Basin Rivers: Winter Blooms, Hyporheic Exchange Effects, and Reservoir-Tailwater Productivity*. Dissertation/Thesis, ProQuest, UMI Dissertations Publishing, Reno.
- Dodds, W. S., Stutzman, L. F., and Sollami, B. J. (1956). Carbon dioxide solubility in water. *Ind. Eng. Chem. Chem. Eng. Data Series* 1, 92–95. doi:10.1021/i460001a018
- Faulds, J. E., Coolbaugh, M., Blewitt, G., and Henry, C. D. (2004). Why is Nevada in hot water? Structural controls and tectonic model of geothermal systems in the northwestern Great Basin. *Geoth. Res. Council Trans.* 28, 649–654.
- Gardner, R., Cooksey, K., Mus, F., Macur, R., Moll, K., Eustance, E., et al. (2012). Use of sodium bicarbonate to stimulate triacylglycerol accumulation in the chlorophyte *Scenedesmus* sp. and the diatom *Phaeodactylum tricornerutum*. *J. Appl. Phycol.* 24, 1311–1320. doi:10.1007/s10811-011-9782-0
- Gardner, R. D., Lohman, E., Gerlach, R., Cooksey, K. E., and Peyton, B. M. (2013). Comparison of CO₂ and bicarbonate as inorganic carbon sources for triacylglycerol and starch accumulation in *Chlamydomonas reinhardtii*. *Biotechnol. Bioeng.* 110, 87–96. doi:10.1002/bit.24592
- Giordano, M., Beardall, J., and Raven, J. A. (2005). CO₂ concentrating mechanisms in algae: mechanisms, environmental modulation, and evolution. *Annu. Rev. Plant Biol.* 56, 99–131. doi:10.1146/annurev.arplant.56.032604.144052
- Hochachka, P. W., and Somero, G. N. (1984). *Biochemical Adaptation*. Princeton, NJ: Princeton University Press.
- Hu, Q., Sommerfeld, M., Jarvis, E., Ghirardi, M., Posewitz, M., Seibert, M., et al. (2008). Microalgal triacylglycerols as feedstocks for biofuel production: perspectives and advances. *Plant J.* 54, 621–639. doi:10.1111/j.1365-313X.2008.03492.x
- Huerlimann, R., De Nys, R., and Heimann, K. (2010). Growth, lipid content, productivity, and fatty acid composition of tropical microalgae for scale-up production. *Biotechnol. Bioeng.* 107, 245–257. doi:10.1002/bit.22809
- Kim, W. (2011). Optimization of culture conditions and comparison of biomass productivity of three green algae. *Bioprocess Biosyst. Eng.* 35, 19–27. doi:10.1007/s00449-011-0612-1
- Leonardi, P. I., Popovich, C. A., and Damiani, M. C. (2011). “Feedstocks for second-generation biodiesel: microalgae’s biology and oil composition” in *Economic effects of biofuel production*. ed. M. A. dos Santos Bernardes (Croatia: In Tech), 318–346. doi:10.5772/23125
- Liao N (2002). *Determination of Orthophosphate in Waters by Flow Injection Analysis Colorimetry*. QuikChem® Method 10-115-01-1-M:17. Loveland, CO: LaChat Instruments.
- Mata, T. M., Martins, A. A., and Caetano, N. S. (2010). Microalgae for biodiesel production and other applications: a review. *Renew. Sust. Energy Rev.* 14, 217–232. doi:10.1016/j.rser.2009.07.020
- McElhane, R. N., and Souza, K. A. (1976). The relationship between environmental temperature, cell growth and the fluidity and physical state of the membrane lipids in *Bacillus stearothermophilus*. *Biochim. Biophys. Acta* 443, 348–359. doi:10.1016/0005-2787(76)90499-8
- Murray, K. E., Shields, J. A., Garcia, N. D., and Healy, F. G. (2012). Productivity, carbon utilization, and energy content of mass in scalable microalgae systems. *Bioresour. Technol.* 114, 499–506. doi:10.1016/j.biortech.2012.03.012
- Pritzlaff, P. (2000). *Determination of Nitrate/Nitrite in Surface and Wastewaters by Flow Injection Analysis*. QuikChem® Method 10-107-04-1-C – 15. Loveland, CO: LaChat Instruments.
- Prokopy, W. R. (2003). *Determination of Ammonia by Flow Injection Analysis*. QuikChem® Method 10-107-06-2-C – 10. Loveland, CO: LaChat Instruments.
- Renaud, S., Parry, D., Thinh, L.-V., Kuo, C., Padovan, A., and Sammy, N. (1991). Effect of light intensity on the proximate biochemical and fatty acid composition of *Isochrysis* sp. and *Nannochloropsis oculata* for use in tropical aquaculture. *J. Appl. Phycol.* 3, 43–53. doi:10.1007/BF00003918
- Samburova, V., Lemos, M., Hiibel, S., Kent Hoekman, S., Cushman, J., and Zielinska, B. (2013). Analysis of triacylglycerols and free fatty acids in algae using ultra-performance liquid chromatography mass spectrometry. *J. Am. Oil Chem. Soc.* 90, 53–64. doi:10.1007/s11746-012-2138-3
- Sato, N., and Murata, N. (1980). Temperature shift-induced responses in lipids in the blue-green alga, *Anabaena variabilis*: the central role of diacylmonogalactosylglycerol in thermo-adaptation. *Biochim. Biophys. Acta* 619, 353–366. doi:10.1016/0005-2760(80)90083-1
- Sheehan, J., Dunahay, T., Benemann, J., and Roessler, P. (1998). *A Look Back at the U.S. Department of Energy’s Aquatic Species Program – Biodiesel from Algae*. Golden, CO: National Renewable Energy Laboratory. Report NREL/TP-580-24190.
- Smith, R. G., and Bidwell, R. (1989). Mechanism of photosynthetic carbon dioxide uptake by the red macroalga, *Chondrus crispus*. *Plant Physiol.* 89, 93–99. doi:10.1104/pp.89.1.93
- Stephenson, P. G., Moore, C. M., Terry, M. J., Zubkov, M. V., and Bibby, T. S. (2011). Improving photosynthesis for algal biofuels: toward a green revolution. *Trends Biotechnol.* 29, 615–623. doi:10.1016/j.tibtech.2011.06.005
- Terry, K. L., and Raymond, L. P. (1985). System-design for the autotrophic production of microalgae. *Enzyme Microb. Technol.* 7, 474–487. doi:10.1016/0141-0229(85)90148-6
- United States Congress Senate Committee On, E., Natural Resources Subcommittee On, E., and Mineral, R. (1984). *Geothermal Energy Development in Nevada’s Great Basin: Hearing Before the Subcommittee on Energy and Mineral Resources of the Committee on Energy and Natural Resources, United States Senate, Ninety-Eighth Congress, Second Session, to Examine the Current Status and Future Needs of Nevada’s Geothermal Energy Industry, Sparks, NV, April 17, 1984*. Washington, DC: U.S. G.P.O.
- Weissman, J. C., and Benemann, J. R. (1979). Biomass recycling and species competition in continuous cultures. *Biotechnol. Bioeng.* 21, 627–648. doi:10.1002/bit.260210408
- White, D. A., Pagarette, A., Rooks, P., and Ali, S. T. (2013). The effect of sodium bicarbonate supplementation on growth and biochemical composition of marine microalgae cultures. *J. Appl. Phycol.* 25, 153–165. doi:10.1007/s10811-012-9849-6

Widjaja, A., Chien, C. C., and Ju, Y. H. (2009). Study of increasing lipid production from fresh water microalgae *Chlorella vulgaris*. *J. Taiwan Inst. Chem. Eng.* 40, 13–20. doi:10.1016/j.jtice.2008.07.007

Wolters, M. (2002). *Determination of Silicate in Brackish or Seawater by Flow Injection Analysis*. QuikChem® Method 31-114-27-1-D – 12. Loveland, CO: LaChat Instruments.

Zhou, W. G., Li, Y. C., Min, M., Hu, B., Chen, P., and Ruan, R. (2011). Local bioprospecting for high-lipid producing microalgal strains to be grown on concentrated municipal wastewater for biofuel production. *Bioresour. Technol.* 102, 6909–6919. doi:10.1016/j.biortech.2011.04.038

Conflict of Interest Statement: The Guest Associate Editor Umakanta Jena declares that, despite being affiliated to the same institution as authors, the review process was handled objectively and no conflict of interest exists. The authors declare that the research was conducted in the absence of any commercial

or financial relationships that could be construed as a potential conflict of interest.

Received: 29 August 2014; accepted: 13 December 2014; published online: 16 February 2015.

Citation: Bywaters KF and Fritsen CH (2015) Biomass and neutral lipid production in geothermal microalgal consortia. *Front. Bioeng. Biotechnol.* 2:82. doi: 10.3389/fbioe.2014.00082

This article was submitted to *Bioenergy and Biofuels*, a section of the journal *Frontiers in Bioengineering and Biotechnology*.

Copyright © 2015 Bywaters and Fritsen. This is an open-access article distributed under the terms of the Creative Commons Attribution License (CC BY). The use, distribution or reproduction in other forums is permitted, provided the original author(s) or licensor are credited and that the original publication in this journal is cited, in accordance with accepted academic practice. No use, distribution or reproduction is permitted which does not comply with these terms.

Pyrolysis of algal biomass obtained from high-rate algae ponds applied to wastewater treatment

Fernanda Vargas e Silva* and Luiz Olinto Monteggia

Institute of Hydraulic Research, Federal University of Rio Grande do Sul, Porto Alegre, Brazil

OPEN ACCESS

Edited by:

Umakanta Jena,
Desert Research Institute, USA

Reviewed by:

Sandeep Kumar,
Old Dominion University, USA
Kaushlendra Singh,
West Virginia University, USA

*Correspondence:

Fernanda Vargas e Silva,
Instituto de Pesquisas Hidráulicas,
Bento Gonçalves 9500, Porto Alegre,
Rio Grande do Sul, Brazil
fervs@globo.com

Specialty section:

This article was submitted to
Bioenergy and Biofuels, a section of
the journal *Frontiers in Energy
Research*

Received: 16 July 2014

Accepted: 10 June 2015

Published: 30 June 2015

Citation:

Vargas e Silva F and Monteggia LO
(2015) Pyrolysis of algal biomass
obtained from high-rate algae ponds
applied to wastewater treatment.
Front. Energy Res. 3:31.
doi: 10.3389/fenrg.2015.00031

This work presents the results of the pyrolysis of algal biomass obtained from high-rate algae ponds treating sewage. The two high-rate algae ponds (HRAP) were built and operated at the São João Navegantes Wastewater Treatment Plant. The HRAP A was fed with raw sewage while the HRAP B was fed with effluent from an upflow anaerobic sludge blanket (UASB) reactor. The HRAP B provided higher productivity, presenting total solids concentration of 487.3 mg/l and chlorophyll a of 7735 mg/l. The algal productivity in the average depth was measured at 41.8 g·m⁻² day⁻¹ in pond A and at 47.1 g·m⁻² day⁻¹ in pond B. Algae obtained from the HRAP B were separated by the process of coagulation/flocculation and sedimentation. In the presence of alum, a separation efficiency in the range of 97% solid removal was obtained. After centrifugation the biomass was dried and comminuted. The biofuel production experiments were conducted via pyrolysis in a tubular quartz glass reactor which was inserted in a furnace for external heating. The tests were carried out in an inert nitrogen atmosphere at a flow rate of 60 ml/min. The system was operated at 400, 500, and 600°C in order to determine the influence of temperature on the obtained fractional yields. The studies showed that the pyrolysis product yield was influenced by temperature, with a maximum liquid phase (bio-oil and water) production rate of 44% at 500°C, 45% for char and around 11% for gas.

Keywords: high-rate algae ponds, pyrolysis, biofuels, wastewater treatment, bioremediation

Introduction

Biomass is considered worldwide as an important source of renewable energy, including electricity, automobile fuel, and as a source of heat for industrial equipment.

Cultures commonly used for energy production are sugarcane, corn, beans, beets, and many others. There are two main factors that define when a culture is appropriate for this process: good dry matter yield per unit of land (dry ton/ha), low area requirement for cultivation, and low costs of energy production from biomass (Dermibas et al., 2009).

However, some research has condemned the use of biofuels, associating its production with possible high food prices. Algae, among the aquatic biomass feedstocks, are considered one of the most promising sources of biofuels due to their unique characteristics. They can accumulate lipids that can be converted into biofuels, present fast proliferation, have the ability to sequester CO₂ from the atmosphere for growth and do not require agricultural land or freshwater for growth or higher water consumption, and also the whole plant matter can be used in converting biofuels processes

(Dismukes et al., 2008; Brennan and Owende, 2010; Jena and Das, 2011; Pate et al., 2011; Yanik et al., 2013; Zhou et al., 2014; Hognon et al., 2015).

Wastewater treatment associated with algae cultivation can offer an alternative way for sustainable renewable biofuels, since the large amount of freshwater needed for algae cultivation can be saved, becoming an environmentally friendly process (Zhou et al., 2014).

In a sewage treatment system, high-rate ponds are characterized by having high algal biomass generation which is an undesirable byproduct for the environment. Its presence in water bodies decreases water quality.

High-rate algae ponds are raceway-type ponds, in which water, algae, and nutrients are continually mixed. A paddle wheel generates a mean horizontal water velocity of approximately 0.15–0.3 m/s. This movement is necessary to avoid sedimentation and stratification. The maximum biomass production (mostly algae) is achieved through better use of lighting per volume. This is ensured by the low depth of the ponds and the constant movement of biomass through mechanical mixing (Nascimento, 2001; Chisti, 2007).

Usually the algal biomass productivity is determined by the measurement of solids found in the ponds.

The algal biomass production costs are mainly covered by the costs of treatment when using wastewater high-rate ponds resulting in lower environmental impacts in terms of water, energy, and fertilizer needs.

The biomass in high-rate algae ponds assimilates the nutrients needed for its growth and becomes responsible for the removal of nutrients from wastewater. This has the advantage of controlling pollution of water resources which contributes to the sustainable use of this technology on an industrial scale (Park et al., 2011; Passos et al., 2013).

The biomass separation process requires an increase in algal suspension concentration typically from 0.02 to 0.06% total suspended solids (TSS) to approximately 2 to 7% solids, which may be higher depending on the target process objective (Uduman et al., 2010).

The algal cells have reduced size, sometimes <30 μm and their density is similar to water with a low sedimentation rate, so to be successful in separation, it is necessary to aggregate the cells. Generally, the process comprises of two steps: the first involving destabilization of algal cells using coagulation followed by sedimentation or flotation. In the second step of the process, it is necessary to increase the biomass content, which is often done by filtration, centrifugation, or thermal processes (Molina Grima et al., 2003; Granados et al., 2012; Cai et al., 2013; Udom et al., 2013).

The algae cell has a negative surface charge, which prevents aggregation. This charge may be reduced or neutralized by the addition of flocculants or multivalent cations, such as cationic polymers that change the zeta potential, which is a measure of particle stability, reducing the repulsive forces. So the action of the attractive Van der Waals forces allows algae agglutination (Wessler et al., 2003; Granados et al., 2012). Salts used for this purpose should be non-toxic, low cost, and have high effectiveness at low concentrations (Molina Grima et al., 2003).

Another advantage of using coagulation/flocculation process is nutrient removal. The presence of nutrients in wastewater,

particularly nitrogen and phosphorus, is a serious environmental problem and is receiving increasing attention. Nitrogen in the form of ammonia can be volatilized and cause air pollution. Phosphorus can permeate into the soil and cause damage to the underground water (Chen et al., 2012). When there are excessive levels of nutrients in the wastewater, they cause eutrophication of water sources, possibly damaging the ecosystem (Cai et al., 2013).

The algal biomass, after thickening, may reach 5–15% solid content, and, being perishable, it must be processed as soon as possible. Essential processes such as thickening and drying usually involve high operational costs. Thus, these steps are considered determining factors regarding the economical feasibility analysis of the overall process (Brennan and Owende, 2010; Uduman et al., 2010). The methods commonly used for thickening biomass are centrifugation and filtration followed by different drying techniques, such as natural, oven, spray, and fluidized bed drying.

There are three basic components in algae biomass: proteins, carbohydrates, and lipids. These oils can then be extracted and converted in to biofuels (Um and Kim, 2009).

The pyrolysis process appears to be an excellent alternative for energy conversion, it presents the advantage of using different sources of organic matter, not being limited by the lipid content, as with biodiesel production processes. The pyrolysis process is based on decomposition of organic compounds present in the total biomass under a controlled environment in the absence of oxygen and atmospheric pressure, resulting in different phases: liquid (bio-oil), gas, and solid (char). It is an endothermic reaction that occurs at a temperature of 300–700°C depending on the characteristics of the material to be pyrolyzed (Martini, 2009; Hognon et al., 2015).

Biomass pyrolysis is considered a renewable process, because biomass is turned in several gases when pyrolyzed. Carbon dioxide, one of the gases formed, is absorbed by the algae for its growth, making the process self-sustainable with no serious contribution to greenhouse effect. The relative yield of each phase generated in the process depends on operating parameters (temperature, heating rate, residence time, and flow rate of inert gas), properties of the biomass (the particle size as well as its moisture), and type of pyrolysis used (slow, fast, or flash pyrolysis) (Balat et al., 2009; Martini, 2009; Akhtar and Amin, 2012; Yanik et al., 2013; Hognon et al., 2015).

In order to obtain high yields of aqueous products, fast pyrolysis is normally used, which is characterized by higher heating rates (1000°C/min) and lower residence times of volatiles (10–20 s). In order to favor solid char formation, slow pyrolysis process with lower heating rates (5–80°C/min) and longer residence times (5–30 min) must be used (Van de Velden et al., 2010; Jena and Das, 2011; Yanik et al., 2013).

The bio-oil generated by biomass pyrolysis is generally cleaner than that from fossil fuels, due to its lower nitrogen and sulfur content. The biomass vaporizes, passes through a process of cracking and condensation, producing a dark brown liquid, consisting of a complex mixture of many different hydrocarbons. This process is most successful in fluidized bed reactors due to high heating rates, rapid devolatilization and easy control (Doshi et al., 2005; Martini, 2009).

Materials and Methods

Biomass Production

Two high-rate algae ponds were constructed in the IPH/UFRGS experimental wastewater treatment unit, at São João Navegantes Wastewater Treatment Plant. This plant is responsible for handling the sewage of the north area of Porto Alegre/RS.

The ponds were operated in closed circuit with the following dimensions: overall height: 0.9 m, length of the straight sections: 30 m, width: 5 m (at the upper edge of the slope) and surface area 320 m², as can be seen in **Figure 1**.

The high-rate algae ponds were operated under two feeding conditions: pond A was fed with raw sewage after pretreatment (screening and grit removal) and pond B was fed with effluent from an upflow anaerobic sludge blanket (UASB) reactor. In order to maximize the process of biomass production, the operating parameters of the ponds were useful depth (Hu): 0.3 m, longitudinal flow speed: 0.3 m/s, and hydraulic detention time (HDT): 3 days.

The pond samples were collected in 20 l plastic containers, directly from the body of the ponds, to provide enough biomass for the pyrolysis experiments.

In order to determine algae biomass productivity, total solids, turbidity, and chlorophyll a were measured weekly.

All experiments to determine these parameters were carried out according to Standard Methods for the Examination of Water and Wastewater [American Public Health Association (APHA) and Awwa (2005)].

Algae Separation and Thickening

Experiments of coagulation/flocculation were performed using the effluent from pond B, which showed better performance in terms of algal biomass production.

The equipment used was VELP Jar Test model F.6/S, composed of 6 jars of 2000 ml each, with agitation and controlled independently.

To evaluate the separation process and the removal of nutrients two coagulants were used, Aluminum Sulfate and Ferric Chloride and two flocculants, Sulfloc 1001 and Tanfloc SL. Their concentration ranges are shown in **Table 1**.

After the separation and removal of all the supernatant from the jars, the algae sludge was submitted to centrifugation for 20 min at 2500 rpm to obtain a sample of about 15–20% of dried solids. After

centrifugation, the biomass was dried at 105°C. Finally, the dried algae were ground in a mortar and stored separately according to the reagent used in the separation process.

Nutrient Removal

Experiments were performed to determine the concentration of nitrogen and phosphorus in effluent ponds before and after coagulation/flocculation. Thus, it was possible to determine the effect of algae upon the separation in the removal of nutrients.

Biomass Pyrolysis

The experiments obtaining biofuel via biomass pyrolysis were performed in a tubular quartz reactor, with the dimensions described in **Figure 2**.

The experiments were run in batches, to allow solid char removal. The process flow used in this work, presented in **Figure 3**, was based on Zhang et al. (2011).

In the process, the inert atmosphere was generated by nitrogen gas (1) and the heating process was provided by an external furnace (2). The condensation was performed in (3), where two condensers in series were immersed in an ice bath. The exit of non-condensable gases was in (4).

The pyrolysis reactor was fed manually with 7 g of dried and ground biomass obtained from the previous step of the process. The biomass was inserted in the reactor using an aluminum foil capsule. After it has been charged, the reactor was closed and the inert atmosphere was provided by a 0.06 l/min nitrogen gas flow.

The pyrolysis runs were started by placing the reactor in a programmable tubular furnace, with a heating rate of 20°C/min. All the runs were made in two steps: heating the sample and an isothermal reaction step, maintaining the desired temperature (400, 500, and 600°C) for 60 min.

The vapors generated passed through two condensers in series, immersed in ice baths maintained at a temperature of about 0°C. At the end of each experiment, the aqueous phase generated by condensation was collected, combined, weighed, and stored. The non-condensable gases were measured by difference. Following the 60 min reaction time, the system was turned off and cooled to room temperature.

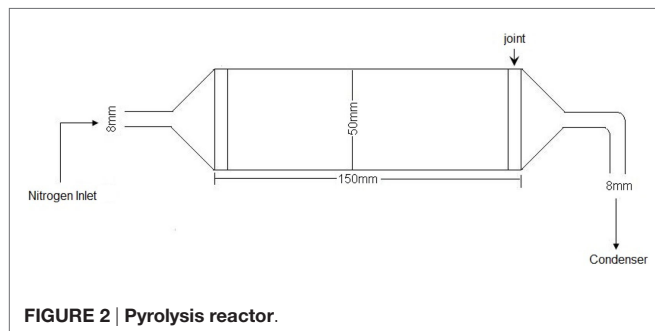
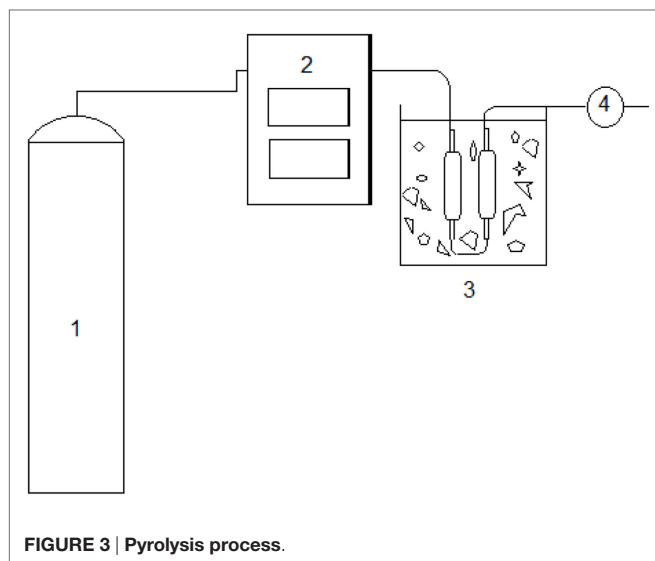
After reaching room temperature, the reactor was opened and the solid fraction (char) was collected, weighed, and stored. The



FIGURE 1 | High-rate algae ponds.

TABLE 1 | Concentration range used.

Product	FeCl ₃ 10%	Al ₂ (SO ₄) ₃ 10%	Sulfloc 20%	Tanfloc 10%
Concentration range (mg/l)	200–300	100–150	250–300	50–100

**FIGURE 2 | Pyrolysis reactor.****FIGURE 3 | Pyrolysis process.**

reactor final mass was also determined, in order to measure the losses by wall adhesion.

The pyrolysis evaluation was performed through yields measurement. Each fraction was determined from the ratio of the weight of respective fraction to initial weight of biomass, expressed as percentage yield, according to Eq. (1).

$$\text{Yield (\%)} = \frac{\text{Fraction mass obtained after pyrolysis}}{\text{Initial algal biomass}} \times 100\% \quad (1)$$

Results and Discussions

Biomass Production

The results of solids, turbidity, chlorophyll a and productivity are shown in **Table 2**, comparing the performance of both biomass production ponds.

In the experiments, we considered the concentration of solids present in effluents and turbidity caused only by the presence of algae. From **Table 2**, it can be noted that pond B in all evaluation parameters showed higher values than those obtained from pond A. Such behavior is explained by the fact that effluent from UASB

TABLE 2 | High-rate ponds performance.

Analysis	Pond A	SD	Pond B	SD
Total solids (mg/l)	433.2	59.2	487.3	56.1
Turbidity (NTU)	41.9	8.9	63.3	13.4
Chlorophyll a (mg/l)	2338	NA	7735	NA
Productivity (g·m ⁻² day ⁻¹)	41.8	NA	47.1	NA

NA, not applicable.

TABLE 3 | Algae biomass productivity.

Authors	System	Biomass productivity (g·m ⁻² day ⁻¹)
Nascimento (2001)	HRAP	21.8
Riaño et al. (2012)	Photobioreactor	1.54
Sturm and Lamer (2011)	Open ponds	12
Terigar and Theegala (2014)	Open tanks	43.4

TABLE 4 | Crops productivity [adapted from Trzeciak et al. (2008)].

Crops	Harvest (month/year)	Biomass productivity (g·m ⁻² day ⁻¹)
Cotton	3	0.38
Peanut	3	0.55
Canola	3	0.60
Sunflowers	3	0.55
Dendê (<i>Elaeis guineensis</i>)	12	6.84
Mamona (<i>Ricinus communis</i> L.)	3	0.41

reactor provided low solid concentration, which facilitated higher solar irradiation in the body of the pond, an essential factor for biomass growth. Thus, the effluent selected for tests of separation, thickening, and the tests for obtaining biofuels was collected from the pond B. **Table 3** shows a comparison among biomass productivity obtained in this work and others presented in the literature.

Table 4 shows the comparison between the productivity of crops commonly used in the biofuels production.

As we can see from both tables, high-rate algae ponds can be a competitive source of biomass, with higher productivities and without need of arable land and fresh water. This system high-rate algae pond (HRAP) presents no seasonality and the biomass can be harvested all year, without competition with food crops.

Algae Separation, Thickening, and Nutrient Removal

The results of algae separation are shown in **Table 5**, based on separation efficiency related to the chemical dosage used. This table also shows the evaluation of nutrient removal for each product.

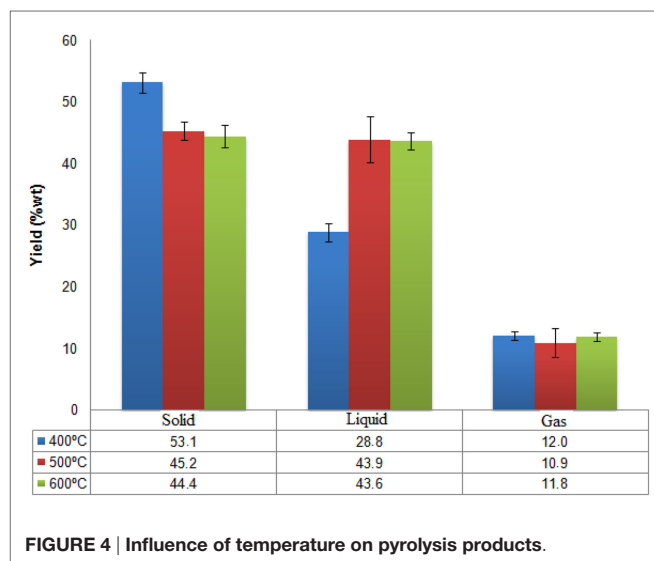
Thus, according to the results shown in **Table 5**, the biomass separated with aluminum sulfate, which was selected as the most convenient chemical due to lower dosage requirement, showed better separation and nutrient removal. The biomass was dried and crushed to be used in the pyrolysis experiments. The efficiency of N and P removal were similar when using Sulfloc 20%, but the dosage required was higher than with sulfate.

Biomass Pyrolysis

The influence of temperature (400, 500, and 600°C) on pyrolysis results are shown in **Figure 4**. According to the results, the

TABLE 5 | Removal obtained and dosage used.

Product	Ferric chloride 10%	Al sulfate 10%	Sulfloc 20%	Tanfloc 10%
Maximum separation (%)	88.4	97.9	94.5	97.5
Concentration (mg/l)	300	150	290	100
P Removal (%)	100	100	100	37.9
N Removal (%)	–	5.5	5.5	–

**FIGURE 4 | Influence of temperature on pyrolysis products.**

temperature of 400°C favors solid phase formation, with an average yield of 53.1%. The aqueous and gaseous phases obtained average yields of 28.8 and 12%, respectively. At 500°C, the yields for solid and aqueous phases were similar, however aqueous phase formation was slightly higher, composed of bio-oil and water. The average yield was 43.9 for solid phase 45.2 for the aqueous phase and 10.9% in the gas phase. At 600°C we can see similar yields between solid and liquid formation, 44.4 and 43.6%, respectively. The average for gas formation at this temperature was 11.8%.

The liquid phase, comprising of bio-oil and water, has a reddish brown color, with a strong and distinctive smoky smell, which

References

- Akhtar, J., and Amin, N. S. (2012). A review on operating parameters for optimum liquid oil yield in biomass pyrolysis. *Renew. Sustain. Energy Rev.* 16, 5101–5109. doi:10.1016/j.rser.2012.05.033
- American Public Health Association (APHA) and Awwa, W. E. F. (2005). *Standard Methods for the Examination of Water and Waste Water*, 21st Edn. American Public Health Association, 4–108; 4–147.
- Balat, M., Balat, M., Kirtay, E., and Balat, H. (2009). Main routes for thermo-conversion of biomass into fuels and chemicals. Part1: pyrolysis systems. *Energy Convers. Manag.* 50, 3147–3157. doi:10.1016/j.enconman.2009.08.014
- Brennan, L., and Owende, P. (2010). Biofuels from microalgae – a review of technologies for production, processing and extractions of biofuels and co-products. *Renew. Sustain. Energy Rev.* 14, 557–577. doi:10.1016/j.rser.2009.10.009
- Cai, T., Park, S. Y., and Li, Y. (2013). Nutrient recovery from wastewater streams by microalgae: status and prospects. *Renew. Sustain. Energy Rev.* 19, 360–369. doi:10.1016/j.rser.2012.11.030
- Chen, R., Li, R., Deitz, L., Liu, Y., Stevenson, R. J., and Liao, W. (2012). Freshwater cultivation with animal waste for nutrient removal and biomass production. *Biomass Bioenergy* 39, 128–138. doi:10.1016/j.biombioe.2011.12.045

confirms the information in the literature about products obtained in the pyrolysis (Jena and Das, 2011; Yanik et al., 2013).

As described in the literature, temperature plays an important role on the yield of the fractions obtained in the pyrolysis process. Studies show that temperatures between 450 and 550°C maximize the yield of bio-oil and, at very high temperatures, secondary reactions of the volatiles may occur, thus decreasing the yield of the liquid phase, which can be seen in **Figure 4**; at 600°C, a small decrease in the aqueous phase yield was observed (Yanik et al., 2013).

For related data, we use an ANCOVA analysis (Analysis of Covariance) with a fixed factor (oven temperature) and a covariate (initial mass of algae) to identify differences in the char mass production. Five replicates were performed for each factor and the software used was SPSS version 18.

The data do not present heteroscedasticity, using the Levene test (p -value of 0.235), the tested factor was significant at a p -value of 0.01. So we went to the *post hoc* analysis, which showed a significant difference between the means of groups, the 400°C group is different from other groups and the 500°C and 600°C are not statistically different from each other.

Conclusion

In this work, the association of wastewater treatment and biofuel production through pyrolysis of algal biomass obtained in high-rate algae ponds was studied. The algal productivity, at the average depth was measured as 41.8 g·m⁻² day⁻¹ for pond A and as 47.1 g·m⁻² day⁻¹ for pond B. The algae were pyrolyzed in a tubular furnace system with external heating at different temperatures. Studies have shown that the pyrolysis process is efficient and the fractions yields are greatly influenced by temperature. Operating under mild conditions, it was possible to obtain maximum yields of 45% at 500°C for aqueous phase (bio-oil and water), 44% for char, and about 11% for gas. As we can see, through this process, it is possible to offer a promising alternative for environmental pollution control with potential economic return.

Acknowledgments

The authors acknowledge CNPq and CAPES for the financial support to this project.

- Dermibas, M. F., Balat, M., and Balat, H. (2009). Potential contribution of biomass to the sustainable energy development. *Energy Convers. Manag.* 50, 1746–1760. doi:10.1016/j.enconman.2009.03.013
- Dismukes, G. C., Carrieri, D., Bennette, N., Ananyev, G. M., and Posewitz, M. C. (2008). Aquatic phototrophs: efficient alternatives to land-based crops for biofuels. *Curr. Opin. Biotechnol.* 19, 235–240. doi:10.1016/j.copbio.2008.05.007
- Doshi, V. A., Vuthaluru, H. B., and Bastow, T. (2005). Investigations into the control of odor and viscosity of biomass oil derived from pyrolysis of sewage sludge. *Fuel Process. Technol.* 86, 885–897. doi:10.1016/j.fuproc.2004.10.001
- Granados, M. R., Ación, F. G., Gómez, C., Fernandez-Sevilla, J. M., and Molina Grima, E. (2012). Evaluation of flocculants for the recovery of freshwater microalgae. *Bioresour. Technol.* 118, 102–110. doi:10.1016/j.biortech.2012.05.018
- Hognon, C., Delrue, F., Texier, J., Gateau, M., Thiery, S., Miller, S., et al. (2015). Comparison of pyrolysis and hydrothermal liquefaction of *Chlamydomonas reinhardtii*. Growth studies on the recovered hydrothermal aqueous phase. *Biomass Bioenergy* 73, 23–31. doi:10.1016/j.biombioe.2014.11.025
- Jena, U., and Das, K. C. (2011). Comparative evaluation of thermochemical liquefaction and pyrolysis for bio-oil production from microalgae. *Energy Fuels* 25, 5472–5482. doi:10.1021/ef201373m

- Martini, P. R. R. (2009). *Conversão Pirolítica de Bagaço Residual da Indústria de Suco de Laranja e Caracterização Química dos Produtos*. Dissertação de Mestrado, PPGQ; Universidade Federal de Santa Maria, Santa Maria.
- Molina Grima, E., Belarbi, E. H., Ación Fernández, F. G., Robles Medina, A., and Chisti, Y. (2003). Recovery of microalgal biomass and metabolites: process options and economics. *Biotechnol. Adv.* 20, 491–515. doi:10.1016/S0734-9750(02)00050-2
- Nascimento, J. R. S. (2001). *Lagoas de Alta Taxa de Produção de Algas Para Pós-Tratamento de Efluentes de Reatores Anaeróbios*. Dissertação de Mestrado, Instituto de Pesquisas Hidráulicas, UFRGS, Porto Alegre.
- Park, J. B. K., Craggs, R. J., and Shilton, A. N. (2011). Wastewater treatment high rate algal ponds for biofuel production. *Bioresour. Technol.*, 102, p. 35–42. doi:10.1016/j.biortech.2010.06.158
- Passos, F., Solé, M., García, J., and Ferrer, I. (2013). Biogas production from microalgae grown in wastewater: effect on microwave pretreatment. *Appl. Energy* 108, 168–175. doi:10.1016/j.watres.2013.10.013
- Pate, R., Klise, G., and Wu, B. (2011). Resource demand implications for US algae biofuels production scale-up. *Appl. Energy* 88, 3377–3388. doi:10.1016/j.apenergy.2011.04.023
- Riaño, B., Hernández, D., and Garcia-González, M. C. (2012). Microalgal-based systems for wastewater treatment: effect of applied organic and nutrient loading rate on biomass composition. *Ecol. Eng.* 49, 112–117. doi:10.1016/j.ecoleng.2012.08.021
- Sturm, B. S. M., and Lamer, S. L. (2011). An energy evaluation of coupling nutrient removal from wastewater with algal biomass production. *Appl. Energy* 88, 3499–3506. doi:10.1016/j.apenergy.2010.12.056
- Terigar, B. C., and Theegala, C. S. (2014). Investigating the interdependence between cell density, biomass productivity, and lipid productivity to maximize biofuel feedstock production from outdoor microalgal cultures. *Renew. Energy* 64, 238–243. doi:10.1016/j.renene.2013.11.010
- Trzeciak, M. B., das Neves, M. B., da Silva Vinholes, P., and Amaral Villela, F. (2008). Utilização de sementes de species oleaginosas para produção de biodiesel. *Inf. Abrates* 18, 30–38.
- Udom, I., Zaribaf, B. H., Halfhide, T., Gillie, B., Dalrymple, O., Zhang, Q., et al. (2013). Harvesting microalgae grown on wastewater. *Bioresour. Technol.* 139, 101–106. doi:10.1016/j.biortech.2013.04.002
- Uduman, N., Ying, Q., Danquah, M. K., Forde, G. M., and Hoadley, A. (2010). Dewatering of microalgal cultures: a major bottleneck to algae-based fuels. *J. Renew. Sustain. Energy* 2. doi:10.1063/1.3294480
- Um, B. H., and Kim, Y. S. (2009). Review: a chance for Korea to advance algal-biodiesel technology. *J. Ind. Eng. Chem.* 15, 1–7. doi:10.1016/j.jiec.2008.08.002
- Van de Velden, M., Baeyens, J., Brems, A., Janssens, B., and Dewil, R. (2010). Fundamentals, kinetics and endothermicity of the biomass pyrolysis reaction. *Renew. Energy* 35, 232–242. doi:10.1016/j.renene.2009.04.019
- Wessler, R. A., Amorim, S., and Cavalli, V. (2003). *Estudo da Viabilidade Técnica e Econômica da Utilização de um Polímero Orgânico Natural Catiônico em Substituição ao Sulfato de Alumínio Convencionalmente Utilizado em Estações de Tratamento de Água (ETA'S)*. Artigo Técnico. Santo André: 33 Assembleia Nacional dos Serviços Municipais de Saneamento; ASSEMAE. Available at: http://www.semasa.sp.gov.br/Documentos/ASSEMAE/Trab_29.pdf
- Yanik, J., Stahl, R., Troeger, N., and Sinag, A. (2013). Pyrolysis of algal biomass. *J. Anal. Appl. Pyrolysis* 103, 134–141. doi:10.1016/j.jaap.2012.08.016
- Chisti, Y. (2007). Biodiesel from microalgae. Research review paper. *Biotechnol. Adv.* 25, 294–306. doi:10.1016/j.biotechadv.2007.02.001
- Zhang, B., Xiong, S., Xiao, B., Yu, D., and Jia, X. (2011). Mechanism of wet sludge pyrolysis in a tubular furnace. *Int. J. Hydrogen Energy* 36, 355–363. doi:10.1016/j.ijhydene.2010.05.100
- Zhou, W., Chen, P., Min, M., Ma, X., Wang, J., Griffith, R., et al. (2014). Environment-enhancing algal biofuel production using wastewaters. *Renew. Sustain. Energy Rev.* 36, 256–269. doi:10.1016/j.rser.2014.04.073

Conflict of Interest Statement: The authors declare that the research was conducted in the absence of any commercial or financial relationships that could be construed as a potential conflict of interest.

Copyright © 2015 Vargas e Silva and Monteggia. This is an open-access article distributed under the terms of the Creative Commons Attribution License (CC BY). The use, distribution or reproduction in other forums is permitted, provided the original author(s) or licensor are credited and that the original publication in this journal is cited, in accordance with accepted academic practice. No use, distribution or reproduction is permitted which does not comply with these terms.



Demineralization of *Sargassum* spp. macroalgae biomass: selective hydrothermal liquefaction process for bio-oil production

Liz M. Díaz-Vázquez^{1*}, Arnulfo Rojas-Pérez¹, Mariela Fuentes-Caraballo¹, Isis V. Robles¹, Umakanta Jena² and K. C. Das³

¹ Department of Chemistry, University of Puerto Rico Río Piedras Campus, San Juan, PR, USA

² Bioenergy Laboratory, Desert Research Institute, Reno, NV, USA

³ College of Engineering, University of Georgia, Athens, GA, USA

Edited by:

S. Kent Hoekman, Desert Research Institute, USA

Reviewed by:

Lixin Cheng, Aarhus University, Denmark

Hao Liu, South China University of Technology, China

*Correspondence:

Liz M. Díaz-Vázquez, Lab CN 202A, Department of Chemistry, University of Puerto Rico Río Piedras Campus, Barbosa Ave-Ponce de León Avenue, San Juan, PR 00931, USA
e-mail: limdiaz@uprrp.edu; lizvazquez@gmail.com

Algae biomasses are considered a viable option for the production of biofuel because of their high yields of oil produced per dry weight. Brown macroalgae *Sargassum* spp. are one of the most abundant species of algae in the shores of Puerto Rico. Its availability in large quantity presents a great opportunity for use as a source of renewable energy. However, high ash content of macroalgae affects the conversion processes and the quality of resulting fuel products. This research studied the effect of different demineralization treatments of *Sargassum* spp. biomass, subsequent hydrothermal liquefaction (HTL), and bio-oil characterization. Demineralization constituted five different treatments: nanopure water, nitric acid, citric acid, sulfuric acid, and acetic acid. Performance of demineralization was evaluated by analyzing both demineralized biomass and HTL products by the following analyses: total carbohydrates, proteins, lipids, ash content, caloric content, metals analysis, Fourier transform infrared-attenuated total reflectance spectroscopy, energy dispersive spectroscopy, scanning electron microscopy, and GCMS analysis. HTL of *Sargassum* spp. before and after citric acid treatment was performed in a 1.8 L batch reactor system at 350°C with a holding time of 60 min and high pressures (5–21 MPa). Demineralization treatment with nitric acid was found the most effective in reducing the ash content of the macroalgae biomass from 27.46 to 0.99% followed by citric acid treatment that could reduce the ash content to 7%. Citric acid did not show significant leaching of organic components such as carbohydrates and proteins, and represented a less toxic and hazardous option for demineralization. HTL of untreated and citric acid treated *Sargassum* spp. resulted in bio-oil yields of 18.4 ± 0.1 and 22.2 ± 0.1 % (ash-free dry basis), respectively.

Keywords: *Sargassum* spp., demineralization, hydrothermal liquefaction, macroalgae bio-oil, biomass conversion

INTRODUCTION

Currently, bio-oil obtained from algae is considered a promising alternative to fossil fuels due to its high energy content (Azadi et al., 2014; Brownbridge et al., 2014) and low life-cycle emissions of greenhouse gases (Li et al., 2011; Azadi et al., 2014). Algae biomass (both microalgae and macroalgae/seaweeds) has higher lipid content and energy content than most lignocellulosic biomass (wood, plants) used for biofuels (Ross et al., 2008). In addition, macroalgae, in particular, are able to regenerate continuously without any special nutrition (Nautiyal et al., 2014; Venteris et al., 2014). In contrast to the high lignocellulosic contents of terrestrial flora, macroalgae are primarily composed of elastic polysaccharides such as alginic acid, laminarin, carrageenan, and agarose that make macroalgae a more suitable feedstock for thermochemical conversion processes (Guiry and Blunden, 1991; Holdt and Kraan, 2011). Recent studies have demonstrated that higher calorific value products can be obtained from macroalgae through hydrothermal liquefaction (HTL) (Peterson et al., 2008; Jena et al., 2011; Toor et al., 2011).

Hydrothermal liquefaction is a process used to obtain bio-crude from wet biomass in moderate to high temperatures (280–370°C) and pressures (10–25 Mpa) (Villadsen et al., 2012), in which water in its subcritical state acts as a highly reactive medium and catalyzes many chemical reactions (Toor et al., 2011). This process is fast and eco-friendly (Peterson et al., 2008) and is energetically efficient because it does not include a drying step as in the pyrolysis process (Bridgwater et al., 1999; Jena and Das, 2011). High reactivity and superior ionic product (K_w) of subcritical water break down biomass complex polymers including polysaccharides, lipids, and proteins into simpler molecules that can be converted into bio-oils with different viscosities (Peterson et al., 2008; Villadsen et al., 2012) depending on the catalysts, solvents, feedstock composition, and pretreatment methods employed. (Zhuang et al., 2012; Neveux et al., 2014; Singh et al., 2015).

Brown macroalgae, *Sargassum* spp., are considered a potential biomass source for energy production due to their relatively fast growth rates, ease of harvesting, and low preproduction cost (Guo et al., 2012). *Sargassum fluitans*, *S. natans*, and *S. filipendula*

are three of the most abundant macroalgae species found at Puerto Rico's coasts. The lipids content of *Sargassum* spp. ranges between 1.0 and 2.5% (total lipids). Li et al. (2012) reported the use of *Sargassum patens* C. Agardh biomass to generate bio-oil via HTL. They reported a bio-oil yield of $(32.1 \pm 0.2)\%$ wt./wt. as dry algae basis) with a calorific value of 27.1 MJ/kg. Another study on HTL of brown algae *Saccharina* ssp. reported a yield of 8.7 and 27.7% of bio-oil depending on the harvest times and harvesting conditions of the macroalgae (Elliott et al., 2013). Blue-green algae and red macroalgae (*Porphyra tenera*) have also been investigated for its bio-oil production through pyrolysis procedures, resulting in a similar calorific values as *S. patens* but with higher yields employing temperatures of 500°C (Bae et al., 2011; Hu et al., 2013). A recent research report described hydrothermal treatments for six types of green algae (Chlorophyta) (Neveux et al., 2014) that produced lower bio-oil yield, 9.7 to 26.2%, of bio-oil than the reported yield for *Sargassum patens* C. Agardh.

Although HTL has the potential to generate high yields of bio-oil, there are some limitations that need to be addressed if macroalgae biomass is used as feedstock. One of the major limitations of using macroalgae to produce biofuels is their high ash content (up to 50%), which reduces the yield and quality of the generated bio-oils and restricts their use in direct combustion and gasification processes (Bach et al., 2014; Neveux et al., 2014). The high ash content of macroalgae is due to the presence of inorganic salts and metals. The effect of inorganic content on the thermal conversion of terrestrial biomass has been well studied and documented; however, the effect of ash content on HTL conversion of marine feedstocks such as macroalgae is not well known (Rowbotham et al., 2013). It is expected that the high inorganic content in macroalgae will affect the physicochemical characteristics of HTL bio-oil and its storage through the catalysis of polymerization reactions.

Most alkali and alkaline earth metals present in algae can either play a catalytic role or act as inhibitors during thermochemical conversions. Ross et al. (2008) reported that the high content of alkaline metals in macroalgae impacted negatively the quality and yield of bio-crude during pyrolysis. There is a need to remove (or reduce) most of the inorganic elements in the biomass. To lower the inorganic content, Ross et al. (2009) employed two demineralization pretreatments of three brown algae species: washing the biomass with nanopure water and with hydrochloric acid solution. It was found that HCl-demineralization treatment was more effective in reducing the amount of metals and increasing the caloric value of the generated pyrolysis product. Shakirullah et al. (2006) published another demineralization study in which they employed chelating agents like EDTA and weak acids like citric acid for coal metal leaching. Their findings showed similar patterns and demineralization potential, removing 64% of the ash content without harm to the carbon content in the samples.

Bio-crudes generated from biomass require further refining by catalytic hydrodeoxygenation and cracking methods. High ash content in macroalgae can bring additional challenges to the catalytic refining of biofuel such as decrease in catalyst activities, poisoning, and coking (Bach et al., 2014; Neveux et al., 2014). It is reported that alkali and alkali earth metals present in lignocellulosic feedstocks inactivated the catalysts used in the downstream

upgrading processes of bio-oil (Liu and Bi, 2011). Although it is already established that metal content impacts biomass thermochemical processing, their role and mechanisms are not well understood and have only been studied for a few types of feedstocks and biomass thermochemical conversion techniques (Liu and Bi, 2011; Jiang et al., 2013).

In this article, we investigate the impacts of different demineralization treatments of macroalgae biomass. Five different treatments were selected for the study: two strong acids (nitric and sulfuric acid), two weak acids (citric and acetic acid), and nanopure water. Due to its abundance in Puerto Rico coast, *Sargassum* spp. were selected for the study. The study focused on analysis of the biomass changes in its physical-chemical composition, and the impact of the pretreatment on the bio-oil yield through the HTL process. The pre-treated and non-treated *Sargassum* spp. biomass were analyzed and compared for their metal contents and organic composition. The quality and chemical composition of the generated bio-oil from untreated and demineralized biomass were compared in terms of energy content and higher heating values (HHVs).

MATERIALS AND METHODS

RAW MATERIAL

Sargassum spp. (a mixture of *S. fluitans*, *S. natans*, and *S. filipendula*) were collected from Naguabo, Puerto Rico, located on the south-east coast of the island facing the Caribbean Sea and Toa Baja, Puerto Rico, located on the north of the island facing the Atlantic Ocean during March–June, 2012. Impurities and salts were removed using nanopure Milli-Q water. Macroalgae biomass was dried at 60°C, pulverized and milled for 6 min using an 8000 M mixer/mill (SPEX CertiPrep, Metuchen, NJ, USA) and stored in a desiccator at room temperature until further analysis.

DEMINERALIZATION METHOD

Demineralization procedures were adapted from the study reported by Jiang et al. (2013). *Sargassum* spp. biomass was submitted to five different demineralization treatments: nanopure Milli-Q water, sulfuric acid (10% v/v), nitric acid (10% v/v), acetic acid (10% v/v), and citric acid (10% w/v). All acids were 99.9% pure and were purchased from Sigma Aldrich. Acid solutions were prepared using nanopure Milli-Q water. In a typical demineralization treatment, 8.0 g of biomass were immersed in 100 mL 10% acid solution (or, just water) to obtain sludge. Algae sludge was magnetically stirred at 28°C and 1000 rpm for 12 h. After demineralization, the samples were filtered and rinsed with an excess of nanopure Milli-Q water until the pH value was neutral. Treated biomass samples were dried in an electric oven at 60°C overnight and stored in a sealed desiccator until further analysis. Demineralization treatments and analyses were done in triplicate and mean values are reported.

BIOMASS CHARACTERIZATION

Biomass biochemical analysis

Untreated and treated *Sargassum* biomass was analyzed for soluble carbohydrates, total proteins, and total lipids content. Anthrone method (Hedge and Hofreiter, 1962), a colorimetric assay, was used to determine the total soluble carbohydrates content as follows: 0.1 g of dry algae was heated in 10 mL HCl 2.5 M, filtered

and neutralized using NaHCO_3 until neutral pH; 1 mL of the resulting solution was mixed with 2 mL of aqueous solution 75% H_2SO_4 and 4 mL of anthrone solution. The absorbance was read at 630 nm using a ultraviolet-visible spectrophotometer (Hach Dr5000). Algal proteins were extracted by a mild digestion using 0.6 M sodium hydroxide solution at 40°C for 12 h. The extracts were filtered, dialyzed against nanopure water for 48 h, and then lyophilized. The protein content in algal biomass was determined by bicinchoninic acid (BCA) assay (Wiechelman et al., 1988) and measured at 562 nm. The total lipid content (%) was determined using an adaptation of the method reported by Bligh and Dyer (1959). Briefly, 1 g of the biomass was homogenized using 15.0 mL of a mixture of solvents [chloroform/(methanol/water) 3:1] using a tissue grinder (Omni® Tissue Master, 125 Watt-Lab Homogenizer with a 7 mm probe tip). Then the homogenate was transferred to a separation funnel and 15 mL of chloroform were added. The aqueous phase was discarded; the organic extract was collected and evaporated to dryness in weighed vials to determine the total lipid content of the sample.

Proximate and metal analysis of untreated and treated *Sargassum* biomass

Moisture, ash, volatile (dry), and fixed carbon contents of untreated macroalgae and solid residues (bio-char) were measured using a thermogravimetric analyzer (TGA), (Leco TGA-701, Leco Corp.) following the ASTM D-5142 method: 1 g sample was heated until 900°C at a rate of 50°C/min. For metal analysis, 100 mL of algae solutions were prepared by adding 0.5 g of samples and were digested in 35 mL of concentrated 69.6% Nitric acid (Fisher scientific, USA) solution. Standard solutions and samples were analyzed in an atomic absorption spectrometer (Perkin Elmer AA analyst 200). Biomass samples were also analyzed using energy dispersive spectroscopy (EDS) X-ray fluorescence (EDAX Detecting Unit PV7757/81 ME) to determine elemental composition. Ash compositions of raw and treated biomass were determined through the use of a muffle furnace. Briefly, three 1.00 g samples of each dry algae biomass were weighed in crucibles and then heated in a muffle furnace at 600°C for 6 h as reported by Ververis et al. (2007). After cooling the samples in a desiccator, the ash content (%) was determined. Results were expressed on a dry algae basis.

Internal energy change (ΔU) of macroalgae biomass

The internal change of energy (ΔU) associated with combustion of the *Sargassum* spp. biomass in the presence of excess oxygen was measured using a bomb calorimeter. The reaction was carried out experimentally in a closed, constant-volume calorimeter (Parr 1341 Plain Jacket Oxygen Bomb 2901EB Ignition unit 115/50/60) and the experimentally measured quantity was the heat associated with the process. Since the change in internal energy is equal to the heat at a constant volume ($\Delta U = q_V$), a measurement of the heat gives ΔU of the combustion reaction directly. The internal energy of combustion was determined from the heat capacity of the system and the temperature rise. All the calculations were done as indicated on the instrument manual and as reported by Garland et al. (2009). The calorimeter calibration and its heat capacity ($C_{\text{calorimeter}}$) calculation were performed using benzoic acid as the reference standard.

FTIR-ATR characterization analysis of macroalgae biomass

Untreated and demineralization treated samples were analyzed using Fourier transform infrared-attenuated total reflectance spectroscopy (FTIR-ATR) (Perkin Elmer Spectrum 100 FTIR spectrometer) to identify the chemical structural differences due to the demineralization processes. For this analysis, 2 mg of sample was ground to obtain a particle size of $\sim 150 \mu\text{m}$. The attenuated total reflectance infrared absorption spectra of the samples were recorded in the frequency range of 4000–450 cm^{-1} and 40 scans were recorded at a resolution of 4 cm^{-1} . Three absorption spectra were obtained for each sample and the average spectra are reported.

Scanning electron microscopy analysis

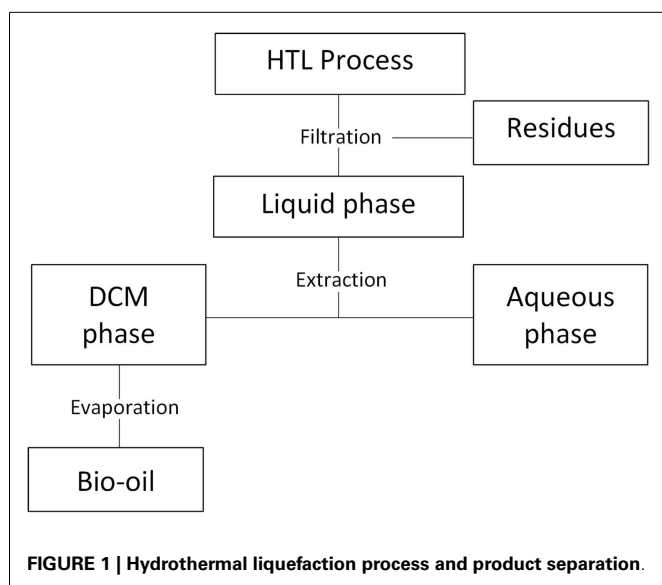
The morphology and surface of gold coated biomass were studied by scanning electron microscopy (SEM) [(JEOL, JSM 6480LV) with low vacuum at 20 kV and 2000 \times magnification factor] to determine its potential change to the physical structure of the macroalgae.

HYDROTHERMAL LIQUEFACTION METHODOLOGY

Hydrothermal liquefaction experiments were carried out in a 1.8 L batch reactor system (Parr Instruments Co. Moline, PA, USA) at 350 \pm 5°C with a holding time of 60 min and stirred at 300 rpm as reported by Jena et al. (2011) (Jena and Das, 2011). Algal slurry was prepared using 80% deionized water and 20% dry algae biomass by weight. In a typical experiment, homogenized algal slurry (~ 500 g) was loaded in the reactor and sealed. The system was purged with He for 3 min and pressurized to 2.03 MPa (295 \pm 2 psi). At the end of the reaction, the reactor was cooled down using tap water flowing through an internal cooling coil that was regulated by a solenoid valve. Gas products were collected in Tedlar® sample bags. HTL products were separated into bio-oil fraction, water soluble fraction, solid residues, and gaseous fraction (Figure 1). The rotor, reactor, and solids residues were washed using dichloromethane (DCM), Sigma Aldrich, USA. The solid product was removed by filtration and the liquid phase product was separated by liquid-liquid extraction. Bio-oil and water soluble products were stored in glass bottles in darkness at 4°C and solids residues (bio-char) were oven dried at 50°C for 24 h and stored for further analysis. All HTL experiments were performed in duplicate.

Analysis of HTL products

Bio-oil and bio-char were analyzed by FTIR-ATR using the procedure described in Section “FTIR-ATR Characterization Analysis of Macroalgae Biomass” for solid samples. For liquid samples, a drop was employed in the same analysis. Elemental C, H, N, S, and O contents in bio-oil and bio-char were measured using a LECO brand (Model CHNS-932) analyzer. Gas chromatography and mass spectroscopy (GC/MS) analysis of bio-oil samples and water soluble products was carried out with an Agilent Technologies 6890N Network GC system, 5973 Network Mass selective Detector and Agilent JW Scientific, DB-5 GC column (5% phenyl and 95% methylpolysiloxane 30 m \times 0.25 mm \times 0.32 mm). The gas fractions were analyzed by gas chromatography coupled to a thermal conductivity detector (GC-TCD Agilent Technologies



G2858A) with a column (5A PLOT) of 10 m × 0.32 mm size and using Helium as mobile phase.

Bio-oil and water soluble product GC/MS procedures. Profiles of volatile and semivolatile compounds present in the bio-oil and residual water samples were analyzed by a gas chromatograph coupled to a mass spectrometer (Agilent Technologies 6890N Network GC system, 5973 Network Mass selective Detector). Bio-oil samples were submitted to a derivatization procedure to improve the detection of alcohol and fatty acids. Briefly, 10 mg of bio-oil were added in a 5 mL reaction vessel with an excess of a silylating reaction mix [BSTFA (*N*, *O*-bis (trimethylsilyl) trifluoroacetamide) and TMCS (trimethylchlorosilane) SUPELCO; Sigma Aldrich]. The reaction mixtures were incubated at 70°C for 30 min. After the derivatization procedure, the samples were diluted to 2.00 mL with DCM and an aliquot of 1 μL was analyzed by GC/MS. The GC/MS method was as follows: sample injection splitless, inlet temperature at 250°C, pulse pressure 25 psi, and flow 1 mL/min; Column DB-5 30 m × 0.320 mm and film 0.21 μm. The MS was in positive ion and total ion scan mode. The GC oven temperature program was as follows: held at initial temperature at 70°C for 1 min, then 5°C/min until 120°C, followed by an increase of 8°C/min until 260°C where it was held for 5 min.

In order to determine the compounds present in the water soluble aqueous co-product (ACP), ACP samples were pre-concentrated using solid phase extraction technique with a 12 cc Oasis™ HLB copolymer with hydrophilic lipophilic balance (HLB) Vac cartridge (Waters Co.) as a stationary phase. About 100 mL of ACP sample was passed through the cartridge; retained compounds were eluted using 10 mL of ethyl acetate and then pre-concentrated with an inert flow of nitrogen to 2.00 mL. Samples were derivatized using the same procedure used for bio-oil samples using BSTFA-TMCS as the silylating agent. The GC/MS method was the same as for bio-oil with the follows changes in the oven temperature program: initial temperature at 40°C held by 2 min, and ramped at 40°C/min until 100°C, 2°C/min until 120°C,

30°C/min until 200°C, 15°C/min until 260°C, 30°C/min until 300, and held for 3 min at that temperature. For bio-oil and water soluble analyses, compounds were identified using a NIST library; only the compounds with a quality identification (R match) of 70% or more and a signal to noise (S/N) ratio ≥ 15 were reported.

Calculation methods: bio-oil and bio-char yield, higher heating value, and energy recovery. Bio-oil and bio-char product yields were calculated separately on an ash and moisture free dry weight basis using the following equation (Li et al., 2012):

$$Y_{\text{PRODUCT}} = \left[\frac{W_{\text{PRODUCT}}}{W_{\text{FEEDSTOCK}} - W_{\text{ASH}} - W_{\text{MOISTURE}}} \right] \times 100 \quad (1)$$

where, Y_{PRODUCT} is the bio-oil or bio-char yield (wt.%) on a dry weight basis, W_{PRODUCT} is the mass of product (g), $W_{\text{FEEDSTOCK}}$ is the mass of macroalgae biomass used in the reactor, W_{ASH} and W_{MOISTURE} are the ash content and moisture content of the feedstock, respectively. The HHVs of the generated bio-oil and bio-char were calculated using the proximate analysis results and the Dulong formula (Landau and Lifshitz, 1980; Qu et al., 2003):

$$\text{HHV (MJ/kg)} = 0.3383C + 1.422 (H - O/8) \quad (2)$$

where C, H, O are the wt.% present in the product.

The chemical energy recovery (ER) was calculated for the bio-crude and bio-char phase according to the following equation (Neveux et al., 2014):

$$\text{ER} = \left(\frac{(\text{HHV}_{\text{PRODUCT}} \times W_{\text{PRODUCT}})}{(\text{HHV}_{\text{FEEDSTOCK}} \times W_{\text{FEEDSTOCK}})} \right) \times 100 \quad (3)$$

RESULTS AND DISCUSSION

EFFECTS OF DEMINERALIZATION ON BIOMASS COMPOSITION AND BIO-OIL YIELD

Material recovery, biochemical composition, and internal energy

The effectiveness of the different biomass demineralization treatments was evaluated considering the impact of the treatments on the biochemical composition of the algae. The yield of bio-oil in HTL depends on the amount of biomolecules such as carbohydrates, proteins, and lipids present in the biomass. Therefore, the most effective treatment should be able to reduce the mineral content of the biomass without losing these molecules. **Table 1** summarizes the impact of the demineralization treatments on the biomass composition. From **Table 1**, it can be concluded that all treatments significantly decrease the biomass ash contents; however, they also reduce the total soluble carbohydrates and total proteins in the biomass. An average total biomass reduction of 36% was observed for all treatments. On the other hand, the percent of lipids extracted from the biomass after the demineralization treatments were higher than with the untreated biomass. This increase in the effectiveness of lipid extraction may be caused by the breakdown of the cellular walls of the macroalgae during the treatments, which makes intracellular lipids more accessible. The treatments did not increase the amount of lipids present in the algae, they maybe just make the extraction process more effective and it is shown in the % of recovery obtained.

Table 1 | Recovery percentage, chemical content and changing in internal energy of algae biomass after the demineralization treatment (all values are reported on dry biomass basis).

Demineralization treatment	% Recovery biomass	Soluble carbohydrates (w/w %)	Ash content (w/w %)	Proteins (w/w %)	Lipids (w/w %)	($-\Delta U$) kJ/g
No treatment	N/A	10 ± 2	27.46 ± 0.04	11.3 ± 0.4	0.3 ± 0.1	11.4 ± 0.2
Nanopure water	61 ± 7	8.3 ± 0.8	12.5 ± 0.4	10.9 ± 0.5	0.7 ± 0.3	11.9 ± 0.4
Acetic acid	66 ± 3	9 ± 1	10.4 ± 0.5	8.1 ± 0.7	0.4 ± 0.5	11.9 ± 0.4
Citric acid	67 ± 3	9 ± 1	7 ± 1	9.4 ± 0.4	0.9 ± 0.4	13.0 ± 0.1
Nitric acid	60 ± 2	9 ± 2	0.99 ± 0.07	8.1 ± 0.5	0.9 ± 0.4	14.0 ± 0.3
Sulfuric acid	65 ± 6	7 ± 4	9 ± 0.5	6.9 ± 0.4	0.9 ± 0.5	12.3 ± 0.9

N/A, not applicable; $-\Delta U$, internal energy.

Among all demineralization treatments conducted in this study, nitric acid was found to be the most effective in reducing the ash contents from 27.64% in the starting biomass to 0.99%, followed by citric acid that resulted in 7% ash content in the treated biomass. These treatments also resulted in lower reduction of soluble carbohydrates and proteins contents, and higher energy content (ΔU) (Table 1). Even nanopure water treatment was able to reduce the ash content significantly suggesting that part of the mineral content lost from *Sargassum*, is composed of water soluble components such as chlorides, nitrates, carbonates, and phosphates as observed for terrestrial biomass (Patwardhan et al., 2010; Jiang et al., 2013).

From Table 1, it can be seen that all demineralization treatments resulted in similar biomass recovery. The change in internal energy ($-\Delta U$) associated with the combustion reaction of the algae biomass was determined by the calorimetric analysis. The change in internal energy was used to estimate the amount of energy the biomass may release. The calorimetric analysis results showed that demineralized biomass releases a higher amount of energy during its combustion. The biomass demineralized with nitric acid releases the highest amount of energy. It may be due to the fact that the removal of the inorganic components allows a more complete combustion of the organic components of the biomass. Also, de-ashing properties of nitric acid solutions have been shown in the demineralization of different types of coals, which is related to a more aggressive digestion (Shakirullah et al., 2006).

Metal analysis of treated and untreated biomass

Treated and untreated *Sargassum* biomass was analyzed for copper (Cu), iron (Fe), magnesium (Mg), manganese (Mn), sodium (Na), and zinc (Zn) content using an atomic absorption (AA) spectrometer. Biomass was analyzed before and after each demineralization (Table 2). The metal content was reduced in the treated biomass for all demineralization treatments. The inorganic acid, sulfuric acid was the most effective treatment in removing Cu, Fe, Mn, and Zn and was followed by another inorganic acid, nitric acid. The organic acids, citric and acetic acid, were found to be effective treatments for the removal of Mg and Mn.

Other elements (Na, K, Si, P, and S) were analyzed using electron dispersive spectroscopy (EDS) and are presented in Table 2. The EDS results also confirmed the reduction in inorganic contents of the biomass in the demineralization treatments. Both EDS and AA

Table 2 | Elemental analysis in untreated and treated biomasses.

Treatment	No treatment	Nanopure water	Acetic acid	Nitric acid	Citric acid	Sulfuric acid
AA RESULTS (ppm)						
Cu	38.5	24	12	n.d	13	n.d
Fe	414.6	403	346	n.d	440	n.d
Mg	21,870	21,663	n.d	789.7	n.d	503
Mn	53	48	n.d	n.d	n.d	n.d
Zn	73	82	71	6	36	13
EDS RESULTS (ppm)						
Na	1800	1300	400	n.d	n.d	1100
K	8000	8400	n.d	n.d	700	n.d
Si	1700	1300	n.d	1000	1300	1300
P	400	n.d	n.d	n.d	n.d	n.d
S	11,600	10,900	11,500	700	9650	60,400 ^a

n.d: below detection limits or not detected.

^aExpected to be high.

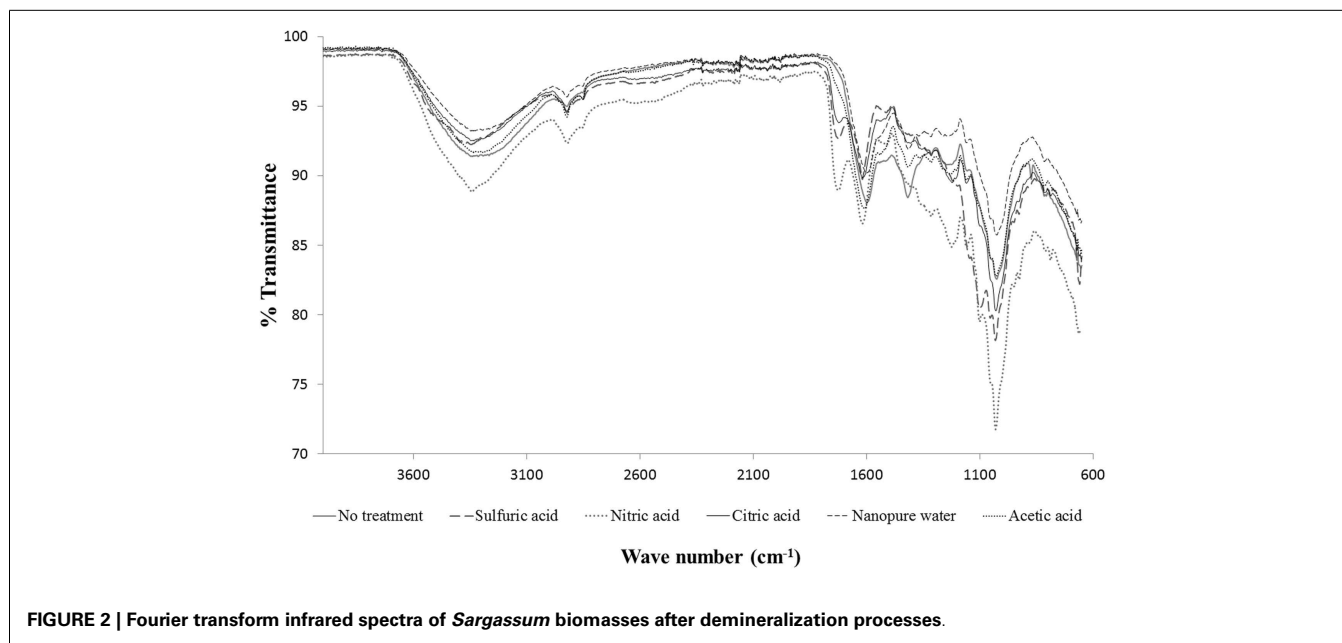
results confirmed the reduction of alkali and alkaline earth metals concentration in *Sargassum* biomass after the treatments.

Treatment of biomass in strong acids is an efficient method for removal of the inorganic elements of the feedstock before its HTL conversion into bio-oil. However, the treatment could also affect the structural and physicochemical properties of the sample. The treatments with weak acids such as citric and acetic acid are less effective than the treatment with strong acids, but are less aggressive removing the organic content of the biomass.

CHARACTERIZATION OF BIOMASS

FTIR-ATR characterization analysis

Fourier transform infrared-ATR analysis was performed to obtain more information on the chemical composition differences in untreated and demineralized *Sargassum* biomass. Figure 2 shows the IR spectra of untreated and treated biomass. Results obtained from FTIR-ATR analysis confirmed that after the demineralization process, the same types of chemical compounds were still present in all treated solids, although FTIR results also revealed that some of the treatments showed losses of structural compounds features. These results agreed with our biochemical composition analysis reported in Table 1. In the mid-infrared spectra, a prominent band

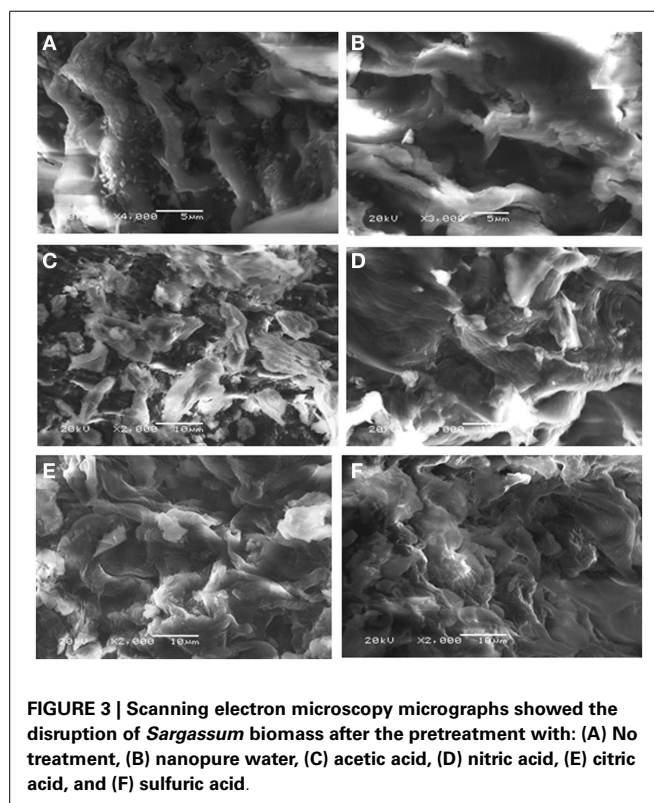


at 3000–3700 cm^{-1} was attributed to O–H stretching vibrations of hydroxyl functional groups in carboxylic, phenolic, and alcoholic compounds. The band at 2800–3000 cm^{-1} was related to =C–H and C–H stretching vibrations. Intensities of the above bands decreased in almost all the solid samples from demineralization treatment, except for the nitric acid treatment. The increase of this band height can be attributed to the presence of residues of nitric acids in the treated samples showing a narrower band in the region of 3491–3550 cm^{-1} . Another relevant band that appeared at a frequency of 1725 cm^{-1} , is attributed to the C=O stretching vibration of free carbonyl groups present in lipids and some polysaccharides such as alginate.

The bands peaks in the region, 1370–1320 cm^{-1} were attributed to O–H, C≡C, and C=O stretching vibrations. The band height at 1350 cm^{-1} decreased with all demineralization treatments. Some bands were observed at 900–1200 cm^{-1} , with the most intense band in this region corresponding to C–O stretching, which might be associated with the polysaccharides (alginate, laminarin, and fucoidan) (Ross et al., 2009). Some of the observed bands were sharper for samples from acids demineralization treatments. The observed changes in this region could be attributed to changes in some of the major constituents due to cross linking reactions between C–OH, C–O–C, and other reactive functional groups present in the biomass (Mayer et al., 2012). The breakdown and leaching of some polysaccharides is suggested from the increase of the bands at 900–1200 cm^{-1} . Similar behavior has also been in terrestrial biomass (Jiang et al., 2013).

Biomass surface analysis (SEM)

Scanning electron microscopy was used to study changes in the biomass surface due to demineralization pretreatments. The SEM micrographs are shown in Figure 3. The micrographs showed that treated algae biomass materials were more porous than untreated algae, and showed distinct differences in the morphology. The untreated biomass showed a defined structure in which small



particles were attached. The biomass treated with nanopure water, acetic acid, and citric acid still showed an almost intact surface when compared with the untreated biomass, but most of the small particles observed on the untreated biomass were removed; only the particles with larger dimensions were noticed on the surface. After treatment with strong acids (nitric acid and sulfuric acid), the structure of the biomass surface seemed to be wrinkled and

fewer particles were seen adhering to the surface, as compared to the weak acid treatments. The changes in morphology of the biomass surface and the analysis of metal composition suggest that the particles observed at the surface of the biomass could be minerals. The strong acid treatment produced the most drastic change in fiber structure of the biomass, demineralization treatments were able to remove the minerals but at the same time they dissolved the polysaccharides (Jiang et al., 2013).

HTL OF UNTREATED AND DEMINERALIZED *SARGASSUM* BIOMASS

Although nitric acid was a better pretreatment for demineralizing the selected biomass, it could be associated with proteins and soluble carbohydrates losses, some structural harm and it is a toxic compound. It was not selected for these reasons and also because it is recommended to avoid the presence of nitrogen in the HTL process. Alvarez et al. (2003) found an increase in nitrogen-containing compounds in the demineralized coal employing nitric acid treatment that could be associated with the release of NO_x during combustion. Although the citric acid demineralization pretreatment did not show the highest demineralization potential, it was selected for further HTL studies due to its low toxicity and its potential to remove inorganic components with a minimum loss of organic compounds (polysaccharides, proteins, and lipids) that are crucial for the HTL process.

Biomass proximate analysis

Proximate analysis of the untreated and demineralized algae biomass (treated with citric acid) was performed and resulted in higher fixed carbon percent ($19.0 \pm 1.0\%$) and lower ash content ($7.0 \pm 0.8\%$) than the untreated feedstock ($9.6 \pm 0.0\%$ fixed carbon and $27.4 \pm 0.9\%$ ash), suggesting that there is higher organic content in the same amount of treated feedstock. As mentioned earlier (see Effects of Demineralization on Biomass Composition and Bio-Oil Yield), demineralized biomass had a lower metal content in the ash. Also, the citric acid treated biomass had a higher percent of volatiles ($73.0 \pm 2.0\%$) and lower moisture content ($4.9 \pm 0.6\%$) than untreated *Sargassum* biomass ($61.5 \pm 0.9\%$ volatiles and $13.3 \pm 0.2\%$ moisture).

Bio-oil and bio-char yield, higher heating value, and energy recovery

Hydrothermal liquefaction reaction conditions of 350°C, 20% solids load, 300 rpm and 60 min reaction time were selected following the settings reported by Jena et al. (2011) (Jena et al., 2011). Bio-oil yields from HTL citric acid treated and untreated

Sargassum biomass are presented in ash-free dry weight basis in **Table 3**. As anticipated from the proximate analysis, a higher bio-oil yield (22.2%) was obtained from the HTL of demineralized *Sargassum* biomass than that of the raw biomass, which had a bio-oil yield of 18.4%. This could be due to more organic content in the same amount of feedstock that validates the demineralization treatment performed. The resulting bio-oil had a HHV of 32.4 and 32.3 MJ/kg in the demineralized and control, respectively, which was significantly higher than that of the obtained by Li et al. (2012), 27.1 MJ/kg. There are no significant differences in elemental carbon, hydrogen, and oxygen composition in bio-oil samples obtained from the untreated and treated biomass (**Table 3**). Both untreated and demineralized biomass produce bio-oil with C, H, and O values comparable to the other studies reported in the literature for the liquefaction of algal biomass (%C 70–73; %H, 7–8; %O 10–11; %S 0–1; and %N 1–7) (Zhou et al., 2010; Anastasakis and Ross, 2011). High oxygen content in bio-oil suggests that a catalysis process before or after the HTL process is required to convert the product in a useful fuel (Li et al., 2012).

Table 3 includes the values for bio-oil ER. A higher energy recovery value ($42.3 \pm 0.1\%$) was obtained for the bio-oil obtained from the demineralized biomass, while only (23.5 ± 0.1) was obtained from the raw biomass. Given that the HHV was not altered, the increase in the ER value may be attributed to the increase in the yield production of bio-oil. **Table 3** also shows that after citric acid treatment and HTL, bio-oil was obtained with slight increase of C/O. This confirms the increase in the potential energy output. Furthermore, S content was minimized, suggesting a more environmental friendly bio-oil product was obtained.

In contrast to the consistency of the elemental composition of the obtained bio-oil, bio-char composition was changed considerably between the untreated and the demineralized biomass as shown in **Table 3**. The untreated biomass produced an organic rich bio-char with higher carbon content 60%, while the bio-char from the demineralized biomass had only 43.47% C. Therefore, a HHV was obtained for it (20.7%) versus 11.5% for the bio-char obtained from the demineralized biomass, suggesting that inorganic substances help preserve the energy output in bio-char although the total yield may be decreased. Although the HHV of bio-char has decreased, the C/O content has also decreased. The reduction in C content in itself is not a desirable thing, but the increase in O is considered desirable because the presence of oxygenated groups in bio-char enhances its properties in soils applications – like its cation exchange capacity (CEC) – as reported in previous studies with terrestrial biomasses and production of

Table 3 | Ultimate analysis, product yield and energy recovery of HTL bio-crude and bio-char product obtained from untreated and demineralized *Sargassum*.

Product	Yield product (%) ^a	C (%)	H (%)	N (%)	S (%)	O (%) ^b	HHV (MJ/kg)	ER (%)	
Citric acid treated biomass	Bio-oil	22.2 ± 0.1	71.54 ± 0.65	8.05 ± 0.29	2.28 ± 0.04	0.07 ± 0.09	18.05 ± 0.92	32.4 ± 1.2	42.3 ± 0.1
	Bio-char	31.3	43.47 ± 1.84	3.67 ± 0.35	1.44 ± 0.15	4.18 ± 2.16	47.24 ± 2.48	11.5 ± 2.5	21.2 ± 0.3
Untreated biomass	Bio-oil	18.4 ± 0.1	70.28 ± 0.51	8.31 ± 0.01	2.65 ± 0.03	0.21 ± 0.05	18.66 ± 0.45	32.3 ± 0.6	23.5 ± 0.1
	Bio-char	29.3 ± 0.1	60.05 ± 1.93	4.08 ± 0.05	2.19 ± 0.02	3.04 ± 0.55	30.65 ± 1.57	20.7 ± 3.0	24.0 ± 0.2

^aAsh-free dry weight basis.

^bObtained by difference.

char (Cheng et al., 2006). The C/O ratio of the produced bio-char suggest that it has a high number of oxygenated functional groups (phenol, hydroxyl, carboxyl among others), a property that can improve its chemisorption ability, increasing its potential to be used to remediate contaminated soils (Jose et al., 2013).

In summary for the HTL primary fuel target, the bio-oil, we observe an increase in yield, lower S, and slightly lower N, along with an increase in ER after the demineralization pretreatment. The generated bio-char have a considerably high energy and higher carbon content than other algae bio-char (Li et al., 2012; Neveux et al., 2014), thus may be a valuable by-product if used for soil application [e.g., as a fertilizers or for remediation purposes (Bird et al., 2012)] or as a feedstock for subsequent thermochemical processes such as pyrolysis (López Barreiro et al., 2013). In terms of ER about 47.2% of the energy present in the original biomass was recovered in the form of bio-oil (19.6%) and bio-char (27.6%) in the HTL of the demineralized biomass, while in the case of the untreated biomass only 28.3% of the energy was recovered. Part of the remaining chemical energy, in both cases may be present in the aqueous phase. As presented in the GCMS analysis of the aqueous residues that follows this section, in both cases there are compounds of energetic value present that may be recovered if a more efficient extraction of the aqueous phase is performed. The ER of the process was improved by the demineralization process, but it still needs to be increased. Our results point that the demineralization pretreatment may be of benefit for the bio-refinery.

Bio-oil chemical composition

ATR-FTIR analysis. The generated bio-oils were analyzed for their chemical composition with ATR-FTIR and the obtained spectra are presented in **Figure 4**. Peaks at 722, 737, and 819 cm^{-1} , O–H bending, shows the presence of aromatic compounds, phenols, esters, and ethers; at 1265 cm^{-1} , C–O stretching for alcohols and with peaks at 1383 and 1458 cm^{-1} , C–H bending, presence of fats; alkenes are detected at 1625 cm^{-1} , C=C stretching; ketones, aldehydes, and carboxylic acids with peak at 1688 cm^{-1} , C=O stretching; alkanes are found at 2875, 2932, and 2965 cm^{-1} , C–H stretching and water with the peak at 3375 cm^{-1} . In the IR-spectrum for the bio-oil obtained from the demineralized biomass, the bands that evidence the presence of alcohols, phenols, esters, ethers, and alkanes are more prominent than in the bio-oil of the raw biomass. Proximate analysis showed that the bio-oil from raw biomass had $1.3 \pm 0.7\%$ of water, while the bio-oil from demineralized biomass had lower water content $0.8 \pm 0.4\%$ w. It is consistent with the FTIR analyses where the band corresponding to OH was more prominent in the bio-oil from raw biomass.

GCMS analysis of the bio-oil product. In general, bio-oil generated from *Sargassum* biomass is a very complex blend of more than 100 compounds that were presumptively identified by GCMS. The chromatograms were analyzed with the NIST library and compounds having quality identification factor higher than 70 were reported. Table S1 in Supplementary Material section shows the compounds identified in the bio-oil obtained from the untreated and demineralized biomass, respectively. Both bio-oil samples obtained from untreated and treated biomass were composed of

alcohols, ketones, aldehydes, phenols, alkenes, fatty acids, esters, aromatics, amino acids, nitrogen-containing heterocyclic compounds, and chlorinated/brominated compounds. The nitrogen-containing heterocyclic compounds, such as indole, could be generated from the decomposition of proteins. In addition, pyrazine derivatives were detected and their presence can be attributed to *Maillard reactions*, which are reaction of sugars and amines (Kruse et al., 2007). The bio-oil obtained from the demineralized biomass has a higher abundance and varieties of fatty acids, alcohols, and hydrocarbons. Oleic acid is the most abundant fatty acid. Only one fatty acid methyl ester was detected in the products, the hexadecanoic acid methyl ester. Different types of ketones and phenols were also identified in the bio-oils, but a higher diversity of phenols was found on the bio-oil obtained from the demineralized biomass. It could be attributed to a more efficient conversion of the polysaccharides and cellulose by reactions of hydrolysis, dehydration, cyclization among other reactions (Shuping et al., 2010; Li et al., 2012). A larger number of polycyclic aromatic compounds were identified in the untreated biomass; these compounds can be associated with an incomplete process.

Analysis of water soluble aqueous co-products. The aqueous fractions obtained with the treated biomass showed a weak acidity (pH = 5.9) as expected for the demineralization process, while untreated biomass showed a weak basicity (pH = 8.0). Table S2 in Supplementary Material list the compounds identified in the water soluble organics produced in HTL of the untreated and the demineralized biomass, respectively. Most of the compounds identified have low molecular weight and are polar. Organic acids such as butanoic, pentanoic, and hexadecanoic acid were detected. Glycerol, an important by product, was found in all the samples. Benzene derivatives and various nitrogen-containing compounds were also identified. In addition, some fatty acids were detected in the water phase suggesting the need for more effective extraction and separation of the different HTL products.

Analysis of gases. The gas fraction produced during the HTL was analyzed by gas chromatography coupled to a thermal conductivity detector for measuring relative CO_2 and CH_4 concentrations. We focus on these two gases because they are main component of the gas mixture. However, there are some research reports that inform the presence of small amounts of C_2H_4 , C_2H_6 , and H_2S when conditions similar to ours are used and in the presence of heterogeneous catalyst in the HTL process (Duan and Savage, 2010).

Carbon dioxide and methane generated from the different biomass feed stocks are presented in **Table 4**. The demineralized *Sargassum* biomass produced a higher amount of CO_2 and CH_4 , than that of the untreated biomass. The detected percentages indicate that there are other components present in the product gases. The higher carbon dioxide content obtained for the demineralized biomass, suggest that the decarboxylation reactions were more productive, leading to obtain a higher bio-oil yield and quality.

CONCLUSION

The efficiency of five demineralization pretreatments (nanopure water, nitric acid, citric acid, sulfuric acid, and acetic acid) of

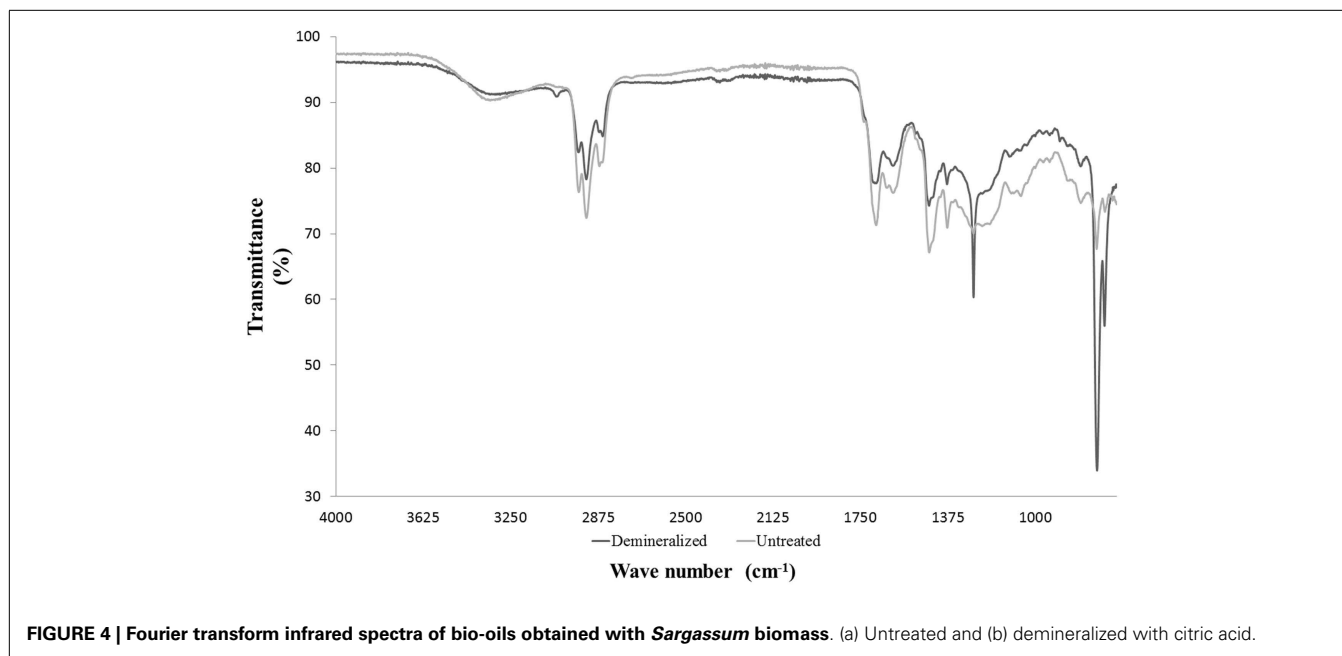


FIGURE 4 | Fourier transform infrared spectra of bio-oils obtained with *Sargassum* biomass. (a) Untreated and (b) demineralized with citric acid.

Table 4 | GC-TCD analysis of the HTL gas fraction obtained for untreated and demineralized *Sargassum* biomass.

Gas fraction	<i>Sargassum</i> spp. (%)	Demineralized <i>Sargassum</i> spp. (%)
CH ₄	0.25 ± 0.01	0.34 ± 0.02
CO ₂	31 ± 1	41 ± 1

Sargassum spp. biomass and the effects of demineralization on HTL conversion were studied. It was found that all the demineralization pretreatments decreased the inorganic contents in the *Sargassum* biomass. However, citric acid was selected as the best option because it was able to remove almost all the mineral content (from 27.46 to 7% ash content) without significantly altering the organic composition and structure of biomass. In addition, it represents a more eco-friendly alternative. HTL process was performed on both demineralized and untreated *Sargassum* biomass. Results showed that demineralized biomass generated a higher bio-oil yield (22.2%) when compared with the untreated biomass (18.4%). The demineralization process did not significantly affect the HHV of the generated bio-oil, but since a higher bio-oil yield and a bio-char with high carbon content were obtained for the demineralized biomass, the net total ER in HTL was an increase from 47.4 to 63.5% when considering the energy associated with the bio-oil and the bio-char products. The chemical composition of the bio-oil obtained from the demineralized biomass confirms that the demineralization process facilitated the generation of a product richer in compounds with higher energy value such as alkanes and fatty acids. The bio-chars obtained from the HTL of the demineralized biomass had a higher percent of fixed carbon and HHV than the original feedstock therefore is suitable for further processing and ER.

ACKNOWLEDGMENTS

This project was supported by a grant from the US DoD Centers of Research Excellence in Science and Technology ARO Grant W911NF-11-1-0218 and the UPR Center for Renewable Energy and Sustainability. Authors are grateful to chemistry students Eduardo Roman, Ana P. Lozada, and Nelson Agosto from UPR-RP and the graduate students Will Costanzo, BSBchE, and Andrew Smola from UGA for their support with some of the analysis. We would like to thank the Material Characterization Center (MCC) at UPR, Rio Piedras Campus for SEM and EDS images.

SUPPLEMENTARY MATERIAL

The Supplementary Material for this article can be found online at <http://www.frontiersin.org/Journal/10.3389/fenrg.2015.00006/abstract>

REFERENCES

- Alvarez, R., Clemente, C., and Gómez-Limón, D. G. (2003). The influence of nitric acid oxidation of low rank coal and its impact on coal structure*. *Fuel* 82, 2007–2015. doi:10.1016/S0016-2361(03)00176-5
- Anastasakis, K., and Ross, A. (2011). Hydrothermal liquefaction of the brown macro-alga *Laminaria saccharina*: effect of reaction conditions on product distribution and composition. *Bioresour. Technol.* 102, 4876–4883. doi:10.1016/j.biortech.2011.01.031
- Azadi, P., Brownbridge, G., Mosbach, S., Smallbone, A., Bhawe, A., Inderwildi, O., et al. (2014). The carbon footprint and non-renewable energy demand of algae-derived biodiesel. *Appl. Energy* 113, 1632–1644. doi:10.1016/j.apenergy.2013.09.027
- Bach, Q.-V., Sillero, M. V., Tran, K.-Q., and Skjermo, J. (2014). Fast hydrothermal liquefaction of a Norwegian macro-alga: screening tests. *Algal Res.* 6(Pt B), 271–276. doi:10.1016/j.algal.2014.05.009
- Bae, Y. J., Ryu, C., Jeon, J. K., Park, J., Suh, D. J., Suh, Y. W., et al. (2011). The characteristics of bio-oil produced from the pyrolysis of three marine macroalgae. *Bioresour. Technol.* 102, 3512–3520. doi:10.1016/j.biortech.2010.11.023
- Bird, M. I., Wurster, C. M., de Paula Silva, P. H., Paul, N. A., and de Nys, R. (2012). Algal biochar: effects and applications. *Glob. Change Biol. Bioenergy* 4, 61–69. doi:10.1111/j.1757-1707.2011.01109.x

- Bligh, E. G., and Dyer, W. J. (1959). A rapid method of total lipid extraction and purification. *Can. J. Biochem. Physiol.* 37, 911–917. doi:10.1139/o59-099
- Bridgwater, A., Meier, D., and Radlein, D. (1999). An overview of fast pyrolysis of biomass. *Org. Geochem.* 30, 1479–1493. doi:10.1016/j.biortech.2012.06.016
- Brownbridge, G., Azadi, P., Smallbone, A., Bhava, A., Taylor, B., and Kraft, M. (2014). The future viability of algae-derived biodiesel under economic and technical uncertainties. *Bioresour. Technol.* 151, 166–173. doi:10.1016/j.biortech.2013.10.062
- Cheng, C.-H., Lehmann, J., Thies, J. E., Burton, S. D., and Engelhard, M. H. (2006). Oxidation of black carbon by biotic and abiotic processes. *Org. Geochem.* 37, 1477–1488. doi:10.1016/j.orggeochem.2006.06.022
- Duan, P., and Savage, P. E. (2010). Hydrothermal liquefaction of a microalga with heterogeneous catalysts. *Ind. Eng. Chem. Res.* 50, 52–61. doi:10.1021/ie100758s
- Elliott, D. C., Hart, T. R., Neuenschwander, G. G., Rotness, L. J., Roesijadi, G., Zacher, A. H., et al. (2013). Hydrothermal processing of macroalgal feedstocks in continuous-flow reactors. *ACS Sustain. Chem. Eng.* 2(2), 207–215. doi:10.1021/sc400251p
- Garland, C. W., Nibler, J. W., and Shoemaker, D. P. (2009). *Experiments in Physical Chemistry*. New York, NY: McGraw-Hill.
- Guiry, M. D., and Blunden, G. (1991). *Seaweed Resources in Europe: Uses and Potential*. Chichester: John Wiley and Sons Ltd.
- Guo, J., Zhuang, Y., Chen, L., Liu, J., Li, D., and Ye, N. (2012). Process optimization for microwave-assisted direct liquefaction of *Sargassum polycystum* C. Agardh using response surface methodology. *Bioresour. Technol.* 120, 19–25. doi:10.1016/j.biortech.2012.06.013
- Hedge, J., and Hofreiter, B. (1962). Determination of reducing sugars and carbohydrates: anthrone colorimetric method. *Methods Carbohydr. Chem.* 1, 389–390.
- Holdt, S. L., and Kraan, S. (2011). Bioactive compounds in seaweed: functional food applications and legislation. *J. Appl. Phycol.* 23, 543–597. doi:10.1007/s10811-010-9632-5
- Hu, Z., Zheng, Y., Yan, F., Xiao, B., and Liu, S. (2013). Bio-oil production through pyrolysis of blue-green algae blooms (BGAB): product distribution and bio-oil characterization. *Energy* 52, 119–125. doi:10.1016/j.energy.2013.01.059
- Jena, U., and Das, K. (2011). Comparative evaluation of thermochemical liquefaction and pyrolysis for bio-oil production from microalgae. *Energy Fuels* 25, 5472–5482. doi:10.1021/ef201373m
- Jena, U., Das, K., and Kastner, J. (2011). Effect of operating conditions of thermochemical liquefaction on biocrude production from *Spirulina platensis*. *Bioresour. Technol.* 102, 6221–6229. doi:10.1016/j.biortech.2011.02.057
- Jiang, L., Hu, S., Sun, L. S., Su, S., Xu, K., He, L. M., et al. (2013). Influence of different demineralization treatments on physicochemical structure and thermal degradation of biomass. *Bioresour. Technol.* 146, 254–260. doi:10.1016/j.biortech.2013.07.063
- Jose, L. G.-E., Luke, B., Eduardo, M.-J., Upal, G., and Tom, S. (2013). “The potential of biochar amendments to remediate contaminated soils,” in *Biochar and Soil Biota*, eds N. Ladygina and F. Rineau (Boca Raton, FL: CRC Press), 100–133.
- Kruse, A., Maniam, P., and Spieler, F. (2007). Influence of proteins on the hydrothermal gasification and liquefaction of biomass. 2. Model compounds. *Ind. Eng. Chem. Res.* 46, 87–96. doi:10.1021/ie061047h
- Landau, L. D., and Lifshitz, E. M. (1980). *Course of Theoretical Physics*. Moscow: Elsevier.
- Li, D., Chen, L., Xu, D., Zhang, X., Ye, N., Chen, F., et al. (2012). Preparation and characteristics of bio-oil from the marine brown alga *Sargassum patens*. *Bioresour. Technol.* 104, 737–742. doi:10.1016/j.biortech.2011.11.011
- Li, Y.-G., Xu, L., Huang, Y.-M., Wang, F., Guo, C., and Liu, C.-Z. (2011). Microalgal biodiesel in China: opportunities and challenges. *Appl. Energy* 88, 3432–3437. doi:10.1016/j.apenergy.2010.12.067
- Liu, X., and Bi, X. T. (2011). Removal of inorganic constituents from pine barks and switchgrass. *Fuel Process. Technol.* 92, 1273–1279. doi:10.1016/j.fuproc.2011.01.016
- López Barreiro, D., Prins, W., Ronsse, F., and Brilman, W. (2013). Hydrothermal liquefaction (HTL) of microalgae for biofuel production: state of the art review and future prospects. *Biomass Bioenergy* 53, 113–127. doi:10.1016/j.biombioe.2012.12.029
- Mayer, Z. A., Apfelbacher, A., and Hornung, A. (2012). Effect of sample preparation on the thermal degradation of metal-added biomass. *J. Anal. Appl. Pyrolysis* 94, 170–176. doi:10.1016/j.jaap.2011.12.008
- Nautiyal, P., Subramanian, K., and Dastidar, M. (2014). Production and characterization of biodiesel from algae. *Fuel Process. Technol.* 120, 79–88. doi:10.1016/j.fuproc.2013.12.003
- Neveux, N., Yuen, A. K., Jazrawi, C., Magnusson, M., Haynes, B. S., Masters, A. E., et al. (2014). Biocrude yield and productivity from the hydrothermal liquefaction of marine and freshwater green macroalgae. *Bioresour. Technol.* 155, 334–341. doi:10.1016/j.biortech.2013.12.083
- Patwardhan, P. R., Satrio, J. A., Brown, R. C., and Shanks, B. H. (2010). Influence of inorganic salts on the primary pyrolysis products of cellulose. *Bioresour. Technol.* 101, 4646–4655. doi:10.1016/j.biortech.2010.01.112
- Peterson, A. A., Vogel, F., Lachance, R. P., Fröling, M., Antal, M. J. Jr., and Tester, J. W. (2008). Thermochemical biofuel production in hydrothermal media: a review of sub- and supercritical water technologies. *Energy Environ. Sci.* 1, 32–65. doi:10.1039/b810100k
- Qu, Y., Wei, X., and Zhong, C. (2003). Experimental study on the direct liquefaction of *Cunninghamia lanceolata* in water. *Energy* 28, 597–606. doi:10.1016/S0360-5442(02)00178-0
- Ross, A., Anastasakis, K., Kubacki, M., and Jones, J. (2009). Investigation of the pyrolysis behaviour of brown algae before and after pre-treatment using PY-GC/MS and TGA. *J. Anal. Appl. Pyrolysis* 85, 3–10. doi:10.1016/j.jaap.2008.11.004
- Ross, A. B., Jones, J. M., Kubacki, M. L., and Bridgeman, T. (2008). Classification of macroalgae as fuel and its thermochemical behaviour. *Bioresour. Technol.* 99, 6494–6504. doi:10.1016/j.biortech.2007.11.036
- Rowbotham, J. S., Dyer, P. W., Greenwell, H. C., Selby, D., and Theodorou, M. K. (2013). Copper (II)-mediated thermolysis of alginates: a model kinetic study on the influence of metal ions in the thermochemical processing of macroalgae. *Interface Focus* 3, 20120046. doi:10.1098/rsfs.2012.0046
- Shakirullah, M., Ahmad, I., Rehman, H., Ishaq, M., Khan, U., and Ullah, H. (2006). Effective chemical leaching and ash depletion of low rank coal with EDTA and citric acid. *J. Chem. Soc. Pak.* 28(1), 56.
- Shuping, Z., Yulong, W., Mingde, Y., Kaleem, I., Chun, L., and Tong, J. (2010). Production and characterization of bio-oil from hydrothermal liquefaction of microalgae *Dunaliella tertiolecta* cake. *Energy* 35, 5406–5411. doi:10.1016/j.energy.2010.07.013
- Singh, R., Bhaskar, T., and Balagurumurthy, B. (2015). Effect of solvent on the hydrothermal liquefaction of macro algae *Ulva fasciata*. *Process Saf. Environ. Prot.* 93, 154–160. doi:10.1016/j.psep.2014.03.002
- Toor, S. S., Rosendahl, L., and Rudolf, A. (2011). Hydrothermal liquefaction of biomass: a review of subcritical water technologies. *Energy* 36, 2328–2342. doi:10.1016/j.energy.2011.03.013
- Venteris, E. R., Skaggs, R. L., Wigmosta, M. S., and Coleman, A. M. (2014). A national-scale comparison of resource and nutrient demands for algae-based biofuel production by lipid extraction and hydrothermal liquefaction. *Biomass Bioenergy* 64, 276–290. doi:10.1016/j.biombioe.2014.02.001
- Ververis, C., Georgioudis, K., Danielidis, D., Hatzinikolaou, D. G., Santas, P., Santas, R., et al. (2007). Cellulose, hemicelluloses, lignin and ash content of some organic materials and their suitability for use as paper pulp supplements. *Bioresour. Technol.* 98, 296–301. doi:10.1016/j.biortech.2006.01.007
- Villadsen, S. R., Dithmer, L., Forsberg, R., Becker, J., Rudolf, A., Iversen, S. B., et al. (2012). Development and application of chemical analysis methods for investigation of bio-oils and aqueous phase from hydrothermal liquefaction of biomass. *Energy Fuels* 26, 6988–6998. doi:10.1021/ef300954e
- Wiechelmann, K. J., Braun, R. D., and Fitzpatrick, J. D. (1988). Investigation of the bicinchoninic acid protein assay: identification of the groups responsible for color formation. *Anal. Biochem.* 175, 231–237. doi:10.1016/0003-2697(88)90383-1
- Zhou, D., Zhang, L., Zhang, S., Fu, H., and Chen, J. (2010). Hydrothermal liquefaction of macroalgae *Enteromorpha prolifera* to bio-oil. *Energy Fuels* 24, 4054–4061. doi:10.1021/ef100151h
- Zhuang, Y., Guo, J., Chen, L., Li, D., Liu, J., and Ye, N. (2012). Microwave-assisted direct liquefaction of *Ulva prolifera* for bio-oil production by acid catalysis. *Bioresour. Technol.* 116, 133–139. doi:10.1016/j.biortech.2012.04.036

Conflict of Interest Statement: The authors declare that the research was conducted in the absence of any commercial or financial relationships that could be construed as a potential conflict of interest. The Guest Associate Editor S. Kent Hoekman

declares that, despite being affiliated to the same institution as author Umakanta Jena, the review process was handled objectively and no conflict of interest exists.

Received: 18 September 2014; accepted: 26 January 2015; published online: 11 February 2015.

Citation: Díaz-Vázquez LM, Rojas-Pérez A, Fuentes-Caraballo M, Robles IV, Jena U and Das KC (2015) Demineralization of *Sargassum* spp. macroalgae biomass: selective hydrothermal liquefaction process for bio-oil production. *Front. Energy Res.* 3:6. doi: 10.3389/fenrg.2015.00006

This article was submitted to Bioenergy and Biofuels, a section of the journal Frontiers in Energy Research.

Copyright © 2015 Díaz-Vázquez, Rojas-Pérez, Fuentes-Caraballo, Robles, Jena and Das. This is an open-access article distributed under the terms of the Creative Commons Attribution License (CC BY). The use, distribution or reproduction in other forums is permitted, provided the original author(s) or licensor are credited and that the original publication in this journal is cited, in accordance with accepted academic practice. No use, distribution or reproduction is permitted which does not comply with these terms.

Optimization of protein extraction from *Spirulina platensis* to generate a potential co-product and a biofuel feedstock with reduced nitrogen content

Naga Sirisha Parimi¹, Manjinder Singh¹, James R. Kastner¹, Keshav C. Das^{1*}, Lennart S. Forsberg² and Parastoo Azadi²

¹ College of Engineering, The University of Georgia, Athens, GA, USA, ² Complex Carbohydrate Research Center, The University of Georgia, Athens, GA, USA

OPEN ACCESS

Edited by:

S. Kent Hoekman,
Desert Research Institute, USA

Reviewed by:

John Chandler Cushman,
University of Nevada, USA
Arumugam Muthu,
Council of Scientific and Industrial
Research, India
Mi Li,
Oak Ridge National Laboratory, USA

*Correspondence:

Keshav C. Das,
Driftmier Engineering Center,
University of Georgia, Room 509,
Athens, GA 30602, USA
kdas@engr.uga.edu

Specialty section:

This article was submitted to
Bioenergy and Biofuels, a section of
the journal Frontiers in
Energy Research

Received: 03 February 2015

Accepted: 10 June 2015

Published: 23 June 2015

Citation:

Parimi NS, Singh M, Kastner JR, Das
KC, Forsberg LS and Azadi P (2015)
Optimization of protein extraction from
Spirulina platensis to generate
a potential co-product and a biofuel
feedstock with reduced nitrogen
content.
Front. Energy Res. 3:30.
doi: 10.3389/fenrg.2015.00030

The current work reports protein extraction from *Spirulina platensis* cyanobacterial biomass in order to simultaneously generate a potential co-product and a biofuel feedstock with reduced nitrogen content. *S. platensis* cells were subjected to cell disruption by high-pressure homogenization and subsequent protein isolation by solubilization at alkaline pH followed by precipitation at acidic pH. Response surface methodology was used to optimize the process parameters – pH, extraction (solubilization/precipitation) time and biomass concentration for obtaining maximum protein yield. The optimized process conditions were found to be pH 11.38, solubilization time of 35 min and biomass concentration of 3.6% (w/w) solids for the solubilization step, and pH 4.01 and precipitation time of 60 min for the precipitation step. At the optimized conditions, a high protein yield of 60.7% (w/w) was obtained. The protein isolate (co-product) had a higher protein content [80.6% (w/w)], lower ash [1.9% (w/w)] and mineral content and was enriched in essential amino acids, the nutritious γ -linolenic acid and other high-value unsaturated fatty acids compared to the original biomass. The residual biomass obtained after protein extraction had lower nitrogen content and higher total non-protein content than the original biomass. The loss of about 50% of the total lipids from this fraction did not impact its composition significantly owing to the low lipid content of *S. platensis* (8.03%).

Keywords: *Spirulina platensis*, protein isolate, high-pressure homogenization, response surface methodology, residual biomass, biofuel feedstock

Introduction

The concept of biorefinery which proposes the integration of biofuel production processes with the extraction of co-product(s) such as proteins, pigments, and other high-value compounds is the path forward to improve the sustainability and economic feasibility of microalgal processing technologies. The high protein (and nitrogen) content of algal feedstock is a major limitation to whole biomass to biofuel conversion processes such as hydrothermal liquefaction (HTL) and anaerobic digestion (AD). High-protein feedstocks result in high nitrogen content in the fuel produced from HTL and

ammonia toxicity in AD (Chen et al., 2008; López Barreiro et al., 2013). Thus, nitrogen removal through protein extraction could potentially improve the feedstock composition for biofuel applications, while generating a useful co-product. Microalgal proteins are comparable to conventional protein sources such as soymeal and eggs, and hence find potential applications in human nutrition and animal feed (Spolaore et al., 2006; Becker, 2007).

Pre-treatments such as mechanical cell lysis, enzymatic, thermal, and chemical treatments result in improved component extraction by complete or partial degradation of the microalgal cell wall, thus, improving the accessibility of the intra-cellular components. High-pressure homogenization and ultrasonication were reported to enhance microalgal protein solubilization, the former being the most effective method (Gerde et al., 2013; Safi et al., 2014). Autoclaving was reported as an effective pretreatment to improve lipid extraction from microalgae (Prabakaran and Ravindran, 2011).

Protein solubility is pH dependent. Highly acidic and alkaline conditions enhance the solubility of algal proteins by inducing net charges on the amino acid residues (Damodaran, 1996). Proteins are least soluble at their isoelectric pH and precipitate out. Thus, solubilization under alkaline conditions followed by precipitation at isoelectric pH is a useful strategy for obtaining crude protein isolates. Several authors reported protein extraction from green algae and cyanobacteria using this method (Choi and Markakis, 1981; Chronakis et al., 2000; Gerde et al., 2013; Safi et al., 2014; Ursu et al., 2014). Other parameters that could impact protein solubility include extraction (solubilization or precipitation) time, solvent/biomass ratio (biomass concentration), and temperature (Abas Wani et al., 2006). High temperature causes protein denaturing and also increases the energy input for the overall process (Goetz and Koehler, 2005). Hence, heat treatment is undesirable in protein isolation processes.

Process optimization and statistical analysis is necessary to maximize protein extraction and determine the independent and interaction effects of various process parameters on the extraction yields. Response surface methodology (RSM) is a popular statistical method for optimization of process parameters while conducting the least number of experiments (Firatligil-Durmus and Evranuz, 2010). Protein extraction process optimization using RSM for non-algal sources and *Chlorella pyrenoidosa* (green algae) was reported previously (Quanhong and Caili, 2005; Zhang et al., 2007; Ma et al., 2010; Wang and Zhang, 2012).

The current study dealt with process optimization for maximizing protein extraction from the cyanobacterium (blue-green alga) *Spirulina platensis*, and the generation of a residual biomass with lower nitrogen content than the original biomass for potential applications as a biofuel feedstock in whole biomass conversion processes such as HTL and AD. Cyanobacteria differ significantly from green algae in cell wall structure and biochemical composition. Unlike the latter which have a recalcitrant cell wall comprising of cellulose and hemicellulose (Payne and Rippin-gale, 2000), cyanobacteria such as *Spirulina* and *Nostoc sp.* have a peptidoglycan-based cell wall (Palinska and Krumbein, 2000). Moreover, they have a higher protein and lower lipid content (Becker, 2007). These differences necessitate the optimization of process parameters for the specific phylum. *S. platensis* was

chosen in the current study for two reasons. First, it is an edible cyanobacterium and hence its protein isolate is expected to have a high nutritive value. Second, it has a very high protein content (Cohen, 1997) and hence the impact of protein isolation on the biochemical composition of the residual biomass would be very striking in this species compared to those with a lower protein content. Although some reports on extraction of proteins from *S. platensis* may be found in the literature, major knowledge gaps on process optimization, component fractionation, and product characterization remain (Devi et al., 1981; Chronakis et al., 2000; Safi et al., 2013b). The current work aimed at filling these gaps in order to understand the fate of various cell components as a result of the fractionation process and identify the bottlenecks in the process. Some of the parameters described in the literature to characterize protein isolates such as protein content, amino acid composition, mineral composition, and molecular weight range of the proteins were reported for the protein isolate obtained in this study (Chronakis et al., 2000; Gerde et al., 2013; Safi et al., 2013a). Such knowledge is very useful in assessing the sustainability, scalability, and economic feasibility of the process.

Materials and Methods

Microalgae

Spirulina platensis was obtained from Earthrise Nutritionals LLC (Calipatria, CA, USA) in dry powder form and was stored in sealed, air tight plastic packages at room temperature prior to use. The dry powder was mixed with deionized (DI) water to form biomass slurry at the desired concentration (solids content).

Protein Isolation Process

Spirulina platensis biomass slurry prepared at the desired concentration was subjected to a protein isolation process (Figure S1 in Supplementary Material) which involved pretreatment of the biomass and subsequent extraction of proteins by solubilization at alkaline pH using 1M NaOH followed by precipitation from the supernatant (obtained from the previous step) at acidic pH using either 1M HCl or 1M HCOOH. The solid-liquid separation after the solubilization and the precipitation steps was achieved by centrifugation at 8670 g for 35 min. The pellet and the supernatant from the solubilization step are henceforth referred to as alkali pellet and alkali supernatant, respectively, and those from the precipitation step are referred to as acid pellet and acid supernatant, respectively. The acid pellet was the protein isolate. The combined fraction of the alkali pellet and acid supernatant was the residual biomass.

Selection of Pretreatment

A 6% slurry of *S. platensis* biomass was subjected to three different pretreatments namely autoclaving, ultrasonication, and high-pressure homogenization. Autoclaving was carried out at 121°C with 103.4 kPa (15 psi) for 30 min. Ultrasonication was carried out using a probe sonicator (Biologics, Inc., VA, USA) at 20% maximum power for 60 min. High-pressure homogenization involved two passes through a high-pressure homogenizer (Constant systems LTD., UK) at 103.4 MPa (15 kpsi). The samples were placed on ice bath during ultrasonication and high-pressure

homogenization, and a chiller was attached to the latter unit to minimize sample heating. The control experiment did not involve any pretreatment. Each of the pretreated and control samples was subjected to protein solubilization at pH 11 for 60 min followed by solid–liquid separation. The treatments were compared based on protein recovery in the supernatant fraction. The cells were observed visually under an optical microscope (400 times magnification).

Optimization of Experimental Conditions

Solubility curve determination

A 6% *S. platensis* biomass slurry was subjected to cell disruption by high-pressure homogenization and separated into aliquots. The pH of each aliquot was adjusted to various values in the range of 2–13 (with a step size of 1 U) using either 1M NaOH or 1M HCl and stirred for 30 min before subjecting to solid–liquid separation. A graph of pH versus protein recovery in the supernatant was plotted to obtain the solubility curve.

Statistical optimization

The design of optimization experiments and the statistical analysis was carried out using SAS-based JMP Pro (version 10) statistical software. A Box–Behnken design based on RSM was employed to optimize the process conditions affecting protein solubilization and precipitation. The optimization range for pH for both the steps was chosen based on the solubility curve data. The range for solubilization and precipitation times was 10–60 min. The 60 min maximum was chosen based on the literature which reported that increasing the solubilization time beyond 60 min did not result in a significant increase in the extracted proteins from pH 11 sonicated, non-defatted algae biomass (Gerde et al., 2013). The chosen range for biomass concentration was 2–10% solids, a typical solids range of harvested algal biomass.

Based on the design, set of 15 and 10 experiments were carried out for the solubilization and precipitation steps, respectively (Tables S1 and S2 in Supplementary Material). A second degree polynomial with the following general equation was fit to the data obtained from the solubilization experiments:

$$Y = A_0 + A_1X_1 + A_2X_2 + A_3X_3 + A_{11}X_1^2 + A_{22}X_2^2 + A_{33}X_3^2 + A_{12}X_1X_2 + A_{13}X_1X_3 + A_{23}X_2X_3 \quad (1)$$

where Y was the protein recovery in the alkali supernatant, X_i ($i = 1, 2, 3$) was the coded dimensionless value of an independent input variable x_i ($i = 1, 2, 3$) in the range of -1 to 1 . The independent input variables were x_1 (pH), x_2 (solubilization time), and x_3 (biomass concentration). A_0 was the constant term, A_i ($i = 1, 2, 3$), A_{ii} ($i = 1, 2, 3$), and A_{ij} ($i = 1, 2, 3; j = 2, 3; i \neq j$) are the linear, quadratic, and interaction regression coefficients. The variables were coded according to the following equation:

$$X_i = (x_i - x_0)/\Delta x_i, i = 1, 2, 3 \quad (2)$$

where x_0 was the real value of the center point of each input variable and Δx_i was the step change.

Protein precipitation from the alkali supernatant was carried out using 1M HCOOH obtained at the RSM optimized conditions.

A second degree polynomial with the following general equation was fit to the data obtained from the precipitation experiments:

$$Y = B_0 + B_1X_1 + B_2X_2 + B_{11}X_1^2 + B_{22}X_2^2 + B_{12}X_1X_2 \quad (3)$$

where Y was the protein recovery in the acid pellet, X_i ($i = 1, 2$) was the coded dimensionless value of an independent input variable x_i ($i = 1, 2$) in the range of -1 to 1 . The independent input variables were x_1 (pH) and x_2 (precipitation time). B_0 was the constant term, B_i ($i = 1, 2$), B_{ii} ($i = 1, 2$), and B_{ij} ($i = 1; j = 2$) were the linear, quadratic, and interaction regression coefficients. The input variables were coded in a manner similar to the solubilization step variables.

The coefficient of determination (R^2) and the scattered plots between the experimental and predicted protein recoveries were obtained. The significance of the regression coefficients of the polynomial equations was determined using the Student's t -test and p value. Optimum process conditions were obtained from the response surface analysis and were experimentally validated.

Analytical Methods

Total Nitrogen, Protein, and Amino Acid Analysis

A HACH high-range total nitrogen assay method (HACH Corporation, Loveland, CO, USA) was used to measure the total nitrogen concentration (mg L^{-1}) in each sample. The nitrogen concentration obtained was multiplied by a factor of 6.25 to obtain the protein concentration (Piorreck et al., 1984; Chronakis et al., 2000; Safi et al., 2013a). A modified Lowry protein assay was used to determine the hydro-soluble protein content (Lowry et al., 1951). Bovine serum albumin (BSA) was used to prepare the standard curve for Lowry protein quantification. Nitrogen content (% N on dry basis) was obtained from the C, H, N, S elemental analysis carried out using a LECO brand analyzer (Model CHNS-932) according to the methods described in ASTM D 5291 and D 3176 (Jena et al., 2011a). Protein content (based on elemental analysis) was determined by multiplying the nitrogen content by the conversion factor of 6.25. Amino acid analysis and quantification was carried out by the University of Missouri Agricultural Experiment Station (Columbia, MO, USA). The proteins in the feed and product fractions were visualized under denatured conditions by SDS-PAGE using a Bio-Rad Miniprotein SystemTM with Any kDTM gels (Bio-Rad Laboratories, Hercules, CA, USA) (Gerde et al., 2013).

Total Solids and Non-Protein Components Analysis

Total solids content was determined by drying the samples at 105°C for 4 h in a conventional oven (Sluiter et al., 2008a). Lipids were extracted by Folch extraction method using chloroform/methanol mixture (2:1 ratio) (Folch et al., 1957), followed by centrifugation at 2600 g for 10 min. The chloroform-soluble fractions were analyzed for fatty acids by preparing fatty acid methyl esters (FAMES) by methanolysis (1M methanolic HCl, 80°C , 16 h) and subjecting to GC-MS analysis using a non-polar DB-1 capillary column equipped with mass selective detector following procedures as described (York et al., 1986). All extracts were first analyzed without any internal standard, allowing the use of behenic acid (C:22:0, 10 μg) as an appropriate internal standard.

Hydroxy fatty acids were subjected to trimethylsilylation following methanolysis to facilitate GC separation; the response factors of common normal chain saturated and unsaturated fatty acid standards, and 2-hydroxy myristic acid standard were normalized relative to that of behenic acid. Ash content was determined after drying the samples in a conventional oven for 4 h and then incinerating them in a furnace at 575°C for 3 h using a slightly modified version of the NREL procedure (Sluiter et al., 2008b). The rest of biomass which comprises predominantly of carbohydrates and small amounts of other cellular components may simply be considered as the carbohydrate fraction for convenience. Thus, the carbohydrate content was determined by the difference (Valdez et al., 2014).

PG Analysis

The product fractions were delipidated by the Folch lipid extraction method described in Section “Total Solids and Non-Protein Components Analysis” and then subjected to PG component analysis. In order to identify and quantify PG amino acids, a portion of the delipidated samples was hydrolyzed in 6M HCl for 16 h at 105°C followed by methanolysis for 4 h at 80°C to yield methyl esters of amino acids, and finally derivatized with heptafluorobutyric anhydride (HFBA), which yields the *N*-heptafluorobutyrate (and *O*-heptafluorobutyrate for Serine and Threonine) derivatives of the PG-derived amino acids (Pons et al., 2003). The method was modified slightly wherein trans-esterification with isoamylalcohol was not performed and 2-amino adipic acid (25 µg) was used as internal standard. The resulting methyl esterified, HFBA derivatives were analyzed by GC-MS analysis using the DB-1 capillary column programed to 240°C. For PG carbohydrate analysis, a separate aliquot was hydrolyzed in 1M HCl for 2 h at 105°C followed by methanolysis for 6 h at 80°C followed by *N*-acetylation (acetic anhydride/pyridine in methanol, 1:1:10 v/v, 45 min, 50°C) and trimethylsilylation using “Tri-Sil” reagent (20 min, 80°C) (York et al., 1986). Carbohydrates were measured relative to the internal standard myo-inositol (20 µg). The resulting HFBA-amino acids and TMS-methyl glycosides of monosaccharide sugars were analyzed separately by GC-MS analysis using a 30 m DB-1 capillary column with electron impact mass fragmentation and detection, using temperature programs optimized for separately analyzing the amino acid and carbohydrate derivatives.

Results and Discussion

Protein Isolation Optimization

Comparison of Different Pretreatments

The results indicated that both high-pressure homogenization and ultrasonication resulted in a higher protein recovery in the supernatant compared to control (Figure S2 in Supplementary Material). High-pressure homogenization was the better of the two pretreatments with a protein recovery of 83.5% as opposed to 69.9% in case of ultrasonication. Microscopic observation of the disrupted cells showed greater cell disruption with the former compared to the latter (Figure S3 in Supplementary Material). Similar trend was reported for various algae and cyanobacteria (Safi et al., 2014; Ursu et al., 2014). Cell counting revealed that

high-pressure homogenization resulted in a near-complete cell lysis with disruption efficiency >99%, thus releasing most of the intra-cellular proteins. Autoclave treatment was the worst among all pretreatments with a protein recovery of only 29%, which was slightly lower than the 32.1% in the control. No visible cell disruption was observed under the microscope for the autoclaved *S. platensis* cells, explaining the lack of improvement in protein recovery. Thus, high-pressure homogenizer-based cell disruption was chosen as a pretreatment for all further protein isolation experiments.

Protein Solubility Curve

The solubility curve (Figure 1) showed that protein solubility (recovery in the supernatant) decreased with increasing pH in the acidic range of 2–4 and increased steadily in the range of 4–7. Least solubility was observed in the proximity of pH 4. High solubility (>75% recovery) was observed in the alkaline range of 7–12. However, under extremely high alkaline conditions (beyond pH 12) the solubility decreased notably. This could be a result of significant protein denaturation and clustering, rendering the proteins insoluble (Haque et al., 2005). The variation in protein recovery was only about 10% in the entire pH range of 6–12, although the trend was irregular. Highest recovery was obtained at pH 11 and closely followed by pH 8. These results differed from those reported for green algae. For *Chlorella vulgaris* the solubilization after cell lysis was 19% higher at pH 12 compared to pH 7 (Ursu et al., 2014). For *Nannochloropsis* species, protein solubilization was reported to increase with increasing pH all the way until 13 (Gerde et al., 2013). Thus, pH 11 and 8 were further explored under different experimental conditions to determine the better of the two for protein solubilization. A 3% *S. platensis* biomass slurry subjected to cell disruption by high-pressure homogenization and protein solubilization resulted in 87.9% protein recovery at pH 11 as opposed to 77.8% at pH 8. Similarly, *S. platensis* biomass at nearly the same solids content but disrupted using ultrasonication resulted in 58.2% protein recovery at pH 11 while only 38.7% at pH 8. Thus, pH 11 was better than 8 for protein solubilization.

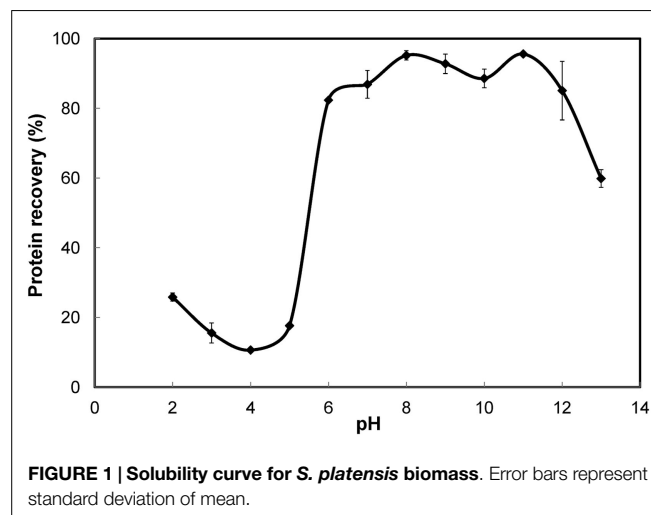


FIGURE 1 | Solubility curve for *S. platensis* biomass. Error bars represent standard deviation of mean.

Optimization of Protein Isolation Using RSM

pH ranges of 10.5–12 and 3–5 that were in the proximity (within 1 U) of the points of highest and least solubility (reported in Section “Protein Solubility Curve”) were chosen for the design of protein solubilization and precipitation optimization experiments, respectively. **Figure 2A** shows the scattered plot between experimentally determined and RSM predicted protein recoveries in the alkali supernatant at different levels of the input variables. The experimental recovery varied from 64.87 to 95.6% (data presented in Table S1 in Supplementary Material). The regression coefficients of the second degree polynomial used to fit the protein recovery data, the standard error in their estimation, and the statistical analysis are presented in **Table 1**. The regression equation obtained from the analysis was as follows:

$$Y = 93.03 - 1.54X_1 + 1.32X_2 - 10.36X_3 - 1.72X_1^2 - 2.33X_2^2 - 9.16X_3^2 - 0.55X_1X_2 - 3.57X_1X_3 + 1.95X_2X_3 \quad (4)$$

The predicted recoveries were highly significant ($p = 0.0027$) and the coefficient of determination (R^2) for this model was 0.97, indicating a good fit. The results from the t -test showed that biomass concentration was a highly significant factor ($p = 0.0001$) in impacting protein recovery. The other two factors, pH, and solubilization time were not significant in the chosen range. However, the interaction of pH and biomass concentration was slightly significant ($p = 0.0522 < 0.1$). Among the quadratic effects, only the quadratic biomass concentration term was highly significant ($p = 0.0015$). The rest of the interaction and quadratic terms were not significant. The optimal values for pH, solubilization time, and biomass concentration determined by RSM were 11.38, 35.32 min, and 3.61% (w/w) solids, respectively, and the predicted value of the response (protein recovery) at these conditions was 96%.

Formic acid is a weak organic acid compared to hydrochloric acid which is a strong inorganic acid. In a comparative study, protein recovery in the acid pellet (protein isolate) was 71.7% when precipitation was carried out using HCl and 71.5% using HCOOH at the same experimental conditions. Thus, the substitution of HCOOH for HCl did not show any significant impact on protein precipitation. The former is more preferable than the latter when the residual biomass is intended to be used for biofuel production processes because chloride ions can corrode reactor vessels in thermochemical processes such as HTL (Kritzer, 2004), and the NaCl formed as a result of NaOH and HCl added during the protein isolation process can be toxic to the microbes in biochemical processes such as AD (Chen et al., 2008). Thus, HCOOH was used for protein precipitation in all further experiments.

Figure 2B shows the scattered plot between experimental and RSM predicted protein recoveries in the acid pellet at different levels of the input variables. The experimental recovery varied from 67 to 74.5% (data presented in Table S2 in Supplementary Material). The regression coefficients of the second degree polynomial used to fit the protein recovery data, the standard error in their estimation, and their statistical analysis are presented in **Table 2**. The regression equation obtained from the analysis is as follows:

$$Y = 73.43 - 0.72X_1 + 1.28X_2 - 5.11X_1^2 + 1.49X_2^2 - 0.48X_1X_2 \quad (5)$$

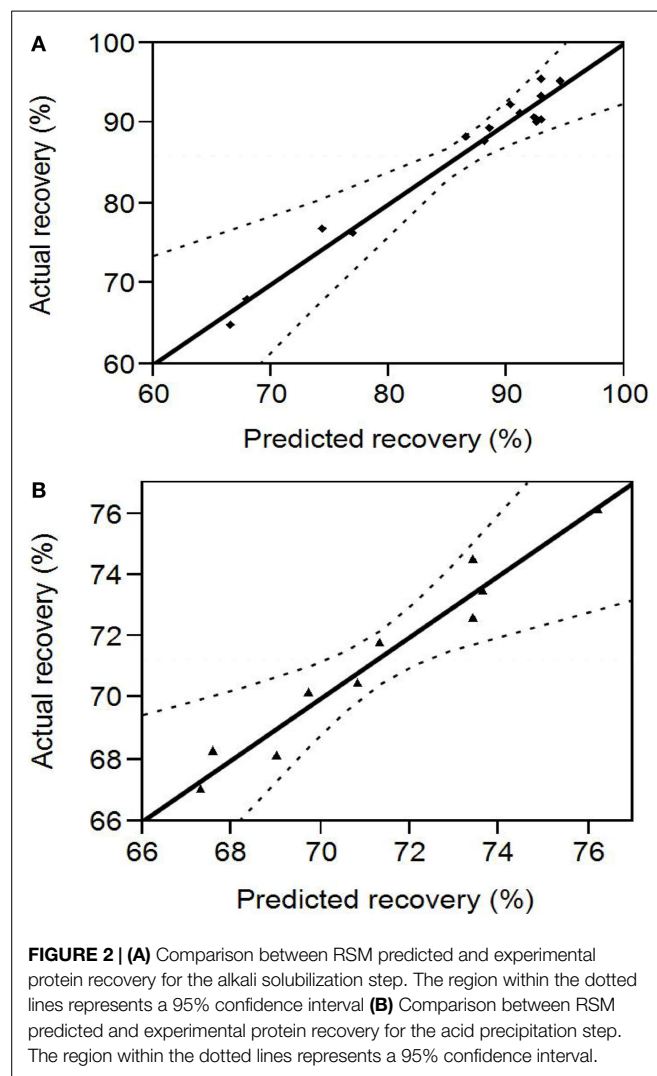


FIGURE 2 | (A) Comparison between RSM predicted and experimental protein recovery for the alkali solubilization step. The region within the dotted lines represents a 95% confidence interval **(B)** Comparison between RSM predicted and experimental protein recovery for the acid precipitation step. The region within the dotted lines represents a 95% confidence interval.

TABLE 1 | Estimate of the regression coefficients for the alkali solubilization optimization model and their statistical significance determined by Student's t -test.

Source	Estimate	SE	t ratio	$p > t $
Intercept	93.03	1.6256	57.23	<0.0001*
X_1	-1.54	0.9955	-1.54	0.1834
X_2	1.32	0.9955	1.32	0.2434
X_3	-10.36	0.9955	-10.4	0.0001*
X_1X_2	-0.55	1.4078	-0.39	0.7134
X_1X_3	-3.57	1.4078	-2.54	0.0522
X_2X_3	1.95	1.4078	1.38	0.2253
X_1^2	-1.72	1.4653	-1.17	0.2941
X_2^2	-2.33	1.4653	-1.59	0.1721
X_3^2	-9.16	1.4653	-6.25	0.0015*

*Significant ($p < 0.05$).

The predicted recoveries were significant ($p = 0.01$) and the coefficient of determination (R^2) for this model was 0.95, indicating a reasonably good fit. The results from the t -test showed that precipitation time was a significant factor ($p = 0.03$) in impacting the protein recovery. The quadratic regression term for pH was

TABLE 2 | Estimate of the regression coefficients for the acid precipitation optimization model and their statistical significance determined by Student's *t*-test.

Source	Estimate	SE	<i>t</i> ratio	<i>p</i> > <i>t</i>
Intercept	73.43	0.5908	124.28	<0.0001*
x_1	0.72	0.4036	1.78	0.1505
x_2	1.28	0.4036	3.18	0.0336*
$x_1 x_2$	-0.48	0.4943	-0.96	0.391
x_1^2	-5.11	0.6472	-7.89	0.0014*
x_2^2	1.49	0.6472	2.31	0.0823

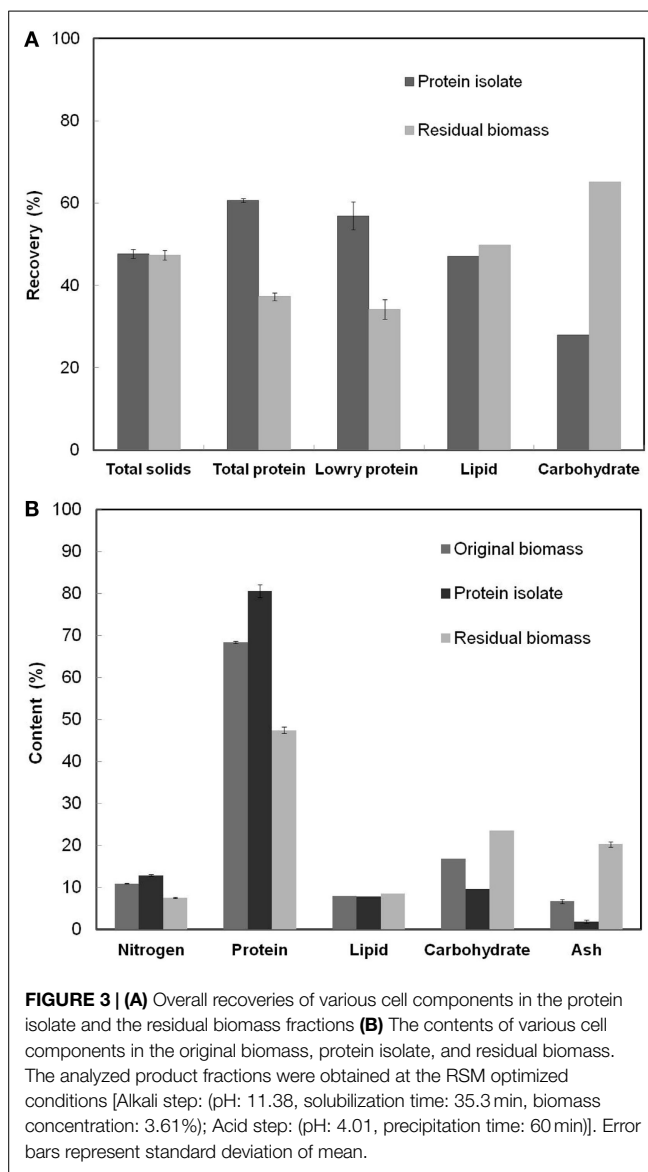
*Significant ($p < 0.05$).

highly significant ($p = 0.0014$) but not the linear term, implying a quadratic dependence of protein recovery on pH in the chosen range. The quadratic term for precipitation time was slightly significant ($p = 0.0823 < 0.1$). However, the interaction of pH and time was not significant implying that both of these factors are independent of each other in the chosen range. The model predicted the solution to be a saddle point. However, based on single parameter profiles, the optimum conditions for maximum protein precipitation were determined as pH 4.01 and precipitation time of 60 min. The predicted value of the response (protein recovery) at these values was 76.2%.

The RSM predicted maximum for overall protein yield after the alkali solubilization and acid precipitation steps was calculated as 73.15%. The experimentally determined protein recovery in the alkali supernatant and acid pellet at the RSM optimized process conditions for the solubilization and precipitation steps were 86 and 70.6%, respectively. Although the experimental recoveries for both the steps were lower than the theoretically predicted values, the variation (10.4 and 7.3%, respectively) was within acceptable limits, considering the scale of operation (the amount of biomass used in each of the optimization experiments was 10 times lower than that used in the protein isolation process at the optimized conditions), handling, and instrumental errors. The overall experimental protein yield at the optimum conditions was 60.7%.

Component Fractionation among the Product Fractions

Figure 3A shows the fractionation of various components between the protein isolate and the residual biomass obtained at the RSM optimized process conditions. The overall yield of total nitrogen and hence the yield of total protein in the protein isolate was 60.7%. This value was higher than the yields reported in the literature for proteins extracted using alkali-acid method from green algae (Gerde et al., 2013; Ursu et al., 2014) but lower than the 80% yield reported for *S. platensis* protein isolates (Devi et al., 1981). The higher yield reported in the latter case was a result of the use of hexane defatted biomass as the starting material and the repeated (three times) aqueous extraction and dialysis steps. Lowry protein assay estimated that 56.9% of soluble proteins were recovered in the protein isolate affecting a lower recovery in the residual biomass. The total solids fractionated almost equally between the two product fractions and so did the total lipids. However, carbohydrate recovery was higher in the residual biomass compared to the protein isolate.



The calculated purity or the protein content (% w/w) in the protein isolate was 80.6%, which was 12.2% higher than *S. platensis* biomass. This value of protein content was higher than that reported in the literature for the protein isolate obtained from *S. platensis* using a slightly different procedure (Chronakis et al., 2000). Recovery of non-protein components in the protein isolate due to co-precipitation of insoluble carbohydrates, cell wall PG fragments (composed of amino sugars), and lipids limited the purity of this fraction. The PG fragments from the cell wall of *S. platensis* did not possibly degrade into their respective sugar and peptide components under the relatively mild pH (=4) condition used in the protein precipitation process resulting in their co-extraction with proteins (Vollmer, 2008). Further, the residual biomass fraction had an undesirably high nitrogen and protein content (7.6 and 47.5%, respectively) indicating incomplete protein extraction, the loss of non-protein components due to co-extraction with proteins and the presence of PG fragments. A PG composition analysis based on the diagnostic markers,

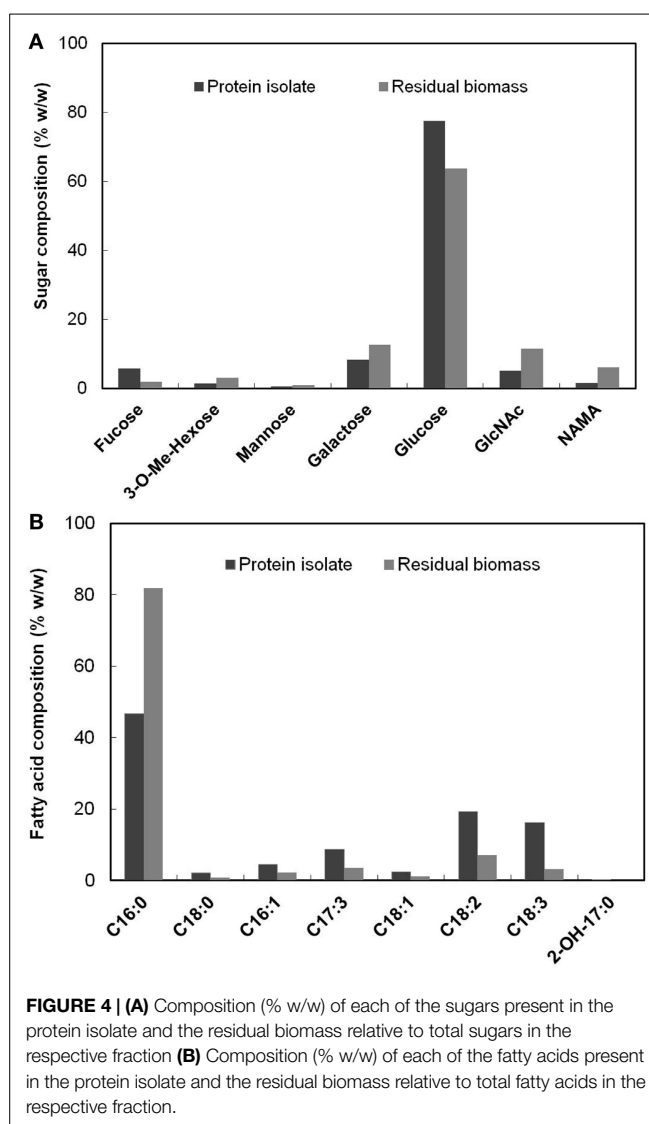
diaminopimelic acid (DAP) and N-acetyl muramic acid (NAMA), revealed the presence of PG fragments in both the protein isolate and the residual biomass fractions. Although the latter had a slightly higher proportion of all PG components compared to the protein isolate, their overall contents were very low compared to other cellular components. The contribution of amino sugars toward the total nitrogen and carbohydrate content in both the fractions was also extremely low (0.16 and 1.39% of the total estimated nitrogen in the two fractions, respectively). Thus, a further reduction in the nitrogen content of the residual biomass may be achieved only by repeated protein extractions involving additional processing steps and/or other unit operations. However, such procedures would demand higher processing costs and other resources, and may negatively impact the scalability of the process. Hence, this idea was not investigated in this work.

Initial Biomass, Protein Isolate, and Residual Biomass Characterization

Figure 3B shows the nitrogen and protein (based on elemental analysis), lipid, carbohydrate and ash contents in the original biomass, the protein isolate, and the residual biomass obtained at the RSM optimized conditions. The original *S. platensis* biomass was comprised of 10.95% nitrogen, 68.4% total protein, and 6.7% ash by weight. Analysis of the protein isolate and the residual biomass revealed higher nitrogen and protein contents and lower lipid, carbohydrate, and ash contents in the protein isolate compared to the residual biomass, which was in accordance with the desired outcome. The former was enriched in proteins while the latter was enriched in non-protein components. Although only 50% of the total lipids were recovered in the residual biomass, this did not have a huge impact on its composition due to the low lipid content of the original *S. platensis* biomass (8.03%).

The PG carbohydrate analysis method described in Section “PG Analysis” also quantified non-PG originated sugars present in the biomass in addition to the PG amino sugars. The relative composition (% w/w) of the detected sugars in the protein isolate and the residual biomass fractions are shown in Figure 4A. A major proportion of the sugars were glucose, which accounted for 77.50 and 63.84% of the total sugars (by weight) in each of these fractions, respectively. This was expected, given that glucose is the most abundant sugar present in *S. platensis* (Shekharam et al., 1987). Galactose accounted for 8.24 and 12.72% in the protein isolate and the residual biomass, respectively. The PG amino sugars NAMA and GlcNAc accounted for 6.11 and 11.39% of the total sugars, respectively in the residual biomass. In the protein isolate the proportions of these amino sugars were 1.52% NAMA and 5% GlcNAc. Small amounts of mannose, 3-methyl hexose and fucose were also detected in both of these fractions.

Figure 4B shows the relative composition (% w/w) of the fatty acids detected by FAMES analysis in the protein isolate and the residual biomass. C16:0 (Palmitic acid) was the dominant fatty acid in both the fractions, as was the case for original *S. platensis* biomass (Cohen, 1997). However, this fatty acid represented 81.83% of the total fatty acids in the residual biomass but only 46.76% of the protein isolate. The latter contained significant amounts of mono- and poly-unsaturated fatty acids (C16–18) while the residual biomass had very small amounts. These and



other fatty acids typically originate from membrane phospholipids where they are acylated to moieties carrying choline (phosphatidyl choline) and other polar head groups (Hoiczky and Hansel, 2000). An α -hydroxy fatty acid (2-OH-C17:0) was detected in low levels in the protein isolate, but not in the residual biomass. These results clearly indicated that the protein isolate was enriched in poly-unsaturated fatty acids while the residual biomass was enriched in saturated fatty acids. The former had a higher proportion of the essential fatty acid, γ -linolenic acid (C18:3) compared to the original *S. platensis* biomass. This and other unsaturated fatty acids can be separated from the protein isolate using methods such as supercritical CO₂ extraction and urea complex formation (Cohen et al., 1993; Mendes et al., 2005) to yield high-value co-products. The lower proportion of unsaturated fatty acids in the residual biomass is favorable for biofuel production processes because they could result in lower oxidative stability (rancidification) of the generated biofuel (Gunstone, 1967).

SDS-PAGE analysis revealed that several lighter (low protein concentration) bands observed in the molecular weight range of

TABLE 3 | Amino acid composition (expressed as g/100 g total amino acids) of the original *S. platensis* biomass and the protein isolate.

Amino acid	Composition	
	Original biomass	Protein isolate
Taurine	0.03	0.03
Hydroxyproline	0.00	0.02
Aspartic acid	10.12	9.86
Threonine ^a	4.92	4.85
Serine	4.32	4.41
Glutamic acid	15.58	13.28
Proline	3.66	3.79
Lanthionine	0.00	0.00
Glycine	5.06	5.24
Alanine	7.48	7.31
Cysteine	1.02	0.99
Valine ^a	6.46	6.91
Methionine ^a	2.38	2.40
Isoleucine ^a	5.85	6.34
Leucine ^a	8.91	9.80
Tyrosine	4.40	5.07
Phenylalanine ^a	4.71	5.16
Hydroxylysine	0.16	0.15
Ornithine	0.09	0.09
Lysine ^a	4.84	4.49
Histidine ^a	1.57	1.69
Arginine	7.30	6.72
Tryptophan ^a	1.14	1.42

^aEssential amino acids.

25–100 kDa in original *S. platensis* biomass were not found in the disrupted biomass implying protein degradation as a result of cell disruption by high-pressure homogenization (Figure S4 in Supplementary Material). The bands around 100 and 55 kDa were the most prominent ones among both the protein isolate and residual biomass fractions, although they were lighter in the latter indicating lower concentration of these proteins in this fraction. Thus, a higher proportion of the high molecular weight proteins fractionated into the protein isolate. Some of the bands observed in the disrupted biomass between 15 and 20 kDa were not observed in the protein isolate and the residual biomass fractions suggesting that these low molecular weight proteins degraded into peptide components during the protein isolation process. Further, the small dark band at the bottom of the gel in the original biomass was observed only in the residual biomass and not in the protein isolate, indicating that the low molecular weight peptides and free amino acids typically present in algae remained in the residual biomass.

The protein isolate obtained at a low ash content of 1.9% was freeze dried and further analyzed for amino acid and mineral contents. The results presented in **Table 3** show that the variation

in the composition of a majority of the amino acids between the protein isolate and the edible original *S. platensis* biomass was low (below 10%). The contents of six out of the eight essential amino acids were slightly higher in the protein isolate. *S. platensis* biomass has widely been accepted as a rich protein source for humans and animals (Becker, 2004) and hence the protein isolate could potentially be used in these applications. The predominant minerals present in the protein isolate were aluminum, calcium, iron, potassium, magnesium, sodium, phosphorus, sulfur, and silicon (Table S4 in Supplementary Material). Except for sodium, the composition of all the elements was lower than original *S. platensis* biomass (Jena et al., 2011b) and hence is within agreeable limits for nutritional purposes. The excess sodium originated from the NaOH added during the solubilization step.

Conclusion

In this study, protein isolation from *S. platensis* cyanobacterium was carried out using the alkali–acid method after cell disruption using high-pressure homogenization. The process conditions were optimized using RSM. At the optimized conditions, the proteins were extracted at a high yield of 60.7% and content of 80.6%. Further improvement of protein extraction was limited by co-fractionation of the non-protein components into the protein isolate and incomplete protein precipitation. The extracted protein isolate was enriched in proteins, essential amino acids, and unsaturated fatty acids, and had a lower ash and mineral content compared to the original biomass. Such a composition is suitable for human food or animal feed applications. The residual biomass had a lower protein and nitrogen content than the original biomass and was enriched in carbohydrates and saturated lipids, a composition better suited for biofuel applications such as HTL and AD.

Acknowledgments

This research was funded in part by the Department of Defense ARO grant W911NF-11-1-0218 (KD, PI) and the Department of Energy grant DE-FG02-93ER20097 (A. Darvill, PI) for the Center for Plant and Microbial Complex Carbohydrates (Complex Carbohydrate Research Center), at the University of Georgia. The authors thankfully acknowledge Dr. David Blum, Paul Volny, and Ron Garrison for their assistance with laboratory analyses and equipment.

Supplementary Material

The Supplementary Material for this article can be found online at <http://journal.frontiersin.org/article/10.3389/fenrg.2015.00030>

References

- Abas Wani, A., Sogi, D., Grover, L., and Saxena, D. (2006). Effect of temperature, alkali concentration, mixing time and meal/solvent ratio on the extraction of watermelon seed proteins – a response surface approach. *Biosyst. Eng.* 94, 67–73. doi:10.1016/j.biosystemseng.2006.02.004
- Becker, E. W. (2007). Micro-algae as a source of protein. *Biotechnol. Adv.* 25, 207–210. doi:10.1016/j.biotechadv.2006.11.002

- Becker, E. W. (2004). “Microalgae in human and animal nutrition,” in *Handbook of Microalgal Culture: Biotechnology and Applied Phycology*, ed. A. Richmond (Oxford: Blackwell Publishing), 312.
- Chen, Y., Cheng, J. J., and Creamer, K. S. (2008). Inhibition of anaerobic digestion process: a review. *Bioresour. Technol.* 99, 4044–4064. doi:10.1016/j.biortech.2007.01.057
- Choi, Y. R., and Markakis, P. (1981). Blue-green algae as a source of protein. *Food Chem.* 7, 239–247. doi:10.1016/0308-8146(81)90029-7

- Chronakis, I. S., Galatanu, A. N., Nylander, T., and Lindman, B. (2000). The behaviour of protein preparations from blue-green algae (*Spirulina platensis* strain Pacifica) at the air/water interface. *Colloids Surf. A Physicochem. Eng. Asp.* 173, 181–192. doi:10.1016/S0927-7757(00)00548-3
- Cohen, Z. (1997). “The chemicals of spirulina,” in *Spirulina Platensis Arthrospira: Physiology, Cell-Biology and Biotechnology*, ed. A. Vonshak (London: CRC Press), 175–204.
- Cohen, Z., Reungjitchachawali, M., Siangdung, W., and Tanticharoen, M. (1993). Production and partial purification of γ -linolenic acid and some pigments from *Spirulina platensis*. *J. Appl. Phycol.* 5, 109–115. doi:10.1007/bf02182428
- Damodaran, S. (1996). “Amino acids, peptides and proteins,” in *Food Chemistry*, ed. O. R. Fennema (New York, NY: Marcel Dekker, Inc.), 321–430.
- Devi, M. A., Subbulakshmi, G., Devi, K. M., and Venkataraman, L. V. (1981). Studies on the proteins of mass-cultivated, blue-green alga (*Spirulina platensis*). *J. Agric. Food Chem.* 29, 522–525. doi:10.1021/jf00105a022
- Firatligil-Durmus, E., and Evranuz, O. (2010). Response surface methodology for protein extraction optimization of red pepper seed (*Capsicum frutescens*). *LWT Food Sci. Technol.* 43, 226–231. doi:10.1016/j.lwt.2009.08.017
- Folch, J., Lees, M., and Sloane-Stanley, G. (1957). A simple method for the isolation and purification of total lipids from animal tissues. *J. Biol. Chem.* 226, 497–509.
- Gerde, J. A., Wang, T., Yao, L., Jung, S., Johnson, L. A., and Lamsal, B. (2013). Optimizing protein isolation from defatted and non-defatted *Nannochloropsis* microalgae biomass. *Algal Res.* 2, 145–153. doi:10.1016/j.algal.2013.02.001
- Goetz, J., and Koehler, P. (2005). Study of the thermal denaturation of selected proteins of whey and egg by low resolution NMR. *LWT Food Sci. Technol.* 38, 501–512. doi:10.1016/j.lwt.2004.07.009
- Gunstone, F. D. (1967). *An Introduction to the Chemistry and Biochemistry of Fatty Acids and Their Glycerides*, 2 Edn. London: Chapman and Hall.
- Haque, I., Singh, R., Moosavi-Movahedi, A. A., and Ahmad, F. (2005). Effect of polyol osmolytes on δ GD, the Gibbs energy of stabilisation of proteins at different pH values. *Biophys. Chem.* 117, 1–12. doi:10.1016/j.bpc.2005.04.004
- Hoiczky, E., and Hansel, A. (2000). Cyanobacterial cell walls: news from an unusual prokaryotic envelope. *J. Bacteriol.* 182, 1191–1199. doi:10.1128/JB.182.5.1191-1199.2000
- Jena, U., Das, K. C., and Kastner, J. R. (2011a). Effect of operating conditions of thermochemical liquefaction on biocrude production from *Spirulina platensis*. *Bioresour. Technol.* 102, 6221–6229. doi:10.1016/j.biortech.2011.02.057
- Jena, U., Vaidyanathan, N., Chinnasamy, S., and Das, K. (2011b). Evaluation of microalgae cultivation using recovered aqueous co-product from thermochemical liquefaction of algal biomass. *Bioresour. Technol.* 102, 3380–3387. doi:10.1016/j.biortech.2010.09.111
- Kritzer, P. (2004). Corrosion in high-temperature and supercritical water and aqueous solutions: a review. *J. Supercrit. Fluids* 29, 1–29. doi:10.1016/S0896-8446(03)00031-7
- López Barreiro, D., Prins, W., Ronsse, F., and Brilman, W. (2013). Hydrothermal liquefaction (HTL) of microalgae for biofuel production: state of the art review and future prospects. *Biomass Bioenergy* 53, 113–127. doi:10.1016/j.biombioe.2012.12.029
- Lowry, O. H., Rosebrough, N. J., Farr, A. L., and Randall, R. J. (1951). Protein measurement with the Folin phenol reagent. *J. Biol. Chem.* 193, 265–275.
- Ma, T., Wang, Q., and Wu, H. (2010). Optimization of extraction conditions for improving solubility of peanut protein concentrates by response surface methodology. *LWT Food Sci. Technol.* 43, 1450–1455. doi:10.1016/j.lwt.2010.03.015
- Mendes, R. L., Reis, A. D., Pereira, A. P., Cardoso, M. T., Palavra, A. F., and Coelho, J. P. (2005). Supercritical CO₂ extraction of γ -linolenic acid (GLA) from the cyanobacterium *Arthrospira* (*spirulina*) maxima: experiments and modeling. *Chem. Eng. J.* 105, 147–151. doi:10.1016/j.cej.2004.10.006
- Palinska, K. A., and Krumbain, W. E. (2000). Perforation patterns in the peptidoglycan wall of filamentous cyanobacteria. *J. Phycol.* 36, 139–145. doi:10.1046/j.1529-8817.2000.99040.x
- Payne, M. F., and Rippingale, R. J. (2000). Evaluation of diets for culture of the calanoid copepod *gladioferens imparipes*. *Aquaculture* 187, 85–96. doi:10.1016/S0044-8486(99)00391-9
- Piorreck, M., Baasch, K.-H., and Pohl, P. (1984). Biomass production, total protein, chlorophylls, lipids and fatty acids of freshwater green and blue-green algae under different nitrogen regimes. *Phytochemistry* 23, 207–216. doi:10.1016/S0031-9422(00)80304-0
- Pons, A., Richet, C., Robbe, C., Herrmann, A., Timmerman, P., Huet, G., et al. (2003). Sequential GC/MS analysis of sialic acids, monosaccharides, and amino acids of glycoproteins on a single sample as heptafluorobutyrate derivatives. *Biochemistry* 42, 8342–8353. doi:10.1021/bi034250e
- Prabakaran, P., and Ravindran, A. D. (2011). A comparative study on effective cell disruption methods for lipid extraction from microalgae. *Lett. Appl. Microbiol.* 53, 150–154. doi:10.1111/j.1472-765X.2011.03082.x
- Quanhong, L., and Caili, F. (2005). Application of response surface methodology for extraction optimization of germinant pumpkin seeds protein. *Food Chem.* 92, 701–706. doi:10.1016/j.foodchem.2004.08.042
- Safi, C., Charton, M., Pignolet, O., Pontalier, P.-Y., and Vaca-Garcia, C. (2013a). Evaluation of the protein quality of *Porphyridium cruentum*. *J. Appl. Phycol.* 25, 497–501. doi:10.1007/s10811-012-9883-4
- Safi, C., Charton, M., Pignolet, O., Silvestre, F., Vaca-Garcia, C., and Pontalier, P.-Y. (2013b). Influence of microalgae cell wall characteristics on protein extractability and determination of nitrogen-to-protein conversion factors. *J. Appl. Phycol.* 25, 523–529. doi:10.1007/s10811-012-9886-1
- Safi, C., Ursu, A. V., Laroche, C., Zebib, B., Merah, O., Pontalier, P.-Y., et al. (2014). Aqueous extraction of proteins from microalgae: effect of different cell disruption methods. *Algal Res.* 3, 61–65. doi:10.1016/j.algal.2013.12.004
- Shekharam, K. M., Venkataraman, L. V., and Salimath, P. V. (1987). Carbohydrate composition and characterization of two unusual sugars from the blue green alga *Spirulina platensis*. *Phytochemistry* 26, 2267–2269. doi:10.1016/S0031-9422(00)84698-1
- Sluiter, A., Hames, B., Hyman, D., Payne, C., Ruiz, R., Scarlata, C., et al. (2008a). “Determination of Total Solids in Biomass and Total Dissolved Solids in Liquid Process Samples”. NREL Technical Report No. NREL/TP-510-42621. Golden, CO: National Renewable Energy Laboratory.
- Sluiter, A., Hames, B., Ruiz, R., Scarlata, C., Sluiter, J., and Templeton, D. (2008b). “Determination of Ash in Biomass”. NREL Technical Report No. NREL/TP-510-42622. Golden, CO: National Renewable Energy Laboratory.
- Spolaore, P., Joannis-Cassan, C., Duran, E., and Isambert, A. (2006). Commercial applications of microalgae. *J. Biosci. Bioeng.* 101, 87–96. doi:10.1263/jbb.101.87
- Ursu, A.-V., Marcati, A., Sayd, T., Sante-Lhoutellier, V., Djelveh, G., and Michaud, P. (2014). Extraction, fractionation and functional properties of proteins from the microalgae *Chlorella vulgaris*. *Bioresour. Technol.* 157, 134–139. doi:10.1016/j.biortech.2014.01.071
- Valdez, P. J., Tocco, V. J., and Savage, P. E. (2014). A general kinetic model for the hydrothermal liquefaction of microalgae. *Bioresour. Technol.* 163, 123–127. doi:10.1016/j.biortech.2014.04.013
- Vollmer, W. (2008). Structural variation in the glycan strands of bacterial peptidoglycan. *FEMS Microbiol. Rev.* 32, 287–306. doi:10.1111/j.1574-6976.2007.00088.x
- Wang, X., and Zhang, X. (2012). Optimal extraction and hydrolysis of *Chlorella pyrenoidosa* proteins. *Bioresour. Technol.* 126, 307–313. doi:10.1016/j.biortech.2012.09.059
- York, W. S., Darvill, A. G., McNeil, M., Stevenson, T. T., and Albersheim, P. (1986). Isolation and characterization of plant cell walls and cell wall components. *Meth. Enzymol.* 118, 3–40.
- Zhang, S., Wang, Z., and Xu, S. (2007). Optimization of the aqueous enzymatic extraction of rapeseed oil and protein hydrolysates. *J. Am. Oil Chem. Soc.* 84, 97–105. doi:10.1007/s11746-006-1004-6

Conflict of Interest Statement: The authors declare that the research was conducted in the absence of any commercial or financial relationships that could be construed as a potential conflict of interest. The Guest Associate Editor S. Kent Hoekman declares that, despite having collaborated with author Keshav C. Das, the review process was handled objectively and no conflict of interest exists.

Copyright © 2015 Parimi, Singh, Kastner, Das, Forsberg and Azadi. This is an open-access article distributed under the terms of the Creative Commons Attribution License (CC BY). The use, distribution or reproduction in other forums is permitted, provided the original author(s) or licensor are credited and that the original publication in this journal is cited, in accordance with accepted academic practice. No use, distribution or reproduction is permitted which does not comply with these terms.



Solvent extraction and characterization of neutral lipids in *Oocystis* sp.

Renil Anthony¹ and Ben Stuart^{2*}

¹ Department of Mechanical Engineering, Ohio University, Athens, OH, USA

² Department of Civil Engineering, Ohio University, Athens, OH, USA

Edited by:

Umakanta Jena, Desert Research Institute, USA

Reviewed by:

Anoop Singh, Ministry of Science and Technology, India

István Barabás, Technical University of Cluj-Napoca, Romania

Daniel Geller, University of Georgia, USA

*Correspondence:

Ben Stuart, 122 Stocker Center, Athens, OH, 45701, USA

e-mail: stuart@ohio.edu

Microalgae are a favorable feedstock for bioproducts and biofuels due to their high oil content, fast growth rates, and low resource demands. Solvent lipid extraction efficiency from microalgae is dependent on algal strain and the extraction solvent. Four non-polar extraction solvents were evaluated for the recovery of neutral cellular lipids from microalgae *Oocystis* sp. (University of Texas at Austin LB2396). Methylene chloride, hexane, diethyl ether, and cyclohexane were selected as the extraction solvents. The lipid extracts were derivatized and analyzed using gas chromatography–mass spectroscopy. All solvent extracts contained hexadecanoic acid, linoleic acid, and linolenic acid; accounting for 70% of total lipid content with a proportional wt% composition of the three fatty acids, except for the hexane extracts that showed only hexadecanoic acid and linoleic acid. While not statistically differentiated, methylene chloride proved to be the most effective solvent for *Oocystis* sp. among the four solvents tested with a total average neutral lipid recovery of 0.25% of dry weight followed by diethyl ether (0.18%), cyclohexane (0.14%), and hexane (0.11%). This research presents a simple methodology to optimize the selection of lipid specific extraction solvents for the microalgal strain selected.

Keywords: microalgae, bioproducts and biofuels, solvent extraction, *Oocystis*, lipids

INTRODUCTION

Microalgae have demonstrated great potential as a feedstock for bioproducts and biofuels. Microalgae have extremely high growth rates with biomass doubling times as short as 3.5 h (Chisti, 2007). Microalgae can be grown in wastewater or brackish water thereby offsetting the requirement for fresh water. In addition to high growth rates, the lipid content of some microalgae strains has been reported as high as 80 wt% of dry biomass when subjected to stressful growth conditions that maximize lipid content (Chisti, 2007).

Microalgae can be fractionated into its major biochemical compounds, namely lipids, carbohydrates, and proteins. These biochemical compounds can then be converted into high value or commodity products such as nutraceuticals/pharmaceuticals, biodiesel from lipids, biosolvents, biogas from carbohydrates, aquaculture or animal feed from proteins, and other bioproducts such as pigments (phycocyanin), antioxidants (biliverdin), or antibacterials (Anthony et al., 2013). Operating on a multi-product platform will be helpful in minimizing the risks of market fluctuations. Hence, while developing extraction methods or processes, care should be taken to avoid damaging any valuable biochemical compounds. Utilizing such a biorefinery approach to produce several products from microalgae has the potential to greatly improve the economic viability and promote industrial scale production and processing of microalgae.

Biodiesel, an alternative diesel fuel, is made from renewable biological sources such as vegetable oils and animal fats (Ma and Hanna, 1999). A variety of feedstock can be used to produce biodiesel such as virgin vegetable oil, waste vegetable oil, animal

fats, and non-edible oils such as Jatropha oil, neem oil, castor oil, and others. The choice of feedstock for biodiesel is contingent upon the natural resources of the particular region where biodiesel production is desired (Demirbas, 2007). Although promising, techno-economic assessments for conventional biodiesel production using crop plants have proved them to be unsustainable due to their low photosynthetic efficiency, huge fresh water requirement to reach maturity, and slow growth rates (Li et al., 2008). Moreover, the use of edible oils for biodiesel is controversial in that it may result in an imbalance in the food supply chain.

Conventional methods of oil extraction such as mechanical pressing, supercritical fluid extraction, enzymatic extraction, hydrothermal liquefaction, ultrasonic assisted extraction, and osmotic shock possess certain technological limitations and/or are economically unsuitable for large-scale microalgal lipid extraction (Herrero et al., 2005). Solvent extraction, on the other hand is a relatively easier method that has been widely used for lipid extraction from microalgae and considered economical for commercial scale systems (Mercer and Armenta, 2011).

Solvent extraction of algal lipids is carried out by organic solvents such as benzene, hexane, acetone, chloroform (Mercer and Armenta, 2011), methylene chloride (Chen et al., 1981), ethanol, isopropanol (Smedes, 1999), or a combination of organic solvents depending on the products desired. Non-polar solvents such as hexane, cyclohexane, and methylene chloride show higher recovery of cellular non-polar or neutral lipids as compared to polar solvents such as methanol and ethanol, which have higher recovery of membrane associated polar lipids (Sakthivel et al., 2011). Furthermore, specific algal strains significantly influence

solvent selection for lipid extraction. Shen et al. (2009) performed lipid extractions on microalgae *Scenedesmus dimorphus* and *Chlorella protothecoides* using hexane and hexane/ethanol solvent systems and found higher lipid recovery with hexane. Fajardo et al. (2007) reported higher lipid recovery with *Phaeodactylum tricornutum* using hexane/ethanol solvent system. In a similar study, methylene chloride recovered the most neutral lipids from *Chlorella* sp. when compared to hexane and chloroform (Guckert et al., 1988). These findings suggest that in addition to the solvent type, the efficiency of lipid recovery is also algal strain dependent.

In this study, four non-polar solvents were chosen as the extraction media to recover neutral lipids from microalgae *Oocystis* sp. using the Soxhlet method. *Oocystis* sp. was chosen due to the potential for lipid production as evaluated under the Aquatic Species Program (ASP). It was desired to determine if the fatty acid profile and quantities from *Oocystis* sp. would be suitable for use as a bioproduct and biofuel feedstock. The four solvents selected were methylene chloride, hexane, diethyl ether, and cyclohexane. These particular solvents were selected based on previous lipid extraction studies on microalgae (Guckert et al., 1988; Shen et al., 2009) and marine samples (Smedes, 1999). The lipid extracts from each solvent were derivatized and analyzed on combined gas chromatography–mass spectroscopy (GC–MS). For this study, no attempt was made to maximize the lipid content of *Oocystis* sp. by nutrient stressing or manipulating other growth conditions. The objectives of this research were; (1) to identify the most efficient solvent among the four in terms of non-polar lipids extracted, and (2) to quantify and characterize the cellular fatty acid profile of *Oocystis* sp.

MATERIALS AND METHODS

The algal strain *Oocystis* sp. was obtained from the University of Texas at Austin (UTEX) culture collection (UTEX # LB2396). Nile Red (9-diethylamino-5H-benzo[a]phenoxazine-5-one), Fatty Acid Methyl Esters (FAMES) mix (C8–C24) and internal standard methyl myristate (C15H30O2) were obtained from Sigma Aldrich (St. Louis, MO, USA) and used as received. HPLC grade n-hexane, methanol, cyclohexane, diethyl ether, and methylene chloride were obtained from Fisher Scientific (Pittsburg, PA, USA). *Oocystis* sp. was grown in closed photobioreactors in artificial sea water media (pH = 7) (McLachan, 1964) as prescribed by Csavina (2008) at an average temperature of 25°C and 0.1 mmol/s/m² light intensity with a 16:08 light/dark cycle. Aeration was provided to facilitate mixing.

Prior to lipid extraction, Nile Red staining was used to detect the non-polar lipid content of *Oocystis* sp. Nile Red is lipid specific and only stains the non-polar lipids within the cell. The fluorescence of the non-polar lipids after being stained with Nile Red can be measured easily on a spectrophotometer (520 nm) (Roessler et al., 1998). According to the lipid optimization studies performed by Csavina et al. (2011), a Nile Red reading of 2000 Fluorescent Standard Units (FSU) suggested a high amount of neutral lipids in the cells. The Nile Red staining procedure followed by Csavina (2008) was adopted to determine time of harvesting. *Oocystis* sp. was harvested by coagulation with a pre-determined dosage of aluminum sulfate. The cells were collected by gravity settling and

washed several times with 1.0 M NaOH to remove the associated aluminum hydroxide prior to oil extraction.

To a sample size of 10 g dry algae, methanol was added while grinding using mortar and pestle to lyse the cells (Guckert et al., 1988). The lysed cells were dried and placed in a cellulose extraction thimble (Whatman no. 2810-338) in the Soxhlet apparatus and the solvents refluxed for 8 h. Extractions were performed in triplicate for each of the four solvents. The derivatization procedure comprised of adding 1 mL of toluene to the reaction test tube containing the extracts followed by 2 mL of 1% sulfuric acid in methanol. The test tube was sealed and heated to 50°C for 8 h. After cooling, 5 mL of 5% sodium chloride in water was added and shaken to dissolve the water soluble elements and encourage phase separation. One milliliter of the top organic phase was transferred to a GC vial for analysis.

The compounds in the lipids extracts were analyzed using a combination of gas chromatography (GC-HP6890) and mass spectrometry (MS-5973) using the parameters provided in **Table 1**. External standard comprising of FAME mix (C8–C24) was used to determine the response factors of the compounds relative to the internal standard, methyl myristate. The response factors were calculated by Eq. 1 as:

$$F = \frac{W_{\text{int}} \times A_i}{A_{\text{int}} \times W_i} \quad (1)$$

where $i = 1, 2, 3, \dots, n$ (where n is defined as the n th FAME), W_{int} and W_i are the weights of the internal standard and the compound peak in consideration, respectively, A_{int} and A_i are the areas of internal standard and the peak in consideration, respectively, and F is the response factor (Grob and Barry, 2004).

For a specific response factor F , the weight of the unknown can be calculated by Eq. 2 (Grob and Barry, 2004) as:

$$W_c = \frac{A_c}{A_{\text{int}}} \times F_c \times W_{\text{int}} \quad (2)$$

where, W_{int} and W_c are the weights of internal standard and unknown (C), respectively, A_{int} and A_c are the areas of internal standard and unknown, respectively, and F_c is the response factor for the compound of interest.

RESULTS AND DISCUSSION

GRAVIMETRIC AND NILE RED ANALYSIS

Nile Red values measured by Csavina (2008) for *Oocystis* sp. on the 7th day of growth was 2000 FSU, which amounted to a 615%

Table 1 | Gas chromatography parameters for the analysis of FAMES.

Parameters	Values
Inlet temperature	260°C
Injection volume	1 μL
Initial temperature	60°C
Ramp	15°C/min
Final temperature	270°C
Carrier gas	Helium

increase in fluorescence suggesting a relatively high neutral lipid content in the cells. For the current research, the average Nile Red fluorescence obtained in the exponential growth phase was 2459 FSU, which represented approximately a 750% increase in fluorescence. *Oocystis* sp. was harvested at this stage by aluminum sulfate and washed prior to oil extraction. Gravimetric analysis revealed a methylene chloride extract weight of 0.54 g followed by hexane, diethyl ether, and cyclohexane with 0.23, 0.20, and 0.20 g, respectively. One of the possible reasons for higher weight of methylene chloride extracts could be due to the higher polarity index of methylene chloride (3.1) when compared to other solvents, which could have better dissolved the polar components of the biomass such as residual media salts or membrane lipids. The

gravimetric analysis measured the total extractable material from *Oocystis* sp., which could include cellular lipids, chlorophyll, proteins, membrane lipids, and residual media salts and the coagulant aluminum hydroxide.

RESPONSE FACTOR

The FAME mix (C8–C24) (external standard) was spiked with methyl myristate (internal standard) and was run to obtain the response factors for the relevant compounds (**Figure 1**). The relevant compounds in the unknown samples were determined as hexadecanoic acid methyl ester (C16:0), linoleic acid methyl ester (18:2), and linolenic acid methyl ester (18:3) eluting at 13.08, 14.07, and 14.17 min, respectively. The response factors for hexadecanoic

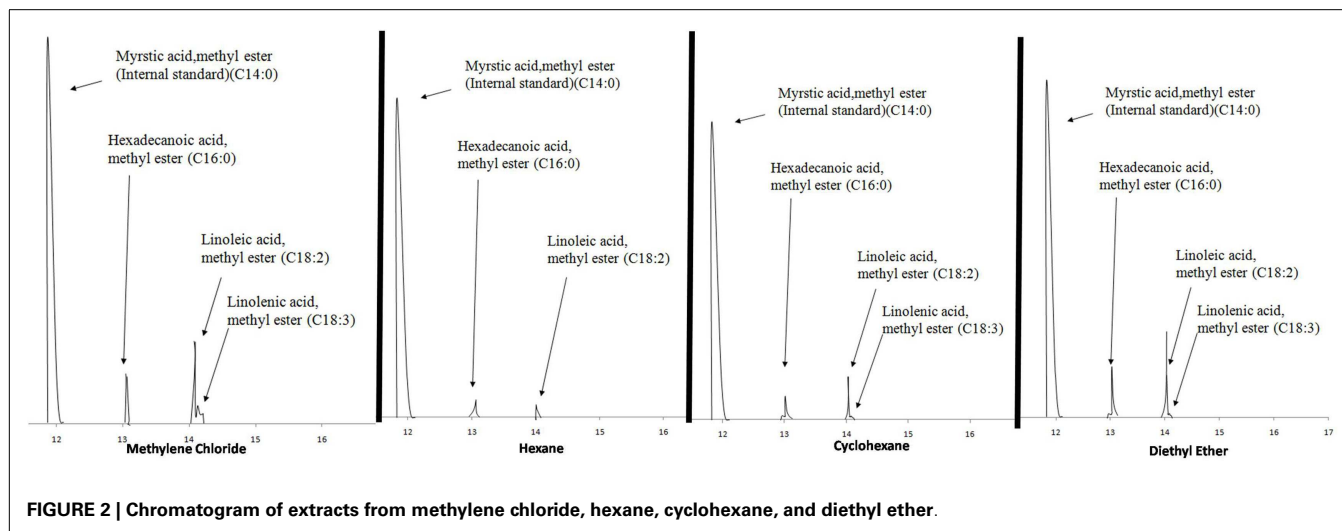
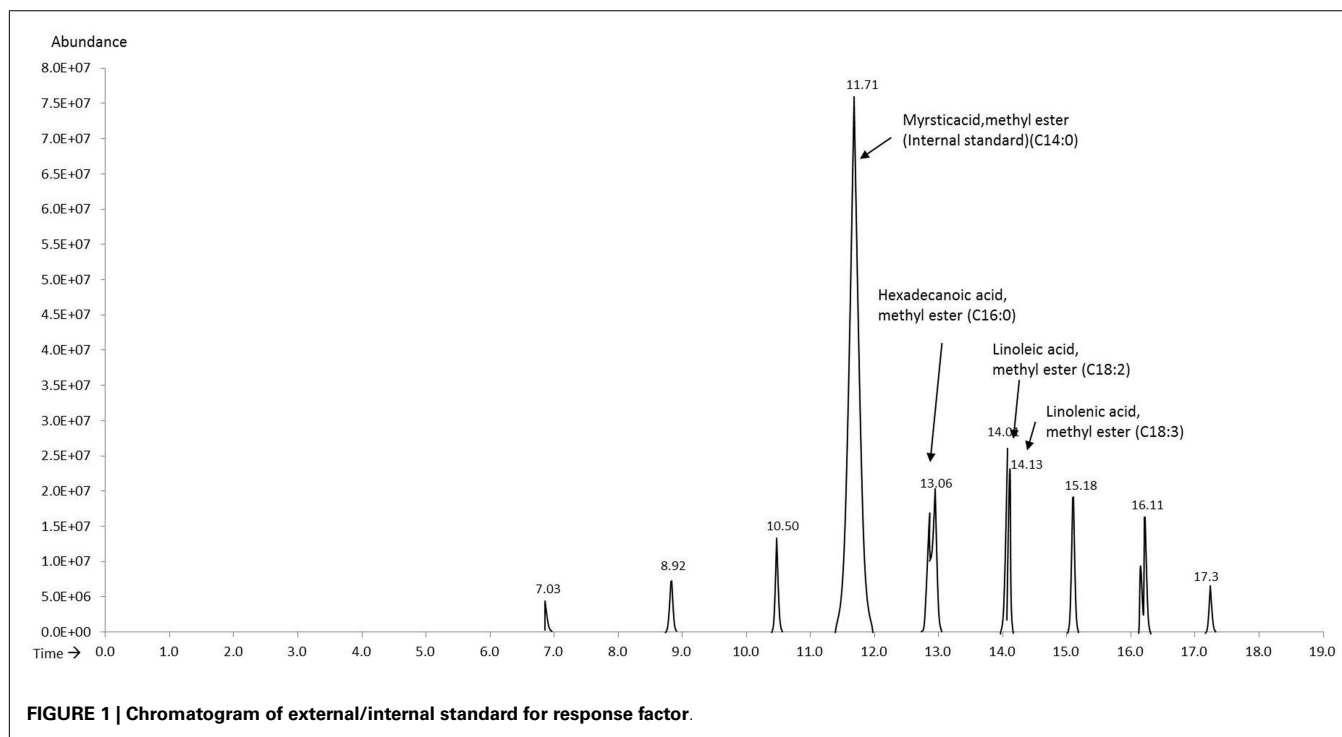


Table 2 | Summary of FAMES from *Oocystis* sp. extracted with the four solvents.

	Total FAMES (mg/g dry wt)	Coefficient of variation (%)	Dry wt (%)	Hexadecanoic acid methyl ester (C16:0) % (w/w)	Linoleic acid methyl ester (C18:2) % (w/w)	Linolenic acid methyl ester (C18:3) % (w/w)
Methylene chloride	2.5 ± 0.1	8.3	0.25	42.7	54.6	2.6
Diethyl ether	1.8 ± 0.2	38.1	0.18	42.5	54.8	2.6
Cyclohexane	1.4 ± 0.2	18.7	0.14	40.9	55.6	3.4
Hexane	1.1 ± 0.1	14.2	0.11	47.0	52.9	ND

ND, non-detectable.

Sums may not equal 100% due to rounding error.

Table 3 | Ryan–Einot–Gabriel–Welsch *post hoc* comparison of lipid yields from extraction solvents.

REGWQ grouping	Mean	N	Solvent
A	24.8	3	Methylene chloride
B A	17.6	3	Diethyl ether
B	14.4	2	Cyclohexane
B	10.7	3	Hexane

Means with the same letter are not significantly different.

acid methyl ester, linoleic acid methyl ester, and linolenic acid methyl ester as calculated using Eq. 1 were 0.57, 0.45, and 0.30, respectively.

QUANTITATIVE ANALYSIS OF FATTY ACID METHYL ESTERS

Methyl myristate was used as the internal standard for quantifying the FAMES in the derivatized extracts. A known volume of methyl myristate was added to the GC vial prior to analysis and the compounds were quantified using Eq. 2. The four extracts consistently showed three peaks eluting between 13 and 15 min, which through mass spectroscopy were identified as hexadecanoic acid methyl ester, linoleic acid methyl ester, and linolenic acid methyl ester except the hexane extracts for which linolenic acid was non-detectable. **Figure 2** shows the chromatograms of the extracts of the four solvents indicating the internal standard and the compounds in the sample.

Table 2 presents the percent composition of the total FAMES extracted. One-way analysis of variance (ANOVA) was performed on the mean values of total neutral lipids for the four solvents with a 95% confidence level with the Ryan–Einot–Gabriel–Welsch (REGWQ) test procedure employed for *post hoc* comparison using Statistical Analysis Software (SAS 9.3). As shown in the REGWQ grouping in **Table 3**, there was a significant difference between the weights of the FAMES extracted by methylene chloride as compared to cyclohexane and hexane, however, there was no significant difference between methylene chloride and diethyl ether. Comparing the average weights of FAMES extracted, methylene chloride was the highest followed by diethyl ether, cyclohexane, and hexane. The extracts from the four solvents showed nearly proportional percent composition of hexadecanoic acid methyl ester, linoleic acid methyl ester, and linolenic acid methyl ester as shown in **Table 2**. Although there are other fatty acids in *Oocystis* sp. in much lower concentrations, these three fatty acids represent

about 70% of the fatty acid profile (Patil et al., 2007) and were the only ones to have been sufficiently produced to be detected as per our growth, extraction, and analytical conditions.

Based on the evaluations conducted under the ASP, *Oocystis* sp. was selected as a candidate for potential bioproduct and biofuel production. Four non-polar solvents were evaluated for their extractability of neutral lipids from *Oocystis* sp. Of the four solvents, methylene chloride (on average) extracted the highest amount of neutral lipids followed by diethyl ether, cyclohexane, and hexane. The success of any bioproduct/biofuel program relies on identifying high lipid producing algal strains and the respective optimum extraction conditions. The economics of bioproduct/biofuel production can further be improved by employing a biorefinery platform to fractionate the biomass thereby, allocating the economic and environmental burdens to all the bioproducts generated, accordingly.

ACKNOWLEDGMENTS

This work was funded in part by a grant from the US Department of Energy (award number DE-FG36-08GO88083).

REFERENCES

- Anthony, R. J., Ellis, J. T., Sathish, A., Rahman, A., Miller, C. D., and Sims, R. C. (2013). Effect of coagulant/flocculants on bioproducts from microalgae. *Biore-sour. Technol.* 149, 65–70. doi:10.1016/j.biortech.2013.09.028
- Chen, I., Shen, C., and Sheppard, A. (1981). Comparison of methylene chloride and chloroform for the extraction of fats from food products. *J. Am. Oil Chem. Soc.* 58, 599–601. doi:10.1007/BF02672373
- Chisti, Y. (2007). Biodiesel from microalgae. *Biotechnol. Adv.* 25, 294–306. doi:10.1016/j.biotechadv.2007.02.001
- Csavina, J. L. (2008). *The Optimization of Growth Rate and Lipid Content from Select Algae Strains*. thesis. Available at: http://etd.ohiolink.edu/view.cgi?acc_num=ohiou1215529734
- Csavina, J. L., Stuart, B. J., Guy Riefler, R., and Vis, M. L. (2011). Growth optimization of algae for biodiesel production. *J. Appl. Microbiol.* 111, 312–318. doi:10.1111/j.1365-2672.2011.05064.x
- Demirbas, A. (2007). Importance of biodiesel as transportation fuel. *Energy Policy* 35, 4661–4670. doi:10.1016/j.enpol.2007.04.003
- Fajardo, A. R., Cerdán, L. E., Medina, A. R., Fernández, F. G. A., Moreno, P. A. G., and Grima, E. M. (2007). Lipid extraction from the microalga *Phaeodactylum tricornutum*. *Eur. J. Lipid Sci. Technol.* 109, 120–126. doi:10.1002/ejlt.200600216
- Grob, R. L., and Barry, E. F. (2004). *Modern Practice of Gas Chromatography*, 4th Edn. Hoboken, NJ: Wiley-Interscience.
- Guckert, J. B., Cooksey, K. E., and Jackson, L. L. (1988). Lipid solvent systems are not equivalent for analysis of lipid classes in the microeukaryotic green alga, *Chlorella*. *J. Microbiol. Methods* 8, 139–149. doi:10.1016/0167-7012(88)90015-2
- Herrero, M., Martín-Álvarez, P. J., Javier Señoráns, F., Cifuentes, A., and Ibáñez, E. (2005). Optimization of accelerated solvent extraction of antioxidants from *Spirulina platensis* microalga. *Food Chem.* 93, 417–423. doi:10.1016/j.foodchem.2004.09.037

- Li, Y., Horsman, M., Wu, N., Lan, C. Q., and Dubois-Calero, N. (2008). Biofuels from Microalgae. *Biotechnol. Prog.* 24, 815–820. doi:10.1021/bp070371k
- Ma, F., and Hanna, M. A. (1999). Biodiesel production: a review. *Bioresour. Technol.* 70, 1–15. doi:10.1016/S0960-8524(99)00025-5
- McLachan, J. (1964). Some considerations of the growth of marine algae in artificial media. *Can. J. Microbiol.* 10, 769–782. doi:10.1139/m64-098
- Mercer, P., and Armenta, R. E. (2011). Developments in oil extraction from microalgae. *Eur. J. Lipid Sci. Technol.* 113, 539–547. doi:10.1002/ejlt.201000455
- Patil, V., Torsten, K., Elisabeth, O., Gjermund, V., and Gislørød, H. R. (2007). Fatty acid composition of 12 microalgae for possible use in aquaculture feed. *Aquacult. Int.* 15, 1–9. doi:10.1007/s10499-006-9060-3
- Roessler, P., Sheehan, J., Dunahay, T., Benemann, J. (1998). *A Look Back at the U.S. Department of Energy's Aquatic Species Program: Biodiesel from Algae*. Books LLC. Reference Series.
- Sakthivel, R., Elumalai, S., and Mohommad Arif, M. (2011). Microalgae lipid research, past, present: a critical review for biodiesel production, in the future. *J. Exp. Sci.* 2, 29–49. Available at: <http://jexpsciences.com/index.php/jexp/article/view/9559>
- Shen, Y., Zhijian, P., Wenqiao, Y., and Enrong, M. (2009). Effect of nitrogen and extraction method on algae lipid yield. *Int. J. Agricult. Biol. Eng.* 2, 51–57. doi:10.3965/ijabe.v2i1.86
- Smedes, F. (1999). Determination of total lipid using non-chlorinated solvents. *Analyst* 124, 1711–1718. doi:10.1039/A905904K

Conflict of Interest Statement: The authors declare that the research was conducted in the absence of any commercial or financial relationships that could be construed as a potential conflict of interest.

Received: 18 September 2014; accepted: 19 December 2014; published online: 20 January 2015.

Citation: Anthony R and Stuart B (2015) Solvent extraction and characterization of neutral lipids in *Oocystis* sp. *Front. Energy Res.* 2:64. doi: 10.3389/fenrg.2014.00064
This article was submitted to *Bioenergy and Biofuels*, a section of the journal *Frontiers in Energy Research*.

Copyright © 2015 Anthony and Stuart. This is an open-access article distributed under the terms of the Creative Commons Attribution License (CC BY). The use, distribution or reproduction in other forums is permitted, provided the original author(s) or licensor are credited and that the original publication in this journal is cited, in accordance with accepted academic practice. No use, distribution or reproduction is permitted which does not comply with these terms.

